



National Library
of Canada

Acquisitions and
Bibliographic Services Branch

395 Wellington Street
Ottawa, Ontario
K1A 0N4

Bibliothèque nationale
du Canada

Direction des acquisitions et
des services bibliographiques

395, rue Wellington
Ottawa (Ontario)
K1A 0N4

Your file Votre référence

Our file Notre référence

NOTICE

The quality of this microform is heavily dependent upon the quality of the original thesis submitted for microfilming. Every effort has been made to ensure the highest quality of reproduction possible.

If pages are missing, contact the university which granted the degree.

Some pages may have indistinct print especially if the original pages were typed with a poor typewriter ribbon or if the university sent us an inferior photocopy.

Reproduction in full or in part of this microform is governed by the Canadian Copyright Act, R.S.C. 1970, c. C-30, and subsequent amendments.

AVIS

La qualité de cette microforme dépend grandement de la qualité de la thèse soumise au microfilmage. Nous avons tout fait pour assurer une qualité supérieure de reproduction.

S'il manque des pages, veuillez communiquer avec l'université qui a conféré le grade.

La qualité d'impression de certaines pages peut laisser à désirer, surtout si les pages originales ont été dactylographiées à l'aide d'un ruban usé ou si l'université nous a fait parvenir une photocopie de qualité inférieure.

La reproduction, même partielle, de cette microforme est soumise à la Loi canadienne sur le droit d'auteur, SRC 1970, c. C-30, et ses amendements subséquents.

University of Alberta

**Characterization and Natural Processes Enhancing Dry
Landscape Reclamation of
Fine Processed Mine Wastes**

by

Richard Peter Stahl



A thesis submitted to the Faculty of Graduate Studies and Research in partial
fulfillment of the requirements for the degree of *Doctor of Philosophy*

in

Geotechnical Engineering

Department of Civil Engineering

Edmonton, Alberta

Spring, 1996



National Library
of Canada

Acquisitions and
Bibliographic Services Branch

395 Wellington Street
Ottawa, Ontario
K1A 0N4

Bibliothèque nationale
du Canada

Direction des acquisitions et
des services bibliographiques

395, rue Wellington
Ottawa (Ontario)
K1A 0N4

Your file Votre référence

Our file Notre référence

The author has granted an irrevocable non-exclusive licence allowing the National Library of Canada to reproduce, loan, distribute or sell copies of his/her thesis by any means and in any form or format, making this thesis available to interested persons.

L'auteur a accordé une licence irrévocable et non exclusive permettant à la Bibliothèque nationale du Canada de reproduire, prêter, distribuer ou vendre des copies de sa thèse de quelque manière et sous quelque forme que ce soit pour mettre des exemplaires de cette thèse à la disposition des personnes intéressées.

The author retains ownership of the copyright in his/her thesis. Neither the thesis nor substantial extracts from it may be printed or otherwise reproduced without his/her permission.

L'auteur conserve la propriété du droit d'auteur qui protège sa thèse. Ni la thèse ni des extraits substantiels de celle-ci ne doivent être imprimés ou autrement reproduits sans son autorisation.

ISBN 0-612-10640-3

Canada

University of Alberta

Library Release Form

NAME OF AUTHOR: *Richard Peter Stahl*

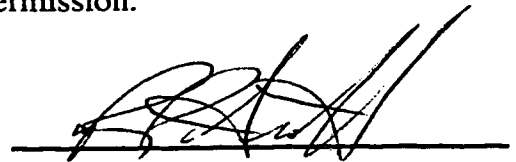
TITLE OF THESIS: *Characterization and Natural Processes Enhancing Dry
Landscape Reclamation of Fine Processed Mine Wastes*

DEGREE: *Dector of Philosophy*

YEAR THIS DEGREE GRANTED: *1996*

Permission is hereby granted to the University of Alberta Library to reproduce single copies of this thesis and to lend or sell such copies for private scholarly, or scientific research purposes only.

The author reserves all other publication and other rights in association with the copyright in the thesis, and except as hereinbefore provided, neither the thesis nor any substantial portion thereof may be printed or otherwise reproduced in any material form whatever without the author's prior written permission.



1403 - 10883 Saskatchewan Drive
Edmonton, Alberta
T6E 4S6


APRIL 18, 1996
Date submitted to FGSR

University of Alberta

Faculty of Graduate Studies and Research

The undersigned certify that they have read, and recommend to the Faculty of Graduate Studies and Research for acceptance, a thesis entitled *Characterization and Natural Processes Enhancing Dry Landscape Reclamation of Fine Processed Mine Wastes* submitted by *Richard Peter Stahl* in partial fulfillment of the requirements for the degree of *Doctor of Philosophy in Geotechnical Engineering*.


Dr. D.C. Sego


Dr. P.K. Robertson


Dr. N.R. Morgenstern


Dr. D. Chanasyk

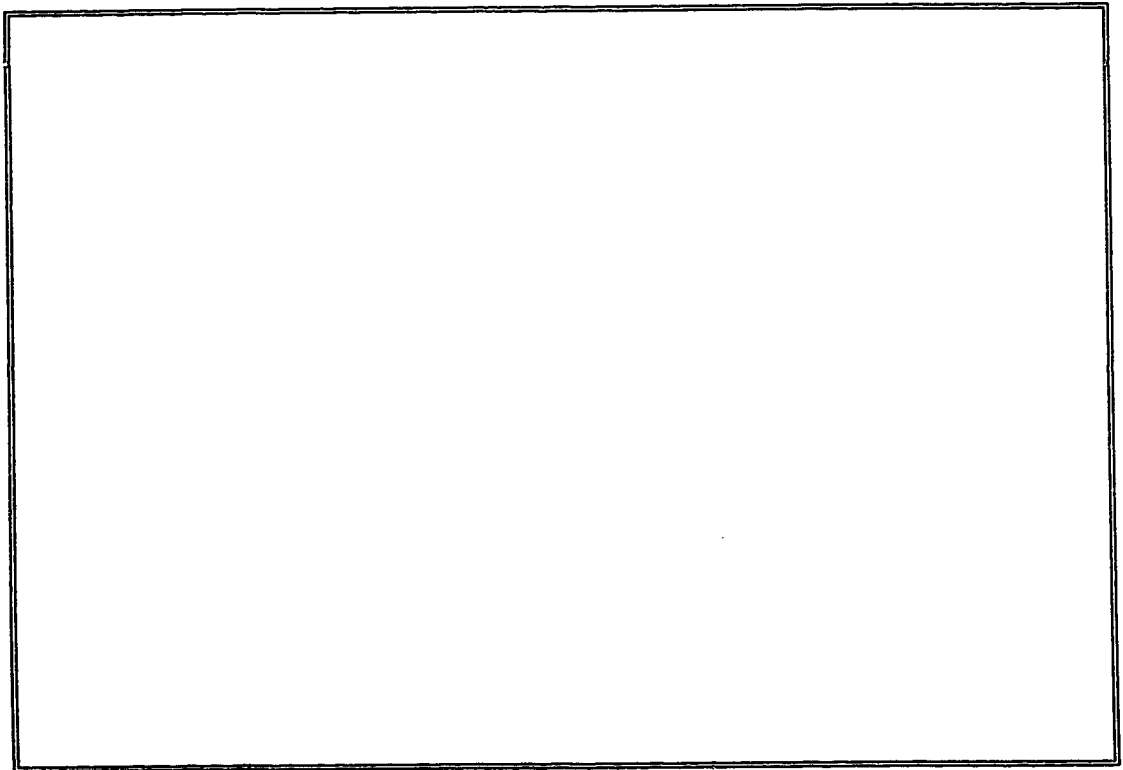

Dr. T.Y. Gan


Dr. J.D. Nelson

APRIL 18, 1996
Date Approved

***The Blood, Sweat, and Tears Shed To Reach
the Summit are Forgotten with the Amplified
Exhilaration Realized Upon Vision of New
Peaks and Horizons.***

- Richard Peter Stahl, 1996 -



to

*Mom, Dad, and Timothy
for all your support, encouragement and
love along the way*

and to

*Gorden who continues to safeguard me
from above*

Abstract

Tremendous volumes and diversity of mine wastes are produced and exist world wide. A large portion of these mine wastes result from ore beneficiation and are transported hydraulically to surface impoundments. These slurried wastes (tailings) may broadly be classified as segregating or nonsegregating, each exhibiting contrasting behavior following deposition. The local or regional geotechnical integrity of these deposits may be limited, creating characterization difficulties and result in problematic dry landscape reclamation. Two tailings deposits of contrasting dimensions, depositional behavior, geotechnical and material properties, which sample the spectrum of tailings facilities were investigated

Characterization of weak tailings deposits requires non-traditional techniques. Three site investigation systems developed to characterize weak deposits included a Plate Load Test apparatus, a Cone Penetration Test apparatus, and a Spectral Analysis of Surface Waves system. Each system was light weight and afforded mobilization to the weak tailings sites using only human effort.

Mechanisms to economically enhance the surface stability and dry landscape reclamation of these weak deposits is available. The mechanisms explored are broadly defined as natural surface enhancement processes and include freeze-thaw consolidation, evaporation, evapotranspiration, and fibre reinforcement of vegetative root systems. Chronological performance monitoring from 1989 to 1996 at a coal tailings facility indicates that these processes are active and have resulted in considerable strength and surface stability enhancement. In addition to highlighting the impact of the various natural enhancement processes, site characterization correlations are confirmed and presented which assist future tailings investigations. Furthermore, extension of a fibre

reinforcing model showed success in prediction of increase in bearing capacity offered by vegetative root systems

The geotechnical integrity of dry landscapes encountered in natural “undisturbed” environments is diverse. Dry landscape reclamation of tailings facilities must satisfy the end-land use, maintain equivalency and behave harmoniously with the regional landscape. Site characterization equipment employed to initially characterize and monitor reclamation progress, coupled with engineering of natural surface enhancement processes are mechanisms to achieve this goal.

Acknowledgments

I would like to express my sincere gratitude to Dr. D.C. Sego who exercised confidence in me and encouraged pursuit of this Ph.D.. Furthermore, his continual technical and financial support, guidance, and constant vision, coupled with patience and flexibility facilitating additional research and athletic endeavors were instrumental for personal growth and is extremely appreciated. Valuable support and encouragement was also provided by Dr. P.K. Robertson. The guidance, experiences, conversations and friendship shared will never be forgotten.

Gratitude is extended to each of the professors within the geotechnical group, particularly Dr. D. Chan, Dr. J.D. Scott, Dr. D.M. Cruden and Dr. N.R. Morgenstern, who contributed to both personnel and professional development during these studies. Special thanks is extended to Dr. Morgenstern who continually exemplifies quality and leadership and is an inspiration for all professionals. I would also like to thank Dr. C.A. Mendoza who further fueled an interest in contaminant remediation and provided guidance towards additional research initiatives.

This research would not have been possible without the financial support provided by several organizations. My most sincere appreciation is extended to The Natural Sciences and Engineering Research Council (NSERC), Luscar Ltd., the Association of Professional Engineers, Geologists, and Geophysicists of Alberta (APEGGA), The Walter H. Johns Foundation, The Boreal Alberta Research Grant Foundation, and The Geotechnical Society of Edmonton.

This research was also made possible through the support in kind provided by Luscar Sterco (1977) Ltd.. The sharing of information, site access, and periodic field support provided by Mr. Dane McCoy, Mr. Bob Latimer, and Mr. Curtis Brinker is greatly appreciated. Suncor Inc. also provided support during the field studies and the efforts behind the scenes by Mr. B. Burns facilitating smooth site investigation periods is appreciated.

The energetic efforts of the geotechnical technicians were critical to this research. The laboratory assistance provided by Christine Hereygers and Steve Gamble was extremely valuable. Special thanks is extended to Gerry Cyre who not only shared his expertise, but also shared in the many miles traveled, long site investigation days, and made the field research experiences truly enjoyable. I am also extremely grateful for the courteous, efficient and tireless secretarial efforts provided during various stages of thesis research by Ms. S. Petaske.

I would also like to thank ConeTec Investigations Ltd. of Vancouver, B.C. who furnished much of the equipment for these investigations. Furthermore, the tremendous support, patients, guidance and friendship shared by Mr. Dave Woeller, Mr. Ilmar Weemee, Mr. Tim Boyd, and Mr. S. Sandeep will be remembered.

To all my friends and colleges at the university, who endured the difficult and happy moments of this adventure, thank you! Very special thanks must go to Barb Hoffman, Richard Dawson, Kevin Biggar, Warren Millar, Sam Proskin, Peter Skopek, Annaji Rao, Marc Adams, and Catherine Fear. Sincere appreciation is sent to my many friends outside the department and university including Karen Calder, John Crabtree, Ken Brass, Grant Andruchow, Michelle Rooney, Wendy Chaboyer, Carmen Ropchan, Carla Fontana, Pat Moore, Ken and Christa Haberstock, Joel and Jody Haberstock, Lee and Michelle Loveridge, The Croteau family, Daniel St. Gelais, Gael Forster, Cheryl and Doug Cox, Gord Polloch, Caroline Lewis, Ann Marie Quinn, and Raymond Stahl. The laughs, experiences, and friendships shared will always be cherished.

Last but not least, the support encouragement and love of my family has been unyielding. Special thanks to my mother who never fails to show me her love and support!

Table of Contents

Chapter 1

Introduction

1.1. INTRODUCTION	1
1.2. RESEARCH BACKGROUND AND OBJECTIVES	4
1.3. ORGANIZATION OF THESIS	6
1.4. REFERENCES	8

Chapter 2

Influence Of Natural Surface Processes On Reclamation Of The Coal Valley Tailings Impoundment

2.1. INTRODUCTION	10
2.2. DEPOSITION HISTORY	11
2.3. RECLAMATION OF COARSE TAILS	12
2.3.1. Shallow Stratigraphy	12
2.3.2. Plate Load Tests	13
2.3.2.1. Theory	13
2.3.2.2. Plate Load Testing Description	14
2.3.2.3. Tests Results	15
2.3.3. Strength Enhancement	17
2.3.3.1. Natural Crusting	17
2.3.3.2. Biological Dewatering And Strength Enhancement	18
2.4. CONCLUSIONS	20
2.5. REFERENCES	21

Chapter 3

Freeze-Thaw Dewatering And Structural Enhancement Of Fine Coal Tails

3.1. INTRODUCTION	31
3.2. FREEZE-THAW	32
3.2.1. General Description	32

3.2.2. Open System Freezing	33
3.2.3. Closed System Freezing	34
3.3. DESIGN PROCESS	36
3.3.1. Background	36
3.3.2. Freezing and Thawing Indices	37
3.3.3. Freezing Model	37
3.3.4. Thawing Model	38
3.3.5. Freeze-Thaw Optimization	40
3.4. FIELD RESULTS	41
3.4.1. Shear Strength Data	41
3.4.2. Normally Consolidated Shear Strengths	42
3.5. FREEZE-THAW CONCEPT FOR EXISTING IMPOUNDMENT	44
3.6. CONCLUSIONS	45
3.7. REFERENCES	45

Chapter 4

Characterization of Fine Processed Mine Tailings Deposits for Purposes of Dry Landscape Reclamation

4.1. INTRODUCTION	57
4.2. TAILINGS FACILITIES	58
4.3. PLATE LOAD TEST (PLT)	59
4.4. CONE PENETRATION TEST (CPT)	61
4.5. SPECTRAL ANALYSIS OF SURFACE WAVES (SASW)	62
4.6. SUMMARY	63
4.7. REFERENCES	63

Chapter 5

Shear Strength And Bearing Capacity Of Fine Coal Tails And Processes Contributing To Their Dry Landscape Reclamation

5.1. INTRODUCTION	70
5.2. INSITU TESTING	71
5.3. UNDRAINED SHEAR STRENGTH	71
5.4. BEARING CAPACITY	73
5.5. SURFACE STABILITY PROCESSES	73
5.5.1. Evaporation/Evapotranspiration	73
5.5.2. Fibre Reinforcement Of Vegetative Root Systems	74
5.6. SUMMARY	76
5.7. REFERENCES	76

Chapter 6

Influence Of Natural Surface Processes On Bearing Capacity And Reclamation Of Fine Coal Tails

6.1. INTRODUCTION	81
6.2. DEPOSIT CHARACTERISTICS	83
6.3. PLATE LOAD TESTS	84
6.3.1. Plate Load Test System	84
6.3.2. Plate Load Test Results	86
6.4. SURFACE STABILITY PROCESSES	88
6.4.1. Evaporation/Evapotranspiration	88
6.4.2. Fibre Reinforcement Of Vegetative Root Systems	92
6.5. SUMMARY AND CONCLUSIONS	96
6.6. REFERENCES	97

Chapter 7

Characterization And Dry Landscape Reclamation Of Mine Tailings

7.1. INTRODUCTION	109
7.2. TAILINGS DEPOSIT CHARACTERISTICS	111
7.3. CHARACTERIZATION	112
7.4. DRY LANDSCAPE RECLAMATION	113
7.4.1. General Reclamation Processes	113
7.4.2. Freeze-Thaw Consolidation	113
7.4.3. Drainage/Evaporation/Evapotranspiration	115
7.4.4. Fibre Reinforcement of Vegetative Root Systems	117
7.5. SUMMARY AND CONCLUSIONS	119
7.6. REFERENCES	120

Chapter 8

Natural Surface Enhancement Process Design Guidelines

8.1. INTRODUCTION	126
8.2. FREEZE-THAW CONSOLIDATION DEWATERING	127
8.2.1. Processes and Models	127
8.2.2. Strength Enhancement and Volume Reduction	128
8.3. EVAPORATION AND EVAPOTRANSPIRATION	130
8.3.1. Background and Models	130
8.3.2. Strength Enhancement	131
8.4. VEGETATIVE ROOT REINFORCEMENT	133
8.5. CONCLUSIONS	134
8.6. REFERENCES	135

Chapter 9

Summary And Conclusions

8.1. SUMMARY AND CONCLUSIONS	137
8.2. SUGGESTED FUTURE RESEARCH	140

Appendix A

Index And Vane Shear Testing At Coal Valley And Suncor NST Cells

A.1. INTRODUCTION	143
A.2. INDEX TABLES	143
A.3. GRAIN SIZE DISTRIBUTIONS	144
A.4. MOISTURE AND SOLIDS CONTENTS	145
A.5. FIELD VANE SHEAR STRENGTH PROFILES	145
A.6. REFERENCES	146

Appendix B

Plate Load Test Results At Coal Valley And Suncor NST Cells

B.1. BACKGROUND	164
B.2. PLATE LOAD TEST RESULTS	165
B.3. MATRIC SUCTIONS AND BEARING CAPACITY	167
B.4. REFERENCES	169

Appendix C

Cone Penetration Tests At Coal Valley And Suncor NST Cells

C.1. BACKGROUND AND SOUNDING RESULTS	188
C.2. INTERPRETATION OF SOIL BEHAVIOR TYPE	193
C.3. SOUNDING AND ANALYSIS COMMENTS	194
C.4. PORE PRESSURE DISSIPATION TESTS	195
C.5. REFERENCES	199

Appendix D

Spectral Analysis Of Surface Waves Investigations At Coal Valley And Suncor NST Cells

D.1. INTRODUCTION	230
D.2. SASW DESCRIPTION	230
D.3. RESULTS	233
D.4. INVESTIGATION AND ANALYSIS COMMENTS	234
D.5. REFERENCES	235

Appendix E

Increased Shear Strength And Bearing Capacity From Vegetative Root Systems

E.1. SHEAR STRENGTH FORMULATIONS	247
E.1.1. Fibre Orientation Effects	251
E.2. THEORETICAL SHEAR STRENGTH AND BEARING CAPACITY PREDICTION	251
E.3. SOIL-FIBRE INTERACTION VARIABLES	256
E.4. PARAMETRIC ANALYSIS OF THEORETICAL MODEL PREDICTIONS	257
E.5. REFERENCES	258

Appendix F

Correlations, Comparisons And Factors From Site Investigation Results

F.1. INTRODUCTION	272
F.2. COMPRESSIBILITY CORRELATIONS	272
F.3. SHEAR WAVE VELOCITY CONFIRMATION	275
F.4. UNDRAINED SHEAR STRENGTH	278
F.5. DISCONTINUITY EFFECTS	283
F.6. REFERENCES	285

List of Tables

Table 3.1	Input Variables for Depth of Frost Predictions for Fine Coal Tails	48
Table 3.2	Input Variables for Depth of Thaw Predictions for Fine Coal Tails	48
Table 3.3	Shear Strength Ratios for Mine Tails (after Schiffman <i>et al.</i> 1988)	49
Table A1	Summary of 1992 Density Measurements at Coal Valley	147
Table A2	Summary of Relative Density Measurements on 1992 Samples	147
Table A3	Summary of 1995 Density and Root Area Ratio Measurements at Coal Valley	148
Table A4	Ash Content and Ash Specific Gravity of Selected 1995/96 Samples at Coal Valley	148
Table A5	Summary of Atterberg Limit Data From Coal Valley	149
Table A6	Summary of Atterberg Limit Data From Suncor NST Cells	149
Table C1	Comparison of Soil Description and Soil Behavior Type at Coal Valley	200
Table C2	Comparison of Soil Description and Soil Behavior Type at Suncor NST	200
Table C3	Summary of Pore Pressure Dissipation Test Results at Coal Valley	201
Table C4	Summary of Pore Pressure Dissipation Test Results at Suncor NST	201
Table C5	Summary of Laboratory Consolidation Data Conducted By Thurber (1992)	202
Table E1	Influence of Soil Properties on Increased Strength and Increased Critical Confining Stress of Fibre Reinforced Soil (<i>developed from Maher, 1988</i>)	260
Table E2	Influence of Fibre Properties on Increased Strength and Increased Critical Confining Stress of Fibre Reinforced Soil (<i>developed from Maher, 1988</i>)	260

List of Figures

Figure 2.1	Coal Valley Waste Streams	23
Figure 2.2a	Plan of Coal Valley Tailings Impoundment	23
Figure 2.2b	Section A-A Through Coal Valley Tailings Impoundment	24
Figure 2.3a	Shallow Stratigraphy at Site 1	24
Figure 2.3b	Shallow Stratigraphy at Site 2	25
Figure 2.3c	Shallow Stratigraphy at Site 3	25
Figure 2.3d	Shallow Stratigraphy at Site 4	26
Figure 2.3e	Shallow Stratigraphy at Site 5	26
Figure 2.4	Modes of Bearing Capacity Failure (<i>after Vesic 1975</i>)	27
Figure 2.5	Plate Load Test Apparatus	27
Figure 2.6	Load vs Settlement and Pressure vs Relative Settlement Response at Site 1	28
Figure 2.7	Plate Load Test Nomenclature and Boundary Conditions	28
Figure 2.8	Bearing Pressures of Surface Tests Relative to Site 1	29
Figure 2.9	Relative Bearing Pressures of Rooted and Below Crust Tailings to Unrooted Surface Tailings	29
Figure 2.10	Influence of Evapotranspiration on Shear Strength and Moisture Content of Tailings (<i>data source: Johnson et al. 1991</i>)	30
<hr/>		
Figure 3.1	Grain Size Distribution of Coal Valley Waste Streams and Pond Fine Tailings	49
Figure 3.2a	Plan of Coal Valley Tailings Impoundment	50
Figure 3.2b	Section A-A Through Coal Valley Tailings Impoundment	50
Figure 3.3	Schematic of Dewatering of a Soil During Freezing (<i>after Konrad and Morgenstern 1983</i>)	51
Figure 3.4	Void Ratio <i>versus</i> Effective Stress Model of Freeze-Thaw	51
Figure 3.5	Idealized Seasonal Temperature Variation at Coal Valley	52

Figure 3.6	Schematic of Freezing Model (<i>modified after Martel 1988</i>)	52
Figure 3.7	Air Freezing Index <i>versus</i> Layer Thickness for Fine Coal Tailings	53
Figure 3.8	Schematic of Thawing Model (<i>modified after Martel 1988</i>)	53
Figure 3.9	Air Thawing Index <i>versus</i> Layer Thickness for Fine Coal Tailings	54
Figure 3.10	Layer Placement Optimization	54
Figure 3.11	Pond Shear Strength Profiles	55
Figure 3.12	Comparison of Theoretical and Actual Pond Shear Strength Profiles	55
Figure 3.13	Proposed Freeze-Thaw Structural Enhancement for Fine Tailings Region of Coal Valley Tailings Impoundment	56
<hr/>		
Figure 4.1	Plan and Section of Coal Valley Tailings Impoundment	65
Figure 4.2	Plan and Section of Suncor's NST Facility	66
Figure 4.3	Plate Load Test (PLT) Apparatus	66
Figure 4.4	Plate Load Test Results at Suncor NST Site 3b	67
Figure 4.5	Plate Load Test Results at Coal Valley's Tailings Impoundment - Site 1	67
Figure 4.6	Cone Penetration Test (CPT) Apparatus	68
Figure 4.7	Cone Penetration Test Results at Suncor NST Site 3b	68
Figure 4.8	Spectral Analysis of Surface Waves System	69
Figure 4.9	Shear Wave Velocity Profile at Suncor NST Site 3b	69
<hr/>		
Figure 5.1	Cross-Section Through Coal Valley Tailings Impoundment	78
Figure 5.2	Shear Strength Profiles from FVST and CPTU at Sites 1 through 4	78
Figure 5.3	Plate Load Test Results from 1991 and 1994 at Sites 1, 2, and 4	79
Figure 5.4	Fibre Reinforcement Model for Inclined Fibres	79
Figure 5.5	Theoretical Increase in Shear Strength from Roots at Site 1	80
<hr/>		
Figure 6.1	Location Map of Coal Valley Mine	100
Figure 6.2	Coal Valley Waste Streams	101
Figure 6.3	Plan and Section of Coal Valley Tailings Impoundment	101
Figure 6.4	Shallow Stratigraphy at Site 2	102
Figure 6.5	Plate Load Test Apparatus	102

Figure 6.6	Plate Load Test Boundary Conditions and Nomenclature	103
Figure 6.7	Selective 1991 Plate Load Tests at Site 2	103
Figure 6.8	Summary of 1991 and 1994 Plate Load Tests at Sites 1 Through 4	104
Figure 6.9	Potential Matric Suctions and Associated Shear Strengths in the Unsaturated Zone	105
Figure 6.10	Typical Evaporation Curve for Sand (<i>modified from Wilson et al. 1994</i> ;	105
Figure 6.11	Laboratory and Model Evaporation, Transpiration and Evapotranspiration Fluxes (<i>modified from Tratch et al. 1995</i>)	106
Figure 6.12	Influence of Evapotranspiration on Shear Strength and Moisture Content of Tailings (<i>data source: Johnson et al. 1991</i>)	106
Figure 6.13	Fibre Reinforcing Models for Inclined Fibres	107
Figure 6.14	Theoretical Increase in Shear Strength from Vegetative Root Systems	107
Figure 6.15	Bearing Capacity Results at Site 1 with Theoretical Increase Resulting from Root Reinforcement	108
<hr/>		
Figure 7.1	Plan and Section of Coal Valley Tailings Impoundment	123
Figure 7.2	Key Natural Enhancement Processes For Dry Landscape Reclamation of Tailings	123
Figure 7.3	Theoretical and Actual Shear Strength Profiles in Pond	124
Figure 7.4	1991 Plate Load Test Results at Site 2 and Site 4	124
Figure 7.5	Fibre Reinforcing Model for Inclined Fibres	125
Figure 7.6	Bearing Capacity Results at Site 1 with Theoretical Increase Resulting from Root Reinforcement	125
<hr/>		
Figure A1	1995 Grain Size Distributions Along Coal Valley Tailings Beach - Site 1	150
Figure A2	1995 Grain Size Distributions Along Coal Valley Tailings Beach - Site 2	150
Figure A3	1995 Grain Size Distributions Along Coal Valley Tailings Beach - Site 3	151
Figure A4	1995 Grain Size Distributions Along Coal Valley Tailings Beach - Site 4	151
Figure A5	Grain Size Distributions Within Coal Valley Tailings Pond	152
Figure A6	Grain Size Distributions of Coal Valley Wastes Streams and Constructed Pond Average	152
Figure A7	1994 Grain Size Distributions Within Suncor NST Cell 3	153
Figure A8	1994 Grain Size Distributions Within Suncor NST Cell 4	153
Figure A9	1994 Grain Size Distributions Within Suncor NST Cell 5	154

Figure A10	Solids Contents Within Coal Valley Pond - Site 1	154
Figure A11	Solids Contents Within Coal Valley Pond - Site 2	155
Figure A12	Solids Contents Within Coal Valley Pond - Site 3	155
Figure A13	1994 Moisture Contents Within Suncor NST Cells	156
Figure A14	1994 Solids Contents Within Suncor NST Cell	156
Figure A15	1991 Field Vane Shear Results Along Coal Valley Tailings Beach	157
Figure A16	1994 Field Vane Shear Results Along Coal Valley Tailings Beach	157
Figure A17	1995 Field Vane Shear Results Along Coal Valley Tailings Beach	158
Figure A18	1989 (Nov) Field Vane Shear Results Within Coal Valley Tailings Pond	158
Figure A19	1990 (Mar) Field Vane Shear Results Within Coal Valley Tailings Pond	159
Figure A20	1990 (Nov) Field Vane Shear Results Within Coal Valley Tailings Pond	159
Figure A21	1991 (Mar) Field Vane Shear Results Within Coal Valley Tailings Pond	160
Figure A22	1993 (Feb) Field Vane Shear Results Within Coal Valley Tailings Pond	160
Figure A23	1994 (Feb) Field Vane Shear Results Within Coal Valley Tailings Pond	161
Figure A24	1995 (Feb) Field Vane Shear Results Within Coal Valley Tailings Pond	161
Figure A25	1996 (Feb) Field Vane Shear Results Within Coal Valley Tailings Pond	162
Figure A26	Average Field Vane Shear Results Within Coal Valley Tailings Pond	162
Figure A27	1994 Field Vane Shear Results Within Suncor NST Cells	163

Figure B1	1991 PLT Results Along Coal Valley Tailings Beach - Site 1	170
Figure B2	1991 PLT Results Along Coal Valley Tailings Beach - Site 2	171
Figure B3	1991 PLT Results Along Coal Valley Tailings Beach - Site 3	172
Figure B4	1991 PLT Results Along Coal Valley Tailings Beach - Site 4	173
Figure B5	1991 PLT Results Along Coal Valley Tailings Beach - Site 5	174
Figure B6	1994 PLT Results Along Coal Valley Tailings Beach - Site 1	175
Figure B7	1994 PLT Results Along Coal Valley Tailings Beach - Site 2	176
Figure B8	1994 PLT Results Along Coal Valley Tailings Beach - Site 4	177
Figure B9	1994 PLT Results Within Suncor NST Cell 3	178
Figure B10	1994 PLT Results Within Suncor NST Cell 4	179
Figure B11	Shear Modulus Relationships from 1991 PLT Results Along Coal Valley Tailings Beach - Site 1	180

Figure B12	Shear Modulus Relationships from 1991 PLT Results Along Coal Valley Tailings Beach - Site 2	180
Figure B13	Shear Modulus Relationships from 1991 PLT Results Along Coal Valley Tailings Beach - Site 3	181
Figure B14	Shear Modulus Relationships from 1991 PLT Results Along Coal Valley Tailings Beach - Site 4	181
Figure B15	Shear Modulus Relationships from 1991 PLT Results Along Coal Valley Tailings Beach - Site 5	182
Figure B16	Shear Modulus Relationships from 1994 PLT Results Along Coal Valley Tailings Beach - Site 1	182
Figure B17	Shear Modulus Relationships from 1994 PLT Results Along Coal Valley Tailings Beach - Site 2	183
Figure B18	Shear Modulus Relationships from 1994 PLT Results Along Coal Valley Tailings Beach - Site 4	183
Figure B19	Shear Modulus Relationships from 1994 PLT Results Within Suncor NST Cell 3	184
Figure B20	Shear Modulus Relationships from 1994 PLT Results Within Suncor NST Cell 4	184
Figure B21	Summary of 1991 and 1994 Plate Load Test Results Along Coal Valley Tailings Beach - Sites 1 to 4	185
Figure B22	Bearing Pressure Increase From 1991 to 1994 Along Coal Valley Tailings Beach	186
Figure B23	Percent Bearing Pressure Increase From 1991 to 1994 Along Coal Valley Tailings Beach	186
Figure B24	Variation in Ultimate Bearing Capacity with Variation in Matric Suction (modified from Fredlund and Rahardjo, 1993)	187
<hr/>		
Figure C1	CPT Profiles - Coal Valley Tailings Beach - Site 1	203
Figure C2	Normalized CPT Data Presented on Soil Behavior Type Charts - Coal Valley Tailings Beach - Site 1	204
Figure C3	Normalized CPT Data Profiles - Coal Valley Tailings Beach - Site 1	205
Figure C4	CPT Profiles - Coal Valley Tailings Beach - Site 2	206
Figure C5	Normalized CPT Data Presented on Soil Behavior Type Charts - Coal Valley Tailings Beach - Site 2	207
Figure C6	Normalized CPT Data Profiles - Coal Valley Tailings Beach - Site 2	208
Figure C7	CPT Profiles - Coal Valley Tailings Beach - Site 3	209

Figure C8	Normalized CPT Data Presented on Soil Behavior Type Charts - Coal Valley Tailings Beach - Site 3	210
Figure C9	Normalized CPT Data Profiles - Coal Valley Tailings Beach - Site 3	211
Figure C10	CPT Profiles - Coal Valley Tailings Beach - Site 4	212
Figure C11	Normalized CPT Data Presented on Soil Behavior Type Charts - Coal Valley Tailings Beach - Site 4	213
Figure C12	Normalized CPT Data Profiles - Coal Valley Tailings Beach - Site 4	214
Figure C13	Estimated PWP (PWP 1) Profiles in Suncor NST Cells 3 and 4	215
Figure C14	Estimated PWP (PWP 2) Profiles in Suncor NST Cells 3 and 4	215
Figure C15	CPT Profiles - Suncor NST Cells - Site 3a	216
Figure C16	Normalized CPT Data Presented on Soil Behavior Type Charts - Suncor NST Cells - Site 3a	217
Figure C17	Normalized CPT Data Profiles - Suncor NST Cells - Site 3a	218
Figure C18	CPT Profiles - Suncor NST Cells - Site 3b	219
Figure C19	Normalized CPT Data Presented on Soil Behavior Type Charts - Suncor NST Cells - Site 3b	220
Figure C20	Normalized CPT Data Profiles - Suncor NST Cells - Site 3b	221
Figure C21	CPT Profiles - Suncor NST Cells - Site 4a	222
Figure C22	Normalized CPT Data Presented on Soil Behavior Type Charts - Suncor NST Cells - Site 4a	223
Figure C23	Normalized CPT Data Profiles - Suncor NST Cells - Site 4a	224
Figure C24	CPT Profiles - Suncor NST Cells - Site 4b	225
Figure C25	Normalized CPT Data Presented on Soil Behavior Type Charts - Suncor NST Cells - Site 4b	226
Figure C26	Normalized CPT Data Profiles - Suncor NST Cells - Site 4b	227
Figure C27	Excess Pore Pressure Dissipation Against Modified Time Factor (T^*) (<i>modified from Teh and Houlsby, 1991</i>)	228
Figure C28	Selected Pore Pressure Dissipation Results From Coal Valley Tailings Beach	228
Figure C29	Comparison Between Laboratory and Field Coefficient of Consolidation Values of Suncor NST	229
<hr/>		
Figure D1	SASW Field and Theoretical Dispersion Curves - Coal Valley Tailings Beach - Site 1	237
Figure D2	SASW Estimated Shear Wave Velocity Profile - Coal Valley Tailings Beach - Site 1	237

Figure D3	SASW Field and Theoretical Dispersion Curves - Coal Valley Tailings Beach - Site 2	238
Figure D4	SASW Estimated Shear Wave Velocity Profile - Coal Valley Tailings Beach - Site 2	238
Figure D5	SASW Field and Theoretical Dispersion Curves - Coal Valley Tailings Beach - Site 3	239
Figure D6	SASW Estimated Shear Wave Velocity Profiles - Coal Valley Tailings Beach - Site 3	239
Figure D7	SASW Field and Theoretical Dispersion Curves - Coal Valley Tailings Beach - Site 4	240
Figure D8	SASW Estimated Shear Wave Velocity Profile - Coal Valley Tailings Beach - Site 4	240
Figure D9	SASW Field and Theoretical Dispersion Curves - Suncor NST Cell 3a	241
Figure D10	SASW Estimated Shear Wave Velocity Profiles - Suncor NST Cell 3a	241
Figure D11	SASW Field and Theoretical Dispersion Curves - Suncor NST Cell 3b	242
Figure D12	SASW Estimated Shear Wave Velocity Profiles - Suncor NST Cell 3b	242
Figure D13	SASW Field and Theoretical Dispersion Curves - Suncor NST Cell 4a	243
Figure D14	SASW Estimated Shear Wave Velocity Profiles - Suncor NST Cell 4a	243
Figure D15	SASW Field and Theoretical Dispersion Curves - Suncor NST Cell 4b	244
Figure D16	SASW Estimated Shear Wave Velocity Profiles - Suncor NST Cell 4b	244
Figure D17	Small Strain Shear Modulus Profiles Along Coal Valley Tailings Beach	245
Figure D18	Small Strain Shear Modulus Profiles Within Suncor NST Cells (With Crust)	245
Figure D19	Small Strain Shear Modulus Profiles Within Suncor NST Cells (Without Crust)	246
Figure D20	Schematic of Typical Shear Modulus Attenuation Curve (<i>modified from Viggiani and Atkinson 1995</i>)	246
<hr/>		
Figure E1	Fibre Reinforcing Model for Perpendicular and Inclined Fibres (<i>modified from Gray and Al-Refeai, 1986</i>)	261
Figure E2	Fibre Reinforcing Model for Inclined Fibres	261
Figure E3	Root Area Ratio (RAR) Profiles Along Coal Valley Tailings Beach	262
Figure E4	Conceptual Model of Shear Zone Development Beneath a PLT on Compressible Root Reinforced Soil	262
Figure E5	Modes of Bearing Capacity Failure: (a) General Shear, (b) Local Shear, (c) Punching Shear (<i>from Craig, 1983</i>)	263

Figure E6	Effect of Shear Zone Displacement (k) and Initial Fibre Inclination (i) on Mobilized Strength Ratio ($\Delta S_R/t_r$)	263
Figure E7	Theoretical Increase in Shear Strenght From Vegetative Root Systems - Coal Valley Tailings Beach - Site 1	264
Figure E8	Theoretical Increase in Shear Strenght From Vegetative Root Systems - Coal Valley Tailings Beach - Site 2	264
Figure E9	Theoretical Increase in Shear Strenght From Vegetative Root Systems - Coal Valley Tailings Beach - Site 3	265
Figure E10	Theoretical Increase in Shear Strenght From Vegetative Root Systems - Coal Valley Tailings Beach - Site 4	265
Figure E11	Theoretical Increase in Bearing Capacity From Vegetative Root Systems - Coal Valley Tailings Beach - Site 1	266
Figure E12	Theoretical Increrse in Bearing Capacity From Vegetative Root Systems - Coal Valley Tailings Beach - Site 2	266
Figure E13	Theoretical Increase in Bearing Capacity From Vegetative Root Systems - Coal Valley Tailings Beach - Site 3	267
Figure E14	Theoretical Increase in Bearing Capacity From Vegetative Root Systems - Coal Valley Tailings Beach - Site 4	267
Figure E15	Parametric Analysis of Theoretical Increase in Bearing Capacity From Vegetative Root Systems - Coal Valley Tailings Beach - Site 1	268
Figure E16	Parametric Analysis of Theoretical Increase in Bearing Capacity From Vegetative Root Systems - Coa. Valley Tailings Beach - Site 2	269
Figure E17	Parametric Analysis of Theoretical Increase in Bearing Capacity From Vegetative Root Systems - Coal Valley Tailings Beach - Site 3	270
Figure E18	Parametric Analysis of Theoretical Increase in Bearing Capacity From Vegetative Root Systems - Coal Valley Tailings Beach - Site 4	271
<hr/>		
Figure F1	Proposed Soil Behavior Type Chart Based on Q_t and G_s/q_t (after Robertson <i>et al.</i> 1995)	287
Figure F2	Q_t versus G_s/q_t Behavior Chart for Coal Valley Tailings Beach - Site 1	288
Figure F3	Q_t versus G_s/q_t Behavior Chart for Coal Valley Tailings Beach - Site 2	288
Figure F4	Q_t versus G_s/q_t Behavior Chart for Coal Valley Tailings Beach - Site 3	289
Figure F5	Q_t versus G_s/q_t Behavior Chart for Coal Valley Tailings Beach - Site 4	289
Figure F6	Q_t versus G_s/q_t Behavior Chart for Suncor NST Cell 3a	290
Figure F7	Q_t versus G_s/q_t Behavior Chart for Suncor NST Cell 3b	290
Figure F8	Q_t versus G_s/q_t Behavior Chart for Suncor NST Cell 4a	291

Figure F9	Q_r versus G_r/q_r Behavior Chart for Suncor NST Cell 4b	291
Figure F10	Shear Wave Velocity Profiles from SASW Modelling and Predicted from CPT Soundings - Coal Valley Tailings Beach - Site 1	292
Figure F11	Shear Wave Velocity Profiles from SASW Modelling and Predicted from CPT Soundings - Coal Valley Tailings Beach - Site 2	292
Figure F12	Shear Wave Velocity Profiles from SASW Modelling and Predicted from CPT Soundings - Coal Valley Tailings Beach - Site 3	293
Figure F13	Shear Wave Velocity Profiles from SASW Modelling and Predicted from CPT Soundings - Coal Valley Tailings Beach - Site 4	293
Figure F14	Shear Strength Profiles from FVST and CPT Soundings Along Coal Valley Tailings Beach	294
Figure F15	Computed N_{kr} Cone Factors Based on Reference FVST Results Along Coal Valley Tailings Beach	294
Figure F16	Shear Strength Profiles from FVST and Predicted from CPT Soundings - Suncor NST Cell 3a	295
Figure F17	Shear Strength Profiles from FVST and Predicted from CPT Soundings - Suncor NST Cell 3b	295
Figure F18	Shear Strength Profiles from FVST and Predicted from CPT Soundings - Suncor NST Cell 4a	296
Figure F19	Shear Strength Profiles from FVST and Predicted from CPT Soundings - Suncor NST Cell 4b	296
Figure F20	Cone Factors Based on Plate Load Tests Conducted in Clays with a Range in Scale of Fabric Feature (Discontinuities) (<i>modified from Powell and Quarterman 1988</i>)	297
Figure F21	Cone Factors Computed from Plate Load Tests Conducted on Root Reinforced Soils Along Coal Valley Tailings Beach	297

List of Symbols

(d_1-d_2)	distance between receivers
$(\sigma-u_a)$	net normal stress
(u_a-u_w)	matric suction
a	cone radius
a	net area ratio
α	solar energy absorptance ratio
A	total cross-sectional area of shear zone
A_f	Skempton's pore pressure parameter at failure
A_p	area of plate
A_R	cross-sectional area of fibres (roots)
$b_{c,q,\gamma}$	bearing capacity factors for tilting footing
B_q	pore pressure ratio
c', c	effective cohesion
C_c	compression index
c_h	coefficient of consolidation (horizontal drainage)
c_v	coefficient of consolidation (vertical drainage)
d	root diameter
D	vane diameter
D_{10}, D_{50}, D_{90}	grain size corresponding to 10%, 50%, 90% finer than
$d_{c,q,\gamma}$	bearing capacity factors for footing depth
D_p	depth of plate
ΔQ	applied pressure to plate
Δq_f	change in bearing capacity
ΔQ_{roots}	theoretical increase in bearing capacity from root reinforcement
D_r	relative density
ΔS_R	theoretical shear strength increase from fibres (roots)
ΔS_u	change in "total stress" shear strength of unsaturated soils
Δu	excess pore pressure
Δu_i	initial excess pore pressure
E	elastic modulus
ε	thickness of frozen fine tails
$e, e_o, e_A, e_B, e'_B, e_C$	void ratio
$E_{o,d,ud}$	small strain drained or undrained elastic modulus
ϕ	angle of internal friction
f	frequency
$F\%$	percent fines
ϕ'	internal angle of friction with respect to $(\sigma-u_a)$

$\phi(f)$	phase velocity
ϕ^h	internal angle of friction with respect to $(u_s - u_w)$
F_R	normalized friction ratio
f_s	friction sleeve resistance
G	Shear Modulus
$g_{c,q,\gamma}$	bearing capacity factors for sloping ground
G_o, G_{max}	small strain shear modulus
$grad T_f$	temperature gradient within frozen fringe
H	vane height
h_c	convective heat transfer coefficient
i	initial orientation angle of fibre with respect to shear surface
I	insolation (rate of solar radiation)
$i_{c,q,\gamma}$	bearing capacity factor for load inclination
I_r	rigidity index (G/s_u)
k	shear distortion ratio
K_{fs}	thermal conductivity of frozen fine tails
kg, kPa, kN	kilogram, kiloPascal, kiloNewton
K_{ss}	thermal conductivity of settled fine tails
L	latent heat of fusion of fine tails
λ	slope of steady state line
L, L_p	load on plate
L_L	liquid limit
L_{min}	minimum length of root to avoid slippage
λ_R	rayleigh surface wavelength
mm, cm, m, m^3	millimeter, centimeter, meter, cubic meters
N_c	bearing capacity factor
$v_{d,ud}$	drained and undrained Poisson's ratio
$N_{\Delta u}$	cone pore pressure factor
N_{kt}	empirical or semi-empirical cone factor
N_q	bearing capacity factor
P_a	atmospheric pressure
PI	plasticity index
P_L	plastic limit
P_u, P_w	pore fluid pressures within frozen fringe
Q	bearing pressure
θ	thickness of frozen fine tails
q_c	initial cone resistance (uncorrected)
q_{c1}	normalized cone resistance
q_{fo}	initial ultimate bearing capacity
Q_{max}	maximum bearing pressure
Q_t	normalized cone resistance
q_t	total cone penetration resistance
ρ	bulk density
ρ	radial vector to point within plastic zone
r	radius of cylindrical cavity
ρ_f	density of frozen fine tails
R_f	friction ratio (f/q_t)

S	settlement
$\sigma'_{A,B}$	effective normal stress
σ'_c	effective consolidation pressure
σ'_{vo}, σ'_v	total vertical effective stress
s, or sec	second
$\sigma, \sigma_{A,B}$	total normal stress
σ_1	major principal stress
σ_3	minor principal stress
$S_{c,q,\gamma}$	bearing capacity factor for footing shape
σ_{crit}	critical confining stress
σ_{ho}	horizontal total stress
σ_{oct}	octahedral stress
SP	segregation potential
SP_o	segregation potential at no applied load
σ_R	tensile stress developed in fibres (roots)
S_u, s_u	undrained shear strength
S_{uo}	"total stress" shear strength of unsaturated soils
σ_{vo}	total vertical stress
t	time
τ	transmittance factor
T	vane torque
t(f)	travel time
T^*	modified time factor
t_{50}	time for 50% dissipation of initial excess pore pressure
T_{ac}	ambient air temperature
T_{at}	ambient air temperature
τ_B	limiting bond stress between soil and root
T_f	freezing temperature of fine tails
τ_f	shear strength of unsaturated soils
t_f	time to freeze
t_R	mobilized tensile strength per unit area of soil
t_{th}	time to thaw
u	penetration pore water pressure
u_a	pore air pressure
u_w	pore water pressure
v	rate of water migration to ice lense
V	total volume of roots and soil
V_R	rayleigh wave velocity
V_R	volume of roots
V_s	shear wave velocity
V_{sI}	normalized shear wave velocity
x	horizontal shear zone displacement
Y	depth of thawed fine tails
ψ	net fibre orientation angle
Y	$q_{cl} - V_{sI}$ correlation parameter
z	shear zone thickness

List of Abbreviations

AE	Actual Evaporation Flux
AFI	Air Freezing Index
ATI	Air Thawing Index
bts	Below Tailings Surface
CPT	Cone Penetration Test
CPTU	Cone Penetration Test with Pore Pressure Measurements (CPT)
EPA	Environmental Protection Agency
FVST	Field Vane Shear Test
LAI	Leaf Area Index
NST	Nonsegregating Tailings
PE	Potential Evaporation Flux
PLT	Plate Load Test
PPD	Pore Pressure Dissipation
RAR	Root Area Ratio (A_R/A)
RS	Relative Settlement (s/D_p)
SASW	Spectral Analysis of Surface Waves
ts	Tailings Surface
US	United States
vtS	Vegetated Tailings Surface

Chapter 1

Introduction

1.1. INTRODUCTION

Tailings refer to any solid form of mine or mill waste, including rock-sized stripping wastes, underground mine muck, and finely ground mill wastes. Staggering quantities of tailings are generated world wide in all facets of the mining industry including the hard rock, coal, potash and oil sands industries. Brumund (1988) reported US EPA data which states annual mine waste generation rates in the order of 1.4 billion tons. These volumes are in addition to the estimated 31 billion tonnes of mine wastes and 13 billion tonnes of tailings generated in the U.S. between 1910 and 1981 (Testra 1994). Mine wastes generated in Canada support these volumes. The oil sands operations in northern Alberta, through annual production of 85 million barrels of high quality synthetic crude (Sheeran 1993) generate 160 million m³ of fluid tailings with a solids content of 40 to 60 % by mass (Suthaker 1995). The Highland Valley Copper mine located in central British Columbia, producing an estimated 160,000 tonnes of copper and 2300 tonnes of molybdenum per annum, generate about 113 million m³ of slurried tailings (Hanson 1992, Dawson 1994).

The slurried form of processed mine wastes resulting from the beneficiation of ore is conventionally hydraulically transported and deposited in surface impoundments. Considering the diversity of ore deposits, and processing and disposal methods, a well established distinction is forwarded regarding the behavior of the slurried tailings streams. These streams may be

broadly classified as segregating and nonsegregating. Segregation refers to the tendency of the solid fraction (or part of it) to settle and create a concentration gradient within the mass, whereas nonsegregating behavior exhibits a uniform distribution of solids throughout the mass. The demands of hydraulic transport and the geotechnical and chemical composition of slurried tailings streams, often prescribe segregating behavior. Hydraulic sorting often transpires following deposition of segregating mixes resulting in distinct regions within the storage facility. Although hydraulic sorting may be advantageous from a containment and stability viewpoint, regional material contrasts within the storage facility may exasperate dry landscape reclamation concerns. Such reclamation concerns have positioned the oil sand industry to evaluate the properties of nonsegregating tailings (NST)¹ to capture/contain, with the aid of coagulating agents, a greater proportion of the mature fine tailings produced from their segregating tailings streams.

Both the heterogeneous or “homogeneous” tailings deposits eventually require reclamation initiatives to achieve the lease-closure landscape requirements. Depending on the regional landscape conditions, the lease-closure landscape requirements may involve a marriage of wet and dry landscape reclamation philosophies, which require geotechnical and environmental (geo-environmental) considerations prior to activation. The geo-environmental concerns include achieving a lease-closure landscape which is self sustaining, geotechnically stable, maintenance free, and exists harmoniously with the regional landscape. In addition to these engineering issues, the reclamation philosophies must also satisfy economical constraints. Often promotion and engineering of mechanisms to satisfy the geo-environmental concerns are also economically practicable. In the case of dry landscape reclamation of fine processed mine wastes which exhibit limited strength and surface stability, such mechanisms include the adoption and engineering of natural processes to enhance strength and stability.

Promotion and optimization of climatic dependent structural enhancement processes is viewed as achieving environmental and economical harmony. Locations in Australia (and other arid climates) boast evaporation fluxes in excess of 4 m per annum (Swarbrick 1992). Evaporative dewatering mechanism with thin layered disposal of Australian coal tailings to achieve volume reduction and strength gain is encouraged (Williams and Morris, 1990).

¹ “NST” has recently been revised to “CT” - *Consolidated Tailings* (Suncor Inc.), *Composite Tailings* (Syncrude Canada Ltd.)

Climatic sponsored structural enhancement processes have been recognized in Canada as well. Freezing of saturated high void ratio fine tailings during winter months, followed by spring and summer thaw, encourage structural enhancement including consolidation/volume reduction and strength gain. Optimization avenues investigated or currently under investigation include chemical addition, layer thickness control, drainage measures, and waste stream combination. Evaporation and freeze-thaw processes not only help address future reclamation concerns, but through volume reduction processes release land for continued tailings storage, and potentially reduce external process water demands through effective capture of the freeze-thaw release water.

Evaporation and freeze-thaw consolidation represent two of the key natural processes explored in this thesis which enhance the surface stability and dry landscape reclamation of fine processed mine wastes. An additional mechanism discussed herein includes dewatering through evapotranspiration, and the reinforcing effects of vegetation and respective root systems. These three key processes are highlighted as a result of the detailed site investigation activities undertaken at the Coal Valley tailings impoundment, located 200 km west and 90 km south of Edmonton, Alberta, and the Suncor Nonsegregating Tailings (NST) Cells, developed on the Suncor Inc. lease located approximately 500 km north of Edmonton.

Significant contrasts with respect to these deposits, in addition to their geological origin and geotechnical properties are forwarded. Firstly, the Coal Valley tailings facility represents the product of a segregating material. Hydraulic sorting dominated the deposition and extreme heterogeneity and regional contrasts exists within the impoundment. Secondly, the horizontal and vertical dimensional limits of the Coal Valley impoundment are one to two orders of magnitude greater than those of the Suncor NST Cells. Furthermore, the age and resulting reclamation maturity of the Coal Valley tailings deposit is several years advanced than that of the NST Cells.

Highlighting the natural processes which enhance the bearing capacity and surface stability of these deposits is one facet of the research initiative. The development of lightweight geotechnical equipment for efficient and detailed site characterization of the deposits was critical. Three systems which required only human effort for mobilization at the weak tailing sites included a

Plate Load Test (PLT) apparatus, a Cone Penetration Test (CPT) apparatus, and a Spectral Analysis of Surface Waves (SASW) system.

The relatively unprecedented nature of the application of these site investigation techniques on the very weak and compressible soils resulted in the exploration and resolution of a variety of issues. These issues include site investigation problems, detailed interpretation of the results, confirmation of existing correlations, and establishment of unique correlations and findings. The analysis conducted in the succeeding chapters and appendices will enhance our understanding of the performance of these deposits, and advance the state-of-art of investigation and analysis.

1.2. RESEARCH BACKGROUND AND OBJECTIVES

This thesis topic originated initially in 1991 as an M.Sc. research project. The Coal Valley mine owned by Luscar Sterco (1977) was proceeding with reclamation activities on their tailings facility. Due to operation constraints, previous tailings reclamation activities at Coal Valley included placement of significant thicknesses of capping material, in excess of 6 m, to satisfy the minimum 1.3 m “initially” required in their Development and Reclamation Approval. The short haul distance between the mining and tailings regions afforded these thicknesses in the past, however, mine development towards the lease boundaries and resulting extensive haul distances economically discourages this practice today. Maintaining environmental commitments, Coal Valley pursued an alternative reclamation/research approach to achieve a dry landscape condition commensurate with the desired equivalent pre-mining land capability. The reclamation research initiative by Coal Valley included selective thin capping, seeding, planting and fertilization practices on the retired tailings impoundment which had reached capacity in 1989.

Taking advantage of this reclamation program, the M.Sc. research scope included the limited geotechnical investigations of the Coal Valley tailings impoundment, followed by a review of the natural surface processes which were enhancing the shear strength, bearing capacity and surface stability of this deposit. Chapters 2 and 3 represent the early findings of this research initiative. In 1993, the research scope was expanded to a Ph.D. level. The resulting objectives of this

subsequent staged research initiative, which were discussed briefly above, are summarized as follows:

- Development/modification of geotechnical site investigation equipment which is light weight requiring only human efforts for mobilization, and can be employed at tailings sites exhibiting limited surface stability.
- Conduct chronological performance monitoring of the reclamation activities at the Coal Valley tailings impoundment.
- Expand the scope of the tailings deposits investigated to include a contrasting ore deposit, tailings product, and tailings deposition facility. The Suncor NST Cell deposits were selected to satisfy this requirement.
- Highlight the contribution of natural surface processes to enhanced dry landscape reclamation bearing capacity and surface stability of tailings.

As a result of the unique characteristics of the tailings deposits investigated and the complimentary nature of the geotechnical site investigation tools, additional assets beyond the initial research scope were achieved, including:

- Development of a “preliminary” model to predict the increase in shear strength and bearing capacity offered by vegetative root systems on compressible tailings.
- Establishment/confirmation of a variety of cone factors to predict field vane shear strengths, and bearing capacity of root reinforced soils.

The results of this expanded scope are included in Chapters 4 through 8, with detailed field results, discussion, and analysis provided in Appendices A through F.

1.3. ORGANIZATION OF THESIS

This thesis is organized into a series of six fundamental chapters (Chapters 2 through 7), with the final chapter providing a selective summary and conclusions. Detailed successive appendices provide investigation results, analysis, and discussion. Each of the chapters has either been published or is awaiting publication in conferences proceedings and/or journals. The chapters have been organized in a relative chronological fashion with each being unique in focus. Some similarities are observed within the later chapters and the reader will observe the successively enhanced analysis sponsored through extended research.

Chapter 2 introduces the Coal Valley Tailings deposit highlighting the various regions within the facility, and the heterogeneous nature of the deposit at the various sites investigated along the beach portion of the impoundment. This chapter presents the results of the plate load tests conducted in 1991, and introduces the processes which have enhanced the surficial shear strength and bearing capacity of the tailings since initially undergoing reclamation activities in 1989.

To complement the investigations along the beach portion of the Coal Valley Tailings impoundment, *Chapter 3* introduces the process of freeze-thaw which is found to consolidate and enhance the shear strength of fine grained high void ratio saturated slurries. The contribution of freeze-thaw to the gradual strength gain of the saturated silt and clay sized particles within the pond portion of the impoundment is presented.

As the scope of the research was expanded from an M.Sc. to a Ph.D. level, so too did the methodologies of characterization. A key problem inherent in characterization of weak tailings facilities is the development of suitable methods to efficiently investigate the geotechnical properties of these materials. *Chapter 4* presents the equipment (PLT, CPT, and SASW) developed/modified which was employed to investigate tailings deposits including the Coal Valley and Suncor NST facilities, which exhibited limited strength and surface stability. Provided the tailings can support human traffic, the modified equipment transcends the requirement of placing access ramps for utilization of traditional truck-mounted equipment.

Chapter 5 presents results of some of the latest investigations, and introduces the correlation of the CPT with the Field Vane Shear test results. A theoretical model which predicts the increase in shear strength of soils as a result of root reinforcement is introduced.

Chapter 6 represents results of the extended chronological site investigation activities at Coal Valley, including a detailed summary and comparison of the 1991 and 1994 PLT's. The topics of evaporation, evapotranspiration and fibre reinforcement of vegetative root systems are discussed in greater detail than that found in Chapter 2. The theoretical model predicting the increase in shear strength of root reinforced soils is extended to predict the increase in bearing capacity of root reinforced compressible tailings.

Chapter 7 includes an update of the investigations conducted within the pond portion of the Coal Valley tailings impoundment previously presented in Chapter 3. The main contribution of this chapter is the presentation/summary of the key processes which may be employed to geotechnically enhance the surface stability of weak tailings deposits with the goal of attaining a suitable dry landscape reclamation condition.

Prior to reading the final concluding chapters, the reader is encouraged to review the issues which are presented in Appendices A through F. **Appendix A** summarizes the index tests and field vane shear tests which were conducted at the two tailings facilities investigated in this research. **Appendix B** includes a complete summary of the plate load test data at these sites. Due to the very weak nature and otherwise unique nature of the tailings deposits investigated, a variety of interesting issues surfaced during analysis of the CPT soundings. These issues are discussed in detail in **Appendix C**.

The SASW technique was employed to determine the shear wave velocity profiles at the tailings sites with the results presented in **Appendix D**. **Appendix E** provides a limited literature review and sequentially outlines the steps selected to predict the increase in shear strength and bearing capacity offered by vegetative root systems. The unprecedented nature of these investigations necessitated the need for confirmation of field results through consideration of published correlations. The detailed and complimentary nature of these field investigations also provide

insight into new correlations which enhance prediction of soil behavior. These correlations, comparisons and calculations are included in *Appendix F*.

Chapter 8 subsequently includes a brief discussion of the methods, models, and investigation techniques which may help guide the utilization of natural surface enhancement processes to achieve a dry landscape.

Based on the previous chapter and appendix findings, *Chapter 9*, provides a synopsis of the key topics discussed, conclusions gathered, and provides recommendations for future research pursuits.

1.4. REFERENCES

- Brumund, W.F., 1988. Waste Management - An Overview of USA Activity from a Geotechnical Perspective. Symposium on Solid Waste Management - Landfill Design: From Concept to Completion. Southern Ontario Section of the Canadian Geotechnical Society, 34 pgs.
- Dawson, R.F., 1994. Mine Waste Geotechnics. Unpublished Ph.D. Thesis, Department of Civil Engineering, The University of Alberta, 239 pgs.
- Hanson, P., 1992. A Temporary Use of the Land at Highland Valley Copper. Canadian Institute of Mining and Metallurgical (CIM) Bulletin, 85(962):71-72.
- Küpper, A.M.A.G., 1991. Design of Hydraulic Fill. Unpublished Ph.D. Thesis, Department of Civil Engineering, The University of Alberta, 525 pgs.
- Liu, Y., Caughill, D., Scott, J.D., and Burns, R., 1994. Consolidation of Suncor Non Segregating Tailings. 47th Canadian Geotechnical Conference, September 21-23, 1994. Halifax, Nova Scotia, pgs 504-513.
- Sego, D.C., Burns, R., Dawson, R., Dereniwski, T., Johnson, R., and Lowe, L., 1993. Dewatering of Fine Tails Utilizing Freeze-Thaw Processes. Fine Tailings Symposium, Proceedings of the Oil Sands - Our Petroleum Future, April 4-7, 1993, Edmonton, Alberta, Paper F17, 25 pgs.
- Sheeran, D.D., 1993. An Improved Understanding of Fine Tailings Structure and Behavior. Fine Tailings Symposium, Proceedings of the Oil Sands - Our Petroleum Future, April 4-7, 1993, Edmonton, Alberta, Paper F1, 11 pgs.

- Suthaker, N.N., 1995. Geotechniques of Oil Sand Fine Tailings. Unpublished Ph.D. Thesis, Department of Civil Engineering, The University of Alberta, 223 pgs.**
- Swarbrick, G.E., 1992. Transient Unsaturated Consolidation In Desiccated Mine Tailings. Unpublished Ph.D. Thesis, School of Civil Engineering, New South Wales, Australia.**
- Testa, S.M., 1994. Geological Aspects of Hazardous Waste Management. CRC Press, Inc., Boca Raton, Florida, 537 pgs.**
- Williams, D.J., and Morris, P.H., 1990. Engineering Properties of Australian Coal Mine Tailings Relevant to their Disposal and Rehabilitation. Proceedings of the Third International Conference on Reclamation, Treatment, and Utilization of Coal Mining Wastes, Glasgow, United Kingdom, pp 49-56.**

Chapter 2

Influence Of Natural Surface Processes On Reclamation Of The Coal Valley Tailings Impoundment¹

2.1. INTRODUCTION

The Coal Valley mine, owned and operated by Luscar Sterco (1977) Ltd., is located approximately 96 km south of Edson, Alberta, in the foothills of the Rocky Mountains. Yearly production of 1.8 million clean tons of coal results in two waste streams, a coarse dry crushed rock and a fine saturated slurried tailings (Figure 2.1). During one stage of mineral extraction and waste stream deposition, an 18.2 hectare impervious impoundment was constructed to contain the fine saturated slurried tailings. This impoundment reached its capacity in 1989 and has been undergoing reclamation.

During deposition of the slurried tailings stream into the impoundment, coarser particles settled more readily while the finer particles were transported to the pond. This segregation resulted in three distinct zones which potentially require different reclamation schemes. These zones are the coarse tailings zone located near the previous discharge point, the fine tail zone located at the

¹ Published Paper:

Stahl, R.P., and Sego, D.C., 1992. Influence of Natural Surface Processes on Reclamation of the Coal Valley Tailings Impoundment. Second International Conference on Environmental Issues and Management of Waste in Energy and Mineral Production, Calgary, Alberta, September 1-4, pgs. 389-400.

pond, and an intermediate zone located between the two extremes. Each zone represents unique problems and challenges for reclamation.

Previous reclamation practices at the Coal Valley mine have included capping the coarser tailings with 3 to 6 m of waste rock to satisfy operational requirements, although only 1.2 m was required by regulation. Greater capping thicknesses were required for softer, saturated fine tailings as the material squeezed under the loads imposed during placement of cap rock. Capping thicknesses in excess of 1.2 m directly affect production costs and thus profits at the mine.

This paper presents some of the natural processes which can assist during the reclamation of both coarse and intermediate tailings. These include freeze-thaw consolidation, desiccation drying, evapotranspiration, and fibre reinforcement of vegetative root systems. Incorporating natural processes during reclamation may lead to more efficient practices, and potentially reduce the short term and long term reclamation costs.

2.2. DEPOSITION HISTORY

A plan and section of the existing impoundment illustrating the approximate coarse and fine tailings zones is shown in Figure 2.2. The locations of the plate load tests sites, the various test boreholes, as well as the present soil capping locations are shown. The impoundment, which initially existed as a series of smaller interconnected cells, was filled with saturated tailings by single point discharge located at the northern end of the impoundment. This discharge location remained stationary during filling of the impoundment. The fine saturated tailings slurry, which entered the impoundment at approximately 35 % solids, had a grain size distribution as shown in Figure 2.1.

Following tailings discharge, many of the coarser particles settled readily from suspension while the remaining slurry was carried further along the beach. It is noted that tailings deposition is a dynamic process and the reader is referred to Kupper (1991) for a detailed description of its

complexity. In general, however, as distance from the discharge point increases, finer particles tend to settle out of suspension. The remaining fine silt and clay size particle are transported to the main decant pond and eventually settle under quiescent conditions while the decant water treated and released. Due to the location of the tailings discharge pipe and the geometry of the impoundment, small ponds housing fine silt and clay size particles formed along some of the edges of the perimeter dyke. These pond locations are variable and represent potentially weak, highly compressible areas. Nonetheless, most of the tailings were deposited in an above water tailings beach with the mean particle size decreasing with distance from the discharge point.

2.3. RECLAMATION OF COARSE TAILINGS

2.3.1. Shallow Stratigraphy

The shallow subsurface stratigraphy at each of the five plate load sites are shown in Figure 2.3. Site 1 is nearest the previous discharge point, approximately 98 m away, and Site 4 is located furthest away, approximately 302 m from the discharge point. Sites 1 through 3 may be described as interlayered silty sand and sandy silt with the occasional sand layer. Site 2, located approximately 162 m from the tailings discharge location, does not display increased fines (material passing the #200 sieve) within the stratigraphy compared to Site 1. However, Site 3 located 250 m from the discharge location, was characterized by a gradual increase in fines content of both the sandy and silty layers, as well as the absence of relatively clean sand layers.

Site 4 which is the test site located closest to the existing pond (Figure 2.2) shows a significant increase in fines content, with the profile described as sandy and clayey silt. A coarser silty sand layer is observed near the surface, however, the silt remains the dominant material.

Site 5 is located approximately 216 m from the discharge point, in the area of soil capping. Based on its location, its shallow stratigraphy would be expected to be a transition between Sites 3 and 4. Surprisingly, Site 5 is composed of uniform sandy and clayey silt layers with no coarse sand layers present. This profile supports the hypothesis that the pond at one time during the

depositional history had advanced along the southern end of the impoundment, or a small detached pond had occupied the location around Site 5.

2.3.2. Plate Load Tests

2.3.2.1. Theory

One of the early sets of bearing capacity equations intended for shallow foundations was proposed by Terzaghi in 1943. Extensions to Terzaghi's bearing capacity equations have been made over the years by Meyerhof, Hansen and Vesic among others (Bowles 1988, Vesic 1975). The most general bearing capacity equation reported by Hansen and Vesic, which is similar to Meyerhof's equation, is as follows:

$$q_{ult} = \underbrace{cN_c s_c d_c i_c g_c b_c}_{(a)} + \underbrace{qN_q s_q d_q i_q g_q b_q}_{(b)} + \underbrace{0.5BN_\gamma s_\gamma d_\gamma i_\gamma g_\gamma b_\gamma}_{(c)} \quad [2.1]$$

This general equation for the ultimate bearing capacity, q_{ult} has three contributing components. The first component (a) is termed the cohesion component and was developed from the theory of plasticity. The second component (b) is the surcharge component which compensates for any surcharge loading above the elevation of the base of the footing. The third component (c) is the self weight component of the material beneath the footing. This component is highly nonlinear and a function of the friction angle and is the dominant term for shallow foundations on dense sands and gravels. The general equation above has components "s, d, i, g, and b" to account for footing shape, footing depth, inclination of load, sloping ground, and tilting footing respectively.

This bearing capacity equation was developed from solutions of rigid-plastic solids of the classical theory of plasticity. The material is assumed to suffer no deformation prior to shear failure, with plastic flow and constant shear stress after failure. Hence, the capabilities of [2.1] and other theoretical bearing capacity equations for predicting ultimate load, or conversely material properties, are limited to incompressible soils or the general shear failure mode.

There exists predominantly three modes of foundation failure as shown in Figure 2.4. (after Vesic 1973, 1975); general shear failure, local shear failure, and punching shear failure. The latter failure mechanism will be discussed herein as it describes the failure mechanism observed at the surface of the tailings. Punching shear commonly occurs in very loose compressible soils, with a failure pattern or ultimate load difficult to distinguish. Increasing load results in vertical compression of the soil beneath the footing. Vertical shear around the footing perimeter develops through continued penetration. The ultimate load or first failure is difficult to distinguish with any certainty, but is commonly taken as the point of break of the load-settlement plot. For very loose compressible soils where the ultimate load may not be easily distinguished, it is recommended to carry the load to settlements of at least 25% of the footing width (Vesic 1975).

The failure mechanism for incompressible soils and described in [2.1] is not applicable for compressible soils which fail in local or punching shear. Consequently, Terzaghi proposed the use of the bearing capacity equation for the general shear mode of failure, with reductions in the cohesion and friction angle values to account for soil compressibility. This proposal is not supported by laboratory or field tests, and displays an incompatibility in bearing capacity upon transition from general shear to local or punching shear. Vesic (1973) and Ismael and Vesic (1981) proposed the use of compressibility factors in the bearing capacity equation. The compressibility factors are a function of the rigidity index which depends on the Poisson's ratio and elastic modulus of the soil.

Length limitations inhibit a detailed discussion of the compressibility factors for the coal tailings. The following discussion will center on the relative plate bearing pressures at the individual sites and not on specific material properties.

2.3.2.2. Plate Load Testing Description

The plate load apparatus used at the Coal Valley Tailings Impoundment is shown in Figure 2.5. This system had an ultimate load capacity in excess of 10 kN, and was designed for ease of transporting by hand.

The punching shear failure mechanism discussed above was observed with all tests. The plate punched into the ground with vertical shear developing around the plate perimeter. The Load-Settlement and Pressure-Settlement curves from Site 1 (Figure 2.6) display the general failure pattern observed at all sites. This pattern is characteristic of that for punching shear as shown in Figure 2.4.

The objective of the tests at each site was to determine the bearing capacity of the natural tailings. The relative contributions of freeze-thaw dewatering, desiccation drying, evapotranspiration and fibre reinforcing effects of the vegetative root system on bearing capacity were also sought. The nomenclature and boundary conditions for the plate load tests are shown in Figure 2.7. Four tests were typically conducted at each site, two on a bare tailings surface and two on a vegetated surface (rooted tailings). At Sites 2 and 3, tests were also conducted approximately 22 cm below the tailings surface. At Site 4, a test could only be conducted a maximum of 12 cm below the tailings surface due to the proximity of the water table. Site 5 was selected to determine the effect of the loosely placed 0.3 m soil capping material on both the bearing capacity of the capping surface as well as the tailings beneath the capping layer.

All the plate load tests (except one) were conducted at a displacement rate in the order of 0.1 mm/sec. At the coarser grained sites, this rate was deemed slow enough for drained conditions. At Sites 4 and 5, this loading rate likely resulted in a partially undrained test.

2.3.2.3. Tests Results

A summary of the plate load test results on the surface of the tailings are best shown in Figure 2.8. The relative bearing capacity of all plate load tests relative to the results at Site 1 (Site 1 referenced at 100%) are presented. The bearing pressures at the respective 10 % and 20 % relative settlements are used for the comparison.

The bearing pressure at Site 2 for both relative settlement levels on both rooted and unrooted tailings increased from that at Site 1 (Figure 2.8). This is due to the presence of the almost

continuous 37 cm thick surficial sand layer at Site 2, compared to the 11 cm thick compressible surficial silt layer at Site 1.

The gradual increase in fines in the shallow stratigraphy at Site 3 compared to that at Site 1 is reflected in the reduced plate load test results. The lower strength is likely due to the highly compressible silt within the stratigraphy, as well as the closer proximity of the water table which reduces the effective shearing resistance of the soil

The tests at Site 4 were conducted as close to the free water surface as feasible. The higher silt content at this site, and the proximity of the water table is reflected in the plate load results. Tests conducted at the surface of both the rooted and unrooted tailings displayed significant reductions in bearing pressure compared to the previous 3 sites.

The plate load tests on the tailings surface at Site 5 reflect the fine nature of the tailings. The bearing pressures on the bare tailings at 10% and 20% relative settlement are similar to those at Site 4, some 86 m further downstream. One test was also conducted on the surface of the capping material to determine its influence on the bearing pressure. This capping material was placed using a dragline and left uncompacted. Although this material is a well graded clayey till with potentially high bearing pressure, its contribution to bearing pressure was limited due to its loose structure and high moisture content (46%). A well graded free draining medium to dense sand would have contributed significantly more to the bearing capacity of a 300 mm diameter plate at this site. Theoretical bearing capacity calculations indicate that a 0.3 m layer of well graded, compacted, free draining sand placed at this site would have produced capacities significantly higher than those measured.

2.3.3. Strength Enhancement

2.3.3.1. Natural Crusting

A comparison of the crust bearing pressures compared to the below crust pressures are shown in Figure 2.9. This figure shows the relative increase (or decrease) in crust bearing pressure compared to that below the crust. Sites 2 and 4 show significant crust bearing pressures at 10% and 20 % relative settlements compared to that below the crust. An increase in crust bearing pressure is not observed at Site 3 (slow test). This is possibly due to the presence of less compressible sandy material with depth.

Among the two tests conducted below the surface at Site 3, one was conducted at a slow rate similar to that of the other surface tests, and one at a rate approximately 50 times faster. This faster test, conducted at a settlement rate of 5 mm/sec, attempted to analyze the strain rate dependence of the plate load test. The faster test exhibited approximately a 20 % increase in bearing pressure at the two respective relative settlements. The higher bearing pressures indicate that undrained or partially undrained conditions prevailed during the fast test with the generation of positive pore pressures. The low permeability of the soil inhibited the drainage, and resulted in pore pressure generation and reduction of the dynamic compressibility of the soil. Vesic (1965) reported similar results with footings on dense sands subjected to transient loads. The increased bearing capacity on dense sands as reported by Vesic, however, is due to dilation of the sand structure along the general shear failure plane causing the generation of negative pore pressures and increased effective stresses. The surficial coal tailings at the Coal Valley Impoundment are very loose and compress when subjected to loads, leading to the generation of excess pore pressure as the material fails in punching shear.

Higher crust strengths which contribute to the higher measured bearing pressures are believed to be due to three factors. The first two are the freeze-thaw dewatering of the fine grained phase of the surficial tailings during the winter and spring seasons, as well as desiccation drying during the summer season. Both factors rely on the development of suction or negative pore water pressures to dewater and consolidate the tailings. Both natural processes dewater the tailings, creating a

consolidated crust. The significance of these two natural processes depend on the climatic conditions in the tailings disposal area. In arid climates, desiccation drying is likely the dominant enhancement process whereas colder climates may rely on freeze-thaw. Williams and Morris (1990) discuss the significance of desiccation drying on dewatering and strength enhancement of Australian coal tailings, and highlight optimization of the crusting by placing the tailings in thin layers for drying. Optimization of freeze-thaw consolidation and dewatering processes of fine tailings in cold climates such as at the Oil Sands operations in Northern Alberta is also seen as a potentially viable solids enhancement technology. Strength enhancement through desiccation drying or freeze-thaw dewatering depend on particle grain size and are only significant with fine grained saturated or partially saturated soils.

The last factor contributing to increased crust bearing pressure is the relative proximity of the water table. As the plate is loaded, a zone or bulb of influence develops which can be predicted using the Boussinesq equations. As the plate fails the tailings in punching shear, part of the bearing capacity develops from compression of the soil beneath the plate, and part is from vertical shear around the perimeter of the plate. For cohesionless soils, the frictional resistance depends on the effective stress. A net increase in pore fluid pressure beneath the plate within the bulb of influence results in reduced effective stress and a reduced bearing pressure.

2.3.3.2. Biological Dewatering And Strength Enhancement

The effects of biological dewatering and strength enhancement at the sites are also illustrated in Figure 2.9. This figure compares the relative bearing pressure of the rooted tailings with that of the unrooted tailings for relative settlements of 10% and 20%. All sites showed increased bearing pressures of the rooted tailings over the unrooted tailings, with significant gains observed at Site 4. At all sites, the root system dewateres the tailings through evapotranspiration. Strength enhancement through evapotranspiration or biological dewatering becomes more pronounced as the particle size of the tailings decreases (as with desiccation drying and freeze-thaw dewatering discussed above). Thus for the fine tailings at Site 4, which consists primarily of silts and clays, significant strength enhancement in the order of 40 % to 50 % is observed. At the more

granular, free draining sites such as Site 1 and Site 2, the material is sufficiently dewatered by gravity and additional dewatering through evapotranspiration is less evident.

The significance of dewatering through the use of different types of vegetation on the strength enhancement of tailings is shown in Figure 2.10. Johnson *et al.* (1991) tested various plants for dewatering and strength enhancement of a sand-fine tailings mix, by placing the plants in lysimeters in a green house for an 11 week period. The sand-fine tailings mixtures were obtained from the Syncrude oil sands extraction plant. Moisture content and shear strength measurements were carried out at 3 depths in the lysimeters with the average shown in the Figure 2.10. Little information was presented on the method used to measure the shear strength, however, it is anticipated that the measurements were conducted without the roots influencing the measured strengths. The influence of biological dewatering on the strength enhancement of fine grained material, shown in this figure, is impressive and warrants further study.

Figure 2.10 illustrates that Reed Canary and Dock exhibit superior dewatering and strength enhancement capabilities compared to other vegetative species. Reed Canary and Dock also were reported to have had the deepest root systems, each reaching the bottom of the 80 cm deep lysimeters within the 11 week study.

Independent field studies at the Coal Valley tailings impoundment support these results. Macyk *et al.* (1991) conducted field research on the effect of different material replacement options on plant growth and tissue characteristics. The authors concluded that rooting depth was directly proportional to water availability and coal tailings did not adversely affect rooting characteristics. Secondly, Reed Canary grass penetrated to greater depths than the other vegetation species including Alfalfa mix, Red Top, Alsike Clover, Timothy, and Red Clover. Reed Canary grass and Alfalfa mix were the dominant vegetation found on the tailings surface during the field study reported in this paper.

Vegetative root systems also provide a mechanical component which contributes to the bearing capacity of the rooted tailings. This contribution is difficult to quantify and would likely depend on factors including root length, depth, root density and the tensile strength of the root fibre.

Much the same as a geogrid reinforces a soil mass, so too would a root system within the tailings. It is expected that the additional bearing pressure of 5 % at 20 % relative settlement at Site 2 for the rooted tailings is due to the reinforcing effects of the root system since strength enhancement through evapotranspiration dewatering would be negligible. Although a measure of the root density beneath the rooted tailings plate load tests was not conducted, Macyk *et al.* (1991) reported an average plant yield of 88 g dry weight of plant material at five sites obtained from five Daubenmire (1959) frames. Through empirical correlations which predict root morphology, this yield provides a useful index to gauge and compare vegetative reinforcing effects of future plate bearing tests on the coal tailings.

2.4. CONCLUSIONS

The following conclusions may be stated following the plate bearing tests conducted on the coal tailings at the Coal Valley Tailings Impoundment.

1. The tailings are deposited in a loose, uncompacted state and fail in punching shear. Traditional bearing capacity formulation were developed for incompressible soils or the general shear failure mechanism and cannot be directly applied to cases of local or punching shear without accounting for compressibility of the tailings.
2. The bearing pressure in general decreases as distance from the tailings discharge increases. The main contributing factor for this decrease in capacity is due to decreasing grain size or increase in fines.
3. The bearing pressures of the rooted tailings were greater than that on unrooted tailings. This is due to evapotranspiration (dewatering) and fibre reinforcement of the root system. In some cases, the bearing pressures of the rooted tailings were 50-60% greater than the unrooted tailings at equivalent strain or relative settlement levels.

4. A consolidated crust has developed at some of the plate load test sites. The crusting is due to desiccation drying during the summer season and freeze-thaw dewatering through the winter and spring seasons. In some cases, crusting has resulted in a 20 to 40 % increase in bearing pressure over that below the crust at equivalent strain levels.

Incorporation of natural processes including freeze-thaw dewatering, desiccation drying, evapotranspiration and fibre reinforcement of vegetative root systems are seen as a cost effective means of solids enhancement of fine coal tailings at the surface of an impoundment. Incorporation of these processes may promote reductions in thickness or even elimination of capping material, increased stability against wind or water erosion, and reduce the short and long term costs associated with reclamation, monitoring and abandonment of tailings impoundments.

2.5. REFERENCES

- Bowles, J.E., 1988. **Foundation Analysis and Design**. McGraw-Hill, Inc..
- Daubenmire, R. 1959. A Canopy - Coverage Method of Vegetational Analysis. *Northwest Science*, 33:43-64.
- Ismael, N.F. and Vesic, A.S., 1981. Compressibility and Bearing Capacity. *Journal of Geotechnical Engineering*, ASCE, No GT. 12, pp. 1677-1691
- Johnson, R.L., Bork, P., Allen, E.A.D., James, W.H., and Kovernny, L., 1991. Oil Sands Sludge Dewatering by Freeze-Thaw and Evapotranspiration "Draft Report". Presented to Syncrude Canada Ltd. and Reclamation Research Technical Advisory Committee, 273 pgs.
- Kupper, A.M.A.G., 1991. Design of Hydraulic Fill. Unpublished Ph.D. Thesis, Department of Civil Engineering, The University of Alberta, 525 pgs.
- Lamb, W.T., and Whitman, R.V., 1969. **Soil Mechanics**. John Wiley & Sons
- Latimer, R.C., Brinker, C.J. and Kintzi, R.P., 1988. Tailings Disposal Options at the Coal Valley Mine. 90th Annual Meeting of Canadian Institute of Mining and Metallurgy, 43 pgs.
- Macyk, T.M, Nikiforuk, F.I., and Widtman, Z.W., 1991. Characterization and Reclamation of Coal Tailing Materials. Report Prepared For Luscar-Sterco (1977) Ltd. 57 pgs.

- Scott, J.D. and Cymerman, G.J., 1984. Prediction of Variable Tailings Disposal Methods. Proceedings of the Symposium on Sedimentation and Consolidation Models, ASCE, 522-544.
- Sego, D.C., 1990. Use of Freeze-Thaw to Assist in Reclamation of a Coal Tailings Pond. Submitted to Luscar Sterco (1977) Ltd. 27 pgs.
- Selvadurai, A.P.S., Bauer, G.E., and Nicholas, T.J., 1980. Screw Plate Testing of a Soft Clay. Canadian Geotechnical Journal, 17:465-472
- Terzaghi, K and Peck, R.B. 1967. **Soil Mechanics in Engineering Practice**. John Wiley and Sons, Inc.
- Thurber Engineering Ltd., 1992. Coal Valley Mine Site Tailings Reclamation Research Project Geotechnical Report. Submitted to Luscar Sterco (1977) Ltd. 80 pgs.
- Vesic, A. S., Banks, D.C., and Woodward, J.M., 1965. An Experimental Study of Dynamic Bearing Capacity of Footings on Sand. Proceedings of the, Sixth International Conference on Soil Mechanics and Foundation Engineering, Montreal, Vol. II, pp. 209-213.
- Vesic, A.S., 1973. Analysis of Ultimate Loads of Shallow Foundations. Journal of Soil Mechanics and Foundation Division, ASCE, 99(1):45-73.
- Vesic, A.S., 1975. Chapter 3 of Winterkorn, H.F., and Fang, H.Y.. **Foundation Engineering Handbook**. Van Nostrand.
- Williams, D.J., and Morris, P.H., 1990. Engineering Properties of Australian Coal Mine Tailings Relevant to their Disposal and Rehabilitation. Proceedings of the Third International Conference on Reclamation, Treatment, and Utilization of Coal Mining Wastes, Glasgow, United Kingdom, pp 49-56.
- Wroth, C.P., 1984. The Interpretation of In Situ Tests. Geotechnique 34(4):449-489.

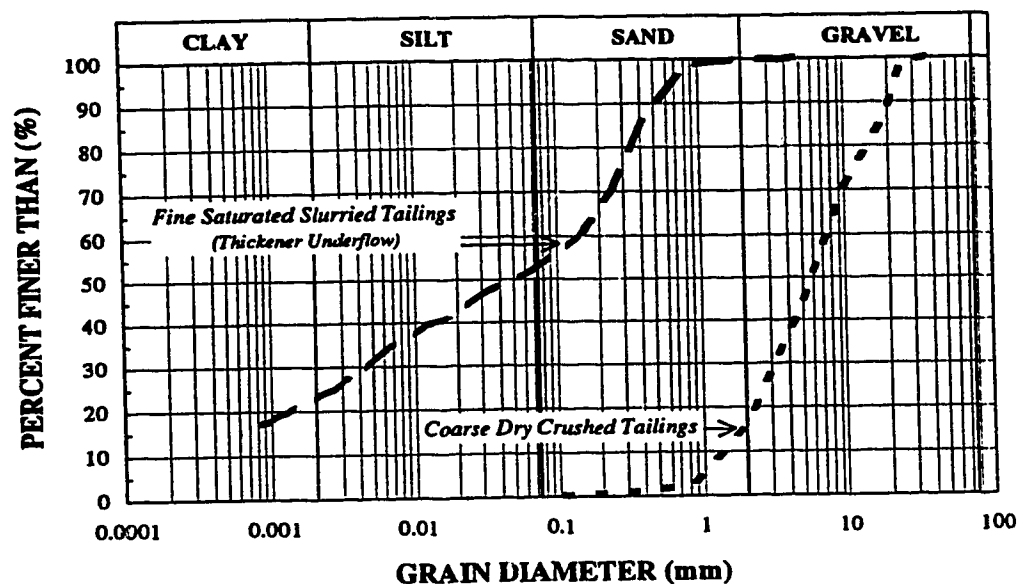


Figure 2.1 Coal Valley Waste Streams

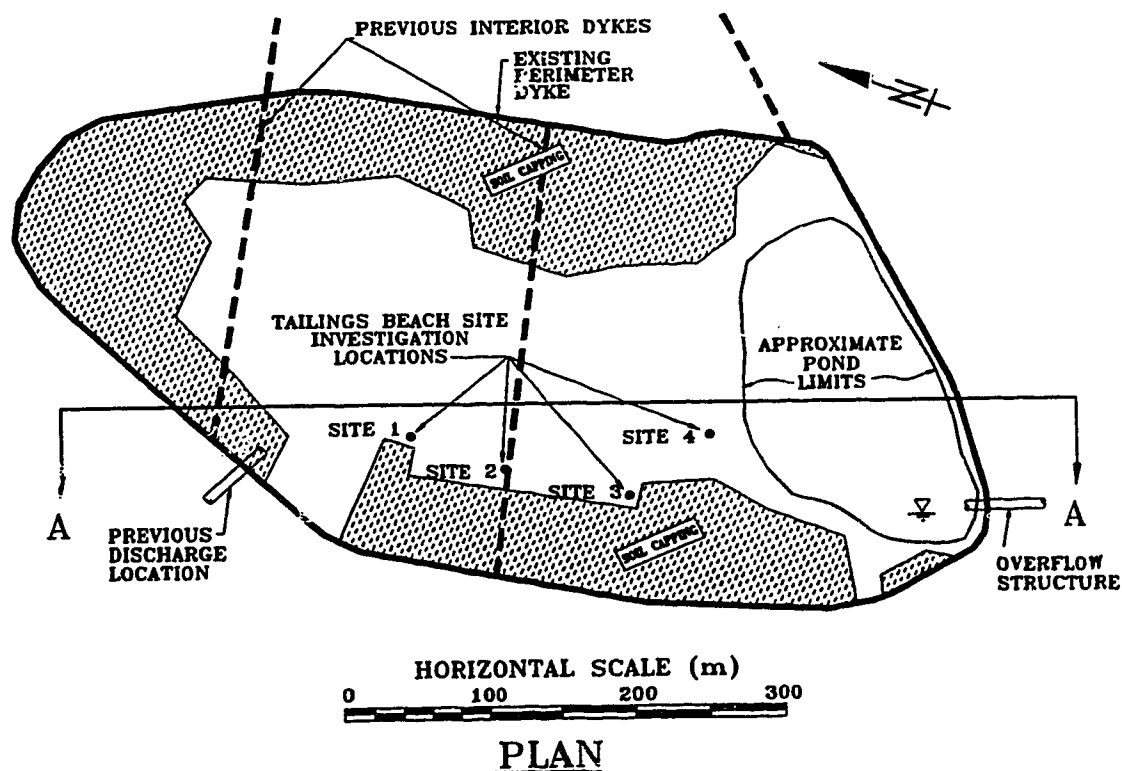


Figure 2.2a Plan of Coal Valley Tailings Impoundment

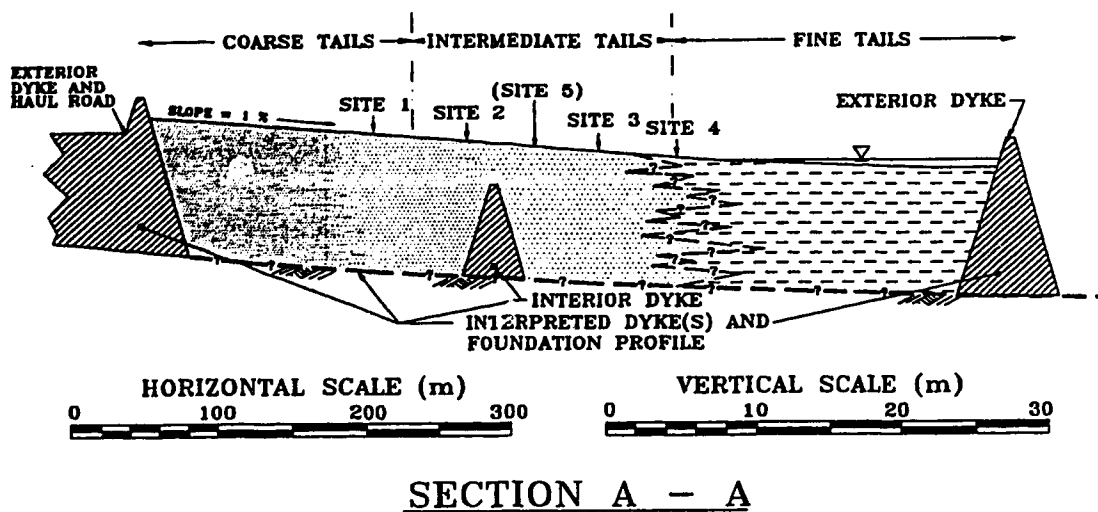


Figure 2.2b **Section A-A Through Coal Valley Tailings Impoundment**

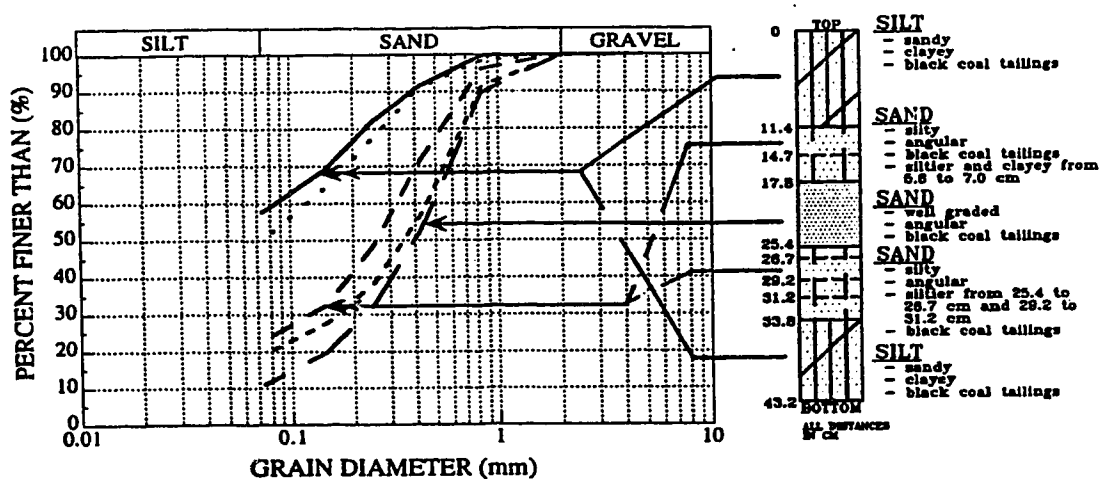


Figure 2.3a **Shallow Stratigraphy at Site 1**

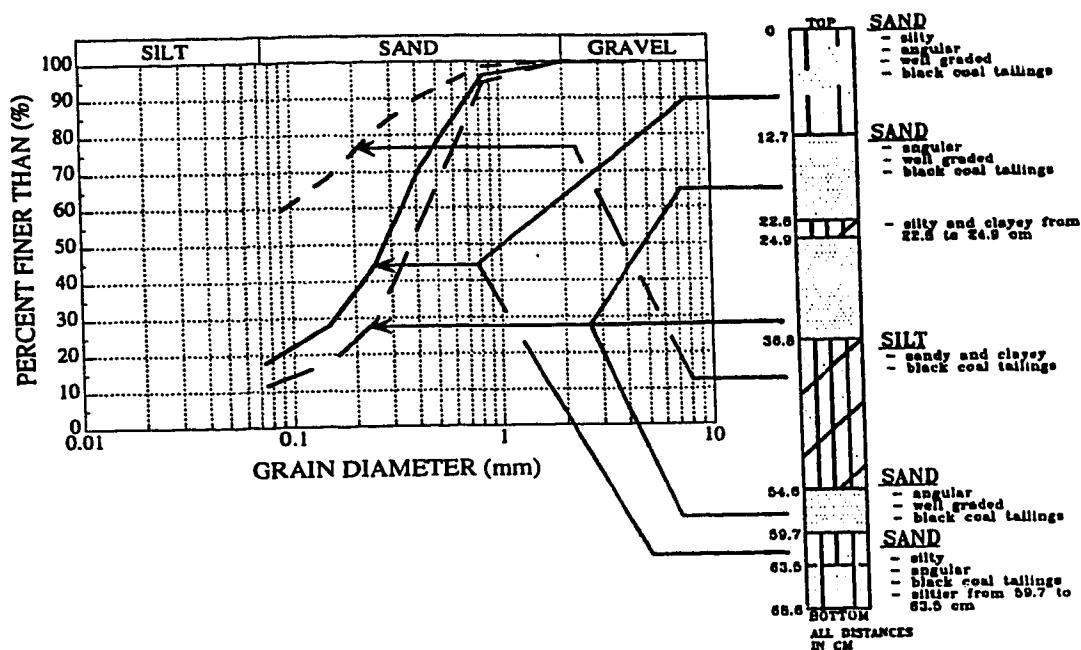


Figure 2.3b Shallow Stratigraphy at Site 2

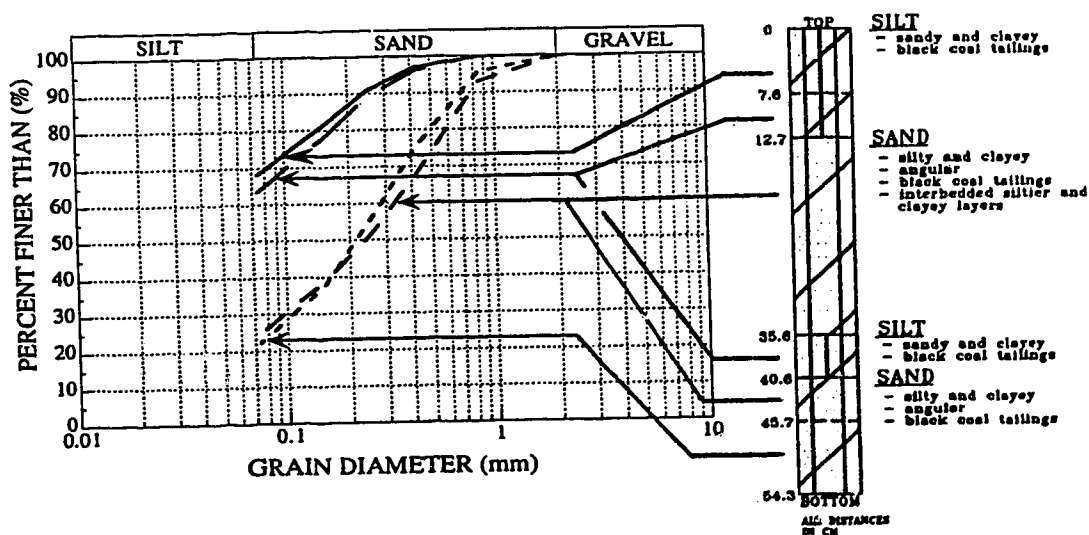


Figure 2.3c Shallow Stratigraphy at Site 3

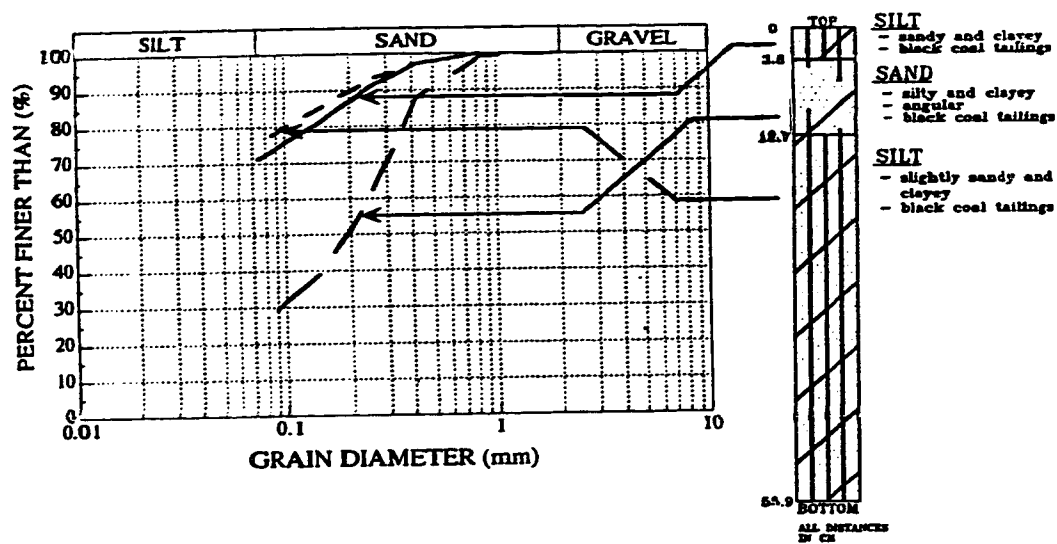


Figure 2.3d Shallow Stratigraphy at Site 4

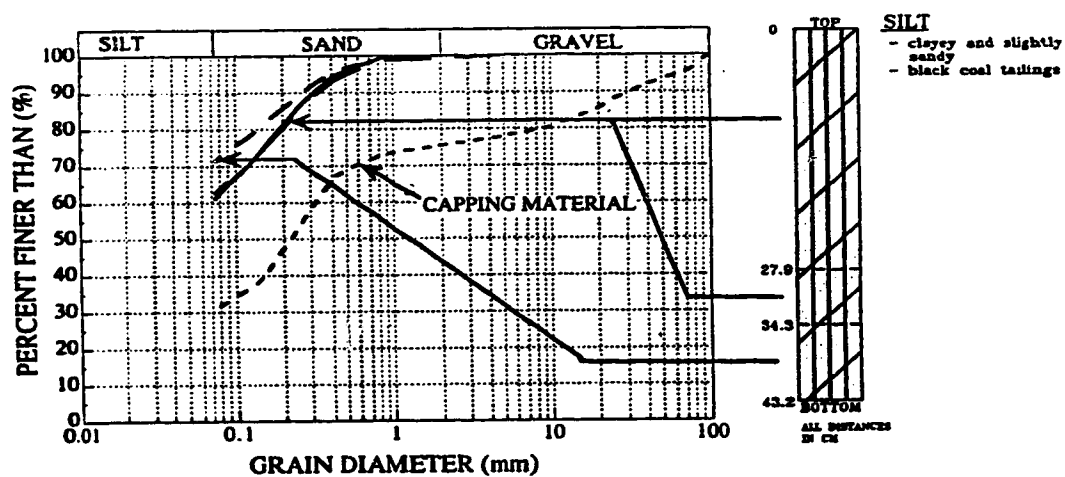


Figure 2.3e Shallow Stratigraphy at Site 5

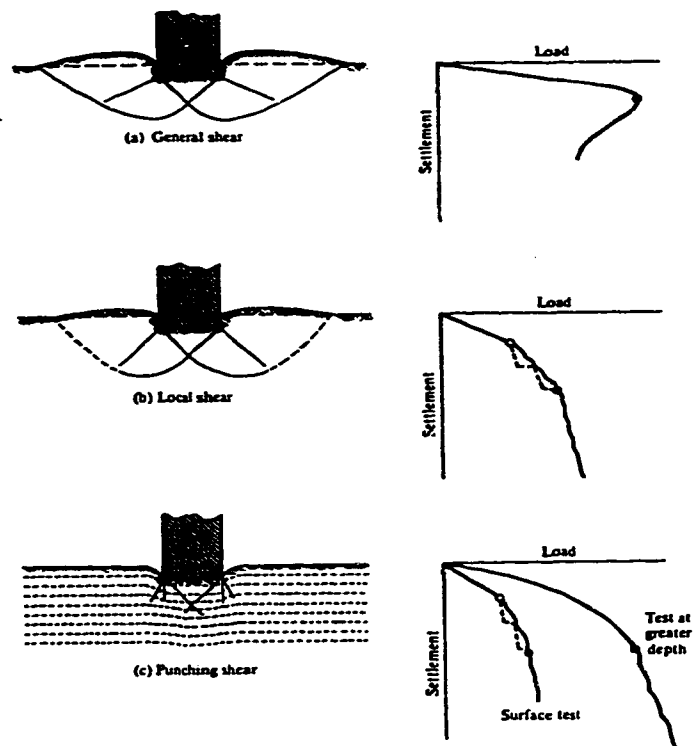


Figure 2.4 Modes of Bearing Capacity Failure (after Vesic 1975)

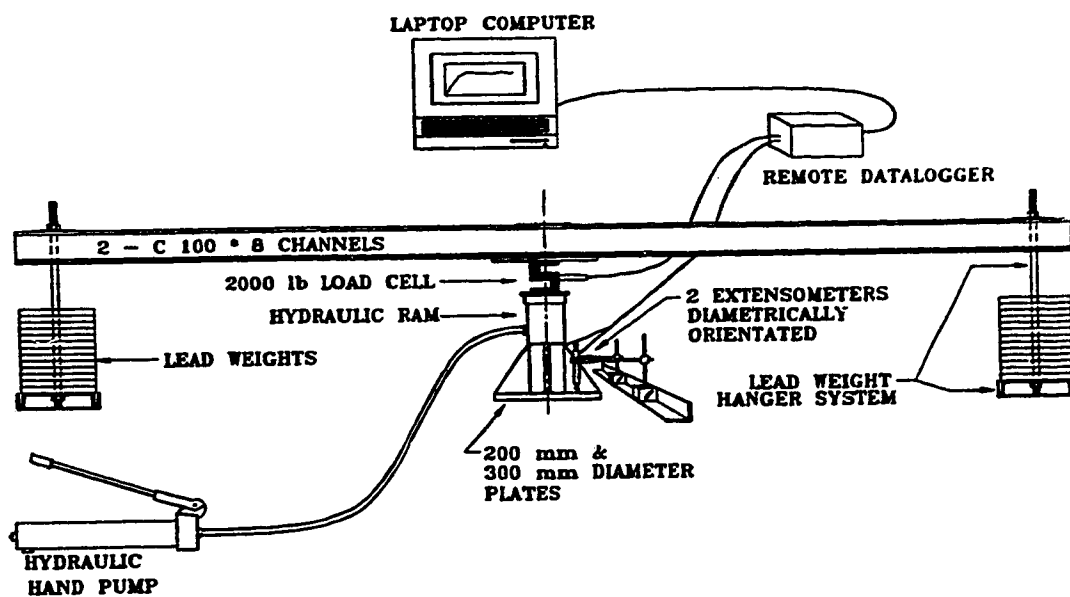


Figure 2.5 Plate Load Test Apparatus

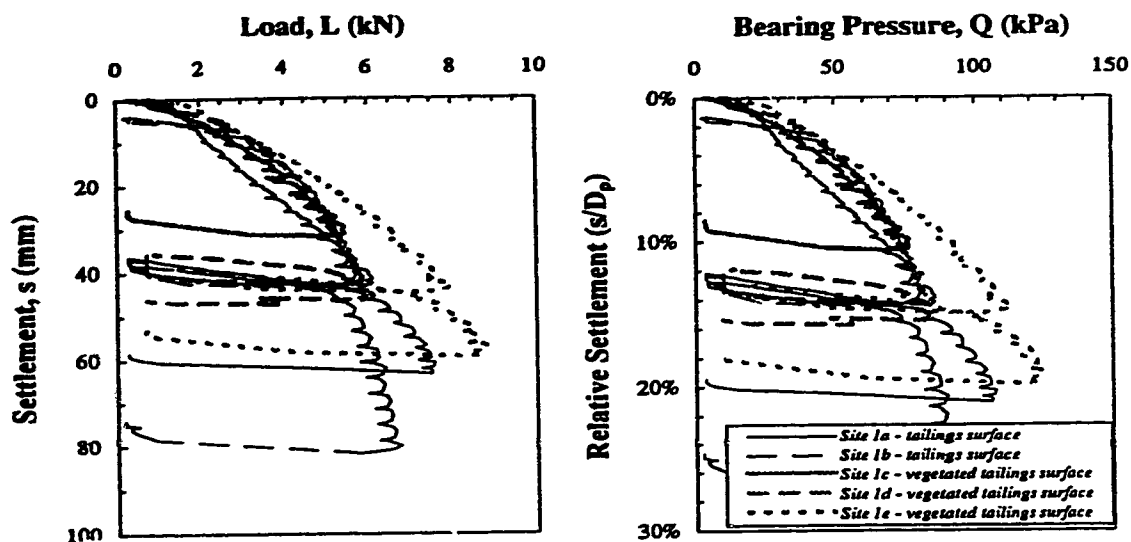


Figure 2.6 Load vs Settlement and Pressure vs Relative Settlement Response at Site 1

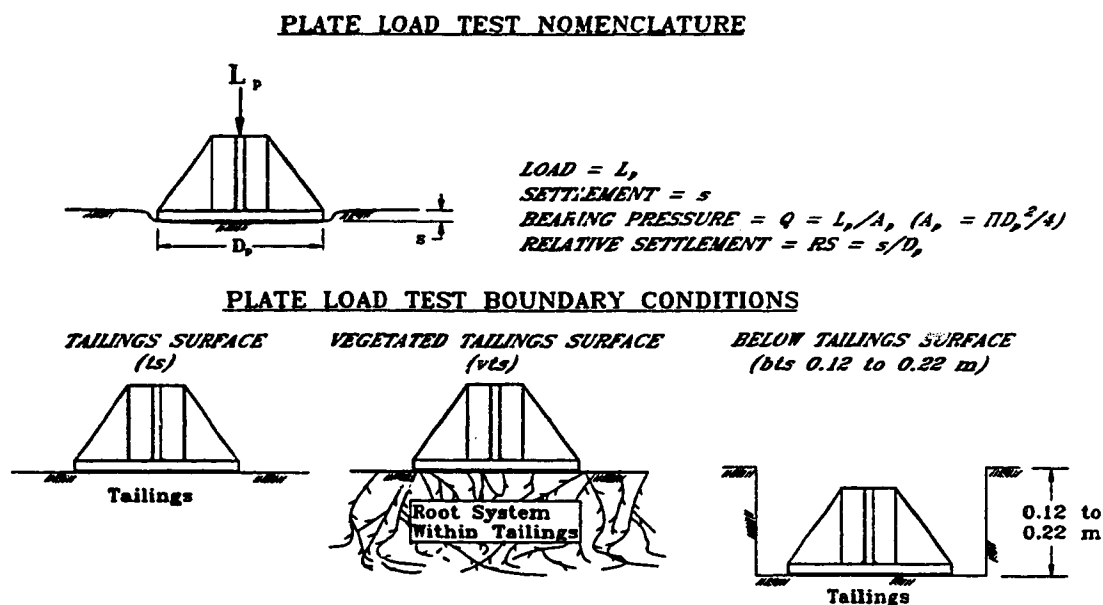


Figure 2.7 Plate Load Test Nomenclature and Boundary Conditions

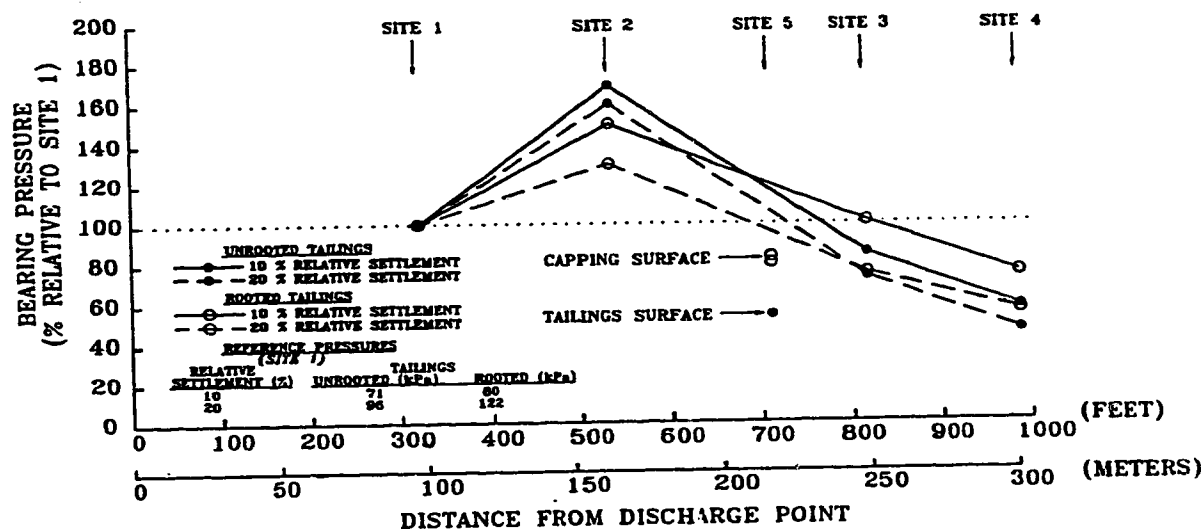


Figure 2.8 Bearing Pressures of Surface Tests Relative to Site 1

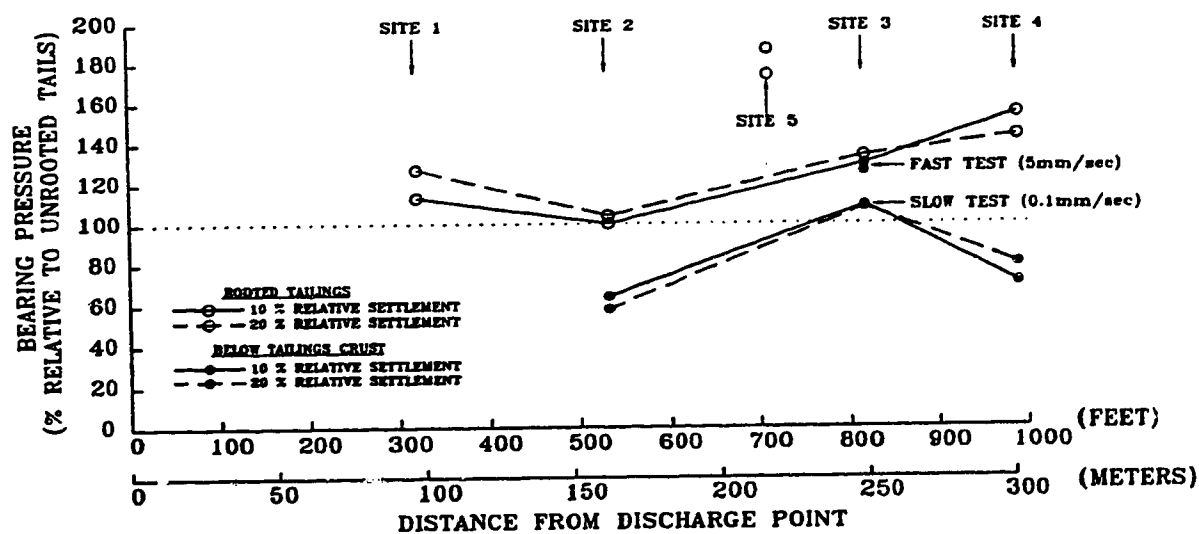


Figure 2.9 Relative Bearing Pressures of Rooted and Below Crust Tailings to Unrooted Surface Tailings

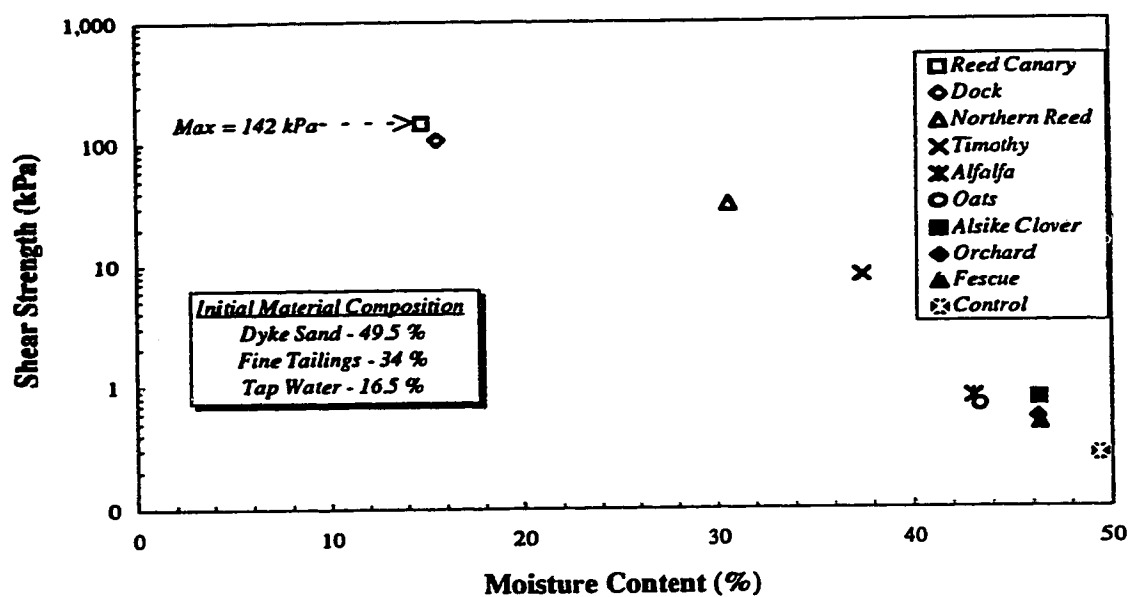


Figure 2.10

Influence of Evapotranspiration on Shear Strength and Moisture Content of Tailings (data source: Johnson et al. 1991)

Chapter 3

Freeze-Thaw Dewatering And Structural Enhancement Of Fine Coal Tails¹

3.1. INTRODUCTION

The Coal Valley mine, owned and operated by Luscar Sterco (1977) Ltd. is located approximately 96 km south of Edson, Alberta in the foothills of the Rocky Mountains. Yearly production of 1.8 million clean tonnes of coal results in generation of two waste streams, a coarse dry crushed rock and a fine saturated slurried tailings (Figure 3.1). During a stage of mineral extraction and waste stream deposition, an 18.2 hectare impervious impoundment was constructed to contain the fine saturated slurried tailings as shown in Figure 3.2a. This impoundment reached its capacity in 1989 and has since been undergoing reclamation.

During deposition of the slurried tailings stream into the impoundment, segregation occurred as coarse particles settled more readily while the finer particles were transported to the pond. Segregation resulted in the development of three distinct zones which potentially require different reclamation schemes. These zones are the coarse, intermediate, and fine tailings regions and are

¹ Published Paper:

Stahl, R.P. and Sego, D.C., 1995. Freeze-Thaw Dewatering and Structural Enhancement of Fine Coal Tails. ASCE Journal on Cold Regions Engineering, 9(3):135-151.

Earlier "Similar" Published Paper:

Stahl, R.P. and Sego, D.C., 1993. Freeze-Thaw Dewatering and Structural Enhancement of Fine Coal Tails. 46th Canadian Geotechnical Conference, Saskatoon, Saskatchewan, September 27-29, pgs. 157-166.

approximately defined in Figure 3.2b. The grain size distribution of the fine tailings region of the impoundment is shown in Figure 3.1.

Previous reclamation practices to achieve dry landscape conditions at the Coal Valley mine have included capping the tailings with 3 to 6 m of waste rock to satisfy operational requirements. These thicknesses were in excess of the 1.2 m initially required by regulation. Greater capping thicknesses were required for the softer saturated fine tailings as material squeezed under the loads imposed during placement of cap rock. Placement of thick capping layers directly affect the production costs and profits at the mine. Freeze-thaw consolidation is viewed as a viable method of reducing or eliminating these excessive material capping requirements.

3.2. FREEZE-THAW

3.2.1. General Description

One of the central mechanisms surrounding the proposed dry landscape reclamation of fine saturated tailings involves freeze-thaw consolidation. The process of consolidation of fine, high void ratio saturated tailings through freeze-thaw has been known for several years. Johnson *et al.* (1989) reported that the concept of freeze-thaw to consolidate saturated materials was initially developed in temperate climates where biological sludges were concentrated from 3-5 % to greater than 30 % solids. Although the use of freeze-thaw to consolidate high void ratio saturated materials may have originated with biological sludges, its effects have been described previously (Andersland and Anderson 1978).

Following the freeze-thaw consolidation of biological sludges, research and development into the dewatering of sludges from municipal wastes sources and dredging operations also developed. Recently, the freeze-thaw consolidation process has developed interest in the mining and mineral extraction industries. In particular, the Oil Sands operations in Northern Alberta are presently evaluating the effects of freeze-thaw consolidation on the dewatering and structural enhancement of their fine tailings derived from the hot water bitumen extraction processes. As discussed by

Sego *et al.* (1993 and 1994), large scale field tests are presently being conducted on oil sands fine tailings incorporating thin layered freeze-thaw disposal of chemically treated fine tailings.

Freezing of a soil-water system involves two process defined as *closed* and *open* system freezing. Both processes occur in nature and several examples were described by MacKay (1972). The effects of closed and open system freezing on the dewatering and structural enhancement were observed with the Coal Valley fine tailings, located within the fine tailings region of the impoundment, and are described in this paper.

3.2.2. Open System Freezing

Open system freezing involves the freezing of *insitu* moisture and additional moisture which migrates to the freezing front within the frozen soil. A mechanistic theory of this process is described by Konrad and Morgenstern (1980). The physical process initiates with the downward freezing of *insitu* pore fluid near the surface. As the frost front progresses, ice nucleates in the water-filled pores with some of the water remaining as unfrozen adsorbed water film around the soil particles. Water from the unfrozen soil, below the frost front, migrates to the front and through the unfrozen water films into the frozen zone under the action of temperature induced suction gradients. The partially frozen zone with pore ice, adsorbed water, and soil particles in a non-equilibrium state is defined as the "Frozen Fringe". Water from below the frost front gradually migrates through the frozen fringe and freezes at the freezing front, feeding a growing ice lense. The latent heat released during freezing of the attracted water retards the advance of the frost front (0°C isotherm). Gradually, as the temperature of the frozen soil decreases, so does the thickness of adsorbed water film around the soil particles. Continued shrinkage of the adsorbed water film layer results in very low permeabilities, eventually stopping the upward flow of attracted water. With the flow of water stopped, the 0°C isotherm continues to advance into the soil until equilibrium conditions are once again reestablished. This ice lense building action results in the development of multiple ice lenses within a frozen soil, potentially causing high uplift stress on overlying structures (Penner, 1974).

Upon observation of the open system freezing process described above with continuity considerations, it is evident that the migration of moisture towards the growing of ice lenses results in a loss of moisture from within the underlying soils. Depending on several factors including the permeability of the underlying soil and the spatial moisture "reservoir" conditions, this process can result in dewatering and consolidation of the unfrozen soil beneath the frost front as illustrated in Figure 3.3. Laboratory and field results on Coal Valley fine tailings indicate that this dewatering of unfrozen saturated tailings occurs and results in significant structural enhancement of tailings found below the frost front.

3.2.3. Closed System Freezing

Open system freezing was previously described as the development of horizontal ice lenses through the migration and freezing of moisture drawn from the underlying soil. Open system freezing includes the presence of an unfrozen soil moisture reservoir. Conversely, closed system freezing may be characterized as freezing of only *insitu* water without the presence of a moisture reservoir. Impermeable boundary conditions, reduced permeabilities, or relative quick freezing rates preclude the migration of moisture from outside the advancing frost front.

Although moisture migration is reduced or eliminated on a macro scale in closed system freezing, migration or redistribution of *insitu* moisture on a micro scale occurs. As described in the open system freezing process, a matrix of pore ice develops which surrounds soil particles and their associated absorbed water layers. The water within these layers is stationary on a macro scale.

Temperature gradients and the associated suction pressures within the partially frozen structure cause the absorbed moisture around the soil particles to migrate towards the ice lense within the closed freezing system. The action of this localized pore fluid flow results in the development of a three-dimensional ice lense matrix. Continued localized moisture migration results in a reduction of the thickness of the absorbed water layers and consolidation of the soil mineral matrix.

For fine grained soils, closed system freezing results in the consolidation of the soil to an overconsolidated "ped" structure. The ped structure is surrounded by a three-dimensional system of ice lenses composed of virtually pure ice with few mineral impurities. This closed system freezing process may also be considered as *undrained freezing* since no change in total moisture content occurs.

The consolidation process during freezing and subsequent thaw of saturated fine tailings subjected to closed system or undrained freezing may be illustrated using the conventional soil mechanics void ratio *versus* effective stress plot shown in Figure 3.4 (Nixon and Morgenstern 1973). The homogenous fine saturated tailings in their *insitu* state prior to freezing is shown in this figure at location A with a void ratio of e_A under a vertical effective stress (self weight) of σ_A' . Considering the entire sample, upon undrained freezing, the sample expands due to a 9 % volume expansion of the voids as the pore fluid changes phase. The entire sample moves to location B' with a void ratio $e_{B'}$. With expansion of the entire sample, the freezing results in the development of a three dimensional segregated structure of consolidated soil peds housed within an ice matrix. Within the soil peds, freezing over consolidates the soil matrix to a void ratio of e_B at location B, under an effective stress of σ_B' .

Upon thaw, water is released as the ice lenses melt and the entire sample returns to location A. The sample at location A after freezing is no longer homogeneous. Rather, a segregated profile exists with the moisture from the thawed ice matrix at the surface, and the consolidated peds formed during the freezing process settled at the bottom (due to density differences). Decanting of the "pure" water from the top of the thawed sample results in the average void ratio decreasing to e_C under an effective stress σ_A' . The void ratio at C includes some moisture reabsorbed during the thawing and ped settling process. This reabsorbed moisture is illustrated as the consolidated peds at location B, swell upon thaw to location C.

The path A-B-C describes the freezing and thawing process within the consolidated peds, whereas path A-B'-C illustrates the freezing, thawing, and decanting of the total sample. The void ratio

reduction from *A* to *C* is directly related to the volume reduction or thaw strain of the total fine tailings.

Research at the University of Alberta indicates that the magnitude of thaw strain and overconsolidation of the soil matrix depend on several factors including initial solids contents, mineral composition, grain size distribution, pore fluid composition, freezing rate and temperature boundary conditions imposed during closed system freezing.

The material at *C* has undergone both a physical and mechanical transformation. Included with the volume reduction (thaw strain) and increased solids content at the lower void ratio, the material has in general an increased permeability, reduced compressibility, and increased shear strength compared to the unfrozen material at *A*. These post freeze-thaw mechanical changes have been discussed by several authors on various materials (Stanczyk *et.al.* 1971), (Nixon and Morgenstern 1973 and 1974), (Chamberlain and Blouin 1978), (Chamberlain and Gow 1979), (Chamberlain 1980), (Johnson *et al.* 1989), (Vahaaho 1991), (Sego and Dawson 1992), (Sego *et al.* 1993), and will not be discussed further.

3.3. DESIGN PROCESS

3.3.1. Background

The first step in considering whether freeze-thaw consolidation can be utilized for dewatering of fine tailings is to evaluate the available energy for freezing and thawing. Stanczyk *et al.* (1971) calculated the energy requirements in terms of calories per gram or kilowatt-hours per ton to cool and freeze phosphate rock slime at varying initial solids contents. Stanczyk points out that theoretical energy computations and cost estimates can be developed assuming idealized freezing cycles utilizing reversible heat exchange processes.

Although freezing and thawing systems may be designed and implemented on a large scale, their costs would be considerable. With this in mind, perhaps the most economical process and energy

source for freeze-thaw is to utilize the natural seasonal temperature fluctuations associated with the climate. Fortunately in most parts of Canada, natural seasonal temperature variations result in alternate freezing and thawing cycles. The subzero temperatures during the Fall and Winter months may be used to freeze the fine tailings, with the warmer temperatures recorded during the Spring and Summer facilitating thaw.

3.3.2. Freezing and Thawing Indices

Prediction of the natural freezing and thawing energy begins with an analysis of the climatic data at the tailings disposal or storage area. Using 30 year monthly temperature averages from 1951 to 1980 (from Environment Canada), the seasonal temperature variation near the Coal Valley site may be approximated as shown in Figure 3.5. For this 30 year period, the average Air Freezing Index (AFI) and Air Thawing Index (ATI) are 1316 °C - days and 1864 °C - days respectively. The mean yearly temperature is approximately +1.5 °C with an average seasonal amplitude of 13.6 °C. The equation describing the seasonal temperature variation approximated for the Coal Valley site is shown in this figure. With the available natural energy sources for freezing and thawing defined, prediction of the potential volumes of freeze-thaw treated material is desired.

3.3.3. Freezing Model

Martel (1988) developed a mathematical model for freezing of sewage sludge which gives the time to freeze a layer of sludge. The model is based on the boundary conditions shown in Figure 3.6, and assumes that the sludge is initially at 0 °C when freezing begins.

The freezing model considers both convective and conductive heat transfer processes to the surface and is given as:

$$t_f = \frac{\rho_f L \epsilon}{T_f - T_{ac}} \left(\frac{1}{h_c} + \frac{\epsilon}{2K_{fs}} \right) \quad [3.1]$$

where

t_f	=	time to freeze
ρ_f	=	density of frozen fine tailings
L	=	latent heat of fusion of fine tailings
ϵ	=	thickness of frozen fine tailings
h_c	=	convective heat transfer coefficient
K_{fs}	=	thermal conductivity of frozen fine tailings
T_f	=	freezing temperature of fine tailings
T_{ac}	=	ambient air temperature

The first and second terms in the brackets of [3.1] account for convective and conductive heat transfer processes respectively. Equation [3.1] was used to predict the depth of freezing of fine coal tailings in terms of the AFI and is presented in Figure 3.7. The input values used to predict the depth of frost are presented in Table 3.1. These values are based on typical values reported by Martel (1988), adjusted for the characteristics and composition of fine coal tailings. Figure 3.7 shows the relative contribution of conduction and convection to the total energy requirements for freezing of a single layer. The energy requirement (ie. the AFI) increases significantly for thicker layers due to the retarding effect of conduction through the frozen tailings as the layer thickness increases. This figure illustrates that an AFI of 1316 °C - days results in a predicted frost penetration of approximately 1.1 m. This prediction is supported by depth of frozen material measurements recorded on the fine coal tailings at the Coal Valley mine.

3.3.4. Thawing Model

The benefits of freeze-thaw such as increased shear strength, increased permeability, and reduced volume and liberation of moisture are realized if the fine tailings frozen during the fall and winter, thaw during the next spring and summer. Thus, in evaluating optimal freezing thicknesses, one must also consider the predicted thaw depth based on the climatic conditions in the area.

The model illustrating the thawing process of frozen fine tailings is shown in Figure 3.8 (after Martel 1988). The mathematical representation for this model is shown as:

$$t_{th} = \frac{\rho_f LY}{T_{at} - T_f + \frac{\alpha \tau I}{h_c}} \left(\frac{1}{h_c} + \frac{\theta Y}{2K_{ss}} \right) \quad [3.2]$$

where

t_{th}	=	time to thaw
ρ_f	=	density of frozen fine tailings
Y	=	depth of thawed fine tailings
L	=	latent heat of fusion of fine tailings
h_c	=	convective transfer coefficient
K_{ss}	=	thermal conductivity of settled fine tailings
T_f	=	freezing temperature of fine tailings
T_{at}	=	ambient air temperature
I	=	insolation (rate of solar radiation)
θ	=	thickness of frozen fine tailings
α	=	solar energy absorptance ratio
τ	=	transmittance factor

Similar to the freezing model, this equation represents the time to thaw a thick frozen layer. The model assumes that the supernatant water released upon thaw is decanted quickly and the settled thawed tailings do not desiccate.

Once again, the first and second terms in the brackets account for the convective and conductive heat transfer processes respectively. The parameters shown in [3.2] are defined in Table 3.2 with the values adjusted for the properties of fine coal tailings. The thawing model was used to predict the depth of thaw of frozen fine coal tailings in terms of the ATI as shown in Figure 3.9. Considering the ATI of 1864 °C - days at the Coai Valley site, a maximum predicted thaw depth of 1.5 m is predicted.

The maximum possible predicted thaw depth of 1.5 m assumes heat transfer only occurs from the tailings surface towards the atmosphere. Detailed design would warrant accounting for heat

transfer processes from the base of the frozen tailings downwards into the unfrozen tailings and foundation (geothermal effects).

3.3.5. Freeze-Thaw Optimization

With the maximum calculated thaw thickness of 1.5 m (neglecting geothermal effects), it is desirable to optimize the placement layer thickness for freezing. As discussed above and shown in Figure 3.7, the predicted frozen thickness at the Coal Valley Impoundment, assuming one layer, is approximately 1.1 m. Considering this model, the freezing process may be optimized by freezing the fine tailings in thin layers. Freezing in multiple thinner layers reduces the retardation effect of heat conduction through the frozen tailings which predominates with thicker layers. Figure 3.10 shows the total frozen layer thickness *versus* placement thickness of individual layers for the air freezing index of 1316 °C - days and 658 °C - days. The latter AFI assumes that 1/2 of the freezing season is required for layer placement and provides a conservative lower bound for design. The actual "usable" AFI would likely lie between this upper and lower bound and depend on the specific season's temperature profile, placement geometry, depositional rate and methodology, and efficiency.

Based on a maximum previously assumed thaw depth of 1.5 m, the optimal multiple placement layer thickness is between 0.31 m and 0.75 m. Greater thicknesses would likely result in non-optimization of the freezing process with respect to the available thaw thickness. Conversely, thicknesses less than the lower bound may result in freezing great thicknesses and development of a remnant frozen fine tailings layers within the stratigraphy following completion of thaw.

As a comparison, if one assumes that an additional 1 m of thaw occurs through geothermal effects (resulting in a total thaw thickness of 2.5 m), the optimal placement layer thickness is between 0.15 m and 0.31 m.

Optimization of the freeze and thaw processes with respect to the available energy sources, placement conditions and variables, results in maximization of the volumes of freeze-thaw

enhanced materials. This reduces the time required and costs associated with structurally enhancing saturated fine grained tailings through freeze-thaw

3.4. FIELD RESULTS

3.4.1. Shear Strength Data

As discussed previously, the tailings impoundment reached full capacity in 1989, at which time reclamation activities were initiated. During the winter months from 1989 through 1993, shear strength profiles of the unfrozen tailings were measured in the fine tailings region of the impoundment. Holes were drilled through the ice and frozen fine tailings using a standard ice auger or a core barrel. The shear strengths were determined using a *Genor* hand held field vane. Due to the expected low strengths of the saturated fine tailings and the shear strength resolution desired, larger non-standard vanes were required and fabricated at the University of Alberta.

The average undrained shear strength profiles from November 1989 to February 1993 are presented in Figure 3.11. This period represents four freeze-thaw seasons. The profiles are based on the average results determined from three sites, except November 1989 and November 1990 which only include profiles from two and one site(s) respectively. The three sites are shown in plan in Figure 3.2a.

The shear strength profiles determined on two separate occasions in the winter of 1989/1990 are virtually identical. The profiles represent that of a normally consolidated soil with increasing shear strength with depth due to increasing effective stress. The shear strength increases linearly from approximately 0.2 kPa at 0.5 m below the ice surface to 1 kPa at a depth of 2 m.

The shear strengths recorded following the initial 1989/1990 profiles show significant gains with time. In terms of relative shear strength increases, the shear strength in February 1993 is approximately 9 times greater at a depth of 1 m, and 5 times greater at a depth of 2 m than the

initial 1989/1990 profile. Beyond a depth of 2 m, the strength appears to increase linearly with depth.

Similarities between the profile for a normally consolidated clay with a desiccated crust, and the February, 1993 profile are evident. For a desiccated normally consolidated clay, the higher shear strength near the surface is due to drying and matrix suctions which consolidate the material and increase the shear strength. Although the surface of the fine coal tailings has always been capped with water and has never been exposed to desiccation processes, it has likely been dewatered through the suctions developed during the freezing process. The suction pressures developed within the frozen fringe encourage migration of pore water, within the unfrozen tailings depth, toward the frost front. This moisture migration results in dewatering and consolidation of the unfrozen tailings.

Space limitations preclude discussion of the laboratory results on the fine coal tailings. However, laboratory experiments have also shown that dewatering and structural enhancement of fine coal tailings occurs both within and beyond the frost front (Sego 1990).

3.4.2. Normally Consolidated Shear Strengths

To provide a relative index for the strength increase due to freeze-thaw and moisture migration processes, conventional concepts of undrained shear strength for normally consolidated fine grained materials are used for comparison. As discussed by Schiffman *et al.* (1988), for hydraulic fill with significant plasticity, undrained shear strength can be evaluated using normalized soil properties approaches developed for natural clays. The undrained shear strength of natural clays is conveniently expressed according to the ratio of s_u/σ_c' where s_u is the undrained shear strength and σ_c' is the effective consolidation pressure. This relationship allows the changes in the undrained strength to be monitored over time with changes in consolidation (induced pore water pressure dissipation).

Several undrained shear strength relationships (s_u/σ_c') for various materials are cited by Schiffman and are presented in Table 3.3. The s_u/σ_c' ratios for fine tailings from various sources

range between 0.2 and 0.3. Considering that normal consolidation conditions apply for most hydraulic fills, the undrained shear strength relationship for natural soils proposed by Bishop and Henkel and discussed by Schiffman may be considered to help refine the s_u/σ_c' ratio estimate. The undrained shear strength ratio was shown to correlate with the plasticity index (PI) and is presented as:

$$\frac{s_u}{\sigma_c'} = 0.18 + 0.0037 (PI) \quad [3.3]$$

Based on the Atterberg Limits conducted on the Coal Valley fine tailings, ($L_L = 70\%$, $P_L = 35\%$, $PI = 35\%$) [3.3] results in an $s_u/\sigma_c' = 0.24$. This value is within the range reported in Table 3.3 and will be used to compare with the field shear strengths.

The theoretical shear strength profile is not complete without account for selfweight consolidation processes resulting in a void ratio reduction and density increase with depth. Considering a bulk unit weight of the tailings measured at the surface of 13.3 kN/m^3 and compression indices, C_c , in the range of 0.3 to 1.0, the theoretical shear strength profiles may be compared with the actual profiles as shown in Figure 3.12.

The theoretical shear strength profiles compare well with the shear strengths measured during the winter of 1989/1990. Furthermore, the slopes of the actual and theoretical strength profiles are similar, supporting the s_u/σ_c' ratio of 0.24 chosen and the range of C_c values selected. Comparison of the theoretical strength profile with the measured profile above a depth of 2 m for the March 1991 profile, and the entire February 1993 profile indicate the freezing process has overconsolidated and strengthened the upper regions of the saturated fine tailings.

The depth of dewatering and consolidation encountered in February 1993 could not be determined due to equipment limitations. It is expected, however, that with increasing depth, the measured shear strength profile would eventually coincide with the calculated profile. It is noted that this calculated profile was based largely on empirical correlations. A detailed theoretical profile would require investigations including laboratory consolidometer tests with shear strength

measurements, and a detailed knowledge of the stratigraphy within the fine tailings at this location.

3.5. FREEZE-THAW CONCEPT FOR EXISTING IMPOUNDMENT

Freeze thaw consolidation is a powerful structural enhancement process for fine saturated high void ratio tailings. Specifications enforced by reclamation regulatory authorities, the Development and Reclamation Review Committee (DRRC) in Alberta, occasionally require that fine saturated tailings areas be returned to dry landscape conditions for wildlife or perhaps productive farm land purposes. Freeze-thaw consolidation is viewed as a viable process to assist the consolidation (dewatering) of fine tailings zones enabling the development of a dry landscape scenario.

An illustration of a possible freeze-thaw consolidation disposal operation at the Coal Valley mine at their abandoned tailings impoundment is illustrated in Figure 3.13. The freeze-thaw operations would incorporate natural freezing to freeze the top layer of fine tailings to a depth of approximately 0.3 m. This thickness should provide sufficient stability for relatively light human and equipment traffic. In order to reduce the freezing retardation effects of conduction and to optimize the volume of freeze-thaw treated material, holes would be drilled through the frozen fine tailings with the underlying unfrozen fine tailings pumped to the surface in thin layers and exposed to the atmospheric thermal conditions. The pumped placement layer thickness could be optimized as discussed previously and this process repeated throughout the freezing season.

The higher temperatures during the spring and summer would thaw the frozen tailings and unlock the benefits developed during freezing including increased shear strength and permeability. This freeze thaw enhancement process could be continued for several seasons until the consistency of the fine tailings changes from that of a slurry to a weak soil. Evaporation coupled with evapotranspiration through introduction of stable, high moisture demand vegetation grown on the thawed tailings results in further dewatering and strengthening. This enhancement is in addition to the fibre reinforcing effects of the vegetative root system. As discussed in Stahl and Sego

(1992), evaporation, evapotranspiration, and fibre reinforcement can significantly contribute to bearing capacity and surface stability of fine coal tailings. These surface enhancement processes following treatment by freeze-thaw can provide sufficient surface stability alone, or through the addition of thin capping layers, to support revegetation and other dry landscape reclamation activities. The goal of which to provide an acceptable, stable reclaimed environment commensurate with the post-mine land use philosophy.

3.6. CONCLUSIONS

The Coal Valley tailings impoundment reached full capacity in 1989 and has been undergoing reclamation activities. Freeze-thaw dewatering and consolidation processes have structurally enhanced the fine coal tailings both within the frost front and at depth due to moisture migration. Four freeze-thaw cycles representing four winters have resulted in a shear strength increase in the fine tailings between 5 and 9 fold. The shear strength has increased from a negligible value to near 5 kPa at the surface. Continued freeze-thaw consolidation processes coupled with evaporation, evapotranspiration, and fibre reinforcement of vegetative root systems help support dry landscape reclamation of these problematic soft, weak soils.

3.7. REFERENCES

- Chamberlain, E.J. and Blouin, S.E. 1978. *Densification by Freezing and Thawing of Fine Material Dredged from Waterways. Proceedings of Third International Conference on Permafrost, Edmonton, Alberta, pp. 623-628.*
- Chamberlain, E.J. and Gow, A.J. 1979. *Effect of Freezing and Thawing on the Permeability and Structure of Soils. Engineering Geology, 13: 73-92.*
- Chamberlain, E.J. 1980. *Overconsolidation Effects of Ground Freezing. Proceedings of the Second International Symposium on Ground Freezing, Trondheim, Norway, pp. 325-337.*
- Johnson, R.L., Bork, P. and Layte, P. 1989. *The Effect of Freezing and Thawing on the Dewatering of Oil Sands Sludges. International Symposium on Reclamation, A Global Perspective, Calgary, Alberta, pp. 687-694.*

- Johnson, R.L., Bork, P., Allen, E.A.D., James, W.H. and Koverny, L. 1991. Oil Sands Sludge Dewatering by Freeze-Thaw and Evapotranspiration - "Draft Report". Presented to Syncrude Canada Ltd. and Reclamation Research Technical Advisory Committee, 273 p.
- Konrad, J-M. and Morgenstern, N.R. 1980. A Mechanistic Theory of Ice Lens Formation in Fine-Grained Soils. *Canadian Geotechnical Journal*, 17: 473-486.
- Latimer, R.C., Brinker, C.J. and Kintzi, R.P. 1988. Tailings Disposal Options at the Coal Valley Mine. 90th Annual Meeting of Canadian Institute of Mining and Metallurgy, p. 43.
- Martel, C.J. 1988. Development and Design of Sludge Freezing Beds. US Army Cold Regions Research and Engineering Laboratory, CRREL Report 88-20.
- McKay, R.J. 1972. The Worlds of Underground Ice. *Annals of the Association of American Geographers*, 62(1): 1-22.
- Morgenstern, N.R. 1981. Geotechnical Engineering and Frontier Resource Development. *Geotechnique* 31(3): 305-365.
- Morgenstern, N.R. and Nixon, J.F. 1971. One Dimensional Consolidation of Thawing Soils. *Canadian Geotechnical Journal*, 8: 558-565.
- Nixon, J.F. and Morgenstern, N.R. 1973. The Residual Stress in Thawing Soils. *Canadian Geotechnical Journal*, 10: 571-580.
- Nixon, J.F. and Morgenstern, N.R. 1974. Thaw Consolidation Tests on Undisturbed Fine-grained Permafrost. *Canadian Geotechnical Journal*, 11: 202-214.
- Nixon, J.F. and McRoberts, E.C. 1973. A Study of Some Factors Affecting the Thawing of Frozen Soils. *Canadian Geotechnical Journal*, 10: 439-452.
- Ogata, N., Kataoka, T. and Komiya, A. 1985. Effect of Freezing-Thawing on the Mechanical Properties of Soil. *Proceedings of the Fourth International Symposium on Ground Freezing*, Sapporo, Japan, pp. 201-207.
- Penner, E. 1974. Uplift Forces on Foundations in Frost Heaving Soils. *Canadian Geotechnical Journal*, 11: 323-338.
- Schiffman, R.L., Vick, S.G. and Gibson, R.E. 1988. Behavior and Properties of Hydraulic Fill Structures. American Society of Civil Engineers, Geotechnical Special Publication, No. 21, Edited by D.J.A. Van Zyl and S.G. Vick, pp. 166-202.
- Sego, D.C., Burns, R., Dawson, R., Dereniowski, T., Johnson, R. and Lowe, L. 1993. Dewatering of Fine Tails Utilizing Freeze-Thaw Process. *Fine Tailings Symposium, Proceedings of the Oil Sands - Our Petroleum Future*, April 4-7, 1993, 25 p.

-
- Sego, D.C. and Dawson, R.F. 1992. Freeze-Thaw Dewatering of Oslo Cold Water Process Fine Tailings. Submitted to Esso Resources Canada Ltd., 50 p.
- Sego, D.C., Dawson, R.F., Dereniwski, T. and Burns, B. 1994. Freeze-Thaw Dewatering to Reclaim Oil Sand Fine Tails to a Dry Landscape. 7th International Cold Regions Engineering Specialty Conference, March 7-9, 1994, Edmonton, pp: 669-688.
- Sego, D.C. 1990. Use of Freeze-Thaw to Assist in Reclamation of a Coal Tailings Pond. Submitted to Luscar Sterco (1977) Ltd., 27 p.
- Stanczyk, M.H., Field, I.L. and Collins, E.W. 1971. Dewatering Florida Phosphate Pebble Rock Slime by Freezing Techniques. U.S. Bureau of Mines, R.I # 7520, 21 p.
- Vahaaho, I. 1991. Effects of Thaw Consolidation on Clay. Proceedings of the Tenth European Conference on Soil Mechanics and Foundation Engineering, Deformation of Soils and Displacement of Structures, Vol II, pp 625-628.

Table 3.1 **Input Variables for Depth of Frost Predictions for Fine Coal Tailings**

Variable	Definition	Value
t_f	Time to freeze	varies
ρ_f	Density of the frozen fine tailings	1130 kg/m ³
ϵ	Thickness of fine tailings layer	varies
L	Latent heat of fusion of fine tailings _(conservative, value for water)	93 W·h/kg
h_c	Average convective heat transfer coefficient	30 W/m ² ·°C
K_{fs}	Thermal conductivity of the frozen fine tailings	2.22 W/m·°C
T_f	Freezing temperature of fine tailings	0°C
T_{ac}	Ambient air temperature during freezing	varies

Table 3.2 **Input Variables for Depth of Thaw Predictions for Fine Coal Tailings**

Variable	Definition	Value
t_{th}	Time to thaw	varies
ρ_f	Density of the frozen fine tailings	1130 kg/m ³
Y	Total depth of thawed fine tailings	varies
L	Latent heat of fusion of fine tailings _(conservative, value for water)	93 W·h/kg
h_c	Average convective heat transfer coefficient	30 W/m ² ·°C
K_{ss}	Thermal conductivity of the settled solids	0.87 W/m·°C
T_f	Freezing temperature of fine tailings	0°C
T_{at}	Ambient air temperature during thaw	varies
I	Insolation (rate of direct solar radiation - 30 yr average)	197 J/s·m ²
θ	Approximate thaw strain	50 %
α	Solar energy absorptance ratio	0.9
τ	Transmittance factor	1.0

Table 3.3 Shear Strength Ratios for Mine Tails (after Schiffman *et al.* 1988)

Description	Shear Strength Ratio
Cycloned Copper Slimes Tailings:	
Field Vane Data	$s_u/\sigma_{vo}' = 0.26$
CIU* Triaxial Test Data	$s_u/\sigma_{1c}' = 0.30$ to 0.33
CAU* Triaxial Test Data	$s_u/\sigma_{1c}' = 0.32$ to 0.34
Normally Consolidated Phosphate Clay Hydraulic Fills	$s_u/\sigma_c' = 0.22$
Cycloned Non-plastic Lead-Zinc Slimes	$s_u/\sigma_c' = 0.20$ to 0.22

*Note: CIU and CAU indicated "Isotropic Consolidation Undrained Triaxial" and "Anisotropic Consolidation Undrained Triaxial" respectively.

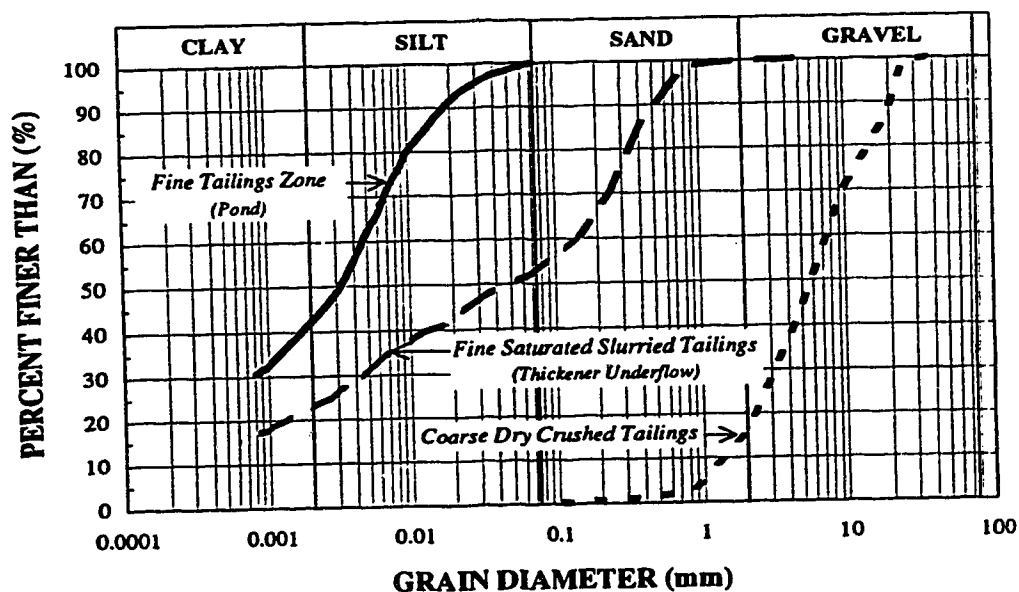


Figure 3.1

Grain Size Distribution of Coal Valley Waste Streams and Pond Fine Tails

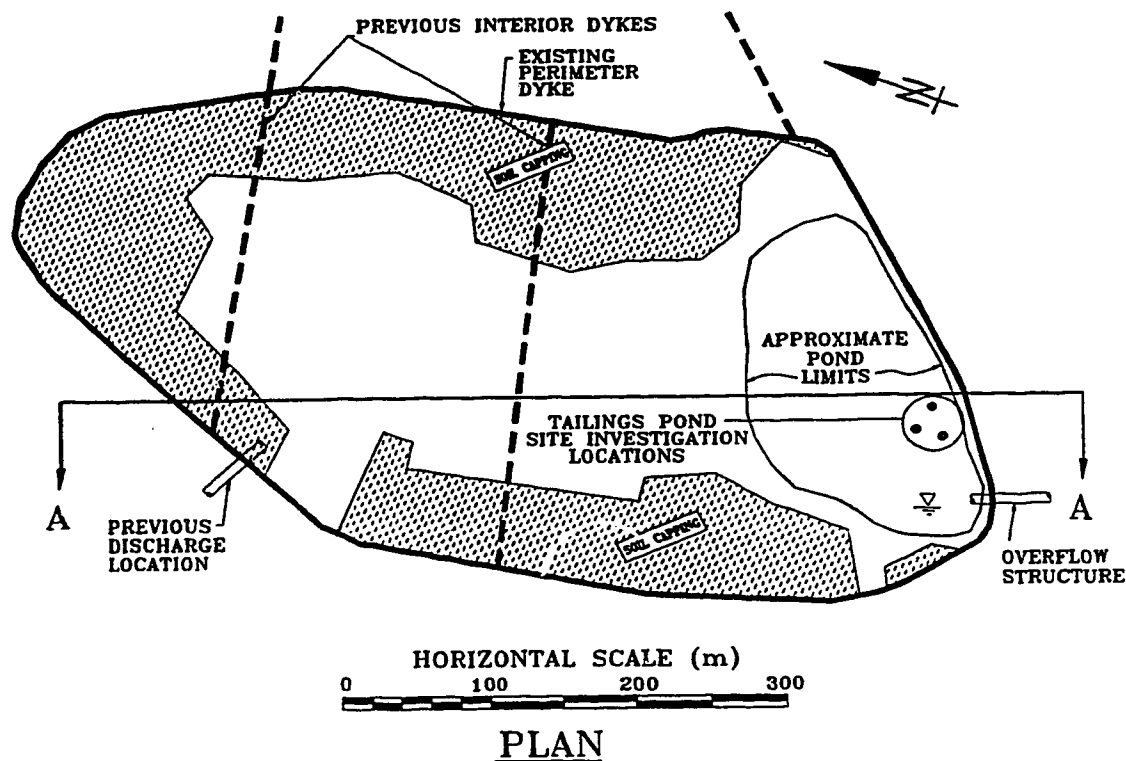


Figure 3.2a Plan of Coal Valley Tailings Impoundment

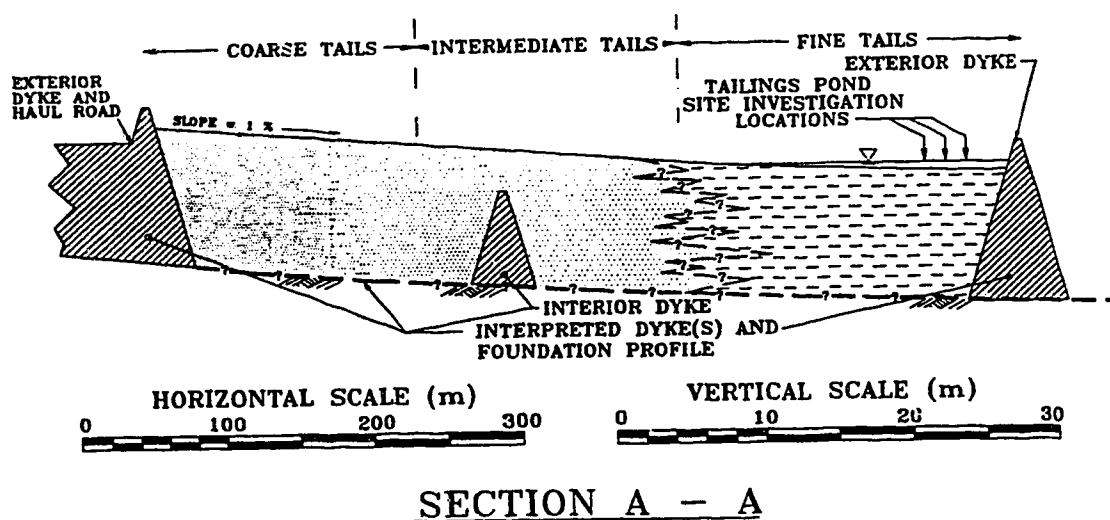


Figure 3.2b Section A-A Through Coal Valley Tailings Impoundment

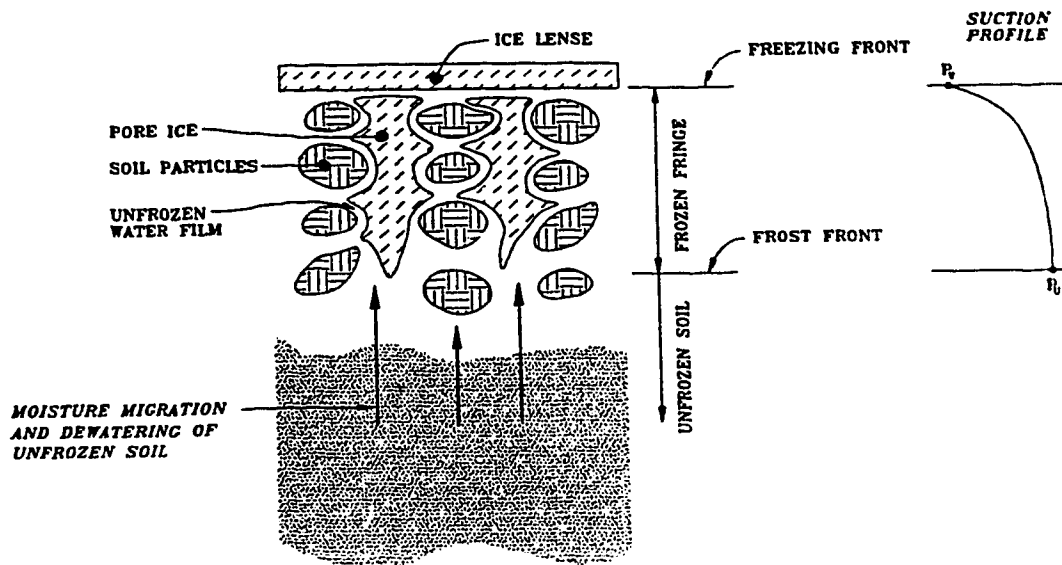


Figure 3.3 Schematic of Dewatering of a Soil During Freezing (after Konrad and Morgenstern 1983)

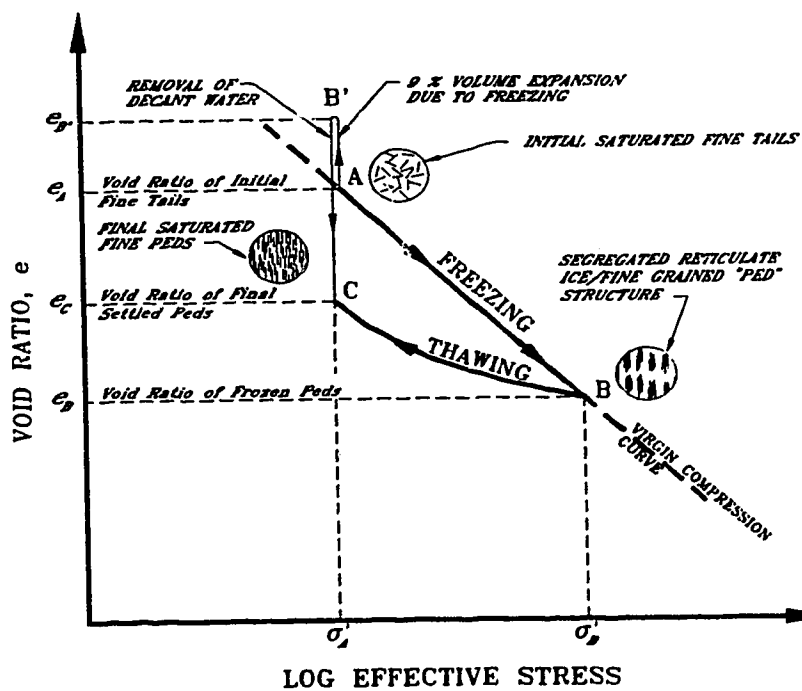


Figure 3.4 Void Ratio versus Effective Stress Model of Freeze-Thaw

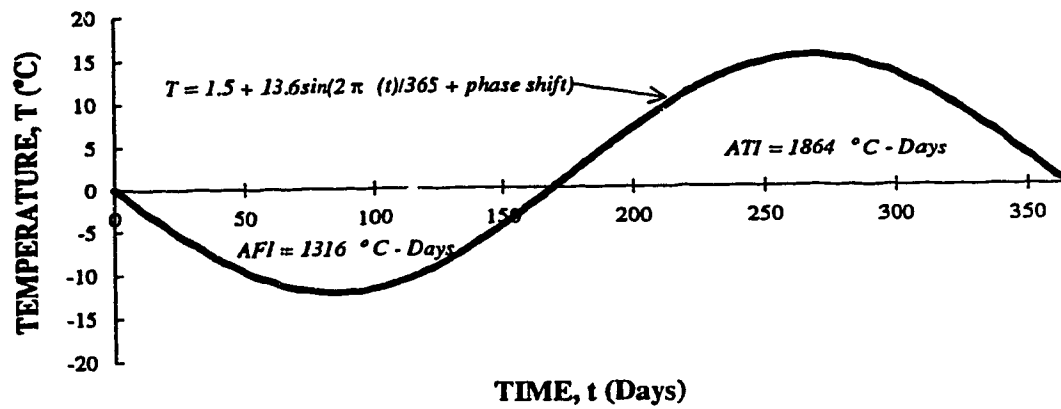


Figure 3.5 Idealized Seasonal Temperature Variation at Coal Valley

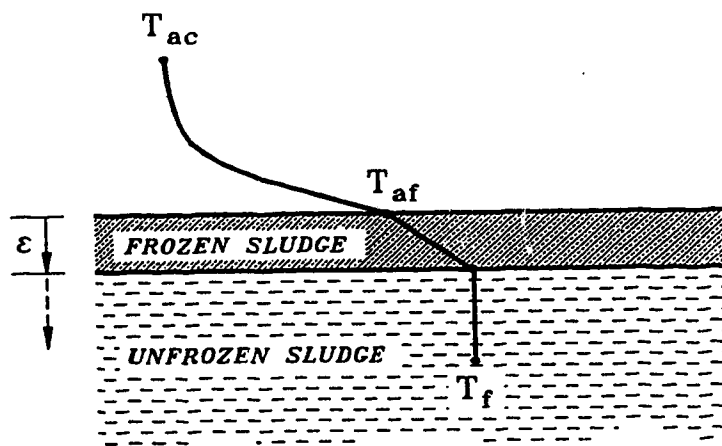


Figure 3.6 Schematic of Freezing Model (modified after Martel 1988)

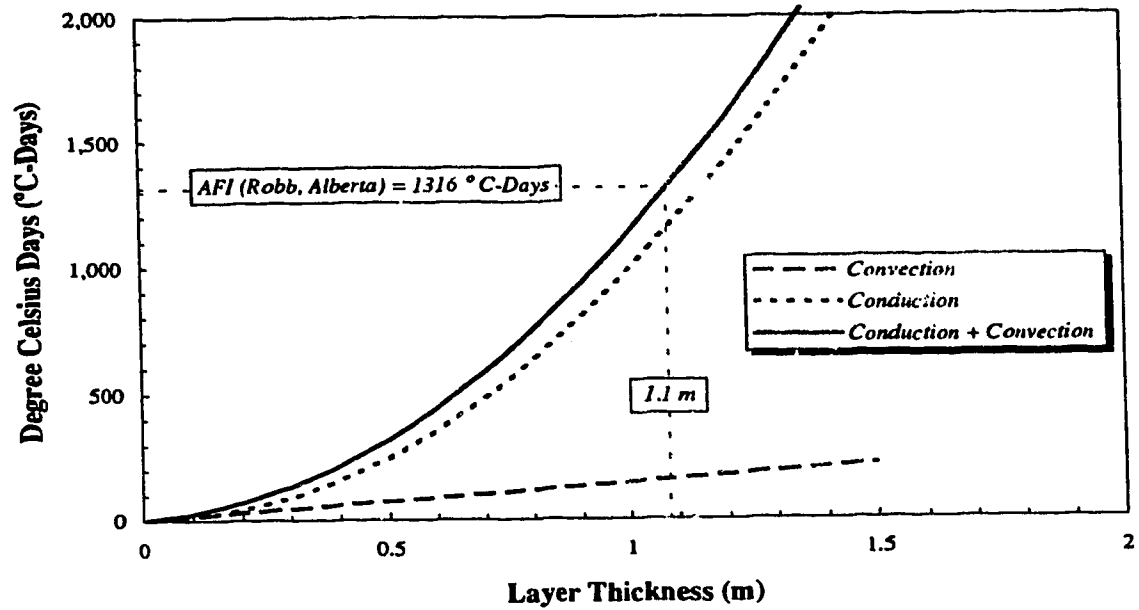


Figure 3.7 Air Freezing Index *versus* Layer Thickness for Fine Coal Tails

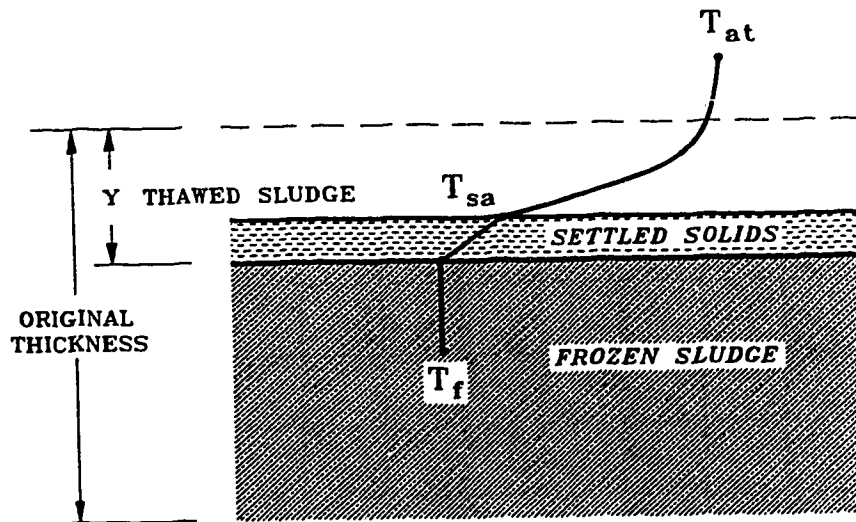


Figure 3.8 Schematic of Thawing Model (*modified after Martel 1988*)

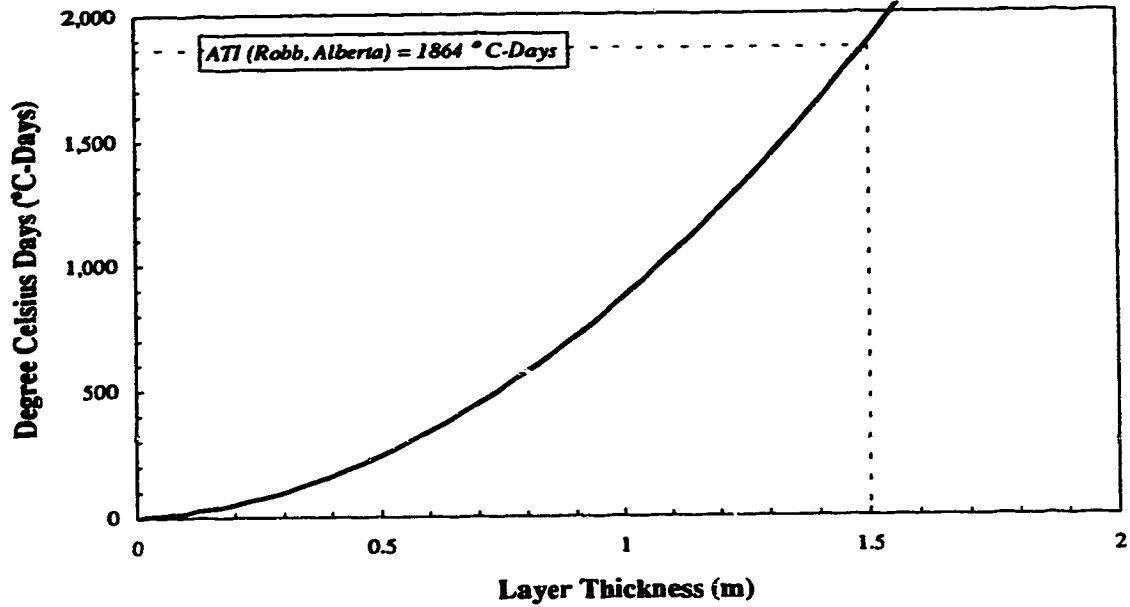


Figure 3.9 Air Thawing Index *versus* Layer Thickness for Fine Coal Tails

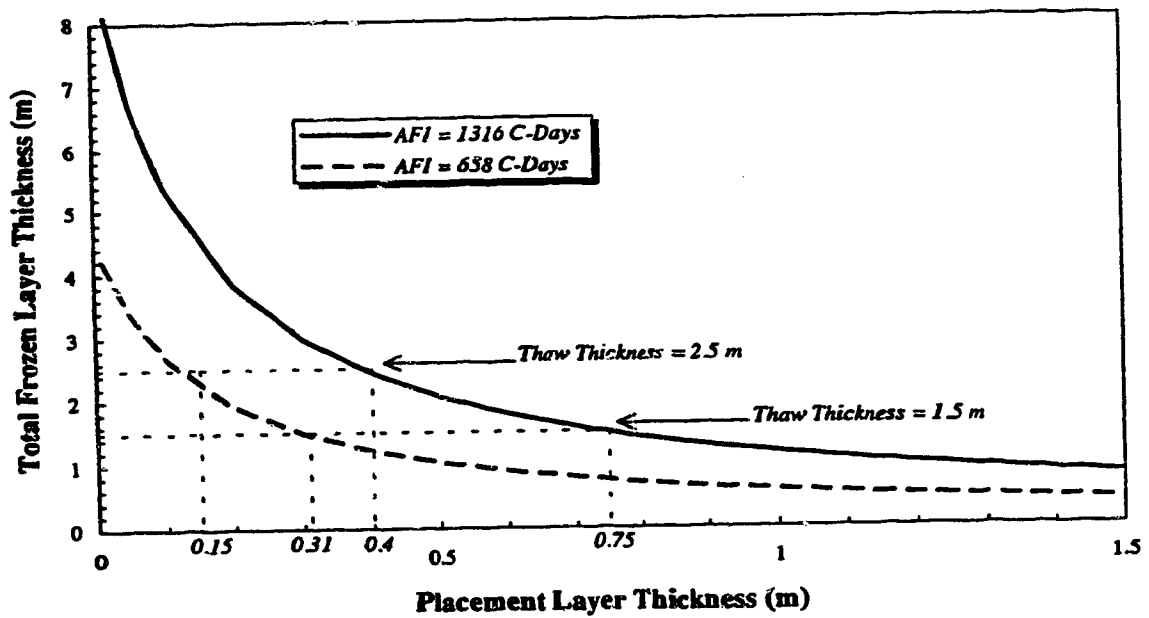


Figure 3.10 Layer Placement Optimization

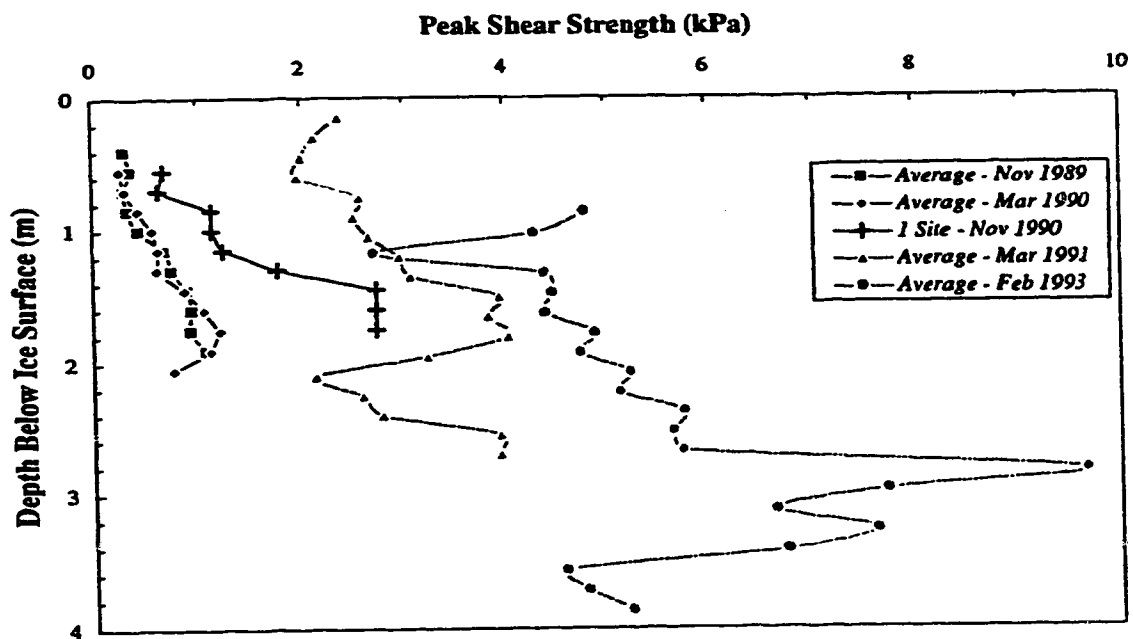


Figure 3.11 Pond Shear Strength Profiles

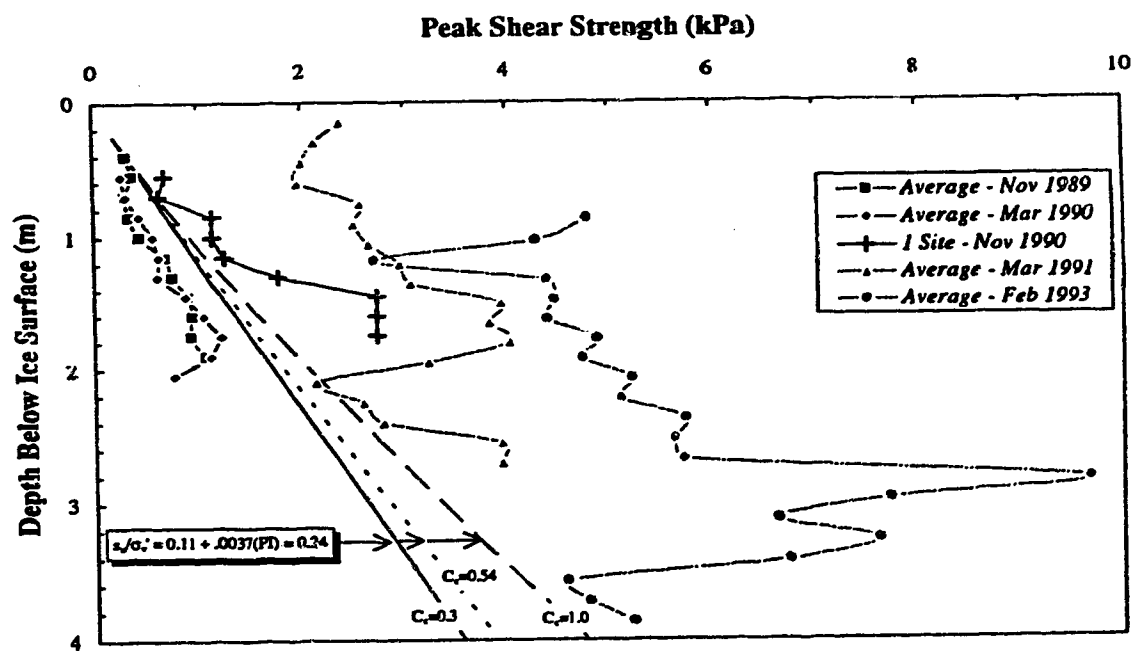


Figure 3.12 Comparison of Theoretical and Actual Pond Shear Strength Profiles

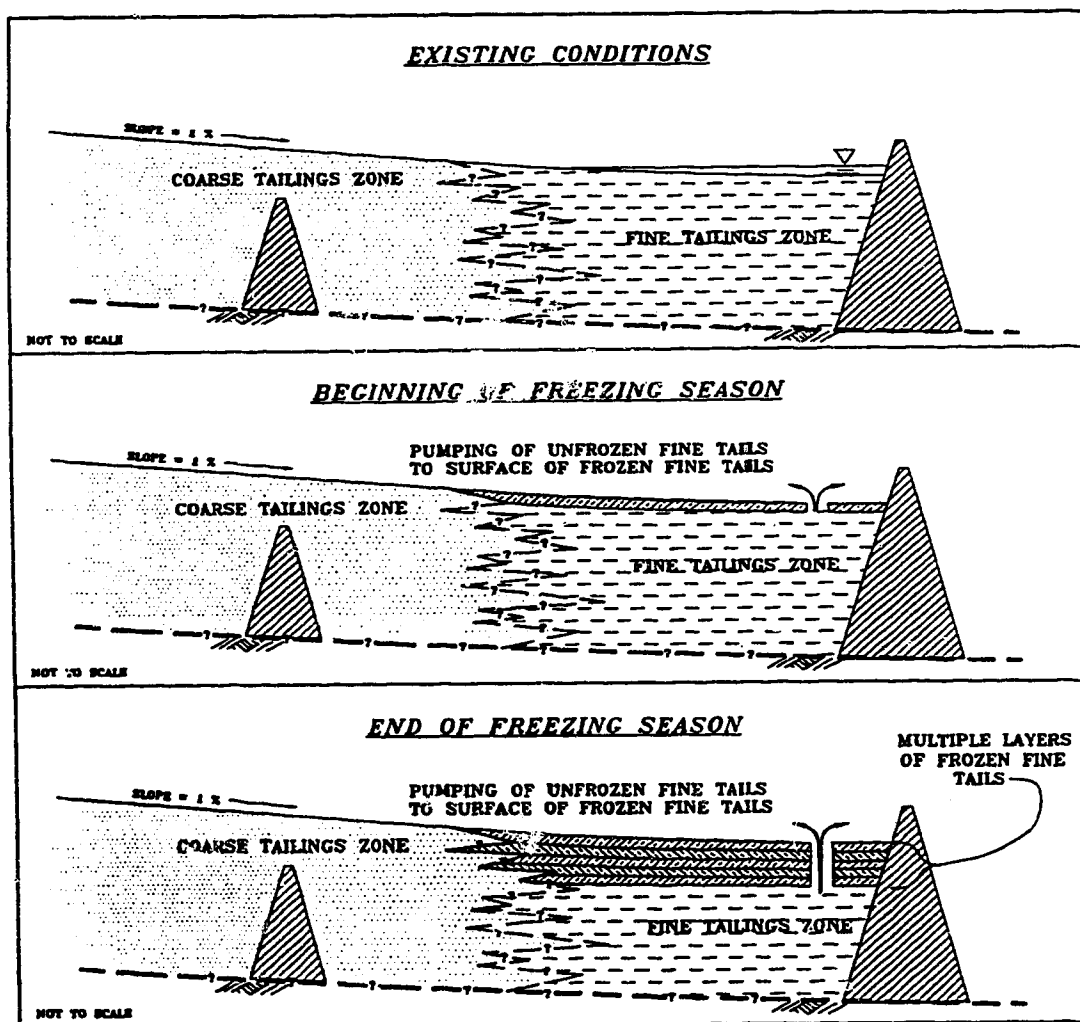


Figure 3.13 Proposed Freeze-Thaw Structural Enhancement for Fine Tails Region of Coal Valley Tailings Impoundment

Chapter 4

Characterization of Fine Processed Mine Tailings for Purposes of Dry Landscape Reclamation¹

4.1. INTRODUCTION

Tremendous volumes of fine processed mine wastes, composed typically of saturated sand, silt and clay, are generated yearly in Canada and around the world. As an example, the total volume of fine tailings produced by the Oilsands operating in northern Alberta is expected to exceed 1 billion cubic meters by the year 2020 (Liu *et al.* 1994). The majority of these mine wastes are deposited in surface impoundments which ultimately require reclamation after reaching capacity. Implementation of reclamation activities firstly requires physical and mechanical characterization of the final deposit to optimize the reclamation program.

Physical and mechanical characterization poses interesting geotechnical challenges due to the typically extremely weak nature and limited bearing capacity of these deposits. Many of these deposits are unable to support traditional truck mounted geotechnical testing equipment.

¹ Published Paper:

Stahl, R.P., Sego, D.C., Robertson, P.K., and Woeller, D., 1996. *Characterization of Fine Processed Mine Tailings Deposits For Purposes of Dry landscape Reclamation, Tailings and Mine Wastes '96, Fort Collins, Colorado, January 16-19, pgs. 515-524.*

Characterization of these fine tailings deposits of limited trafficability encouraged the development of three geotechnical testing systems. The first included a light weight Plate Load Test (*PLT*) system which could directly define the load-settlement behavior and bearing capacity of the tailings surface. The next system developed included a light weight frame capable of conducting Cone Penetration Test (*CPT*) soundings to a depth of at least 5 m. The last system includes the Spectral Analysis of Surface Waves (*SASW*) technique which provides a shear wave velocity profile of the near surface deposits. These lightweight geotechnical testing systems are described herein.

This equipment has been used to characterize two fine tailings deposits in Alberta for purposes of dry landscape reclamation. These deposits are the Coal Valley tailings impoundment located at the Coal Valley Mine located approximately 200 km east and 90 km south of Edmonton, and the Suncor Nonsegregated Tailings facility located approximately 500 km north of Edmonton. At the completion of deposition, both tailings deposits had limited trafficability and could not support loads much greater than human traffic. However, the deposits were effectively characterized using the modified lightweight testing equipment described above. The following presents some of the geotechnical results obtained at these tailings facilities.

4.2. TAILINGS FACILITIES

The Coal Valley Tailings Deposit, described by Stahl and Sego (1992) and Stahl and Sego (1993) is located at the Coal Valley mine which is owned and operated by Luscar Sterco (1977) Ltd.. The tailings impoundment, shown in Figure 4.1, is approximately 18.2 hectares in area and since reaching full capacity in 1989 has been undergoing reclamation activities. Fine processed saturated coal tailings slurry at a solids content of approximately 35% solids content were deposited into the impoundment through overboard depositional techniques. The segregating nature of the tailings slurry coupled with the depositional dynamics resulted in the development of a vertical and horizontal heterogeneous deposit with a general trend of decreasing grain size with increasing distance from the discharge point towards the pond. The grain size of the

heterogeneous shallow subsurface at the sites, varied approximately from well graded sand and silty sand at Site 1 to a sandy, clayey silt at Site 4.

The Suncor Oilsands Nonsegregated Tailings (NST) program included the construction of 5 geomembrane lined cells and one unlined U-shaped cell as discussed by Caughill *et al.* (1994) and shown in Figure 4.2. Without conditioning, the Suncor tailings (as do most mine tailings) segregate upon deposition with the water and fines separating from the sand. The ponds which house the fines and water have very low solids contents, exhibit very slow consolidation rates, and present problematic containment and abandonment issues. The nonsegregating tailings field trial at Suncor, prevent separation of fines and water from the slurried tailings upon deposition and eliminates some of the aforementioned problematic issues associated with the segregating tailings. The field test pits shown in Figure 4.2 were filled with NST produced on site using a small pilot plant. The NST were produced by connecting a slipstream of one of Suncor's main tailings lines to a hydrocyclone. The underflow from the hydrocyclone was conditioned with mature fine tails, with a solids content of approximately 30%, from a nearby tailings pond, then pumped to the test cells. Sulfuric acid and lime were added to the pumped tails to flocculate the fines (material <44 microns) and encourage a nonsegregating tailings slurry. Detailed background regarding the test cells, tailings mixes, chemical additions, and depositional variables is provided by Caughill *et al.* (1994). The sites characterized are located in cells 3 and 4 with their locations shown in Figure 4.2. The final NST deposit when characterized in October, 1994, approximately one year after deposition, may be described as a silty sand with a solids content of approximately 82 %.

4.3. PLATE LOAD TEST (PLT)

The Plate Load Test (PLT) apparatus employed at the Coal Valley and Suncor NST tailings sites is schematically shown in Figure 4.3. The relative remote nature of these tailings sites and the generally weak, yet potentially variable nature of the deposits dictated the following design criteria for the PLT apparatus.

- i. High load capacities (10 kN) required to fail a 300 mm diameter plate at the coarser grained, stronger tailings sites.
- ii. Light weight, easily dismantled and transported with human effort to all (particularly the weakest) tailings sites.
- iii. Computerized load and settlement monitoring for accurate determination of load-deformation characteristics and ultimate failure load.
- iv. Settlements as much as 50 % of footing diameter (100 to 150 mm) may be required to determine large strain load-deformation characteristics and ultimate failure load in soils exhibiting punching shear failure.

A variety of tailings surface conditions were investigated at the Coal Valley tailings deposit. The 1991 field testing program included tests on the bare, unvegetated tails, the sparsely vegetated tails, and tailings at depths of approximately 0.1 to 0.2 m. The tests on the "vegetated tails" were conducted following removal of surface vegetation in order to capture the influence of the vegetative root system on bearing capacity. The enhanced vegetative cover experienced during the 1994 investigation program precluded tests on bare, unvegetated tails and only tests conducted on vegetated tails and tails at depth could be conducted. Surface plate load tests, conducted at the Suncor NST facility in 1994, could only be conducted on the partially desiccated tailings surface. No vegetation was present. Furthermore, the elevated pore water pressure conditions experienced at the Suncor NST Cells 3 and 4 prevented plate load tests being conducted at depth.

The PLT data from both Coal Valley and Suncor is plotted in terms of Pressure (Q) versus Settlement (s), and Pressure versus Relative Settlement (RS) where:

$$Pressure = Q = \frac{Load(L_p)}{Plate Area(A_p)} \quad [4.1]$$

and

$$Relative Settlement = RS = \frac{Settlement(s)}{Plate Diameter(D_p)} \quad [4.2]$$

The punching failure mechanism discussed by Vesic (1973) was observed with all tests. Figure 4.4 illustrates the punching behavior observed at Site 3b of the Suncor MST deposits. Note that the ultimate failure loads is in the range of human traffic (40 kPa). As contrast, illustrating the variability in load-deformation behavior of tailings surfaces, the plate load test results obtained in 1994 at the Coal Valley tailings impoundment (Site 1) is illustrated in Figure 4.5.

4.4. CONE PENETRATION TEST (CPT)

The cone used for the investigations was a ASTM standard electronic cone. The pore pressure element to record penetration, dissipation, and static pore water was located directly behind the cone tip. Coupled between the cone and the push rods was a friction reducer to reduce frictional resistance along the rods.

The low capacity cone employed, using a load cell of 2.5 tons, provides a greater sensitivity and accuracy when investigating weak and/or highly compressible soils. The capacities for the cone tip, friction sleeve, and pore pressure element were 2.5 MPa, 0.25 MPa, and 1.73 MPa respectively. Data was recorded using a Hogentogler data acquisition system.

As with the plate load test design requirements, the CPT system had to be light weight and easily transported using human effort, yet capable of supplying in excess of 4 kN of pushing force for the desired 5 m of penetration. The system developed used a Nilcon Vane Shear pushing frame with modifications to the head assembly to facilitate cone pushing. A schematic of the complete pushing frame and CPT equipment provided by ConeTec Investigations Ltd. is illustrated in Figure 4.6. The pushing frame could be easily dismantled into two pieces and transported to the testing sites.

The initial CPT data of total cone resistance, (q_t), was plotted versus depth where (Robinson 1990):

$$q_t = q_c + (1 - a)u \quad [4.3]$$

where q_c is the total cone penetration resistance, u is the pore water pressure recorded behind the cone tip and a is the net area ratio equal to 0.85.

In addition to the total cone resistance information, the data includes plots of the friction resistance, (f_s), pore pressure, (u), and friction ratio, (R_f) versus depth. The friction ratio helps classify the soil according to behavior under CPT penetration and is defined as:

$$R_f = \frac{f_s}{q_c} \times 100\% \quad [4.4]$$

The CPT data obtained from the Suncor NST Site 3a is shown in Figure 4.7.

4.5. SPECTRAL ANALYSIS OF SURFACE WAVES (SASW)

SASW method is a non-intrusive *insitu* test that uses the principles of elasticity and surface wave dispersion to determine the shear wave velocity, V_s with depth at a site. The shear wave velocity, which is primarily a function of void ratio and effective confining stress, can be used to evaluate *insitu* state, small strain moduli (strains of less than 0.001 percent), and susceptibility to liquefaction (Cunning *et al.* 1994).

Following the forward modeling procedure and the matching of the theoretical dispersion curve with the field dispersion curve using a Windows based forward modeling program entitled WinSASW, the key parameters developed from the modeling include the shear wave velocity and layer thickness. The shear wave velocity may subsequently be used to develop profiles of soil small strain modulus with depth. The small strain shear modulus, G_0 , and small strain drained or undrained elastic modulus, $E_{o,d,ud}$ may be computing using:

$$G_o = \rho V_s^2 \quad \text{and} \quad E_{o,d,ud} = 2(1 + \nu_{d,ud})G_o \quad [4.5]$$

where $\nu_{d,ud}$ are the appropriate drained and undrained Poisson's ratio of the soil.

As described by Robertson *et al.* (1995), the small strain shear modulus, coupled with the cone penetration profile provides a powerful characterization tool for identification of "unusual" soils which are either highly compressible, or exhibit cemented or aged properties. Identification of "unusual" soils exhibiting these properties, which maybe encountered in tailings deposits, provides opportunity to make modifications to the empirical CPT correlations to reflect soil behavior.

4.6. SUMMARY

Three lightweight geotechnical testing systems were developed to characterize fine processed mine tailings which exhibit limited bearing capacity and which would be unable to be characterized using conventional geotechnical testing methods. The equipment developed included a plate load test apparatus to evaluate the punching shear load-deformation behavior of the surficial tailings. The next system included the cone penetration test system which could help define material type and empirically defined mechanical properties. The third system, entitled the Spectral Analysis of Surface Waves technique determines the shear wave velocity profile at a site. The small strain shear modulus determined from the shear wave velocity profile, coupled with the cone penetration test information provides a powerful tool for evaluating "unusual" soils which are highly compressible or have been influenced through aging or cementation.

4.7. REFERENCES

- Addo, K., and Robertson, P.K., 1992. Shear Wave Velocity Measurement of Soils Using Rayleigh Waves. *Canadian Geotechnical Journal* 29:558-568.

- Caughill, D.L., Scott, J.D., Lui, Y., Burns, R., Shaw, W.H., 1994. 1993 Field Program on Nonsegregating Tailings at Suncor Inc. 47th Canadian Geotechnical Conference, September 21-23, Halifax, Nova Scotia, p. 524-536.
- Cunning, J.C., Robertson, P.K. and Sego, D.C., 1994. Shear Wave Velocity to Evaluate In-situ State of Sands. 47th Canadian Geotechnical Conference, September 21-23, Halifax, Nova Scotia, p. 307-316.
- Lui, Y., Caughill, D., Scott, J.D., Burns, R., 1994. Consolidation of Suncor Nonsegregating Tailings. 47th Canadian Geotechnical Conference, September 21-23, Halifax, Nova Scotia, p. 504-513.
- Robertson, P.K., 1990. Soil Classification Using The Cone Penetration Test. Canadian Geotechnical Journal, 27:151-158.
- Robertson, P.K., Fear, C.E., Woeller, D.J., and Weemee, I., 1995. Estimation of Sand Compressibility from Seismic CPT. 48th Canadian Geotechnical Conference, September 25-27, 1995, Vancouver, B.C..
- Stahl, R.P. and Sego, D.C., 1992. Influence of Natural Surface Processes on Reclamation of the Coal Valley Tailings Impoundment. Second International Conference on Environmental Issues and Management of Waste in Energy and Mineral Production, Calgary, Alberta, September 1-4, pp. 389-400.
- Stahl, R.P. and Sego, D.C., 1993. Freeze-Thaw Dewatering and Structural Enhancement of Fine Coal Tails. 46th Canadian Geotechnical Conference, Saskatoon, Saskatchewan, September 27-29, pp. 157-166.
- Stokoe, K.H., and Nazarian, S., 1985. Use of Rayleigh Waves in Liquefaction Studies. ASCE proceedings of Measurement and Use of Shear Wave Velocity for Evaluating Dynamic Soil Properties. pp. 1-17.
- Vesic, A.S., 1973. Analysis of Ultimate Loads of Shallow Foundations. Journal of Soil Mechanics and Foundation Division, ASCE. 99(1).45-73.

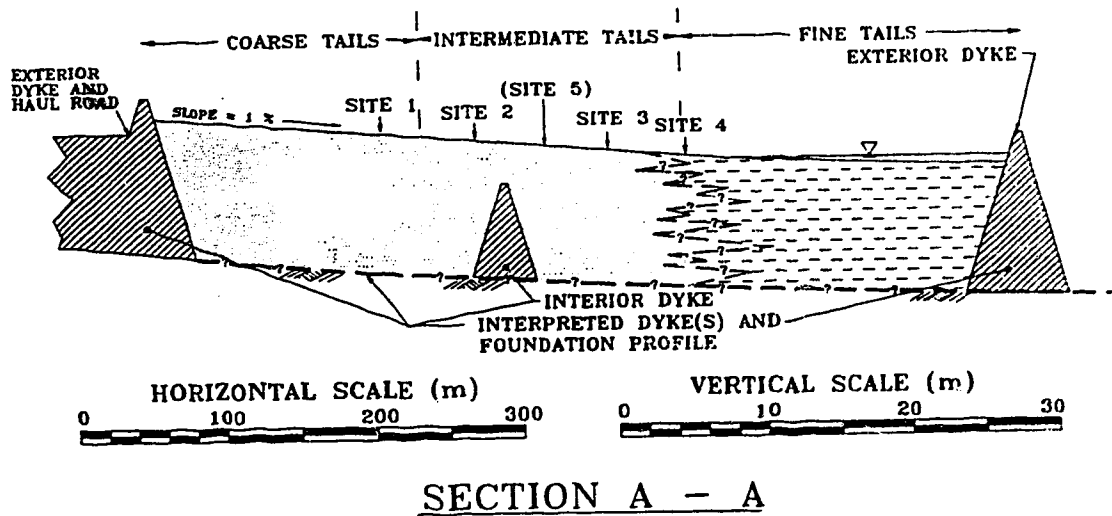
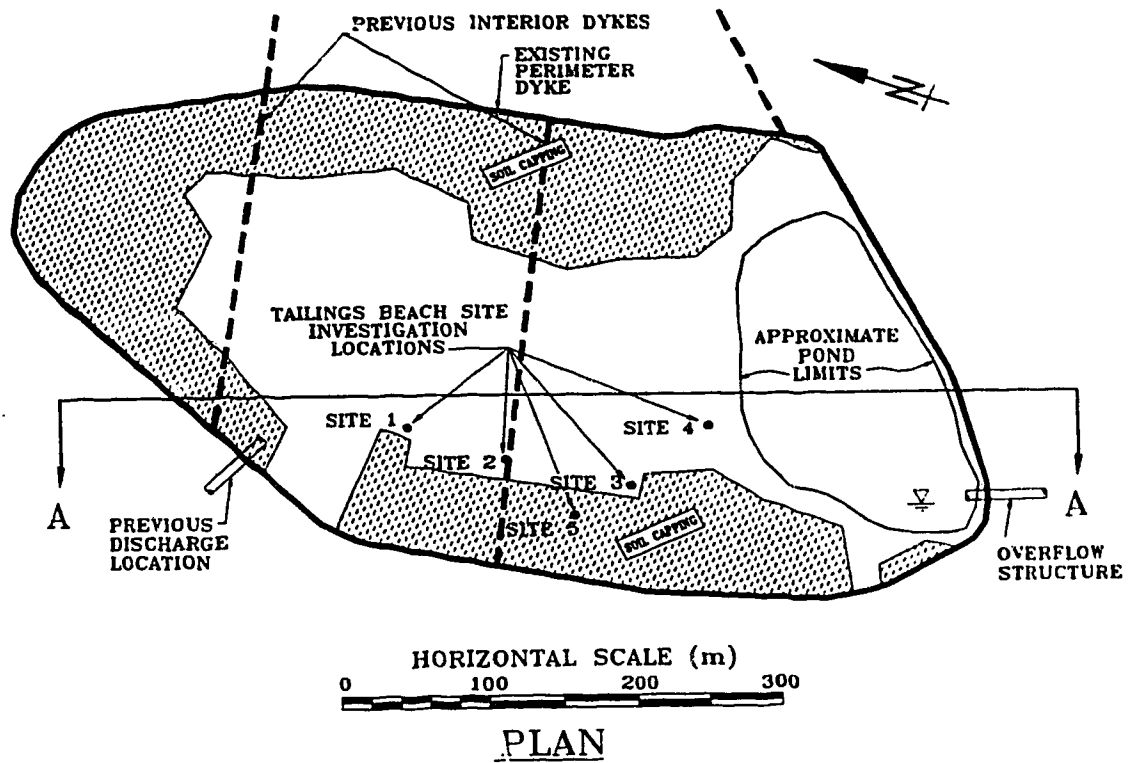


Figure 4.1

Plan and Section of Coal Valley Tailings Impoundment

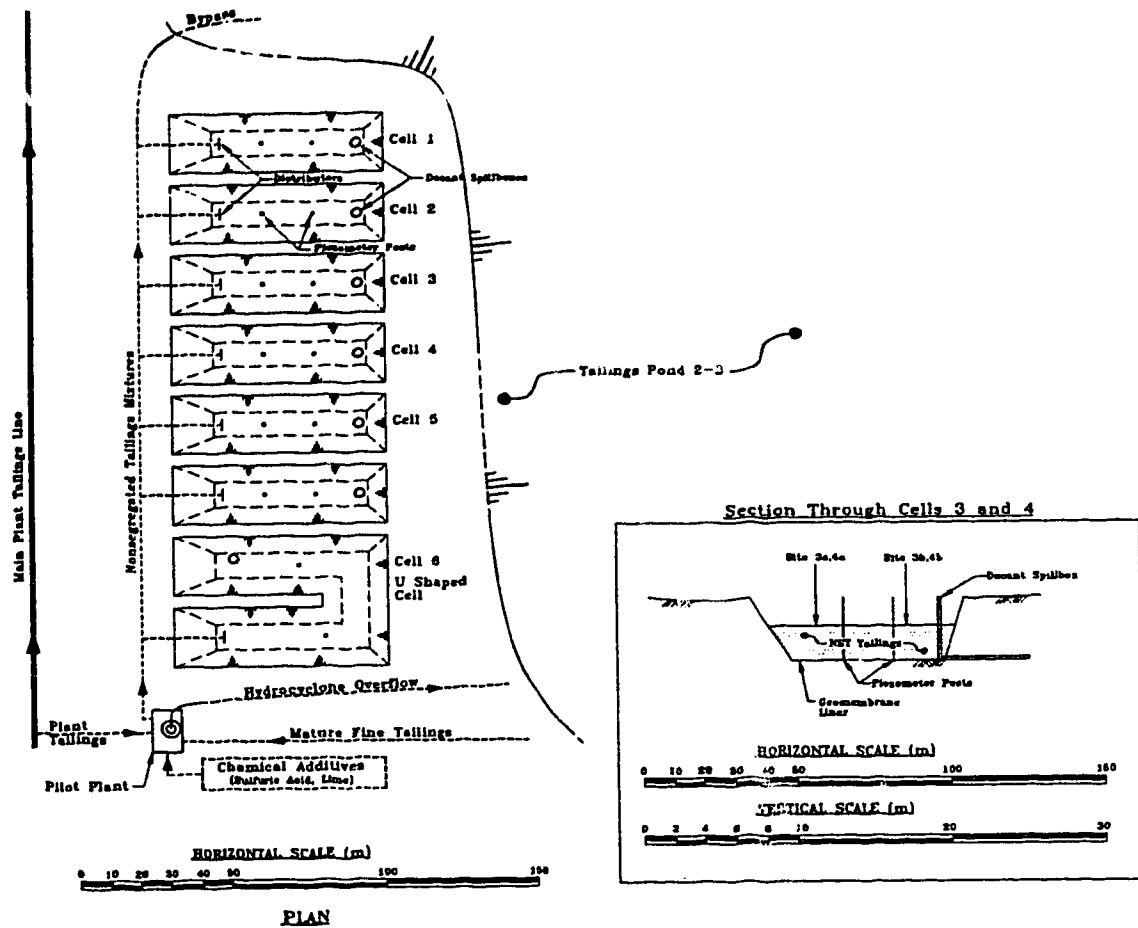


Figure 4.2 Plan and Section of Suncor's NST Facility

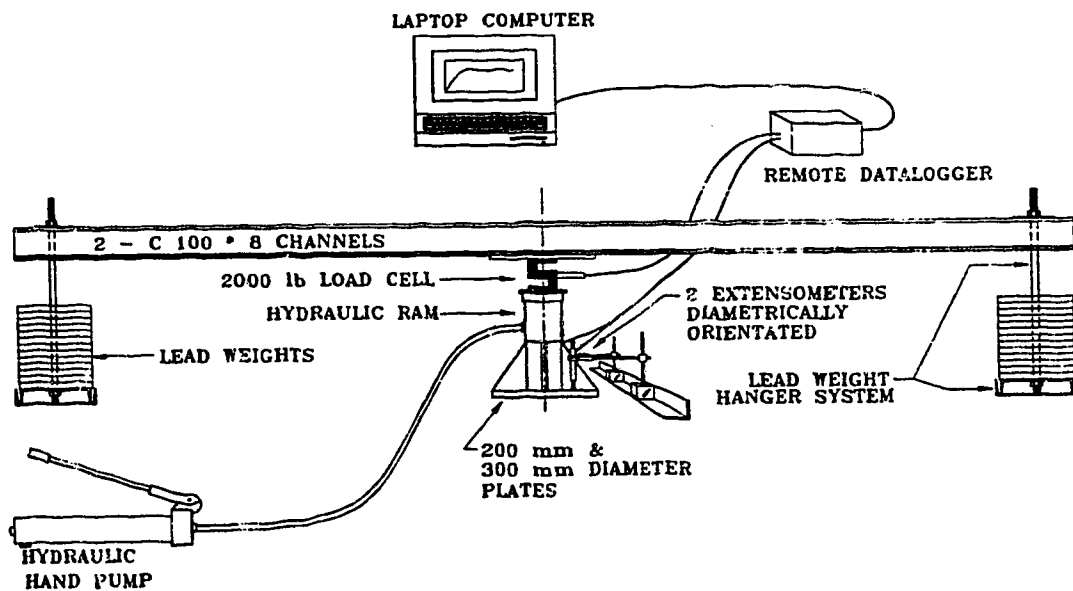


Figure 4.3 Plate Load Test (PLT) Apparatus

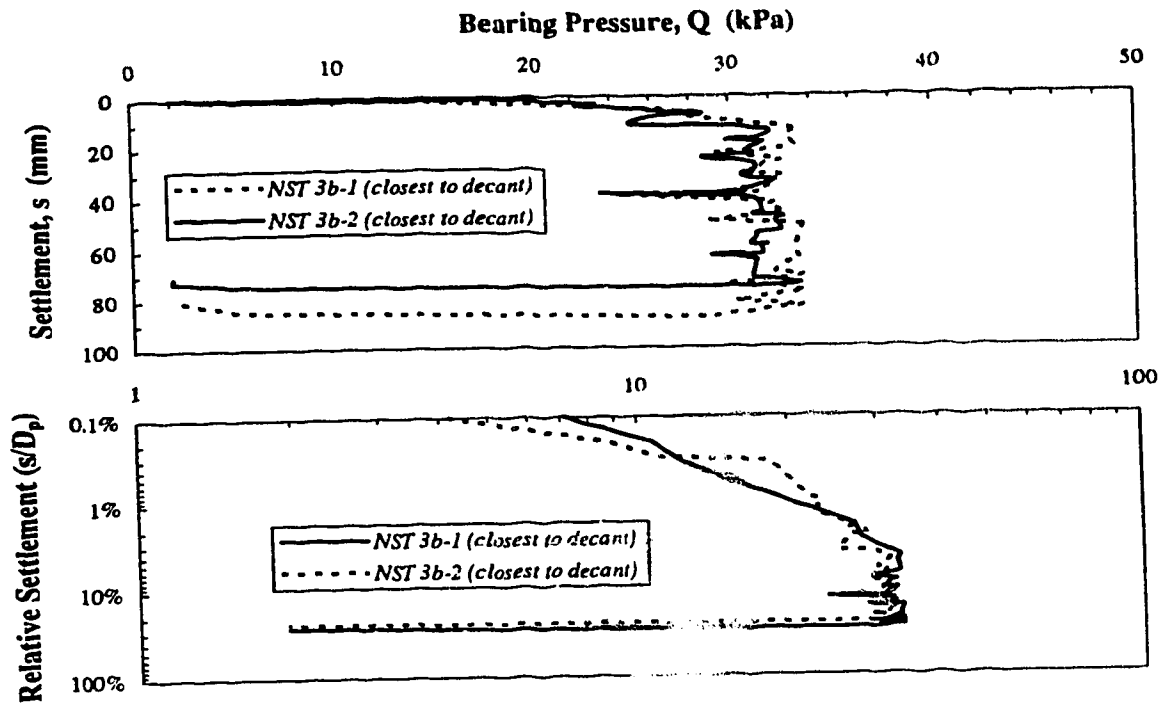


Figure 4.4 Plate Load Test Results at Suncor NST Site 3b

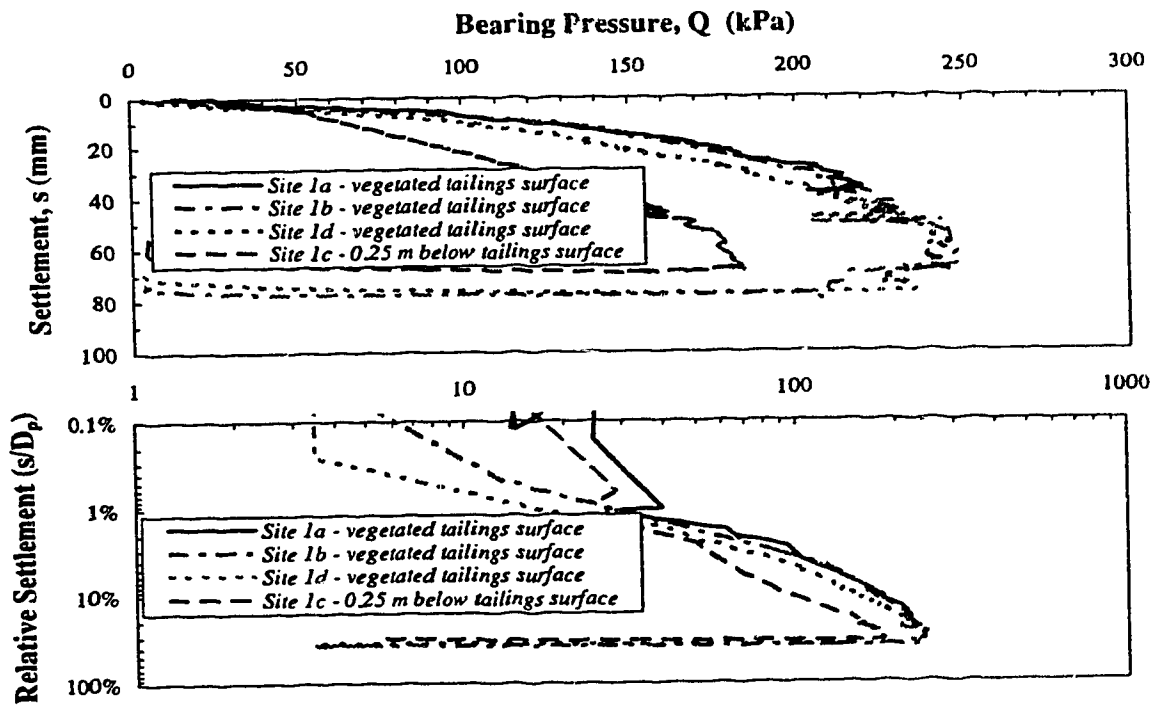


Figure 4.5 Plate Load Test Results at Coal Valley's Tailings Impoundment - Site 1

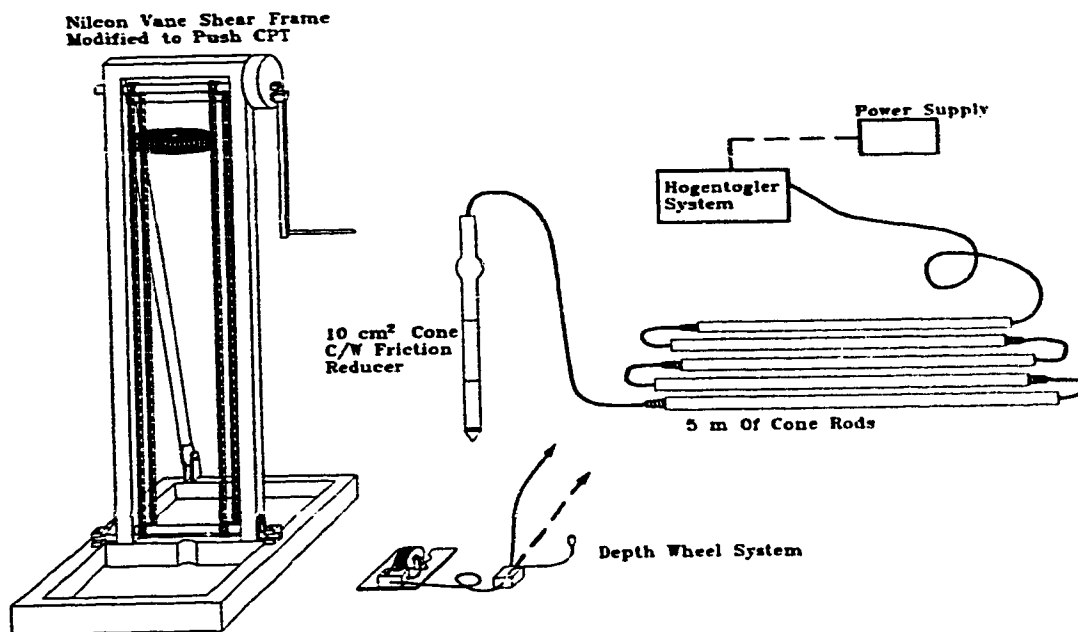


Figure 4.6 Cone Penetration Test (CPT) Apparatus

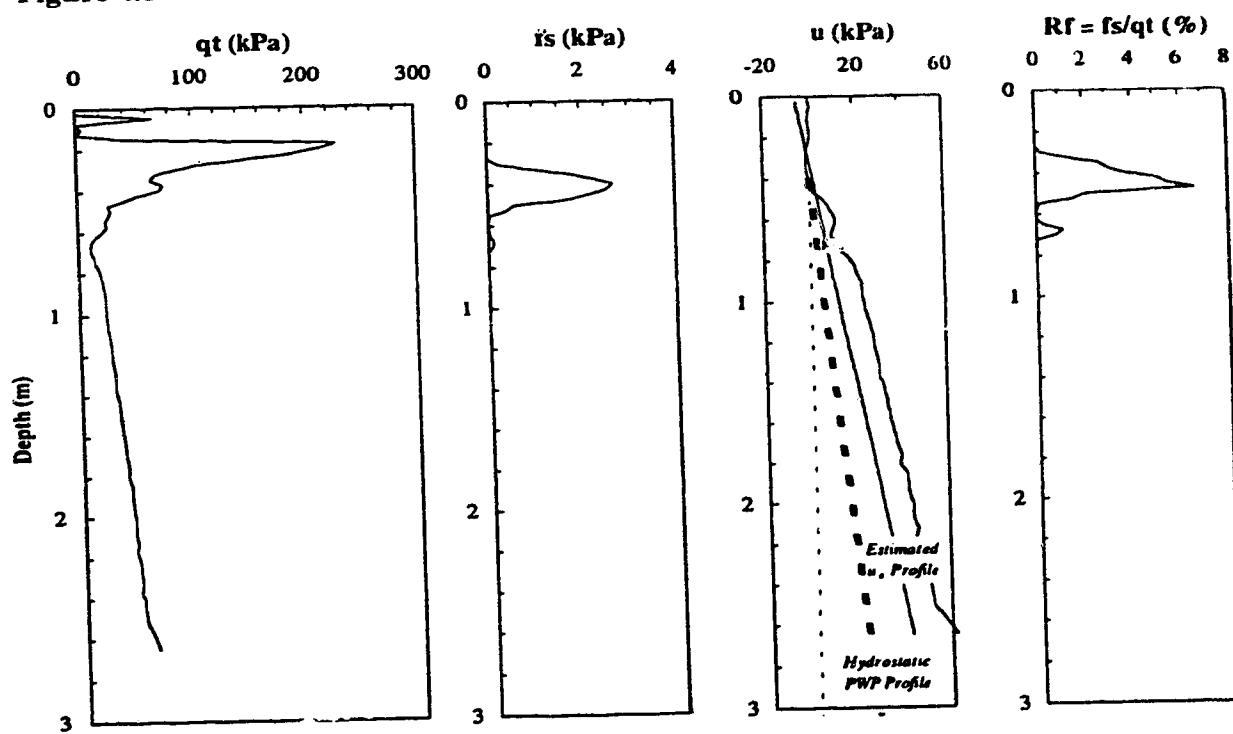


Figure 4.7 Cone Penetration Test Results at Suncor NST Site 3b

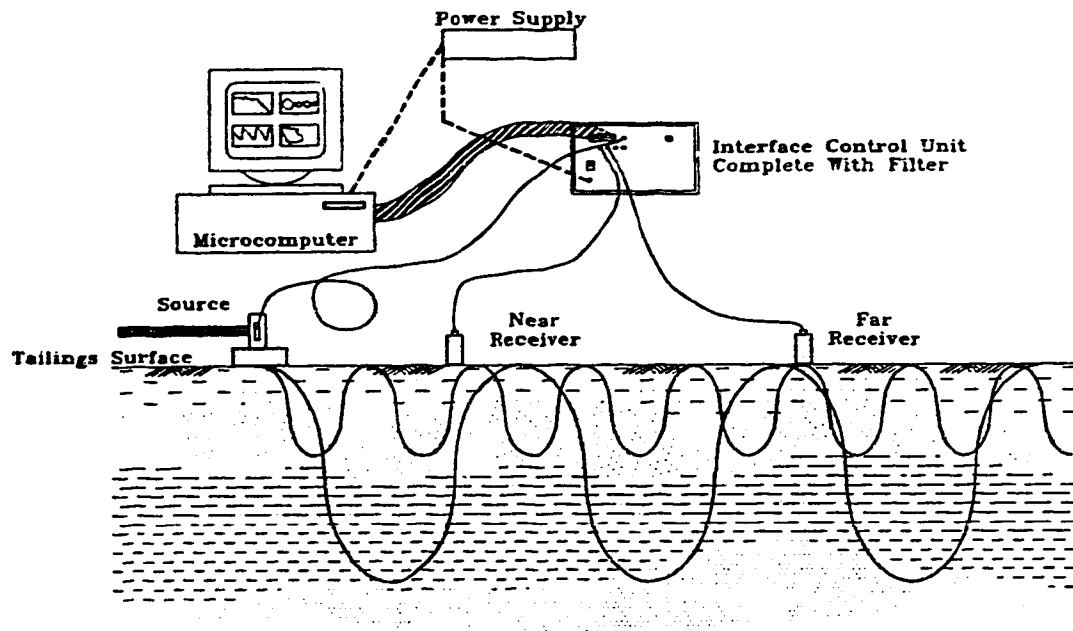


Figure 4.8 Spectral Analysis of Surface Waves System

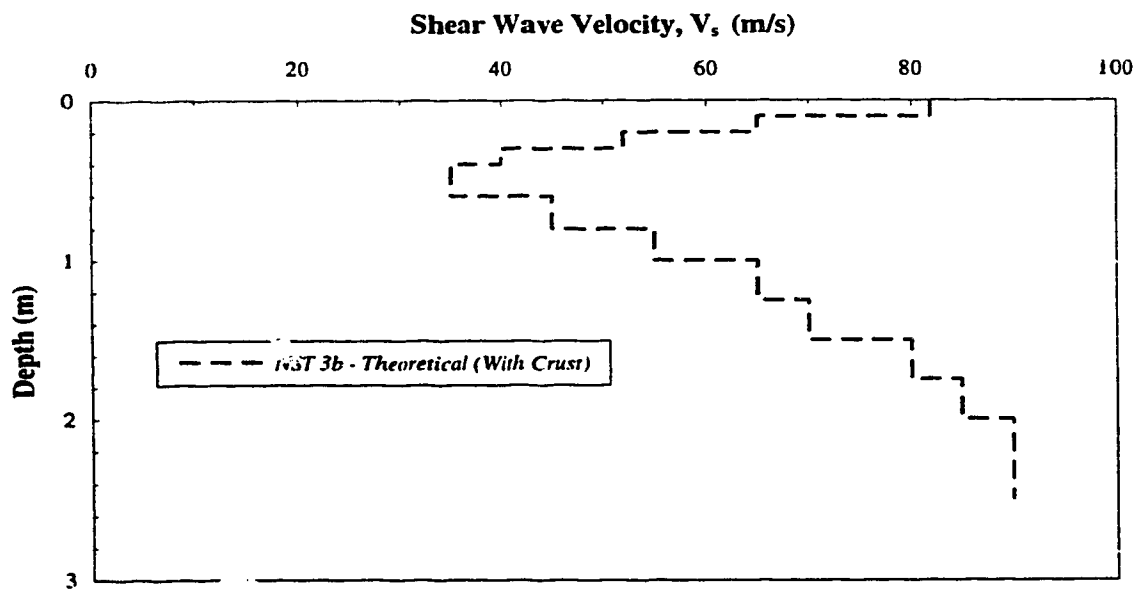


Figure 4.9 Shear Wave Velocity Profile at Suncor NST Site 3b

Chapter 5

Shear Strength And Bearing Capacity Of Fine Coal Tailings And Processes Contributing To Their Dry Landscape Reclamation¹

5.1. INTRODUCTION

The Coal Valley mine owned and operated by Luscar Sterco (1977) Ltd., located approximately 200 km east and 100 km south of Edmonton, Alberta, developed an 18.2 hectare impoundment to contain fine saturated coal tailings. During deposition of the slurried tailings stream, segregation occurred as coarser particles settled along the depositional beach with finer particles transported to the pond to undergo sedimentation. Segregation resulted in the development of three zones including the coarse tailings region near the discharge point, the fine tailings region at the pond, and an intermediate region located between the two extremes. Figure 5.1 includes a section through the impoundment illustrating these zones as well as the site investigation locations. Details highlighting the depositional dynamics and shallow subsurface stratigraphy at each of the sites are provided by Stahl and Sego (1992).

Upon completion of deposition in 1989 and during the initial stages of dry landscape reclamation, the majority of the deposit was extremely weak and could not support human traffic. The

¹ Submitted Paper:

Stahl, R.P., Sego, D.C., and Robertson, P.K., 1996. Mechanical Properties of Coal Tails and Natural Processes Contributing to Their Reclamation. Second International Conference on Environmental Geotechnique, IS-OSAKA '96, Osaka, Japan, November 5-8, 6 pgs.

reclamation activities since 1989 have included localized soil capping, aerial and nonaerial seeding and fertilization. Natural processes contributing to the reclamation objective include drainage, evaporation, evapotranspiration, fibre reinforcement of vegetative root systems, and freeze-thaw consolidation. The site investigation activities along the depositional beach will highlight the influence of evaporation, evapotranspiration and fibre reinforcement on the increased strength and surface stability of the coal tails. The impact of freeze-thaw on consolidation and strength gain of the fine saturated tails within the pond is discussed by Stahl and Sego (1995) and will not be presented.

5.2. INSITU TESTING

A variety of *insitu* tests were conducted along the tailings beach and in the pond region following the impoundment reaching full capacity. The key site investigation techniques which are discussed herein include the Field Vane Shear Test (FVST), Cone Penetration Test with pore pressure measurements (CPTU), and Plate Load Test (PLT). The FVST results were obtained using a Nilcon vane shear device. Both the CPTU and PLT apparatus, which required only human effort to transport them to the various sites, are discussed by Stahl *et al.* (1996).

5.3. UNDRAINED SHEAR STRENGTH

The undrained shear strength was determined along the beach portion of the impoundment using the FVST assuming that the shear strength, S_u is equal to:

$$S_u = \frac{T}{\pi D^2 [H/2 + D/6]} \quad [5.1]$$

where T is the maximum applied torque, and D and H are the diameter and height of the vane respectively. Although several papers discuss the impact of factors including sensitivity and related progressive failure effects, shear stress distribution, failure rate, and anisotropy

(Mahmoud 1988, De Alencar *et al.* 1988), no corrections were applied to the shear strengths determined using [5.1].

The undrained shear strength may be derived from the CPTU profiling information using the corrected cone tip resistance, q_t , or the excess pore water pressure, Δu , generated during penetration (Robertson and Campanella 1983, Robertson and Van Impe 1987). Considering, q_t , the shear strength, S_u , may be estimated by

$$S_u = \frac{q_t - \sigma_{vo}}{N_{kt}} \quad [5.2]$$

where σ_{vo} is the total vertical stress, and N_{kt} is the empirical or semi-empirical cone factor. Models to describe the cone tip resistance and corresponding shear strength are based on classical bearing capacity theory, cavity expansion theory, or the strain path method (Teh and Houlsby 1991). The latter two methods require an estimation of the rigidity index, I_r , of the soil which is the ratio of the undrained shear modulus to the undrained shear strength. Based on an estimated I_r of about 60, a preliminary “first-cut analysis” N_{kt} of 16 was chosen to predict the shallow subsurface shear strength profile at all four sites along the impoundment.

The undrained shear strengths at Sites 1 through 4 determined using the FVST and [5.1] and the CPTU and [5.2] are shown in Figure 5.2. This figure illustrates that the preliminary N_{kt} factor was satisfactory in predicting an S_u from the CPTU in the same range as that predicted by the FVST. It is expected that efforts to “fine-tune” the N_{kt} values, considering the vertical and horizontal heterogeneity within the subsurface, would produce more closely matching shear strength profiles. It is observed that in general, the average shear strength at depth, and the thickness of the surface crust due to evapotranspiration, decrease in a downstream fashion from Site 1 near the initial tailings discharge to Site 4 near the pond.

5.4. BEARING CAPACITY

A variety of PLT boundary conditions were investigated along the depositional beach with the results from the 1991 and 1994 investigation programs compared in Figure 5.3. The PLT results, which exhibited punching shear failure mechanism as discussed by Vesic (1975), indicate that the maximum bearing pressure increased substantially from 1991 to 1994. Sites 1, 2, and 4 displayed an increase and percent increase in capacity at maximum settlement of 140 kPa (150%), 60 kPa (40%), and 80 kPa (190%) respectively. In addition, the 1994 PLT results displayed a decrease in slope of the load-settlement behavior (increase in modulus) compared to the 1991 results. The increased bearing capacity and modulus is mainly reflective of the enhanced reinforcement provided by the developing vegetative root system. Finally, the PLT results from both years indicate that the surface bearing capacity is greater than that at depth. The bearing capacity reduction observed with depth in 1991 PLT's is believed to result from a decrease in matric suction and shear strength with depth. Although matric suctions were not measured, visual observations of a desiccated crust resulting from evaporation support this theory. The bearing capacity reductions observed with depth in the 1994 PLT's are believed to result from a coupled effect of reduced matric suction and reduced reinforcement of the vegetative root system. The effects of matric suction and vegetative root systems on shear strength are presented below.

5.5. SURFACE STABILITY PROCESSES

5.5.1. Evaporation/Evapotranspiration

The processes of evaporation, evapotranspiration, and drainage along the Coal Valley tailings impoundment results in the development of a two phase geotechnical subsurface system which includes a variable thickness unsaturated zone at the surface and a saturated zone at depth.

The shear strength of unsaturated soils may be defined in terms of two stress variables, $(\sigma - u_a)$ and $(u_a - u_w)$, as (Fredlund *et al.* 1978, Fredlund and Rahardjo 1993):

$$\tau_f = c' + (\sigma - u_a)_f \tan \phi' + (u_a - u_w)_f \tan \phi^b \quad [5.3]$$

where c' is the effective cohesion parameter, σ , u_a , u_w denote total stress, pore air pressure, and pore water pressure, $(\sigma - u_a)_f$ is the net normal stress on the failure plane at failure, $(u_a - u_w)_f$ is the matric suction on the failure plane at failure, ϕ' is the angle of internal friction with respect to net normal stress, and ϕ^b is the angle of internal friction with respect to matric suction. The shear strength of saturated soils is a special case of [5.3] where the u_a term of the stress variable $(\sigma - u_a)$ equals the u_w value and $(u_a - u_w)$ approaches zero. Based on [5.3], the *insitu* shear strength and bearing capacity can change as a result of changes to matric suction in response to changes in climatic conditions such as evaporation, evapotranspiration, and precipitation. Evidence to the possible variation in matric suction in response to these environmental factors, namely evaporation and evapotranspiration, was observed with the reduced bearing capacities recorded at depth, as discussed above.

5.5.2. Fibre Reinforcement Of Vegetative Root Systems

The effects of fibre reinforcement on the increased shear strength of soils has been discussed extensively in the literature (Gray and Ohashi 1983, Gray and Al-Refeai 1986, Maher 1988, Waldron and Dakessian 1981, and others). The focus of the literature is directed towards increased stability of natural or artificially constructed slopes or embankments.

To better predict the strength and bearing capacity increase of root reinforced soil, a force-equilibrium model discussed in the literature (Gray and Al-Refeai 1986) was chosen. The initial model which includes fibres orientated perpendicular (not shown) and inclined ($i < 90^\circ$) to the shear zone is illustrated in Figure 5.4. Considering the orientation of roots intersecting the developing shear zone beneath a PLT, the initial model was modified to include roots which initially are orientated in a compression condition ($i > 90^\circ$) as shown in Figure 5.4. Roots in a compression orientation do not contribute to shear strength until the deformation of the shear

zone causes sufficient rotation to develop tensile stresses. Based on the model, the predicted strength increase, ΔS_R , from regular arrays of multiple, orientated inclined fibres is given by:

$$\Delta S_R = t_R [\sin(90 - \psi) + \cos(90 - \psi) \tan \phi] \quad [5.4]$$

$$\text{where } \psi = \arctan \left[\frac{I}{k + (\tan i)^{-1}} \right] \quad [5.5]$$

and t_R is the mobilized tensile strength of the fibres per unit area of soil; ϕ is the angle of internal friction of the soil; i is the initial orientation angle of the fibre with respect to the shear surface; k is the shear distortion ratio ($k = x/z$) with z being the thickness of the shear zone and x being the horizontal shear displacement. The mobilized tensile strength per unit area of soil is given as:

$$t_R = \left(\frac{A_R}{A} \right) \sigma_R \quad [5.6]$$

with σ_R equal to the tensile stress developed in the fibres within the shear zone, A_R is the cross-sectional area of the roots within the shear zone and A is the total cross-sectional area of the shear zone.

The modified model was further modified to address the complex stress-strain paths associated with PLT's conducted on compressible tailings which fail in punching shear. The modifications, include considerations for shear strain distribution, variation of root orientation in the subsurface, and possible root slippage or pullout near the tailings surface. With the root area measurements made at Site 1, the modified model was used to predict the ΔS_R profile shown in Figure 5.5. The step wise distribution of ΔS_R is reflective of the root measurement frequency of the expected continuous nonlinear decreasing shear strength profile. It is noted that the increase in ΔS_R with increasing surface settlement of a footing and resulting increasing shear distortion ratio, k , reflects the rotation of some of the roots within the shear zone from a compression orientation (no contribution to strength) to a tension orientation. This nonlinear ΔS_R profile was subsequently coupled with bearing capacity theory to predict the increase in bearing capacity resulting from

root reinforcement. The predicted increase in bearing capacity as a result of root reinforcement was approximately equal to that determined at Site 1 between 1991 and 1994 of 140 kPa. Similar successful predictions of the increase in bearing capacity were obtained at the other sites within the tailings impoundment.

5.6. SUMMARY

Shear strength profiles were determined along the depositional beach of the Coal Valley tailings impoundment using FVST and the CPTU, and both devices showed good comparison. In addition, the profiles indicated that the average shear strength and thickness of the desiccated crust decreased with distance from the discharge point.

Plate load tests conducted along surface of the impoundment indicated that bearing capacity and modulus of the tailings ~~increased~~ considerably from 1991 to 1994. The increase in bearing capacity and modulus was mainly attributed to the ~~soil reinforcing~~ effect of the developed vegetative root system.. A fibre reinforcing model discussed in the literature was modified to predict the theoretical increase in bearing capacity from root systems. Plate load tests conducted below the surface of the tails indicated lower bearing capacity than those conducted at the surface. Increased matric suction and increased shear strength at the surface as a result of evapotranspiration are believed to contribute to the higher capacity. Both fibre reinforcement of vegetative root systems and evapotranspiration processes were shown to increase surface stability of the coal tails and thus enhance future dry landscape reclamation.

5.7. REFERENCES

- De Alencar, J.A., Chan, D.H., Morgenstern, N.R., 1988. Progressive Failure in the Vane Test. Vane Shear Strength Testing in Soils: Field and Laboratory Studies, ASTM STP 1014, A.F. Richards, Ed., pp 150-165.

- Fredlund, D.G., 1995. The Scope of Unsaturated Soil Mechanics: An Overview. First International Conference on Unsaturated Soils, Paris, France, 23p.
- Fredlund, D.G., Morgenstern, N.R., and Widger, R.A., 1978. The Shear Strength of Unsaturated Soils. *Canadian Geotechnical Journal*, **15**(3): 313-321.
- Fredlund, D.G., Rahardjo, H., 1993. **Soil Mechanics For Unsaturated Soils**. John Wiley & Sons, Inc. New York., 517 pp.
- Gray, D.H., and Al-Refeai, T., 1986. Behavior of Fabric-Versus Fibre-Reinforced Sand. *ASCE Journal of Geotechnical Engineering* **112**(8) 804-821.
- Gray, D.H., and Ohashi, H., 1983. Mechanics of Fibre Reinforcement in Sand. *ASCE Journal of Geotechnical Engineering* **109**(3): 335-353.
- Maher, M.H., 1988. Static and Dynamic Response of Sands Reinforced With Discrete, Randomly Distributed Fibres. Ph.D. Thesis, The University of Michigan.
- Mahmoud, M., 1988. Vane testing in Soft Clays. *Ground Engineering*, Oct., pp 36-40.
- Robertson, P.K., and Campanella, R.G., 1983. Interpretation of Cone Penetrometer Tests. Part II: Clay. *Canadian Geotechnical Journal*, **20**(4):734-745.
- Robertson, P.K., and Van Impe, W.F., 1987. Cone Penetration With Pore Pressure Measurement. *Belgisch Comité voor Ingenieursgeologie, B.C.I.G.*, Belgium, Dec. 1987, 60 pgs.
- Stahl, R.P. and Sego, D.C. 1992. Influence of Natural Surface Processes on Reclamation of the Coal Valley Tailings Impoundment. Second International Conference on Environmental Issues and Management of Waste in Energy and Mineral Production, Calgary, Alberta, September 1-4, pp. 389-400.
- Stahl, R.P. and Sego, D.C., 1995. Freeze-Thaw Dewatering and Structural Enhancement of Fine Coal Tails. *ASCE Journal on Cold Regions Engineering*, **9** (3):135-151.
- Stahl, R.P., Sego, D.C., Robertson, P.K., and Woeller, D., 1996. Characterization of Fine Processed Mine Tailings Deposits For Purposes of Dry Landscape Reclamation, Tailings and Mine Wastes '96, Fort Collins, Colorado, January 16-19, 1996.
- Teh, C.I., and Houlsby, G.T., 1991. An Analytical Study of the Cone Penetration Test in Clay. *Geotechnique* **41**(1): 17-34.
- Vesic, A.S., Chapter 3 of Winterkorn, H.F., and Fang, H.Y., 1975. **Foundation Engineering Handbook**, Van Nostrand.
- Waldron, L.J. and Dakessian, S., 1981. Soil Reinforcement by Roots: Calculation of Increased Soil Shear Resistance From Root Properties. *Soil Science* **132**(6): 427-435.

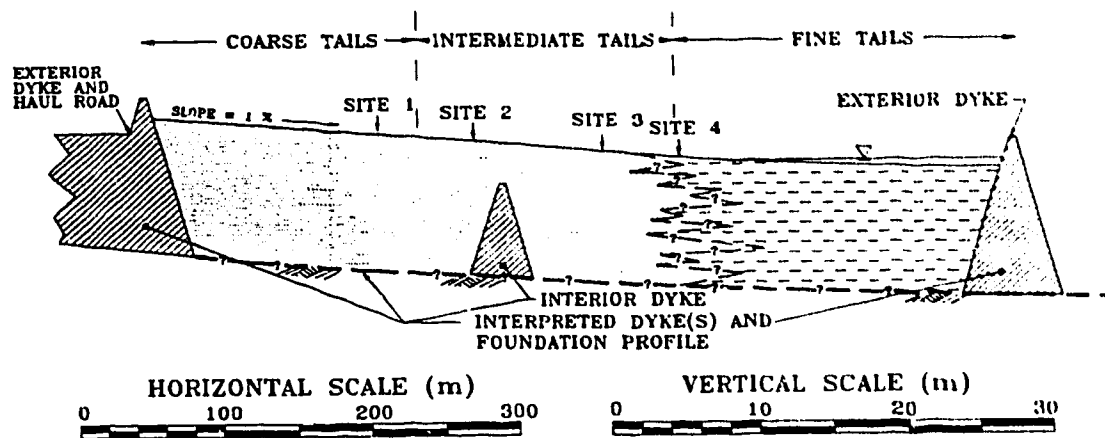


Figure 5.1 Cross-Section Through Coal Valley Tailings Impoundment

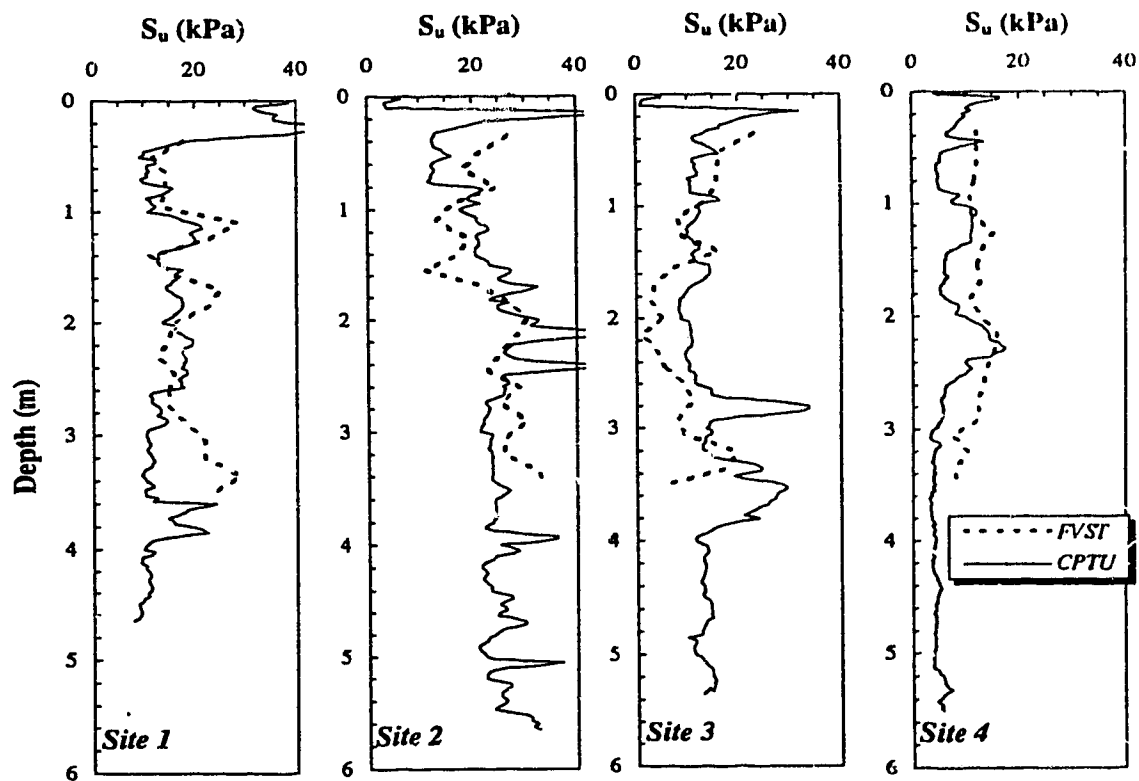


Figure 5.2 Shear Strength Profiles from FVST and CPTU at Sites 1 through 4

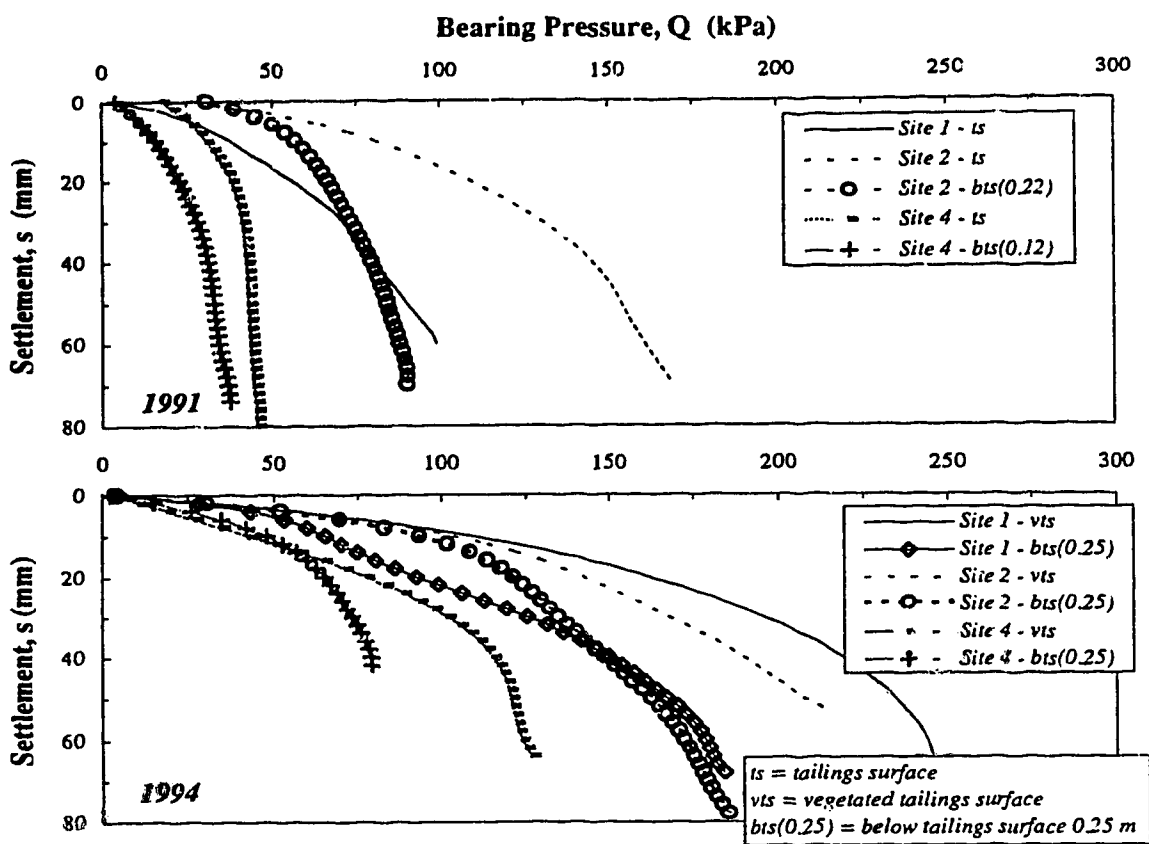


Figure 5.3 Plate Load Test Results from 1991 and 1994 at Sites 1, 2, and 4

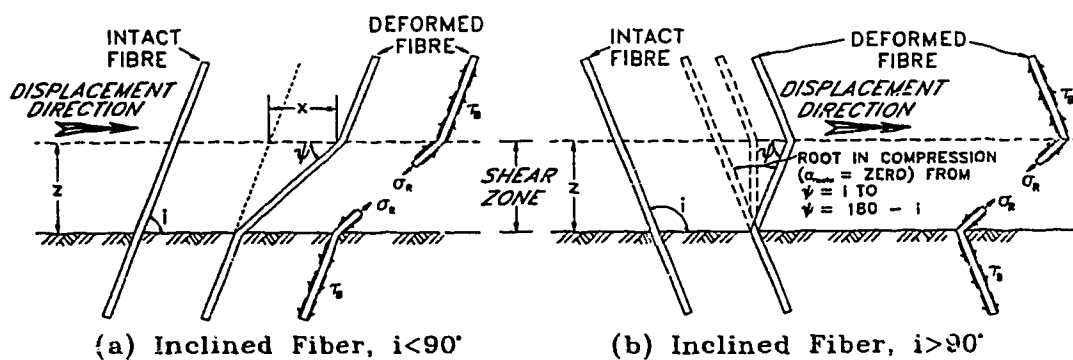


Figure 5.4 Fibre Reinforcement Model for Inclined Fibres

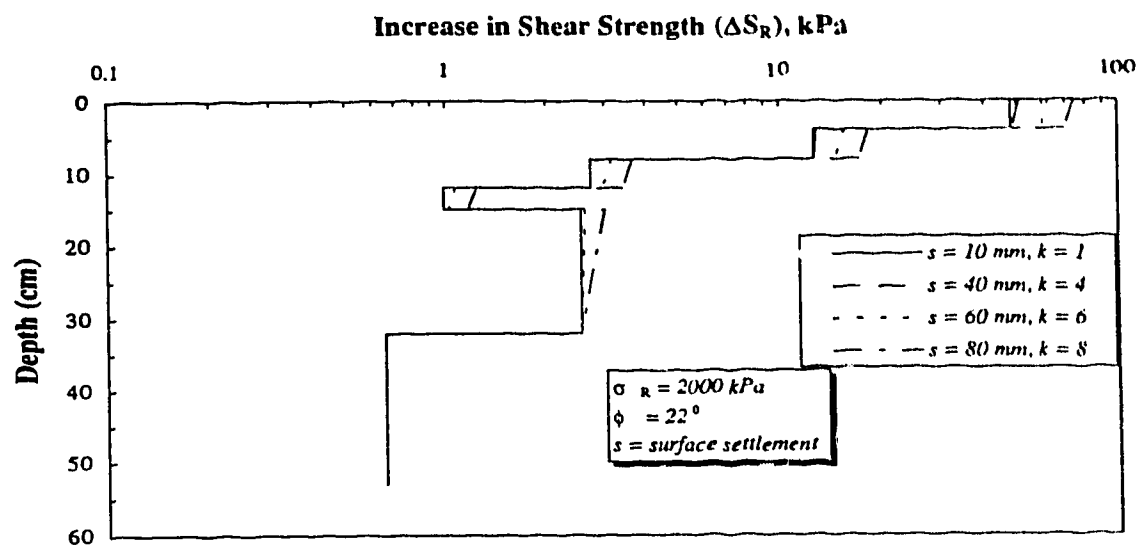


Figure 5.5 **Theoretical Increase in Shear Strength from Roots at Site 1**

Chapter 6

Influence Of Natural Surface Processes On Bearing Capacity And Reclamation Of Fine Coal Tails¹

6.1. INTRODUCTION

The Coal Valley mine, owned and operated by Luscar Sterco (1977) Ltd., is located in the foothills of the Rocky Mountains approximately 200 km west and 90 km south of Edmonton, Alberta as shown in Figure 6.1. Yearly production of 1,800,000 clean tons of coal results in two waste streams; a coarse dry crushed rock and a fine saturated slurried tailings with the associated grain size distributions illustrated in Figure 6.2. During one stage of mineral extraction and waste stream deposition, an 18.2 hectare impervious impoundment was constructed to contain the fine saturated slurried tailings which originated from the thickener underflow. A plan and cross-section of the impoundment, which reached full capacity in 1989 and has since been undergoing reclamation activities, is presented in Figure 6.3 (Stahl and Sego 1992). At that time the surficial soils within the impoundment were very weak and could not safely support human traffic.

As stated by Ziemkiewicz and Gallinger (1989), for reasons of revegetation and dust control, Alberta legislation requires that all coal tailings be covered with either suitable overburden or soil

¹ Submitted Paper:

Stahl, R.P., and Sego, D.C., 1995. Influence of Natural Surface Processes on Bearing Capacity and Reclamation of Fine Coal Tails. paper submitted for review to the Canadian Mining and Metallurgical Bulletin, December, 1995, 29 pgs.

to usually 1 to 1.5 m in depth. Coal Valley's development and reclamation approval states that if tailings interfere with reclamation issues including landscape stability, groundwater, surface water and revegetation they must be covered with at least 1.3 m of suitable material (McCoy 1992).

Previous tailings reclamation practices at the Coal Valley mine have included capping the coarser tailings with 3 to 6 m of waste rock to satisfy operational requirements. Greater capping thicknesses were required for softer, saturated fine tails as the material displaced under the loads imposed during placement of cap rock (Latimer *et al.* 1988, Sego 1990). Previously, neighboring mining and tailings reclamation areas with associated short trucking distances allowed for these thicknesses. However, continued mine expansion and increasing distance between mining and tailings reclamation areas economically discourage these extensive capping thicknesses, as well as the minimum 1.2 m thickness required by regulation should the tailings interfere with reclamation including landscape stability. Economics coupled with environmental concerns prompted consideration of alternative, natural surface enhancement processes which would enhance tailings surface stability and encourage the dry landscape reclamation.

This paper presents the results of field investigations conducted along the impoundment which include sampling and plate load tests. The sampling program defined the nature of the deposit highlighting the physical variability and heterogeneity of the soils, and the vegetative root area profiles along the impoundment. The plate load tests define the mechanical properties of the surficial soils and changes with time as a result of natural surface enhancement processes. The main processes include evaporation, evapotranspiration, and fibre reinforcement of root systems of the planted vegetative cover. These processes which directly influence bearing capacity and surface stability are evaluated, considering the matric suction and shear strength development as a result of evaporation and evapotranspiration, and theoretical models which define the increase in shear strength of root reinforced soils. The natural process of freeze-thaw consolidation which enhances the strength of the fine tailings within the pond area is discussed by Stahl and Sego (1995) and will not be presented here.

6.2. DEPOSIT CHARACTERISTICS

Figure 6.3 highlights the circumferential regions of the impoundment which have received limited soil capping, the previous tailings discharge location, the pond and overflow structure, and the four site investigation locations. The site investigation locations, designated as Sites 1 through 4, are located about 100 m, 160 m, 250 m, and 300 m respectively from the previous discharge location.

The impoundment, which initially existed as a series of smaller interconnected cells, was filled with saturated tailings by single point discharge. The discharge location remained unchanged during deposition and is located at the northwest corner of the impoundment. The fine saturated tailings slurry entered the impoundment at approximately 35 % solids and had a grain size distribution as shown in Figure 6.2.

During hydraulic deposition of the slurried tailings stream into the impoundment, the segregating tailings were hydraulically sorted. Hydraulic sorting refers to the separation of hydraulically deposited materials in different granulometric fractions as a result of the hydraulic flow characteristics. Küpper (1991) reports Soviet standards specifications on hydraulic fills which state that hydraulic sorting must be considered in all cases where:

$$D_{90}/D_{10} \geq 5 \quad [6.1]$$

and/or

$$D_{60}/D_{30} > 2.5 \quad [6.2]$$

The D_{90} , D_{60} , and D_{10} , denote the grain size corresponding to 90%, 60%, and 10% finer than. The tailings grain size distribution present in Figure 6.2 had ratios well in excess of the limits presented in [6.1] and [6.2] and displayed hydraulic sorting within the impoundment. In general, hydraulic sorting resulted in a decrease in mean grain size (D_{50}) and an increase in the amount of fines ("F%", material < 74 mm) with distance from the discharge point. Based on weighted averages of the shallow *heterogeneous* (discussed below) subsurface grain size distributions at Sites 1 through 4, the average D_{50} 's and (F%) were 0.19 mm (36%), 0.25 mm (28%), 0.16 mm

(38%), and 0.04 mm (70%) respectively. It is noted that Site 2, which has a greater D_{50} and lower $F\%$ than Site 1 yet is located further downstream, is adjacent to a remnant (possibly high flow velocity) depositional channel. This potential localized high velocity channel likely encouraged the coarser localized shallow deposit (Küpper 1991).

Hydraulic sorting of the segregating slurry resulted in roughly three tailings zones as shown in Figure 6.3. These zones are the coarse tails zone located near the previous discharge point, the fine tails zone located at the pond, and an intermediate zone located between the two extremes. These zones, particularly the pond region, potentially require different initiating natural surface enhancement processes to reclaim them to a dry landscape condition.

The *heterogeneous* shallow subsurface stratigraphy alluded to above is illustrated in Figure 6.4, which includes the shallow soil profile obtained at Site 2 (Stahl and Sego 1992). The profile, approximately 70 cm deep, was simplified to include 7 distinct silt or sand dominant layers. This same level of small scale heterogeneity was observed at the other testing sites located in Figure 6.3. As discussed by Küpper (1991), the prevailing continuous variation in type and strength of flow in time and space causes variation in localized deposit characteristics. In the case of a sandy hydraulic fill, deposition dynamics create heterogeneities on the scale of centimeters to meters in plan and on the scale of millimeters to centimeters in depth (Küpper 1991).

6.3. PLATE LOAD TESTS

6.3.1. Plate Load Test System

The Plate Load Test (*PLT*) apparatus employed at Coal Valley is schematically illustrated in Figure 6.5 (Stahl *et al.* 1996). The relative remote nature of these tailings sites and the generally weak, yet potentially variable nature of the deposits dictated the following *PLT* apparatus design specifications.

1. High load capacities (10 kN) required to fail a 300 mm diameter plate at the coarser grained, stronger tailings sites.
2. Light weight, easily dismantled and transported with human effort to all (particularly the weakest) tailings sites.
3. Computerized load and settlement collection and storage for accurate determination of load-deformation characteristics and ultimate failure load.
4. Settlements of as much as 50 % of footing diameter (100 to 150 mm) may be required to determine large strain load-deformation characteristics and ultimate failure load in soils exhibiting punching shear failure.

As shown in Figure 6.5, the *PLT* apparatus consisted of beam and hanger system with 20 to 30 kg lead weights providing the reaction load. The beam was designed according to *Limits States Design* following specifications outlined in the Handbook of Steel Construction (CISC 1982). The load transmitted to the 200 mm or 300 mm diameter stiff aluminum plates was applied through a hand actuated hydraulic ram reacting against the underside of the reaction beam. A 10 kN load cell recorded the load and two extensometers located diametrically on the plate recorded settlements. The extensometers were secured to a 2.5 m long steel angle, founded outside the zone of influence of the loaded plate. The load and settlement information were recorded at either one or two second intervals by a datalogger and subsequently downloaded to a laptop computer.

A variety of surficial boundary conditions were investigated at the Coal Valley tailings deposit as schematically illustrated in Figure 6.6. The boundary conditions investigated during the field investigation program included tests on the bare, unvegetated tails, the sparsely vegetated tails, and the tailings at depths of approximately 0.1 to 0.2 m. The tests on the “vegetated tails” were conducted following removal of surface vegetation in order to capture the influence of the vegetative root system on bearing capacity. The boundary conditions investigated during the 1994 investigation program did not include the bare, unvegetated tailings due to the enhanced development of the vegetative cover.

6.3.2. Plate Load Test Results

The *PLT*'s exhibited a punching shear failure mechanism which is indicative of very loose, compressible soils (Vesic 1973, Vesic 1975, Ismael and Vesic 1981). This failure pattern or ultimate load is difficult to distinguish, as increasing load results in compression of soil beneath the footing and vertical shear development at the footing perimeter with increasing penetration. Although difficult to distinguish, the ultimate load or first failure is commonly taken as the point of break in the load-settlement plot.

The *PLT* data from Coal Valley was analyzed in terms of Bearing Pressure (Q) versus Settlement (s), and Pressure versus Relative Settlement (RS) where:

$$\text{Bearing Pressure} = Q = \frac{\text{Load } (L_p)}{\text{Plate Area } (A_p)} \quad [6.3]$$

and

$$\text{Relative Settlement} = RS = \frac{\text{Settlement } (s)}{\text{Plate Diameter } (D_p)} \quad [6.4]$$

Figure 6.7 illustrates the punching shear pressure-settlement behavior observed in 1991 from representative *PLT*'s at Site 2. This behavior was similar at the other sites investigated for both years. The results from 31 *PLT*'s conducted in 1991 and 1994 are summarized for the capacities at 10% *RS*, 20% *RS*, and maximum bearing pressure (Q_{max}) versus distance from discharge point in Figure 6.8. It is noted that *PLT*'s were not conducted at Site 3 in 1994. The following observations are formulated from the field test results.

- The test results for 1991 and 1994 at 10% *RS*, 20% *RS*, and Q_{max} indicate a general decrease in bearing capacity with increasing distance from the discharge point. The decrease in capacity (shear strength) reflects the decreasing grain size and higher pore pressures within the deformed soil beneath the loaded plate. The higher pore pressures are a combination of reduced hydraulic conductivity which limit drainage, evaporation and evapotranspiration

dewatering processes, and increased proximity of the water table to the tailings surface particularly at Site 4.

- The 1991 tailings surface (*ts*), vegetated tailings surface (*vts*) and 1994 below tailings surface (*bts*) results indicate generally an increase in bearing pressure at Site 2 compared to that at Site 1. This likely reflects the coarser nature (D_{50} , $F\%$) and resulting higher soil strength of the deposit at Site 2 (compared to Site 1), as discussed above.
- In all cases, the 1991 and 1994 *PLT*'s conducted at the surface were considerably greater than those conducted below the surface. Acknowledging that heterogeneities are present and provide influences, the greater surface (compared to below tailings surface) bearing capacity is believed through enhanced dewatering and matric suction development sponsored by evaporation and evapotranspiration, coupled with fibre reinforcement of vegetative root systems. Both these processes which enhance surficial capacities are discussed below. Fibre reinforcing effects are observed to play a very small role in the increased surface bearing capacity in 1991. The fibre reinforcing effects on increased surface bearing capacity are much more pronounced in 1994 due to the enhanced development of the vegetative cover.
- Lastly, the 1994 surface and below surface bearing capacities were considerably higher than the respective 1991 surface and below surface bearing capacities at all sites. In particular, comparing the increase from 1991 tailings surface (*ts*) to 1994 vegetated tailings surface (*vts*), Sites 1, 2 and 4 displayed an increase and percent increase in capacity of 140 kPa (150%), 60 kPa (40%), and 80 kPa (190%). A modified theoretical fibre reinforcing model applied to the vegetative root systems and stress-strain conditions imposed beneath the *PLT* on compressible tailings support these increases.

6.4. SURFACE STABILITY PROCESSES

6.4.1. Evaporation/Evapotranspiration

The processes of evaporation, evapotranspiration, and drainage along the Coal Valley tailings impoundment results in the development of a two phase geotechnical subsurface system which includes a variable thickness unsaturated zone at the surface and a saturated zone at depth. As discussed by Fredlund (1995), the geotechnical properties of soils may be described under the umbrella of generalized soil mechanics which includes the strength, compressibility, and permeability of a majority of saturated and unsaturated soils. The theories which embrace the unsaturated portion of a soil profile have saturated behavior as a special case. Most geotechnical and geoenvironmental projects involve understanding the behavior of unsaturated soils. Consideration of the mechanics of unsaturated soils is not without precedent in tailings projects including the design of soil covers, moisture and contaminant migration, and seepage through unsaturated soils. The following discussion is restricted, however, to the development of shear strength of unsaturated soils which influence the surficial bearing capacity of the coal tails.

The shear strength of unsaturated soils, τ_f , may be defined in terms of two stress variables, $(\sigma - u_a)$ and $(u_a - u_w)$, as presented in Fredlund *et al.* (1978), Fredlund and Rahardjo (1993) as:

$$\tau_f = c' + (\sigma - u_a)_f \tan \phi' + (u_a - u_w)_f \tan \phi^b \quad [6.5]$$

where c' is the effective cohesion parameter, σ , u_a , u_w denote total stress, pore air pressure, and pore water pressure, $(\sigma - u_a)_f$ is the net normal stress on the failure plane at failure, $(u_a - u_w)_f$ is the matric suction on the failure plane at failure, ϕ' is the angle of internal friction with respect to net normal stress, and ϕ^b is the angle of internal friction with respect to matric suction. The shear strength of saturated soils is a special case of [6.5] where the u_a term of the stress variable $(\sigma - u_a)$ equals the u_w value and $(u_a - u_w)$ approaches zero. Based on [6.5], the *insitu* shear strength and bearing capacity change through matric suction variations in response to climatic or environmental conditions such as evaporation, evapotranspiration, and precipitation.

In addition to time dependent matric suction variations developed through environmental conditions, matric suctions will also vary spatially particularly with depth. Figure 6.9 schematically illustrates the stress variable profiles which may exist in the subsurface environment composed of a saturated and unsaturated zone. Focusing on the pore water pressure profiles in the unsaturated zone, several matric suction conditions and associated variations with depth may exist. These matric suction profiles translate to shear strength variations illustrated in Figure 6.9. As discussed in Section 6.3.2, the increase in surface bearing capacity compared to below tailings surface bearing capacity in the 1991 *PLT*'s results from the matric suction and shear strength increase caused by the excessive evaporation profile illustrated in Figure 6.9. Although matric suctions were not measured, visual observations of a desiccated crust resulting from evaporation support this hypothesis. Due to the enhanced vegetative cover, the bearing capacity increase at the surface (compared to below tailings surface bearing capacities) observed in the 1994 *PLT*'s result from a coupled effect of increased matric suction and increased reinforcement of the vegetative root system. Although vegetative root systems enhance the surficial shear strength irrespective of matric suction profiles, for clarity its effect is only illustrated on the excessive evaporation shear strength profile in Figure 6.9.

The development or variation of matric suctions within the soil occur through changes in moisture content via drainage, infiltration, evaporation and plant transpiration with a combined term of evapotranspiration. Drainage and for that matter infiltration are gravity driven processes depending mainly upon soil properties such as hydraulic conductivity. Evaporation from a soil surface is more complicated and controlled by both climatic conditions which define the potential rate of evaporation, and soil properties such as saturated and unsaturated hydraulic conductivity (Wilson *et al.* 1994).

These complications and associated non-linearity of evaporation from a soil surface is illustrated in Figure 6.10. This figure represents the ratio of actual evaporation flux (*AE*) to potential evaporation flux (*PE*) versus water availability. The *PE* is defined as the upper or maximum rate of evaporation from a pure water surface under given climatic conditions. Stage I is the maximum or potential rate of drying that occurs when the soil surface is at or near saturation and is determined by climatic conditions with moisture migration controlled by hydraulic

conductivity. As drying proceeds to Stage II, the soil surface begins to desaturate and the AE falls below the PE as the conductive properties decrease. Continued drying decreases the AE to a residual value of Stage III where the liquid-water phase is discontinuous and the water molecules only migrate to the surface through vapour diffusion.

With continued drying the thin surficial desiccated zone, which effectively seals the underlying material limiting moisture migration to only vapour diffusion pathways, experiences a decrease in water content, reduction in hydraulic conductivity, and an increase in matric suction and shear strength. The thickness of this strengthened crust is critical to the surface stability of weak tails. As modelled by Wilson *et al.* (1994) for a given PE , the duration of Stage I (high AE , and possibly increased thickness of desiccated crust) is extended with increasing saturated hydraulic conductivity. Abu-Hejleh (1993) has shown analytically for a soft clay that the degree of dewatering and the crust thickness development through desiccation is reduced for high evaporation rates which result in rapid crust development, and effective termination of AE and sealing of the underlying material. Acknowledging this sealing effect, dependent upon factors including hydraulic conductivity and potential evaporation rates, Williams and Morris (1990) highlighted optimization of evaporation processes by placing Australian coal tails in thin layers for drying to enhance dewatering and shear strength development.

In addition to thin layer placement and evaporation optimization, the dewatering and strength gain limitations at depth imposed by a sealing desiccated crust may be circumvented through development of biological dewatering pathways offered through transpiration of vegetative root systems. Transpiration was differentiated into a three flux rate stages, each stage dependent upon the leaf area index (LAI) of the plant canopy as discussed by Ritchie (1972). These stages include a “zero” transpiration stage at a $LAI < 0.1$, a nonlinear transpiration stage from $0.1 \leq LAI \leq 2.7$, and a maximum potential transpiration stage at $LAI > 2.7$.

Tratch *et al.* (1995) describes a model incorporating these transpiration stages discussed by Ritchie (1972) with a soil evaporation model outlined by Wilson *et al.* (1994). This “evapotranspiration” model was applied to a laboratory experiment conducted on a instrumented 60 cm column of silty soil with surface vegetation evapotranspiring under controlled conditions.

The laboratory and model results from Tratch *et al.* (1995) are presented in Figure 6.11. The evaporation, transpiration, and evapotranspiration fluxes from Tratch *et al.* (1995) are presented as a ratio of the *PE* moisture flux similar to the representative evaporation curve for sand in Figure 6.10. It is noted that the measured potential evaporation and evapotranspiration profiles in Figure 6.11 are approximate representations of the actual detailed and variable data provided by Tratch *et al.* (1995).

Six surface flux stages were observed by Tratch *et al.* (1995), three involving evaporation only and three involving evaporation and transpiration fluxes. The first three evaporation stages which include the first 17 days are reminiscent of the evaporation curve presented in Figure 6.10. Matric suctions along the 60 cm soil column on Day 16 indicated that only the top approximately 10 cm had undergone dewatering with matric suctions greater than 40 kPa established, with only the upper 1-2 cm developing matric suctions greater than 200 kPa.

Day 17 (Figure 6.11) denotes the initiation of transpiration processes as the *LAI* exceeded 0.1, with continually increasing transpiration flux to day 40 when the vegetative canopy reached a *LAI* value of 2.7 and maximum potential transpiration (Ritchie 1972, Tratch *et al.* 1995). At that stage the potential transpiration flux approximately equated the *PE* flux. The total evapotranspiration flux corresponded to the *PE* flux until day 47 when moisture limiting conditions were applied by terminating moisture flux into the base of the soil column. Moisture limiting conditions resulted in reduced evapotranspiration flux, sample drying, progressive root growth, and development of matric suctions at depth. After 86 days of evapotranspiration, moisture content measurements indicated that on average, the enhanced dewatering through transpiration had resulted in the development of matric suctions of about 200 kPa in the upper 33 cm, decreasing to 70 kPa at the base of the 60 cm soil column. These matric suctions through enhanced dewater by evapotranspiration processes contribute to increased shear strength (Equation [6.5]) and surficial soil stability.

The significance of dewatering, matric suction development and increased shear strength through evapotranspiration processes is further emphasized in Figure 6.12. Johnson *et al.* (1991) investigated the dewatering and shear strength enhancement capabilities of nine plant species

cultivated for 11 weeks in lysimeters filled with a sand-fine tails mix. Average moisture content and shear strength measurements were recorded with the best four dewatering plant species noted in the figure. Little information was presented on the method used to measure shear strength, however, it is anticipated that the measurements were conducted without the roots influencing the measured strengths. This figure illustrates that Reed Canary and Dock appear superior to other native grasses for dewatering and strength enhancement of the tailings mixtures. These species also were reported to have had the deepest root systems, each reaching the bottom of the 80 cm deep lysimeters within the 11 week study. The deep rooting pattern of Reed Canary is supported by field studies along the coal tailings impoundment reported by Macyk *et al.* (1991). Furthermore, Reed Canary and Alfalfa mix were the dominant vegetative species along the impoundment during the study period (Macyk *et al.* 1991).

Although the work by Tratch *et al.* (1995) and Johnson *et al.* (1991) are independent studies on different materials, they nonetheless embraced the effects of evapotranspiration processes on the dewatering, development of matric suctions, and enhancement of shear strength of unsaturated soils. These studies support the increase in surface, compared to below tailings surface, bearing capacity as a result of matric suction changes observed with the (1994 and particularly 1991) *PLT*'s at Coal Valley.

6.4.2. Fibre Reinforcement Of Vegetative Root Systems

The effects of fibre reinforcement on the increased shear strength of soils has been discussed extensively in the literature (Waldron 1977, Waldron and Dakessian 1981, Ziemer 1981, Gray and Ohashi 1983, Gray and Al-Rafeai 1986, , Maher 1988, Sotir and Gray 1989, Maher and Gray 1990, Al-Rafeai 1991, Terwilliger and Waldron 1991, Day 1993). The focus of much of the literature is directed towards the effect of natural vegetation root systems or artificially placed natural, metal or synthetic fibres on the increase in stability of natural or constructed slopes or embankments.

Based on the stress-strain response of fibre reinforced soils, the effect of roots is to provide an increase in the effective cohesion of the soil with no effect on the internal angle of friction (Gray

and Ohashi 1983, Sotir and Gray 1989, Day 1993). Several simplistic formations are presented in the literature which attempt to predict the increase in shear strength of root permeated soils. These equations which generally only require volume percentage of roots within the soil or area percentage of root across a shear plane, are based on specific soil types, root strength and morphology. The specifics of these formulations limits their applicability and prevents their confident utilization in prediction of the enhanced bearing capacity of root permeated compressible tailings.

To analyze the effect of vegetative root systems on bearing capacity of the tails, a force-equilibrium model discussed in the literature (Gray and Al-Refeai 1986) was chosen. The initial model which includes fibres orientated perpendicular (not shown) and inclined ($i < 90^\circ$) to the shear zone is illustrated in Figure 6.13. Considering the orientation of roots intersecting the developing shear zone beneath a *PLT*, the initial model was modified to include roots which initially are orientated in a compression condition ($i > 90^\circ$) as shown in Figure 6.13. Roots in a compression orientation do not contribute to shear strength until the deformation of the shear zone causes sufficient rotation to develop tensile stresses. Based on the model, the predicted strength increase, ΔS_R , from regular arrays of multiple, orientated inclined fibres is given by:

$$\Delta S_R = t_R [\sin(90 - \psi) + \cos(90 - \psi) \tan \phi] \quad [6.6]$$

$$\text{where } \psi = \arctan \left[\frac{I}{k + (\tan i)^{-I}} \right] \quad [6.7]$$

and t_R is the mobilized tensile strength of the fibres per unit area of soil; ϕ is the angle of internal friction of the soil; i is the initial orientation angle of the fibre with respect to the shear surface; k is the shear distortion ratio ($k = x/z$) with z being the thickness of the shear zone and x being the horizontal shear displacement. The mobilized tensile strength per unit area of soil is given as:

$$t_R = \left(\frac{A_R}{A} \right) \sigma_R \quad [6.8]$$

with σ_R equal to the tensile stress developed in the fibres within the shear zone, A_R is the cross-sectional area of the roots within the shear zone and A is the total cross-sectional area of the shear zone.

The modified model was further modified to address the complex stress-strain paths associated with *PLT*'s conducted on compressible tailings which fail in punching shear. These preliminary modifications based on the expected soil-fibre interaction mechanics beneath a loaded plate are summarized as follows:

- In accordance with the initial random orientation of fibres intersecting the shear zone beneath the *PLT*, 50% of the fibres are assumed to initially be in a compression orientation with no contribution to bearing capacity. Shear zone development following load application and plate settlement results in gradual fibre rotation from compression to tension orientation with a corresponding increasing percentage of fibres contributing to bearing capacity.
- The loose compressible nature of the tailings which exhibit punching shear failure realize non-uniform strain and associated shear zone deformation beneath the plunging plate. This analysis considered the shear strains within the shear zone as a result of surface settlement to vary linearly with a maximum at the surface and zero at a depth equal to D_p .
- The theoretical ΔS_R in the upper approximately 5 cm was reduced by about 50 % to account for possible root slippage due to limited stress development length. The reduction is based on estimates of the minimum length of root, L_{min} required to avoid slippage as outlined by Waldron (1972).

In summary, these modifications attempt to consider variation of root orientation in the subsurface, variable shear strain distribution at depth, and possible root slippage or pullout near the tailings surface. With the root area profile measurements obtained at Site 1, the modified model was used to predict the ΔS_R profile shown in Figure 6.14 for an estimated lower bound root tensile strength, σ_R , of 2000 kPa. The step wise distribution of ΔS_R is reflective of the root

measurement frequency of the expected continuous nonlinear decreasing shear strength profile. It is noted that the increase in ΔS_R with increasing surface settlement of a footing and resulting increasing shear distortion ratio, k , reflects the rotation of some of the roots within the shear zone from a compression orientation (no contribution to strength) to a tension orientation as discussed above.

This nonlinear ΔS_R profile was subsequently coupled with bearing capacity theory to predict the increase in bearing capacity resulting from root reinforcement. The increase in bearing capacity, ΔQ_{roots} , resulting from root reinforcement was determined using, as a framework, the cohesion component formulation of the general bearing capacity equation (Bowles 1988, Vesic 1973, Vesic 1975) shown as:

$$\Delta Q_{roots} = N_c s_c \Delta S_R \quad [6.10]$$

where N_c is the bearing capacity factor for cohesion (5.14), s_c is the shape factor for a circular footing (1.2), and ΔS_R is the theoretical shear strength from root reinforcement as shown in Figure 6.14.

The theoretical contribution of vegetative root systems to increase bearing capacity at Site 1 using [6.10] and the profile in Figure 6.14 is illustrated in Figure 6.15. This figure illustrates the 1994 vegetated tailings surface (*vt*) bearing capacity profile, and the 1991 tailings surface (*ts*) profile coupled with the theoretical contribution from root reinforcement. The bearing capacity contribution from root reinforcement considers “estimated” (Schiechl 1980, Naeth 1995) root tensile strengths, σ_R , ranging from 2000 kPa to 3000 kPa which likely reflect lower bound values for Reed Canary vegetation. These lower bound estimates of σ_R provide for conservatism and indirectly account for potential root rupture beneath the loaded plate.

Although several preliminary assumptions and estimates were made to model the soil-root interaction mechanics beneath a *PLT* on compressible tails at Coal Valley, the predicted increase in bearing capacity is within the same range as the 1994 vegetated tailings surface (*vt*) results

and is very encouraging. Considering the 1991 and 1994 *PLT*'s were likely conducted 1 to 2 m apart, these results are even more encouraging considering the localized heterogeneity prevalent at the individual sites as outlined in Section 6.2. Similar successful predictions of the increase in bearing capacity were obtained at the other sites within the tailings impoundment.

6.5. SUMMARY AND CONCLUSIONS

The site investigation activities conducted along the Coal Valley tailings impoundment in 1991 and 1994 provide the following conclusions.

1. The segregating tailings underwent hydraulic sorting along the impoundment resulting in a decrease in mean grain size, D_{50} , and an increase in fines % F , with distance from the discharge point.
2. The dynamics of hydraulic deposition created horizontal and vertical heterogeneity with vertical heterogeneity on a scale of millimeters to centimeters.
3. The loose nature of the tails result in the *PLT*'s exhibiting a punching shear failure mechanism.
4. The bearing capacities at 10% *RS*, 20% *RS*, and Q_{max} , in general decrease with increasing distance from the discharge point mainly as a result of reduced grain size and increased pore water pressure (reduced matric suction).
5. The *PLT*'s conducted at the tailings surface had considerably greater bearing capacities than those at depth. The increased capacity with elevation results from increased matric suction and increased fibre reinforcing effects of vegetative root systems.
6. The 1994 *PLT*'s had higher capacities than the 1991 *PLT*'s. The main factor contributing to the increased capacity is the enhanced vegetative growth and resulting fibre reinforcing effect of the vegetative root systems.

Considering the theme of unsaturated soil mechanics and the associated shear strength formulation, the processes and effect of evaporation and evapotranspiration on matric suction and shear strength development were discussed. Evaporation and evapotranspiration on matric

suction and shear strength development of two independent soils were presented. The contribution of vegetative root systems to increased shear strength and bearing capacity was evaluated using a theoretical model established in the literature, subsequently modified to address the idealized stress-strain pattern beneath the *PLT*. This modified model showed success in predicting the increase in surface bearing capacity observed at Site 1 between 1991 to 1994 as a result of vegetative development.

The natural surface enhancement processes of evaporation, evapotranspiration, and fibre reinforcement of vegetative root systems have considerably enhanced the bearing capacity and surface stability of the initially very weak impoundment materials which could not safely support human traffic. These environmentally conscience natural processes promote adoption of dry landscape reclamation philosophies with potential thickness reductions or elimination of soil capping, and reduced short and long term reclamation costs.

6.6. REFERENCES

- Abu-Hejleh, A.N.M., 1993. Desiccation Theory for Soft Soils. Ph.D. Thesis, The University of Colorado. 211 pgs.
- Al-Refeai, T.O., 1991. Behavior of Granular Soils Reinforced with Discrete Randomly Orientated Inclusions. *Geotextiles and Geomembranes* 10: 319-333.
- Bowles, J.E., 1988. **Foundation Analysis and Design**. McGraw-Hill, Inc..
- Canadian Institute of Steel Construction, (CISC), 1982. *Handbook of Steel Construction*, Third Edition, Universal Offset Limited, Markham, Ontario.
- Day, R.W., 1993. Surficial Slope Failure: A Case Study. *ASCE Journal of Performance of Constructed Facilities* 7(4): 264-269.
- Fredlund, D.G., 1995. The Scope of Unsaturated Soil Mechanics: An Overview. First International Conference on Unsaturated Soils, Paris, France, 23p.
- Fredlund, D.G., Morgenstern, N.R., and Widger, R.A., 1978. The Shear Strength of Unsaturated Soils. *Canadian Geotechnical Journal*, 15(3): 313-321.

- Fredlund, D.G., and Rahardjo, H., 1993. **Soil Mechanics For Unsaturated Soils.** John Wiley & Sons, Inc. New York., 517 pp.
- Gray, D.H., and Al-Refeai, T., 1986. Behavior of Fabric-Versus Fibre-Reinforced Sand. **ASCE Journal of Geotechnical Engineering** **112(8)** 804-821.
- Gray, D.H., and Ohashi, H., 1983. Mechanic: of Fibre Reinforcement in Sand. **ASCE Journal of Geotechnical Engineering** **109(3)**: 335-353.
- Ismael, N.F. and Vesic, A.S., 1981. Compressibility and Bearing Capacity. **Journal of Geotechnical Engineering**, ASCE, No GT. 12, pp. 1677-1691
- Johnson, R.L., Bork, P., Allen, E.A.D., James, W.H., and Koverny, L., 1991. Oil Sands Sludge Dewatering by Freeze-Thaw and Evapotranspiration "Draft Report". Presented to Syncrude Canada Ltd. and Reclamation Research Technical Advisory Committee, 273 pgs.
- Küpper, A.M.A.G., 1991. Design of Hydraulic Fill. Unpublished Ph.D. Thesis, Department of Civil Engineering, The University of Alberta, 525 pgs.
- Latimer, R.C., Brinker, C.J. and Kintzi, R.P., 1988. Tailings Disposal Options at the Coal Valley Mine. 90th Annual Meeting of Canadian Institute of Mining and Metallurgy, 43 pgs.
- Macyk, T.M., Nikiforuk, F.I., and Widtman, Z.W., 1991. Characterization and Reclamation of Coal Tailing Materials. Report Prepared For Luscar-Sterco (1977) Ltd. 57 pgs.
- Maher, M.H., 1988. Static and Dynamic Response of Sands Reinforced With Discrete, Randomly Distributed Fibres. Ph.D. Thesis, The University of Michigan.
- Maher, M.H., and Gray, D.H., 1990. Static Response of Sands Reinforced with Randomly Distributed Fibres. **ASCE Journal of Geotechnical Engineering** **116(11)**: 1661-1677.
- McCoy, D., 1992. Personal Communications. Environmental Supervisor, Luscar Sterco (1977) Ltd., Edson, Alberta.
- Naeth, M.A., 1995. Personal Communications. Assistant Professor, Department of Renewable Resources, The University of Alberta, Edmonton, Alberta.
- Ritchie, J.T., 1972. Model for Predicting Evaporation from a Row Crop with Incomplete Cover. **Water Resources Research**, **8(5)**:1204-1213.
- Schiechl, H., 1980. **Bioengineering for Land Reclamation and Conservation.** University of Alberta Press, Edmonton, Alberta, 400 pgs.
- Sego, D.C., 1990. Use of Freeze-Thaw to Assist in Reclamation of a Coal Tailings Pond. Submitted to Luscar Sterco (1977) Ltd. 27 pgs.

- Sotir, R.B., and Gray, D.H., 1989. Fill Slope Repair Using Soil Bioengineering Systems. *Journal of Public Works*, **120**(13): 37-40, 77.
- Stahl, R.P. and Sego, D.C., 1992. Influence of Natural Surface Processes on Reclamation of the Coal Valley Tailings Impoundment. *Second International Conference on Environmental Issues and Management of Waste in Energy and Mineral Production*, Calgary, Alberta, September 1-4, pp. 389-400.
- Stahl, R.P. and Sego, D.C., 1995. Freeze-Thaw Dewatering and Structural Enhancement of Fine Coal Tails. *ASCE Journal on Cold Regions Engineering*, **9** (3):135-151.
- Stahl, R.P., Sego, D.C., Robertson, P.K., and Woeller, D., 1996. Characterization of Fine Processed Mine Tailings Deposits For Purposes of Dry landscape Reclamation. *Tailings and Mine Wastes '96*, Fort Collins, Colorado, January 16-19, 1996.
- Terwilliger, V.J., and Waldron, L.J., 1991. Effects of Root Reinforcement on Soil-Slip Patterns in the Transverse Ranges of Southern California. *Geological Society of America Bulletin* **103**: 775-785.
- Thurber Engineering Ltd., 1992. Coal Valley Mine Site Tailings Reclamation Research Project Geotechnical Report. Submitted to Luscar Sterco (1977) Ltd. 80 pgs.
- Tratch, D.J., Wilson, G.W., and Fredlund, D.G., 1995. An Introduction to Analytical Modelling of Plant Transpiration for Geotechnical Engineers. *Proceedings, 48th Canadian Geotechnical Conference*, Vancouver, B.C., pgs 771-789.
- Vesic, A.S., 1973. Analysis of Ultimate Loads of Shallow Foundations. *Journal of Soil Mechanics and Foundation Division, ASCE*, **99**(1):45-73.
- Vesic, A.S., 1975. Chapter 3 of Winterkorn, H.F., and Fang, H.Y.. *Foundation Engineering Handbook*. Van Nostrand.
- Waldron, L.J. and Dakessian, S., 1981. Soil Reinforcement by Roots: Calculation of Increased Soil Shear Resistance From Root Properties. *Soil Science* **132**(6): 427-435.
- Waldron, L.J., 1977. The Shear Resistance of Root-Permeated Homogeneous and Stratified Soil. *Soil Science Society of America*, **41**: 843-849
- Williams, D.J., and Morris, P.H., 1990. Engineering Properties of Australian Coal Mine Tailings Relevant to their Disposal and Rehabilitation. *Proceedings of the Third International Conference on Reclamation, Treatment, and Utilization of Coal Mining Wastes*, Glasgow, United Kingdom, pp 49-56.
- Wilson, G.W., Fredlund, D.G., and Barbour, S.L., 1994. Coupled Soil Atmosphere Modelling for Soil Evaporation. *Canadian Geotechnical Journal*, **31**(2):151-161.

Ziemer, R.R., 1981. Roots and the Stability of Forested Slopes. International Association of Hydrological Sciences, Publication No. 132: 343-361.

Ziemkiewicz, P.F., and Gallinger, R., 1989. Overview of Tailings Reclamation in Western Canada. Proceeding of Syposium entitled "Reclamation, A Global Perspective". Calgary, Alberta, Aug. 27-31, pp 707-716.

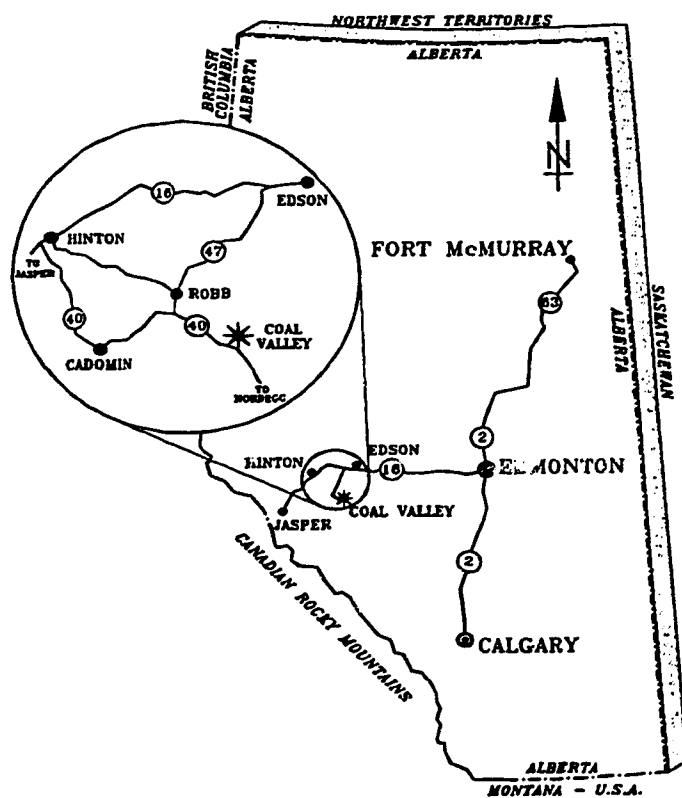


Figure 6.1

Location Map of Coal Valley Mine

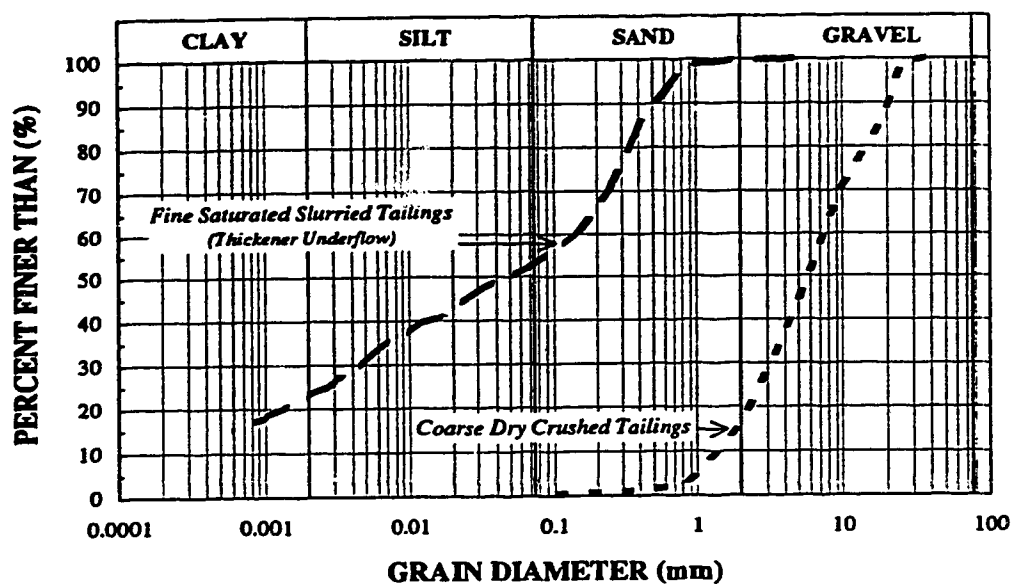


Figure 6.2 Coal Valley Waste Streams

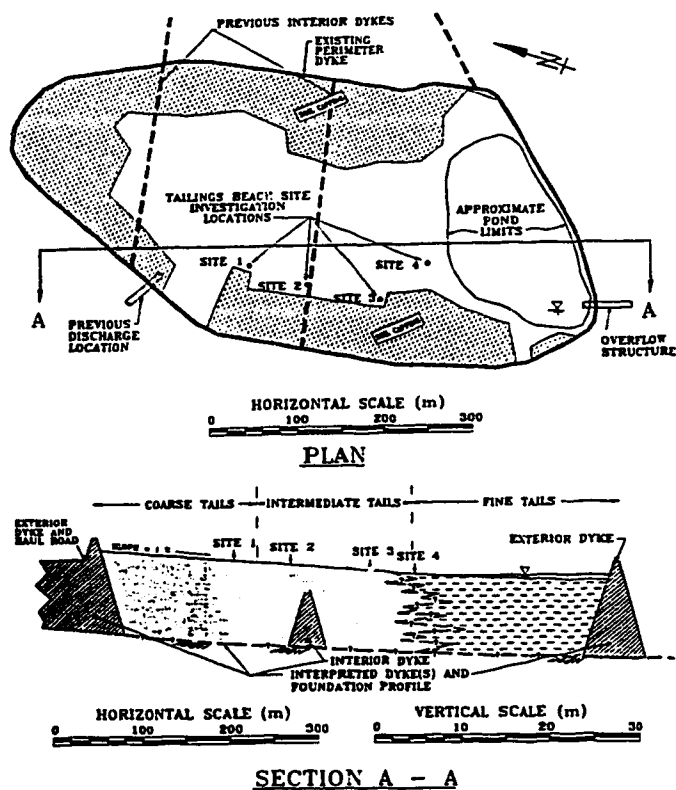


Figure 6.3 Plan and Section of Coal Valley Tailings Impoundment

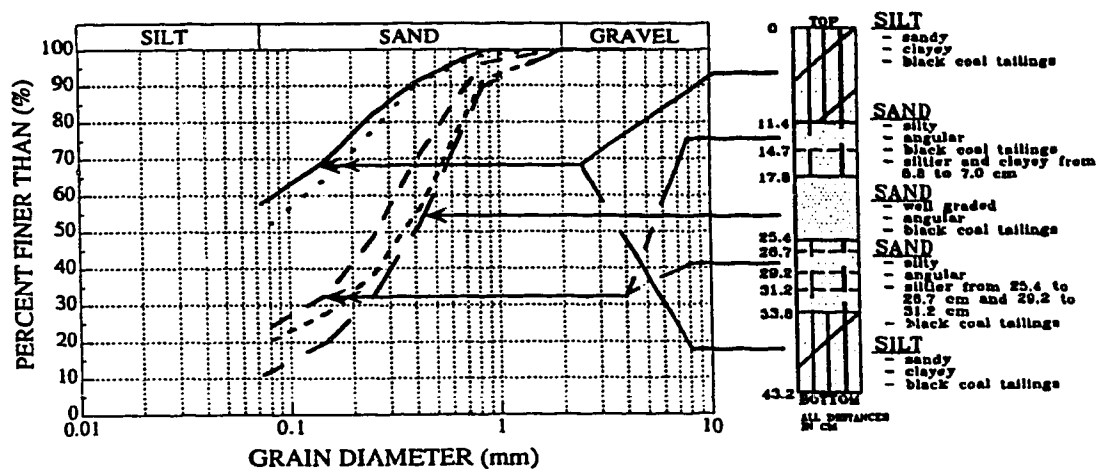


Figure 6.4 Shallow Stratigraphy at Site 2

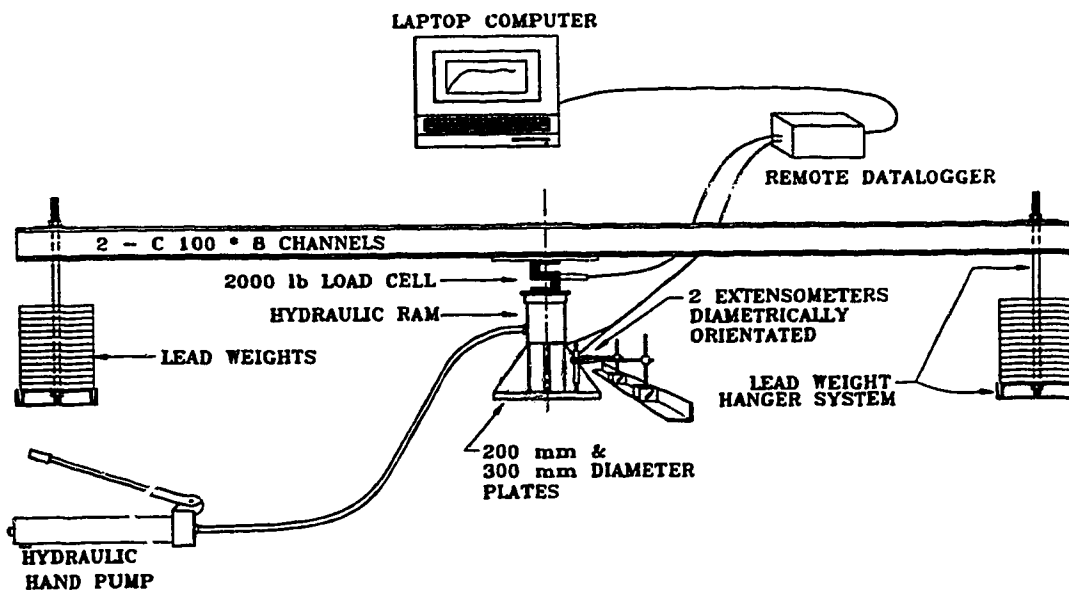


Figure 6.5 Plate Load Test Apparatus

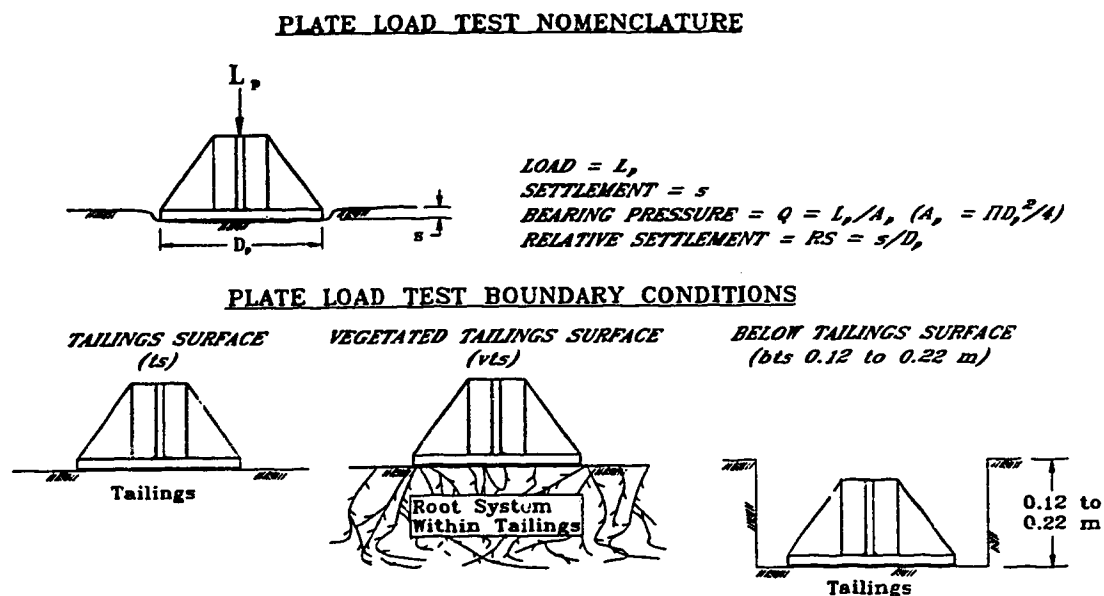


Figure 6.6 Plate Load Test Boundary Conditions and Nomenclature

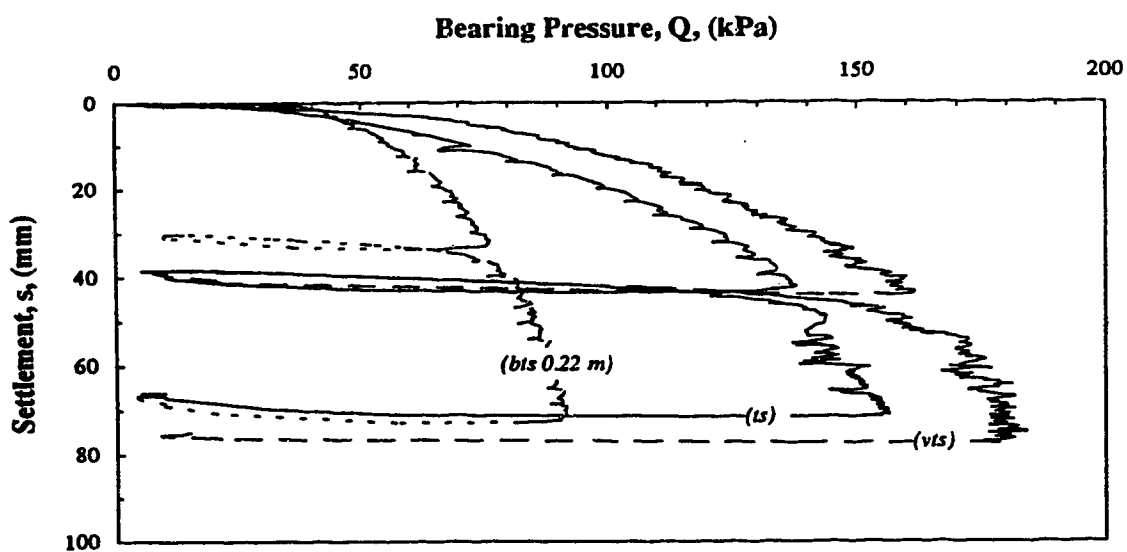


Figure 6.7 Selective 1991 Plate Load Tests at Site 2

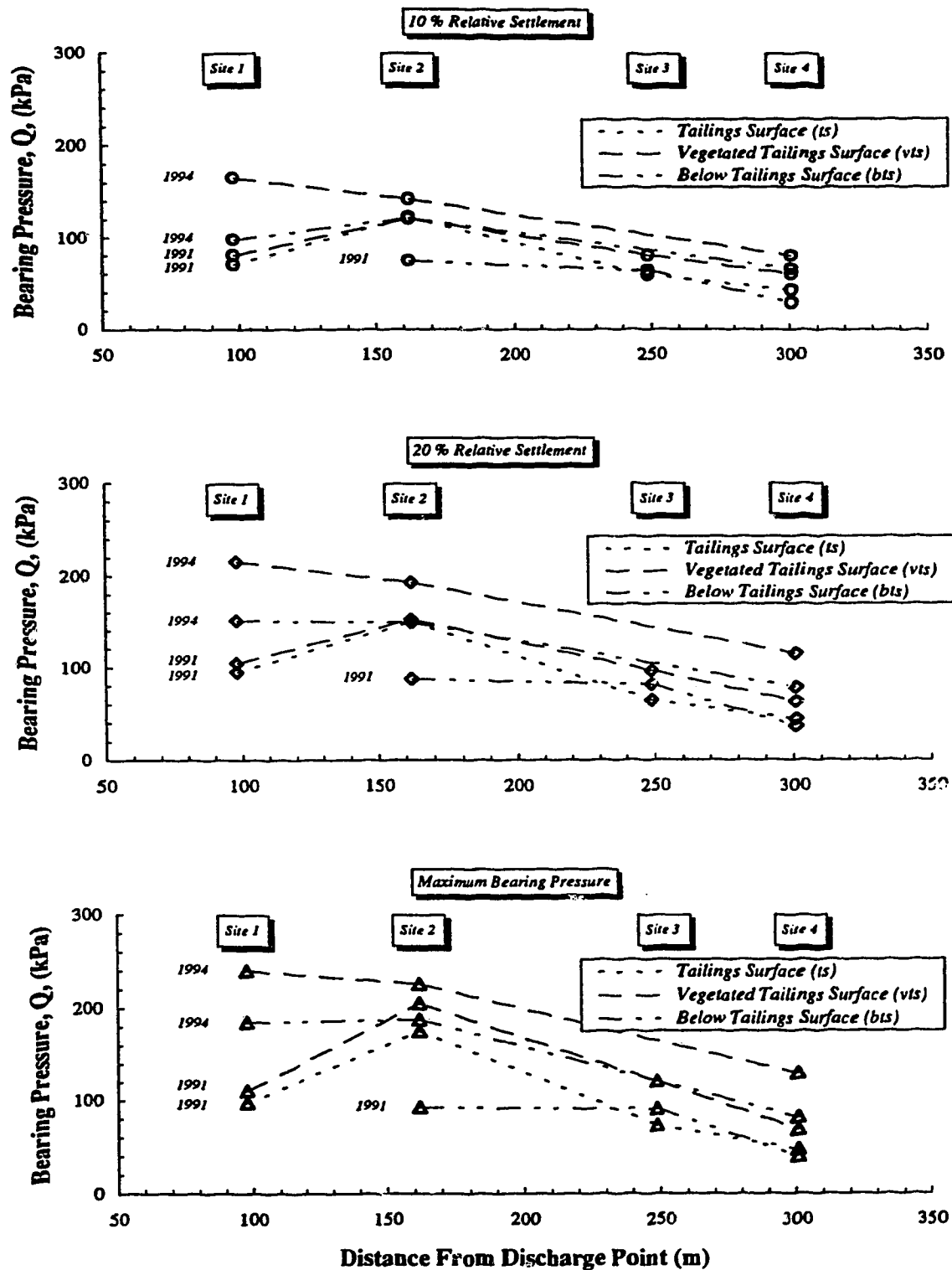


Figure 6.8

Summary of 1991 and 1994 Plate Load Tests at Sites 1 Through 4

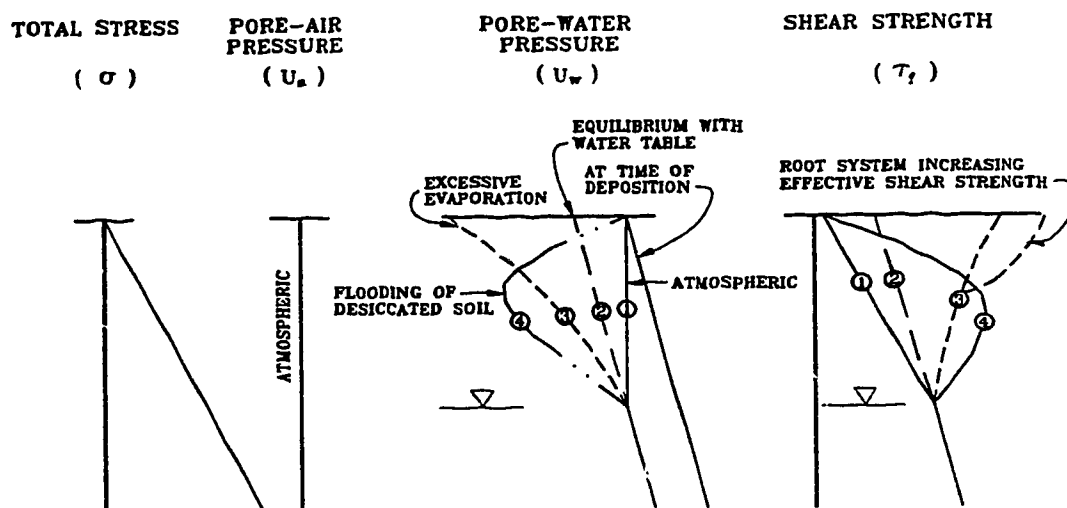


Figure 6.9 Potential Matric Suctions and Associated Shear Strengths in the Unsaturated Zone

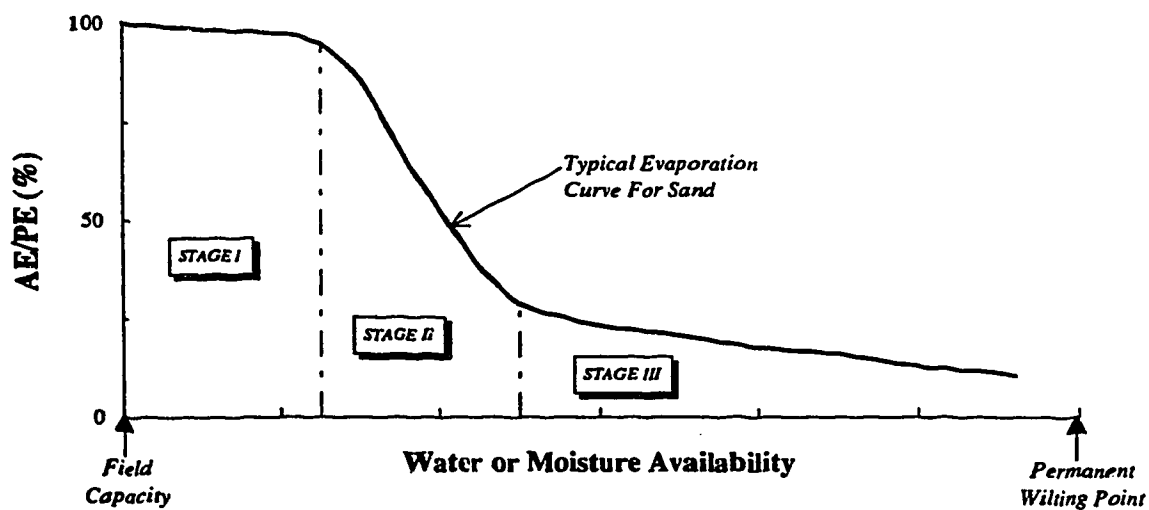


Figure 6.10 Typical Evaporation Curve for Sand (modified from Wilson et al. 1994)

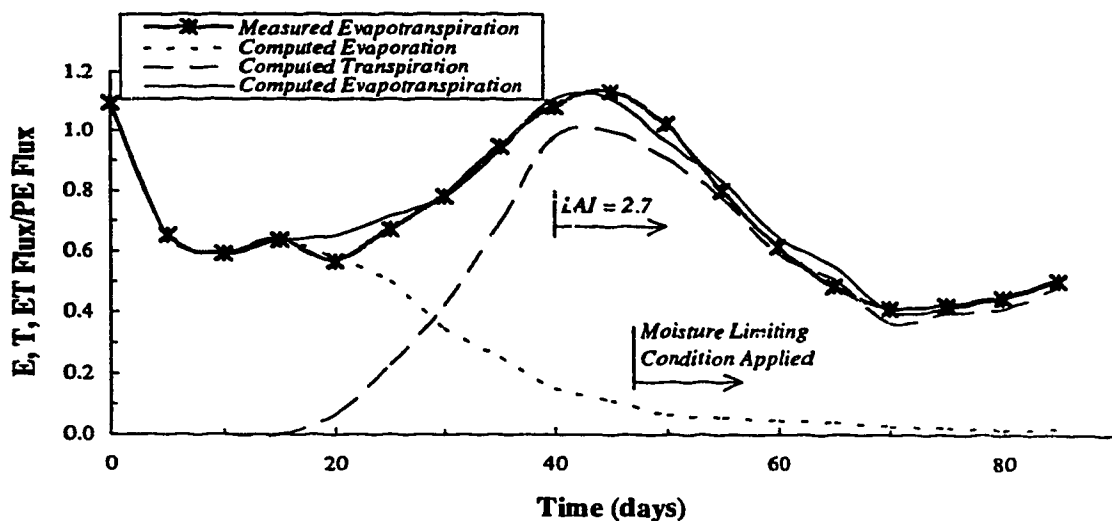


Figure 6.11 Laboratory and Model Evaporation, Transpiration and Evapotranspiration Fluxes (modified from Tratch et al. 1995)

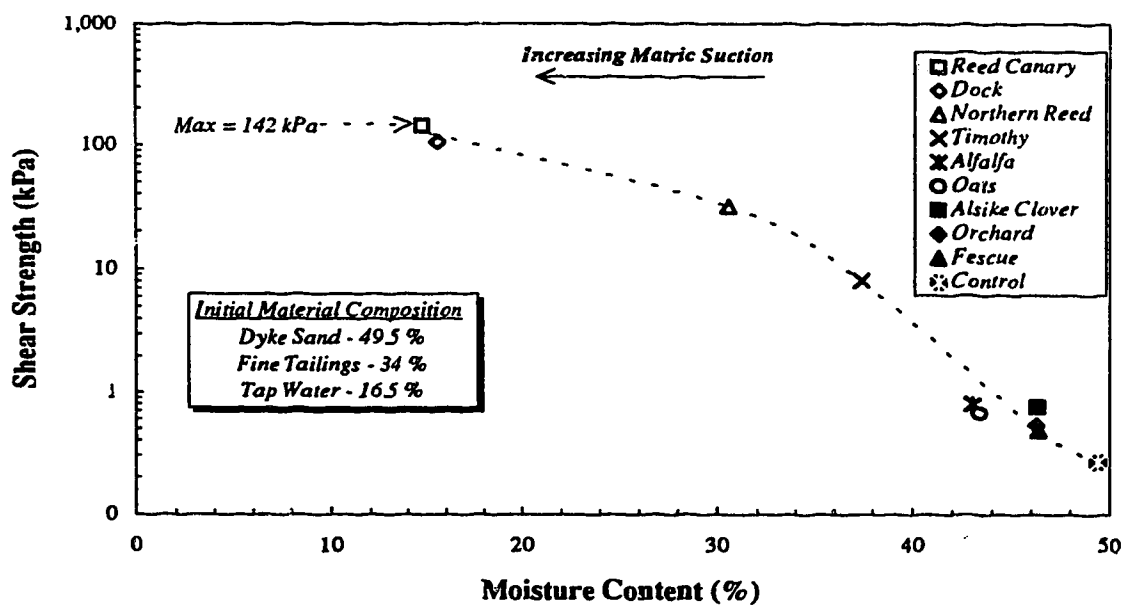


Figure 6.12 Influence of Evapotranspiration on Shear Strength and Moisture Content of Tailings (data source: Johnson et al. 1991)

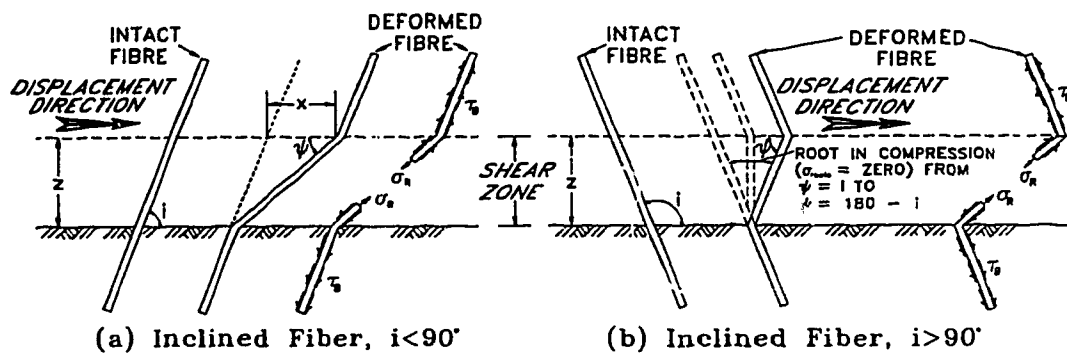


Figure 6.13 Fibre Reinforcing Models for Inclined Fibres

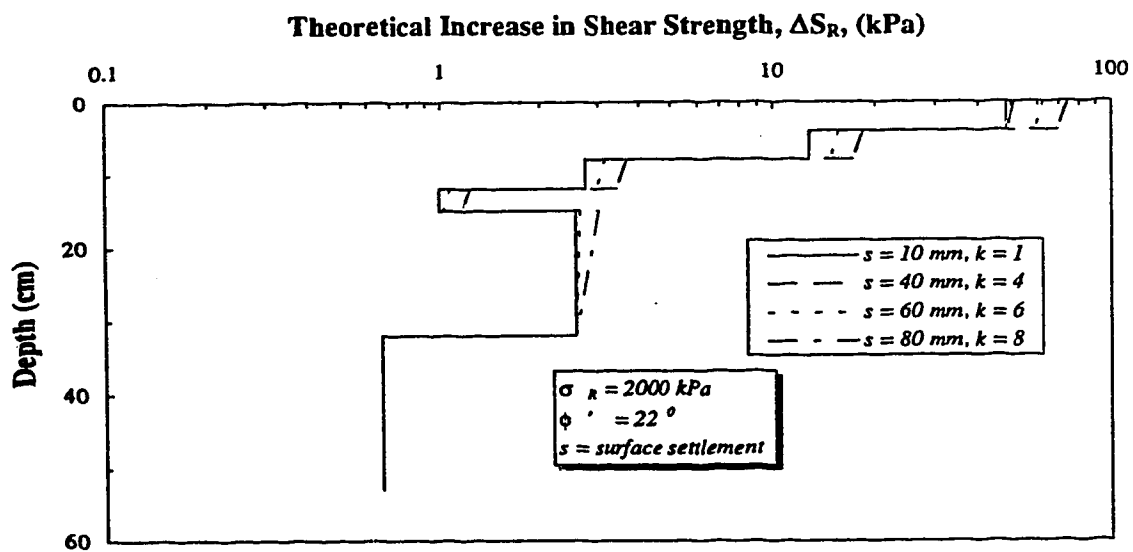


Figure 6.14 Theoretical Increase in Shear Strength from Vegetative Root Systems

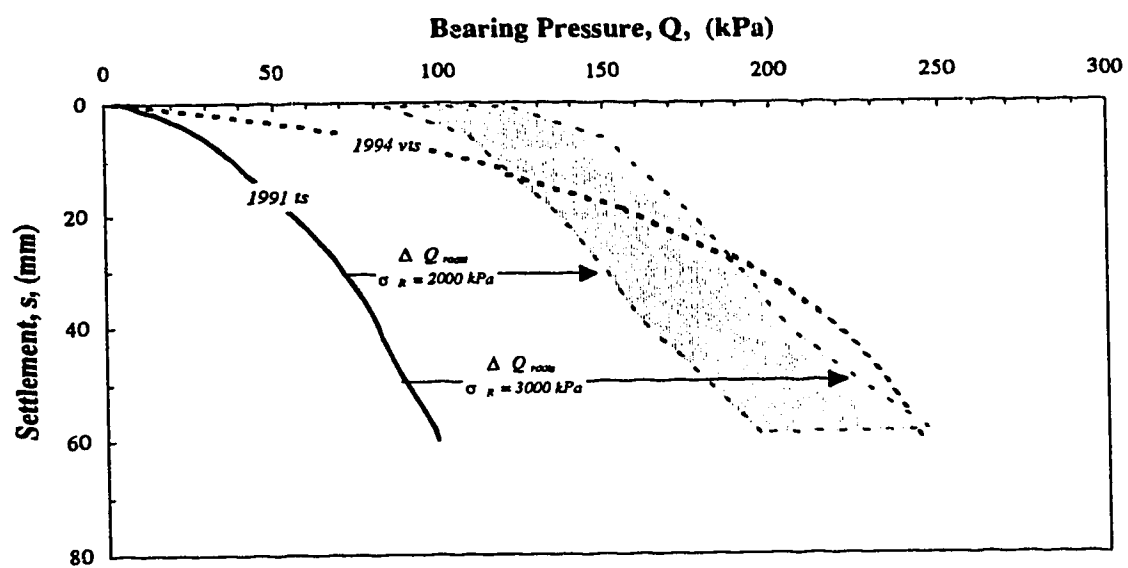


Figure 6.15

Bearing Capacity Results at Site 1 with Theoretical Increase Resulting from Root Reinforcement

Chapter 7

Characterization And Dry Landscape Reclamation Of Mine Tailings¹

7.1. INTRODUCTION

Tailings refer to any solid form of mine or mill waste, including rock-sized stripping wastes, underground mine muck, and finely ground mill wastes. The annual production of mining wastes in the U.S. totals 1.4 billion tons per year according to 1986 data from the US EPA (Brumund 1988). Furthermore, EPA information estimates that about 31 billion metric tons of mine wastes and 13 billion metric tons of tailings were accumulated in the U.S. between the years 1910 and 1981 (Testra 1994). Examples in Western Canada which the authors have direct experience and which support these volumes firstly include the oil sands mining operations (Suncor Inc. and Syncrude Canada Ltd.) in Northern Alberta, Canada. The annual combined mining, processing, and beneficiation of 84 million m³ of oil sands, producing annually 85 million barrels of high quality synthetic crude (Sheeran 1993), results in the annual generation of 160 million m³ of fluid tailings with a solids content of 40% to 60% by mass (Suthaker 1995). Several surface impoundments have been constructed to house these tailings, one of the largest measuring approximately 25 km² in area with a height ranging from 32 to 90 m.

¹ Submitted Paper:

Stahl, R.P., and Sego, D.C., 1996. Characterization and Dry Landscape Reclamation of Mine Tailings. paper submitted to the Third International Symposium on Environmental Geotechnology, June 10-12, 1996, 10 pgs.

The Highland Valley Copper mine, a hard rock mining operation in central British Columbia, mines and processes approximately 130,000 metric tons of ore per day. Benefication of the ore yields a copper and molybdenum concentrate stream (over 1000 metric tons per day) with the remainder constituting the tailings stream (Sporleder 1989). The slurried portion of the tailings stream is deposited into a surface impoundment developed through the construction of two dams which intersect the valley floor. This impoundment is 10 km long, will measure 5 km in width, and reach a storage capacity of 2.7 billion metric tons of tailings (Sporleder 1989).

A smaller tailings facility which will be discussed herein, but which encompasses many of the reclamation issues faced by these larger facilities, is the Coal Valley tailings impoundment located approximately 200 km west and 90 km south of Edmonton, Alberta. This tailings impoundment, shown in Figure 7.1, is operated by Luscar Sterco (1977) Ltd. and measures approximately 18.2 hectares in area. Fine saturated coal tailings generated during the annual production of 1.8 million clean tons of coal, were previously pumped at a solids content of 35% into this impoundment. Reclamation activities were subsequently initiated in 1989 when this impoundment reached full capacity.

Our ability to produce these tremendous volumes of mine wastes and associated containment facilities is impressive. However, the limited shear strength and bearing capacity of some of these deposits prevent effective characterization of the surficial soils for the purposes of dry landscape reclamation. With reference to the investigations conducted along the Coal Valley tailings impoundment, a distinction is made regarding the hydraulic transport of slurried tailings, and the resulting grain size distribution along the impoundment. The geotechnical testing equipment which was developed/modified to characterize the limited bearing capacity surface materials is outlined, and the natural processes which have enhanced the shear strength, bearing capacity, and surface stability of the tailings at Coal Valley from 1989 to the present are discussed.

7.2. TAILINGS DEPOSIT CHARACTERISTICS

The behavior of slurried tailings during hydraulic transport may be classified as segregating or nonsegregating. Segregation refers to the tendency of the solid fraction (or part of it) to settle and create a concentration gradient within the mass. Nonsegregating behavior maintains a uniform distribution of solids throughout the mass. Segregating or nonsegregating behavior of a slurry depends upon the type of carrier fluid, type and amount of chemicals additives, type, concentration, and grain size distribution of the solids, and the flow conditions (Küpper 1991). The tailings deposited into the Coal Valley impoundment were segregating and subsequently underwent hydraulic sorting along the beach following deposition.

Hydraulic sorting refers to the separation of hydraulically deposited materials in different granulometric fractions as a result of the hydraulic flow characteristics. In general, hydraulic sorting results in a decrease in mean grain size (D_{50}) and an increase in the amount of fines (" $F\%$ ", material $< 74\text{mm}$) with distance from the discharge point. Based on weighted averages of the shallow heterogeneous subsurface grain size distributions at Sites 1 through 4 located along the beach portion of the impoundment shown in Figure 7.1, the average D_{50} 's and ($F\%$) were 0.19 mm (36%), 0.25 mm (28%), 0.16 mm (38%), and 0.04 mm (70%) respectively. The material sampled from the pond portion of the impoundment (Figure 7.1) had a D_{50} of 0.0024 mm and $F\%$ of 100%. It is noted that Site 2 had a comparatively greater D_{50} and lower $F\%$ than Site 1 yet is located further downstream. This anomaly is explained by the remnant (possibly high flow velocity) depositional channel adjacent Site 2 which likely encouraged the coarser localized shallow deposit (Küpper 1991). In addition to hydraulic sorting, the beach tailings sites investigation locations displayed considerable heterogeneity on the scale of centimeters as illustrated in Stahl and Sego (1992, 1995b), and supported by Küpper (1991).

7.3. CHARACTERIZATION

Tailings are generally of no direct economic value and their disposal adds to the cost of mineral production. Consequently, the objective of all mine operators is to dispose of the tailings as cheaply as possible (Klohn 1982). Although this philosophy is not completely correct today in light of environmental and reclamation concerns shared by mine operators, the method of disposal in the past and present commonly produces loose, sometimes impervious, and potentially liquefiable tailings (Morgenstern and Küpper 1988). Characterization of these low strength deposits using conventional geotechnical techniques may require construction of thick soil ramps complete with a geotextile separation layer to support the geotechnical investigation equipment as employed to investigate a copper tailings deposit as discussed by Vidic *et al.* (1995). East (in Ulrich and East 1996) verbally outlined in his presentation the placement of access ramps measuring upto 12 m thick to investigate weak tailings deposits.

The shallow subsurface characterization of limited bearing capacity deposits discussed herein was achieved without access ramp construction through development/modification of traditional geotechnical testing equipment. The equipment developed/modified includes a Plate Load Test (*PLT*) apparatus, a Cone Penetration Test (*CPT*) apparatus, and Spectral Analysis of Surface Waves (*SASW*) system to determine the shear wave velocity profile of the tailings. All three testing apparatuses had stringent specification for load capacity, sensitivity and range, and foremost had to fulfill a minimum weight requirement enabling transport to, and investigations at, some of the weaker sites requiring only human effort. Details of the specifications and illustrations of the *PLT*, *CPT*, and *SASW* apparatuses are provided in Stahl *et al.* (1996). For reasons of testing history and ensuing detailed analysis, the results from the *PLT*'s along the beach portion of the impoundment will only be presented. Similarly, the historic site investigations within the pond region using the *Genor* Field Vane Shear Test (*FVST*) apparatus will also only be discussed.

7.4. DRY LANDSCAPE RECLAMATION

7.4.1. General Reclamation Processes

The increase in shear strength, bearing capacity, surface stability and the dry landscape reclamation of soft tailings may require the removal of water to increase intergranular stress and strength, and or the addition of reinforcing or strengthen agents as discussed in Barth (1986). The immense areas which these tailings occupy, however, favor efficient and cost effective reclamation solutions supporting the adoption and engineering of natural processes which dewater and reinforce the surficial tailings. Figure 7.2 summarizes the key natural processes which strengthen the slurried tailings follow deposition. This figure highlights the two extremes produced following hydraulic sorting of a segregating slurry, with a non-segregating slurry relying on similar natural processes for shear strength, bearing capacity and surface stability enhancement. It is emphasized that these generic processes (*ie. consolidation may include osmotic and selfweight*) are not mutually exclusive (*ie. consolidation may be induced through matric suction changes from evaporation/evapotranspiration*). The processes which will be discussed herein include freeze-thaw consolidation, drainage, evaporation, evapotranspiration, and fibre reinforcement of vegetative root systems.

7.4.2. Freeze-Thaw Consolidation

The processes of consolidation of fine, high void ratio saturated tailings through freeze-thaw has been known for several years, and has been successfully evaluated and validated using large scale field tests on oil sand fine tailings as discussed by Sego *et al.* (1993 and 1994). Freezing of these saturated tailings results in the generation of negative pore pressures (sponsored through surface tension differences) between the unfrozen water surrounding the mineral particles and the ice within the voids. The negative pore pressures induce moisture migration from the unfrozen water to the growing ice lense and ultimate consolidation of the mineral grains. The ensuing frozen mass includes a segregated reticulate ice and consolidated fine grained soil “ped” structure.

The “open system freezing” process which occurs in nature as a result of sub-zero winter temperatures is active within the pond portion of the Coal Valley tailings impoundment. As the

fine saturated tailings freeze downwards as a result of sub-zero ambient air temperatures, a segregated reticulate ice/fine grained consolidated soil “ped” structure develops above the downward advancing frost. Steady state thermal conditions are eventually established between the freezing front below the surficial frozen tailings and the unfrozen tailings at depth. This condition result in the formation of near horizontal ice lenses (perpendicular to the upward heat flow towards the surface) just above the 0 °C isotherm as water is drawn from the unfrozen tailings at depth. This “open system freezing” process is contrary to “closed system freezing” or “undrained freezing” where migration of free water to the freezing front from the unfrozen soil is restricted.

Thawing of the segregated ice profile and settling of the consolidated soil “peds” through density differences with the vertical migration of moisture from the segregated reticulate ice and horizontal ice lenses results in net consolidation (volume reduction) of the fine tailings. The fine tailings also experience mechanical changes including reduced compressibility, increased shear strength, with the composite thawed soil “ped” structure also realizing increased permeability (Sego *et al.* 1993, 1994).

The impact of cyclical freeze-thaw sponsored through seasonal temperature variations within the pond region (Figure 7.1) of the Coal Valley tailings impoundment is illustrated in Figure 7.3. This figure includes the average undrained shear strengths below the ice surface, determined in the unfrozen tailings, using the FVST apparatus. The shear strength profiles determined on two separate occasions in the winter of 1989/1990 (following completion of deposition) are virtually identical and coincide with the normally consolidated shear strength profiles estimated for three compression indices ($C_c = 0.3, 0.54, \text{ and } 1.0$), based on the plasticity index ($PI = 35\%$) of the tailings (Stahl and Sego 1995a).

Based on the mechanics of freeze-thaw, visual observations in the field, and laboratory studies, two regions along the post 1990 field shear strength profiles are defined. The boundary for these two regions at a depth of 1.2 m is approximately located at the inflection point of the profiles. As confirmed in laboratory tests (Sego 1990) the inflection point is associated with a zone of thick ice lenses which resulted from upward moisture migration induced through suction gradients in

the freezing zone as discussed above for open system freezing. The upper region, which displays shear strengths considerably greater than the 1989/1990 profiles, includes tailings which have experienced post freeze-thaw consolidation and strength gain as discussed above. Although the trend of increasing shear strength with decreasing depth in this upper region is reminiscent of a clay deposit with a desiccated crust, a water cap has always been maintained within the pond and the tailings have not been subjected to drying.

The lower region (below 1.2 m) has also experienced considerable strength gain beyond the initial 1989/1990 profiles. As illustrated in Figure 7.3, the strength gain in this region is likely the result of self weight and freeze-thaw inspired upward moisture migration which consolidate and strengthen the fine tailings. Although heterogeneities influence shear strength and variability thereof, the slope of the shear strength profile beyond the 1.2 m depth is similar to the theoretically estimated profile considering the C_c of 1.0.

7.4.3. Drainage/Evaporation/Evapotranspiration

The processes of drainage, evaporation, and evapotranspiration along the surficial beach portion of the Coal Valley tailings impoundment results in the development of a two phase geotechnical subsurface system which includes a variable thickness unsaturated zone at the surface and a saturated zone at depth. The thickness of the unsaturated zone decreases with increasing proximity to the pond. Drainage and for that matter infiltration are gravity driven processes depending mainly upon soil properties such as hydraulic conductivity. Evaporation from a soil surface is more complicated and controlled, by both climatic conditions which define the potential rate of evaporation, and soil properties such as saturated and unsaturated hydraulic conductivity (Wilson *et al.* 1994). Transpiration offered by vegetative root systems is also dependent upon the hydraulic conductivity of the soil, the water availability of the subsurface, the root type and morphology, as well as the leaf area index (*LAI*) of the vegetative canopy as discussed by Ritchie (1972). Transpiration processes which effectively dewater the soil at depth beyond pure evaporation is illustrated in laboratory studies by Tratch *et al.* (1995) and further discussed in Stahl and Sego (1995b). The dewatering of these tailings and ensuing development of an

unsaturated zone and enhanced shear strength which supports dry landscape reclamation activity warrants consideration.

The shear strength of unsaturated soils, τ_f , may be defined in terms of two stress variables, $(\sigma - u_a)$ and $(u_a - u_w)$, as presented in Fredlund *et al.* (1978), Fredlund and Rahardjo (1993) as:

$$\tau_f = c' + (\sigma - u_a)_f \tan \phi' + (u_a - u_w)_f \tan \phi^b \quad [7.1]$$

where c' is the effective cohesion parameter, σ , u_a , u_w denote total stress, pore air pressure, and pore water pressure, $(\sigma - u_a)_f$ is the net normal stress on the failure plane at failure, $(u_a - u_w)_f$ is the matric suction on the failure plane at failure, ϕ' is the angle of internal friction with respect to net normal stress, and ϕ^b is the angle of internal friction with respect to matric suction. The shear strength of saturated soils is a special case of [7.1] where the u_a term of the stress variable $(\sigma - u_a)$ equals the u_w value and $(u_a - u_w)$ approaches zero. Based on [7.1], the *insitu* shear strength and bearing capacity change through matric suction variations in response to climatic or environmental conditions such as evaporation, evapotranspiration, and precipitation.

In addition to time dependent matric suction variations developed through environmental conditions, matric suctions will also vary spatially particularly with depth. The relative temporary seasonal arid conditions experienced during the *PLT* site investigations conducted in the summers of 1991 and 1994 at Coal Valley support an excessive evaporation matric suction profile (Stahl and Sego 1995b) reminiscent of a decreasing matric suction with increasing depth. Although matric suctions were not measured, visual observations of a desiccated crust support this hypothesis. This excessive evaporation profile and resulting increase in matric suction and shear strength at the surface (compared to at depth) is illustrated using *PLT* results shown in Figure 7.4. This figure includes some the 1991 *PLT*'s conducted at Sites 2 (strongest), and Site 4 (weakest) on the tailings surface (*ts*), vegetated tailings surface (*vt*), and below the tailings surface (*bts* 0.22m). The number following the *bts* acronym refers to the depth of the *PLT* below the tailings surface.

Considering the *ts* and *bts* tests, these sites generally displayed an increased bearing capacity at the surface compared to at depth. Although soil heterogeneities influences the results, the increase in capacity at the surface is believed mainly from higher matric suctions and resulting higher shear strengths. In addition, the *PLT*'s conducted on the vegetated tailings surface generally displayed the greatest capacity. The mechanics surrounding the increased capacity experienced at the vegetated tailings sites is analyzed below.

7.4.4. Fibre Reinforcement of Vegetative Root Systems

The effects of fibre reinforcement on the increased shear strength of soils has been recognized for several decades (Stahl and Sego 1995b). Although several simplistic empirical formations are presented in the literature which attempt to predict the increase in shear strength of fibre or root permeated soils, they are limited in their application (Stahl and Sego 1995b). Consequently, to model the effect of vegetative root systems on bearing capacity of the tailings, a force-equilibrium model discussed in the literature (Gray and Al-Refeai 1986) was chosen. The initial model which includes fibres orientated perpendicular (not shown) and inclined ($i < 90^\circ$) to the shear zone is illustrated in Figure 7.5. Considering the orientation of roots intersecting the developing shear zone beneath a *PLT*, the initial model was modified to include roots which initially are orientated in a compression condition ($i > 90^\circ$) as shown in Figure 7.5. Roots in a compression orientation do not contribute to shear strength until the deformation of the shear zone causes sufficient root rotation to develop tensile stresses. Based on the model, the predicted strength increase, ΔS_R , from regular arrays of multiple, orientated inclined fibres is given by:

$$\Delta S_R = t_R [\sin(90 - \psi) + \cos(90 - \psi) \tan \phi] \quad [7.2]$$

$$\text{where } \psi = \arctan \left[\frac{I}{k + (\tan i)^{-1}} \right] \quad [7.3]$$

and t_R is the mobilized tensile strength of the fibres per unit area of soil; ϕ is the angle of internal friction of the soil; i is the initial orientation angle of the fibre with respect to the shear surface; k is the shear distortion ratio ($k = x/z$) with z being the thickness of the shear zone and x being the horizontal shear displacement. The mobilized tensile strength per unit area of soil is given as:

$$t_R = \left(\frac{A_R}{A} \right) \sigma_R \quad [7.4]$$

with σ_R equal to the tensile stress developed in the fibres within the shear zone, A_R is the cross-sectional area of the roots within the shear zone and A is the total cross-sectional area of the shear zone.

The modified model was further modified to address the complex stress-strain paths associated with *PLT*'s conducted on compressible tailings which fail in punching shear. In summary, these modifications attempt to consider variation of root orientation in the subsurface, variable shear strain distribution at depth, and possible root slippage or pullout near the tailings surface.

The increase in bearing capacity, ΔQ_{roots} , resulting from root reinforcement was determined using, as a framework, the cohesion component formulation of the general bearing capacity equation (Bowles 1988, Vesic 1973, Vesic 1975) shown as:

$$\Delta Q_{roots} = N_c s_c \Delta S_R \quad [7.5]$$

where N_c is the bearing capacity factor for cohesion (5.14), s_c is the shape factor for a circular footing (1.2), and ΔS_R is the theoretical shear strength from root reinforcement defined in [7.2].

With recent root area profile measurements, the theoretical contribution of vegetative root systems to bearing capacity using [7.2] through [7.4] and [7.5] with the aforementioned modifications is shown for Site 1 in Figure 7.6. This figure illustrates the 1994 vegetated tailings surface (*nts*) bearing capacity profile, and the 1991 tailings surface (*ts*) profile coupled with the theoretical contribution from root reinforcement. The bearing capacity contribution from root reinforcement considers "estimated" (Schiechl 1980, Naeth 1995) root tensile strengths, σ_R , ranging from 2000 kPa to 3000 kPa which likely reflect lower bound values for Reed Canary vegetation which was the dominant vegetation on the tailings. These lower bound estimates of σ_R

provide for conservatism and indirectly account for potential root rupture beneath the loaded plate.

Although several preliminary assumptions and estimates were made to model the soil-root interaction mechanics beneath a *PLT* on compressible, heterogeneous tailings at Coal Valley, the predicted increase in bearing capacity is within the same range as the 1994 vegetated tailings surface (*vts*) results and is very encouraging. Similar successful predictions of the increase in bearing capacity were obtained at the other sites within the tailings impoundment.

7.5. SUMMARY AND CONCLUSIONS

Mine wastes in the form of slurried tailings, which are typically deposited in surface impoundments, can be very loose, weak, exhibit limited bearing capacity and surface stability, and present difficulties with respect to characterization and dry landscape reclamation. Three key geotechnical investigation systems were developed/modified to facilitate characterization of these weak deposits utilizing only human effort, with only the results from the Plate Load Test (*PLT*) along the beach portion of the impoundment discussed herein. In addition, the results from the Field Vane Shear Test (*FVST*) apparatus, employed to characterize the pond portion of the impoundment, were also included.

The key natural processes which enhance the shear strength, bearing capacity, and surface stability of the tailings were outlined. Cyclic freeze-thaw consolidation coupled with freezing and self weight induced moisture migration and consolidation have considerably enhanced the shear strength of the saturated silt and clay within the pond region of the impoundment. Drainage, evaporation, and evapotranspiration processes have dewatered the surficial tailings, increased the matric suction, and enhanced the shear strength and bearing capacity of the heterogeneous, compressible tailings at the surface. The contribution of vegetative root systems to increased shear strength and bearing capacity was evaluated using a modified theoretical model. This modified model showed success in predicting the increase in surface bearing capacity observed at

The adoption/engineering of these and other natural processes to enhance the surficial strength, bearing capacity, and surface stability of tailings encourages dry landscape reclamation philosophies with potential thickness reduction, or elimination of soil capping with reduced short and long term reclamation costs.

7.6. REFERENCES

- Barth, R.C., 1986. Reclamation Technology for Tailings Impoundments - Part I: Containment. *Journal of Mineral and Energy Resources*, **29**(1):1-25.
- Bowles, J.E., 1988. **Foundation Analysis and Design**. McGraw-Hill, Inc., New York, 1004 pgs.
- Brumund, W.F., 1988. Waste Management - An Overview of USA Activity from a Geotechnical Perspective. Symposium on Solid Waste Management - Landfill Design: From Concept to Completion. Southern Ontario Section of the Canadian Geotechnical Society, 34 pgs.
- Fredlund, D.G., and Rahardjo, H., 1993. **Soil Mechanics For Unsaturated Soils**. John Wiley & Sons, Inc. New York., 517 pgs.
- Fredlund, D.G., Morgenstern, N.R., and Widger, R.A., 1978. The Shear Strength of Unsaturated Soils. *Canadian Geotechnical Journal*, **15**(3): 313-321.
- Gray, D.H., and Al-Refeai, T., 1986. Behavior of Fabric-Versus Fibre-Reinforced Sand. *ASCE Journal of Geotechnical Engineering* **112**(8) 804-821.
- Klohn, E.J., 1982. The Developments of Current Tailings Dam Design and Construction Methods. *Journal of Mineral and Energy Resources* **25**(5):1-15.
- Küpper, A.M.A.G., 1991. Design of Hydraulic Fill. Unpublished Ph.D. Thesis, Department of Civil Engineering, The University of Alberta, 525 pgs.
- Naeth, A., 1995. Personal Communications. Assistant Professor, Department of Renewable Resources, The University of Alberta, Edmonton, Alberta.
- Ritchie, J.T., 1972. Model for Predicting Evaporation from a Row Crop with Incomplete Cover. *Water Resources Research*, **8**(5):1204-1213.
- Schiechtl, H., 1980. **Bioengineering for Land Reclamation and Conservation**. University of Alberta Press, Edmonton, Alberta, 400 pgs.

- Sego, D.C., 1990. Use of Freeze-Thaw to Assist in Reclamation of a Coal Tailings Pond. Submitted to Luscar Sterco (1977) Ltd., 27 pgs.
- Sego, D.C., Burns, R., Dawson, R., Dereniwski, T., Johnson, R., and Lowe, L., 1993. Dewatering of Fine Tails Utilizing Freeze-Thaw Processes. Fine Tailings Symposium, Proceedings of the Oil Sands - Our Petroleum Future, April 4-7, 1993, Edmonton, Alberta, Paper F17, 25 pgs.
- Sego, D.C., Dawson, R.F., Dereniwski, T., and Burns, B., 1994. Freeze-Thaw Dewatering to Reclaim Oil Sand Fine tails to a Dry Landscape. 7th International Cold Regions Engineering Specialty Conference, March 7-9, 1994, Edmonton, Alberta, pgs 669-688.
- Sheeran, D.D., 1993. An Improved Understanding of Fine Tailings Structure and Behavior. Fine Tailings Symposium, Proceedings of the Oil Sands - Our Petroleum Future, April 4-7, 1993, Edmonton, Alberta, Paper F1, 11 pgs.
- Sporleder, L.E., 1989. Highland Valley Copper, A World-Class Copper Partnership. Engineering and Mining Journal, 190(8):44-46.
- Stahl, R.P. and Sego, D.C., 1992. Influence of Natural Surface Processes on Reclamation of the Coal Valley Tailings Impoundment. Second International Conference on Environmental Issues and Management of Waste in Energy and Mineral Production, Calgary, Alberta, September 1-4, pgs. 389-400.
- Stahl, R.P. and Sego, D.C., 1995a. Freeze-Thaw Dewatering and Structural Enhancement of Fine Coal Tails. ASCE Journal on Cold Regions Engineering, 9 (3):135-151.
- Stahl, R.P., and Sego, D.C., 1995b. Influence of Natural Surface Enhancement Processes on Bearing Capacity and Reclamation of Fine Coal Tails. paper submitted for review to the Canadian Mining and Metallurgical Bulletin, December, 1995, 29 pgs.
- Stahl, R.P., Sego, D.C., Robertson, P.K., and Woeller, D., 1996. Characterization of Fine Processed Mine Tailings Deposits For Purposes of Dry landscape Reclamation. Tailings and Mine Wastes '96, Fort Collins, Colorado, January 16-19, pgs 515-524.
- Suthaker, N.N., 1995. Geotechniques of Oil Sand Fine Tailings. Unpublished Ph.D. Thesis, Department of Civil Engineering, The University of Alberta, 223 pgs.
- Testa, S.M., 1994. **Geological Aspects of Hazardous Waste Management**. CRC Press, Inc., Boca Raton, Florida, 537 pgs.
- Tratch, D.J., Wilson, G.W., and Fredlund, D.G., 1995. An Introduction to Analytical Modelling of Plant Transpiration for Geotechnical Engineers. Proceedings, 48th Canadian Geotechnical Conference, Vancouver, B.C., pgs 771-789.

- Ulrich, B.F., and East, D.R., 1996. Experiences with Insitu Tests in Mine Tailings for Reclamation and Facility Expansion. Tailings and Mine Wastes '96, Fort Collins, Colorado, January 16-19, pgs 505-513.
- Vesic, A.S., 1973. Analysis of Ultimate Loads of Shallow Foundations. Journal of Soil Mechanics and Foundation Division, ASCE, **99**(1):45-73.
- Vesic, A.S., 1975. Chapter 3 of Winterkorn, H.F., and Fang, H.Y.. **Foundation Engineering Handbook**. Van Nostrand.
- Vidic, S.D., Beckwith, G.H., and Mayne, P.W., 1995. Profiling Mine Tailings With CPT. Proceedings of the International Symposium on Cone Penetration Testing, "CPT'95", Linköping, Sweden, October 4-5, pgs 607-612
- Wilson, G.W., Fredlund, D.G., and Barbour, S.L., 1994. Coupled Soil Atmosphere Modelling for Soil Evaporation. Canadian Geotechnical Journal, **31**(2):151-161.

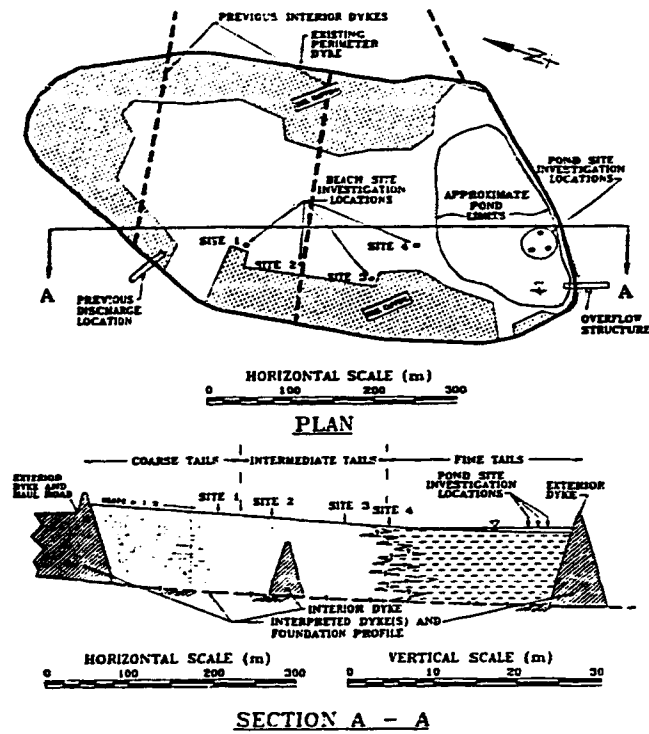


Figure 7.1 Plan and Section of Coal Valley Tailings Impoundment

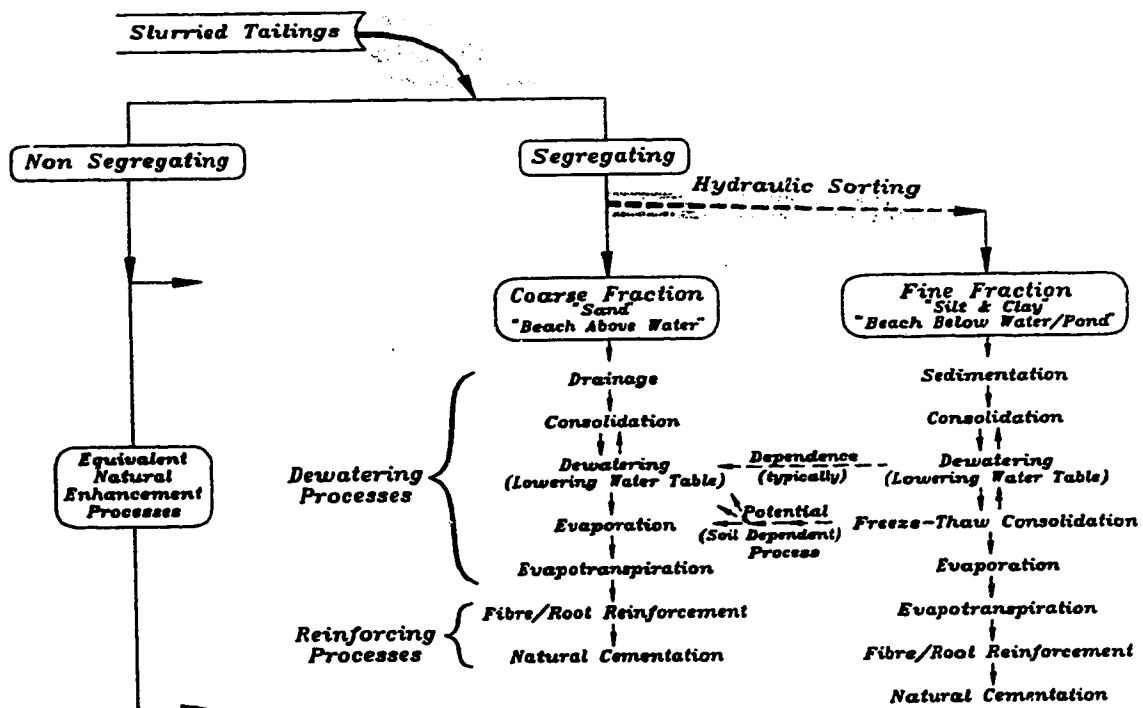


Figure 7.2 Key Natural Enhancement Processes For Dry Landscape Reclamation of Tailings

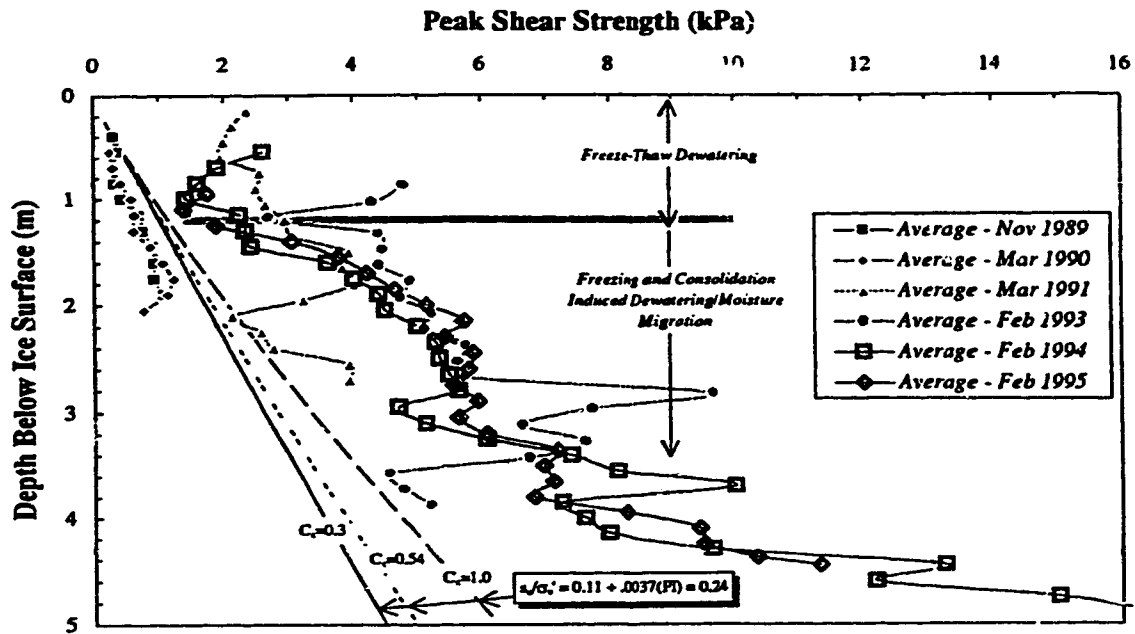


Figure 7.3 Theoretical and Actual Shear Strength Profiles in Pond

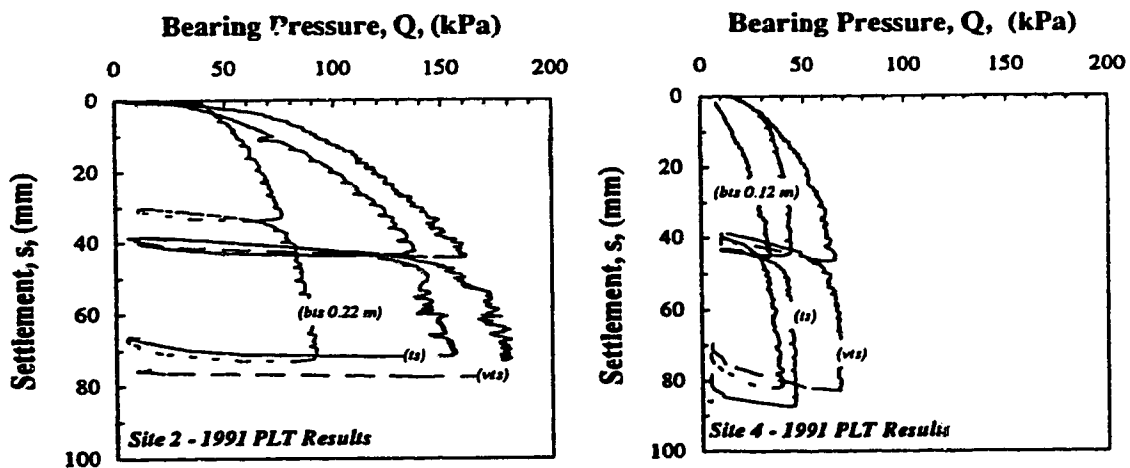


Figure 7.4 1991 Plate Load Test Results at Site 2 and Site 4

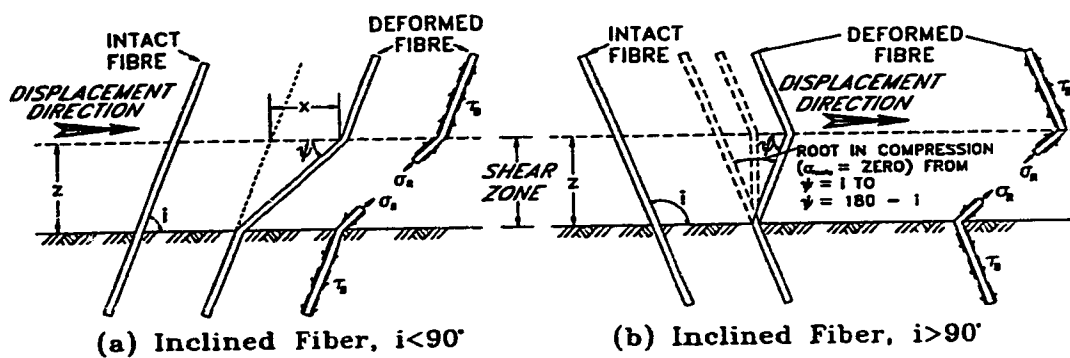


Figure 7.5 Fibre Reinforcing Model for Inclined Fibres

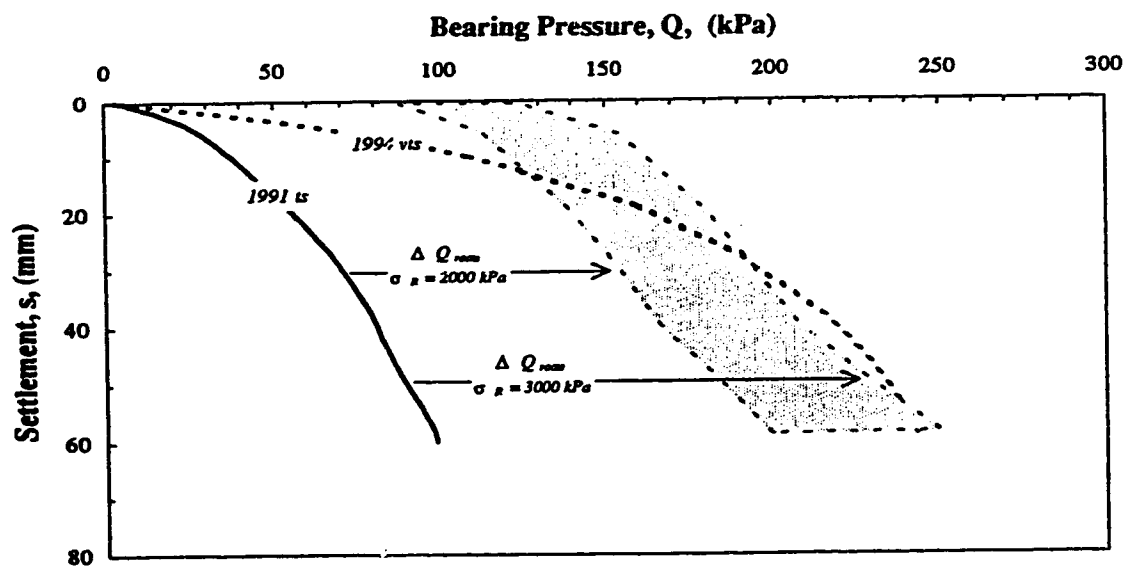


Figure 7.6 Bearing Capacity Results at Site 1 with Theoretical Increase Resulting from Root Reinforcement

Chapter 8

Natural Surface Enhancement Process Design Guidelines

8.1. INTRODUCTION

Reclamation of mine wastes requires a synergy of techniques to achieve the desired landscape which is economically and environmentally acceptable and is harmonious with regional analogues. A multitude of wet and dry landscape scenarios may be envisioned and achieved. Herein, a focus is placed on natural techniques to reclaim fine processed mine wastes to the desired dry landscape. Although the following discussion is applicable to a variety of tailings deposits, the underlying theme of this chapter centers on the Coal Valley tailings facility. The following briefly summarizes methods, models and investigation techniques which help promote dry landscape reclamation activities and provide a framework for regulatory approval. As in the previous chapters and successive appendices, the natural surface enhancement processes discussed in the following include freeze-thaw consolidation, evaporation, evapotranspiration, and fibre reinforcement of vegetative root systems. Processes including drainage and selfweight consolidation as presented in Chapter 7, Figure 7.2, are additional factors which help achieve the desired dry landscape goal.

8.2. FREEZE-THAW CONSOLIDATION DEWATERING

8.2.1. Processes and Models

Structural enhancement of fine grained tailings pond materials through natural surface processes firstly requires reduction or elimination of the water cap to exposure the fine tailings to the environmental loading conditions (freeze-thaw, evaporation → evapotranspiration). Horizontal finger drains, vertical drains, with well managed decant structures can help achieve this goal.

Climatic temperature conditions dictate the volume of fine tailings which may be structurally enhanced through freeze-thaw. Contingent on the site specific climatic freezing and thawing indices, the thin layer freezing and thawing models developed by Martel (1988) may be used to optimize freeze-thaw treated volumes. This is a closed system freezing model where migration of external water outside the freezing zone is restricted. Optimization of the freezing process through thin layer placement and the relatively limited thaw potential of the Canadian climate dictate a thaw controlled processes (i.e. unable to completely thaw the material frozen during the previous winter). Extension of the Martel (1988) model to include additional heat sources to enhance thaw such as warm ground and a warm water cap as outlined by Dawson and Sego (1993) may be considered.

A more passive utilization of freeze-thaw benefits includes the open system freezing and thawing process where thick tailings deposits are subjected to climatic temperature variations as in the case at Coal Valley. Thermally induced suction gradients may not only consolidate the mineral particles into peds as in the closed system process, but the segregating potential of the saturated soil may sponsor moisture migration from outside the freezing zone. As outlined by Konrad and Morgenstern (1983) and Konrad (1994) and illustrated in Chapter 3, Figure 3.3, suction pressures developed within the frozen fringe on the warm side of the warmest ice lense encourage moisture migration from the underlying unfrozen soil. The characteristics of the freezing soil and propensity for moisture migration is best represented by the Segregation Potential. The Segregation Potential, SP , is defined as the ratio of the rate of water migration to the warmest ice lense, v , to the overall temperature gradient within the frozen fringe, $grad T_f$. The SP may be determined from laboratory freezing tests which record water intake and temperature profile with

time. Based on laboratory step-freezing tests (Sego 1990), the SP of the Coal Valley fine tailings is about $120 \times 10^{-5} \text{ mm}^2/\text{sec} \cdot ^\circ\text{C}$. Davila *et al.* (1993) discusses prediction of SP_o (equivalent to SP at low stresses) based on the grain size distribution and liquid limit of the fine fraction. Based on available data, the boundary between high and low frost susceptible soils is assumed to be at $SP_o = 50 \times 10^{-5} \text{ mm}^2/\text{sec} \cdot ^\circ\text{C}$ (Davila *et al.* 1993). This SP value predicted for the Coal Valley fine tailings is well above this boundary SP value indicating that the tailings are highly frost susceptible. Highly frost susceptible soils experience significant heave and ice lense development through migration of moisture at depth beyond the freezing zone.

The suction pressures developed within the frozen fringe which encourage moisture migration may be determined using the theoretical model presented in Konrad (1994). Considering one-dimensional freezing, and assuming homogeneity of the unfrozen tailings and continuum of the pore fluid, the suction pressure at the frost front theoretically extends throughout the depth of the unfrozen fine tailings deposit. Practically, however, dewatering and consolidation (overconsolidation) of the unfrozen fine tailings near the ice lense results in localized reduced hydraulic conductivity that ultimately impedes moisture migration from the tailings at depth. In the case of high void ratio fine tailings, prediction of the "significant depth" of influence for dewatering and strength gain through thermally induced suction gradients may be achieved using finite strain consolidation models.

8.2.2. Strength Enhancement and Volume Reduction

Repeated freeze-thaw cycles of the Coal Valley fine tails subjected to closed system freezing in the laboratory (Sego 1990) resulted in continued shear strength increase in excess of 10 kPa, with thaw strains of 20 to 25 %. Thaw strains in excess of 50 % have been obtained with oil sand fine tails (Dawson and Sego 1993, Sego *et al.* 1993a). In addition to reduced volume and increased shear strength, the remnant consolidated ped structure formed during freezing results in post thaw geotechnical enhancement including reduced compressibility and increased hydraulic conductivity (Dawson and Sego 1993)

During open system freezing, the relatively high *SP* of the Coal Valley fine tails resulted in moisture migration and horizontal ice lense development within the field and laboratory. Laboratory experiments illustrated that thermal induced suction gradients within the frozen fringe reduced the moisture content of the unfrozen fine tails on the warm side of the ice lense from 85% to about 50% (Sego 1990). Field shear strengths profiles (Chapter 7, Figure 7.3) within the pond above the depth of frost penetration indicate freeze-thaw has enhanced the shear strength from zero to between 2 kPa and 4 kPa. Shear strengths below the depth of frost penetration indicate moisture migration sponsored through thermally induced suction gradients increased the shear strength by 2 to 4 kPa beyond that predicted via selfweight consolidation. This shear strength increase was recorded throughout the profile depth (3 to 4 m) and may have extended deeper.

Given the potential strength enhancement and consolidation benefits of freeze-thaw, investigation activities to evaluate the possibilities of incorporating this process to help achieve a dry landscape include:

- Small scale laboratory closed system freeze-thaw consolidation tests to evaluate potential thaw strain, strength and hydraulic conductivity enhancement. Parameters for the Martel (1988) models should also be obtained.
- Laboratory open system freezing tests to evaluate segregation potential and propensity for additional subsurface moisture migration and dewatering of never frozen material.
- Laboratory parametric analysis to evaluate thermal and drainage boundary conditions, layer thicknesses, freezing and thawing rates, and potential enhancement through chemical additions (Sego *et al.* 1993b).
- Implementation of field trials using lysimeters, constructed cells along the tailings beach, or the existing fine tails pond (Chapter 3, Figure 3.13) to evaluate shear strength development and thaw strain under field conditions. Thermistors to evaluate frost penetration, coupled with strength and moisture content measurements help evaluate large scale field performance.

8.3. EVAPORATION AND EVAPOTRANSPIRATION

8.3.1. Background and Models

Evaporation is an important process enhancing consolidation and shear strength development. The consolidation and shear strength development for unsaturated soils through matric suction development is presented in Fredlund and Rahardjo (1993). As with freeze-thaw, evaporation is a climatic dependent process. The net annual evaporation (evaporation - precipitation) at Coal Valley is near zero, however, net summer evaporation is about 200 mm (Canadian Climatic Normals). This is compared with annual evaporation rates up to and exceeding 4 m in more arid climates like Australia (Fahey and Fujiyasu 1993).

A variety of models with varying complexity are presented in the literature which may help predict the sedimentation and desiccation of high void ratio fine grained mine wastes. A semi-empirical approach is described in Swarbrick (1992), a more complex theoretical approach is presented in Abu-Hejleh (1993), and a purely empirical method is mentioned in Fahey and Fujiyasu (1993). Such models may be employed to predict the sedimentation, consolidation, and desiccation of fine grained tailings pond materials following deposition in an arid climate.

A soil evaporation model described in Wilson *et al.* (1994) may help predict the moisture flux along the consolidated tailings beach and the fine tails within the pond following post freeze-thaw consolidation. The coupled heat and mass transfer model can predict soil evaporation rates, water content, matric suction, and surface temperature profiles. This model may be used to predict the matric suction and resulting shear strength development of the subsurface soils as a result of evaporation.

As soil surfaces desaturate with evaporation, the evaporative flux decreases and the depth of soil enhancement through dewatering becomes limited. Newson *et al.* (1996) reports the depth of influence of evaporative flux on shear strength of saline gold tailings was limited to 10 cm, and Burns *et al.* (1993) highlights that effective dewatering of tailings occurs if thin layers (0.1 m to 0.2 m) are placed. In addition to the reduced evaporation from unsaturated soil surfaces,

permeants as described in Newson *et al.* (1996) or bitumen in the fine tails as discussed by Burns *et al.* (1993) can hinder evaporation from near surface materials.

The moisture flux restriction associated with an unsaturated surface soil may be circumvented through development of biological pathways offered through transpiration of vegetative root systems as discussed in Chapter 6. Tratch *et al.* (1995) extended the soil evaporation model discussed by Wilson *et al.* (1994) to include the effects of transpiration. The effects of evaporation and evapotranspiration on moisture content profiles within a laboratory lysimeter experiment were effectively predicted using the theoretical model (Tratch *et al.* 1995). Based on the soil water characteristic curve presented in Tratch *et al.* (1995), soil matric suctions between 70 kPa and 200 kPa developed within the lysimeter.

The depth of dewatering of deep rooting plants is significant with some species extending to depths of 2 to 3 m (Ravina 1983). In 1991, vegetative root systems at Coal Valley had extended to a depth of 1 m within the tailings (Macyk *et al.* 1991). Trees may extend their roots to considerably greater depths with significant moisture reduction and matric suction development occurring within a radius about 1 to 1.5 times the tree height (Ravina 1983). High matric suctions may be sponsored through evapotranspiration processes, with an upper limit for most plants of pF^1 4.2 (\cong 1500 kPa) which is regarded as the vegetative wilting point. Drought tolerant plants may develop matric suctions in the order of pF 4.5 (\cong 3100 kPa) (Williams and Pidgeon 1983). As illustrated in Chapter 6, Figure 6.12, the dewatering potential of vegetation is species dependent with reed canary, dock, northern reed, and timothy most effective in dewatering the tailings mix in this figure. The same is true for trees with Biddle (1983) reporting that the moisture demands of poplar, willow, oak and elm are much higher compared to various other species.

8.3.2. Strength Enhancement

The shear strength enhancement through matric suction development sponsored through evaporation and evapotranspiration processes is defined in Equation [6.5]. Fredlund and

¹ $pF = \log_{10} h$ (h is the height of water in cm)

Rahardjo (1993) report ϕ^h values for various soils generally from 16° to 26° . Considering the matric suctions predicted from Tratch *et al.* (1995) of 70 to 200 kPa, and a lower ϕ^h angle of 16° , a shear strength increase from evapotranspiration of 20 kPa to 57 kPa is predicted. Swarbrick (1992) measured matric suctions in mine wastes in the field within the same order of magnitude, with near surface matric suctions measured in laboratory experiments up to about 1000 kPa. This high matric suction translates to a predicted ($\phi^h = 16^\circ$) shear strength increase of 290 kPa. Swarbrick and Fell (1991) show peak shear strengths of mine tailings resulting from evaporation approaching 100 kPa within the field, and exceeding 200 kPa in the laboratory.

Matric suction development through evaporation within the Suncor NST Cells increased the cone tip resistance near the surface compared to that at depth. Higher strengths within the upper 0.2 to 0.4 m provided sufficient support for human foot traffic. Shear strengths predicted in the surficial materials (Appendix F) were between 10 and 20 kPa, approximately 10 to 20 fold greater than that at depth. Shear strengths and bearing capacities were also enhanced within the surficial material along the beach portion of the Coal Valley tailings impoundment due to a coupled effect of evaporation, evapotranspiration, and fiber reinforcement of vegetative root systems.

It is important to highlight that evidence suggests a non-linear decreasing relationship for ϕ^h with increasing matric suction (Fredlund and Rahardjo 1993). Results show that ϕ^h decreases after the matric suction has increased beyond 100 to 200 kPa. An example is provided in Fredlund and Rahardjo (1993) illustrating a soil with an initial ϕ^h of 25.5° , which subsequently decreases beyond a matric suction of 50 kPa, reaching a steady value of 7° after a matric suction of 300 kPa is reached.

Should climatic conditions encourage shear strength enhancement through evaporation and evapotranspiration, the benefits are highly dependent on the hydrological conditions within the tailings. A maintained high water table and insufficient drainage measures reduce the potential benefits. Investigations to evaluate potential large scale field performance may include:

- Laboratory drying experiments considering volume change, matric suction and shear strength development.

- Laboratory experiments to evaluate parameters for input into atmospheric drying models for prediction of field performance.
- Field trials using instrumented lysimeters, cells, and/or the existing tailings beach to evaluate soil evaporation/evapotranspiration. Measurements should include matric suction and shear strength profiles, with plate load tests and possible cone penetration test to evaluate capacities and mobilized strengths.
- Investigation and cataloging of indigenous or possibly exogenous or genetically engineered vegetative species which may survive within, and effectively dewater the tailings.

8.4. VEGETATIVE ROOT REINFORCEMENT

Although the shear strength development through matric suction can be significant, reduction or elimination of this component with reduced shear strength and bearing capacity may transpire through precipitation or inundation by flooding. The mechanical component of roots, however, will continually provide reinforcement. Various empirical formulations to predict the increase in shear strength are presented in the literature as discussed in Appendix E. A theoretical formulation was adopted in attempts to quantify the shear strength and bearing capacity increase offered through root reinforcement. The theoretical formulations indicated that significant shear strength increases from root reinforcement may be expected (Appendix E). Theoretical formulations predict a 50 kPa to 150 kPa increase in bearing capacity along the Coal Valley tailings beach resulting from root reinforcement. The theoretical formulations provide a framework for preliminary prediction of the mechanical contribution of roots to structural enhancement of tailings. It is noted that detailed sampling and laboratory separation techniques were required to exactly quantify the root area ratio (*RAR*) profiles within the subsurface. It is recognized that *RAR* quantifying operations may require less efforts in the future through employment of the Daubenmire (1959) technique with developed or established root morphology correlations (McCoy 1996).

In addition to the vegetative root system mechanically reinforcing the tailings, tall grasses, legumes and other vegetation may provide addition reinforcement in the event that capping is

required. Folding of the vegetative stalks along the surface during capping placement provides a reinforcing component similar in function (not capacity) to that of a geotextile layer. In addition, decay of the capped vegetation provides nutrients for the successive vegetative species.

As highlighted above considering evapotranspiration, primary investigations to utilize the mechanical component of vegetative systems (roots and stalks) should include cataloging of vegetative species which exhibit satisfactory survival rates within the tailings. Secondary considerations during vegetative optimization will include root (and possible stalk) morphology which dictates degree of mechanical enhancement, and magnitude of potential transpiration dewatering.

8.5. CONCLUSIONS

Several processes may be coupled to enhance the surface stability of tailings deposits and dry landscape reclamation. Freeze-thaw processes serve to dewater and strengthen the fine grained portion of the tailings. Various optimization techniques are available including chemical addition, thin layer placement, drainage and consolidation measures.

The hydrological component associated with evaporation and evapotranspiration serve to further dewater coarse and fine tailings, increase the shear strength and structural integrity through matric suction development. In addition, the mechanical reinforcing components of roots structural enhance the tailings surface, with vegetative stalks providing increased surface stability in the event of capping operations.

These natural enhancement processes are not restrictive and may be coupled with additional tailings management techniques discussed in the literature and used in industry including codisposal operations, sand spiking, and production of nonsegregating tailings mixes.

8.6. REFERENCES

- Abu-Hejleh, A.N.M., 1993. Desiccation Theory for Soft Soils. Ph.D. Thesis, The University of Colorado. 211 pgs.
- Biddle, P.G., 1983. Patterns of Soil Drying and Moisture Deficit in the Vicinity of Trees on Clay Soils. *Geotechnique*, **33**:107-126.
- Burns, R., Cuddy, G., and Lahaie, R., 1993. Dewatering of Fine Tails by Natural Evaporation. Proceedings of the Oil Sands - Our Petroleum Future Conference (Fine Tailings Symposium), Edmonton, Alberta, April 4-7, Paper F16, 36 pgs.
- Canadian Climatic Normals (1951-1980) (1961-1990), Atmospheric Environment Service, Environment Canada.
- Daubenmire, R. 1959. A Canopy - Coverage Method of Vegetational Analysis. *Northwest Science*, **33**:43-64.
- Davila, R.S., Sego, D.C., and Robertson, P.K., 1993. Surface Area Criteria Applied to Segregation Potential. Proceedings of the 46th Canadian Geotechnical Conference, Saskatoon, Saskatchewan, pgs. 333-342.
- Dawson, R.F., and Sego, D.C., 1993. Design Concepts for Thin Layered Freeze-Thaw Dewatering Systems. Proceedings of the 46th Canadian Geotechnical Conference, Saskatoon, Saskatchewan, pgs. 283-292.
- Fahey, M., and Fujiyasu, Y., 1994. The Influence of Evaporation on the Consolidation Behavior of Gold Tailings. Proceedings of the First International Congress on Environmental Geotechnics, Edmonton, Alberta, July 11-15, pgs. 481-486.
- Fredlund, D.G., and Rahardjo, H., 1993. **Soil Mechanics For Unsaturated Soils**. John Wiley & Sons, Inc. New York., 517 pgs.
- Konrad, J.M., 1994. Sixteenth Canadian Geotechnical Colloquium: Frost Heave in Soils: Concepts and Engineering. *Canadian Geotechnical Journal*, **31**(2):223-245.
- Konrad, J.M., and Morgenstern, N.R., 1983. Frost Susceptibility of Soils in Terms of Their Segregation Potential. Proceedings of the Fourth International Permafrost Conference, pgs. 660-665.
- Macyk, T.M, Nikiforuk, F.I., and Widtman, Z.W., 1991. Characterization and Reclamation of Coal Tailing Materials. Report Prepared For Luscar-Sterco (1977) Ltd. 57 pgs.
- Martel, C.J. 1988. Development and Design of Sludge Freezing Beds. US Army Cold Regions Research and Engineering Laboratory, CRREL Report 88-20.

- McCoy, D., 1996. Personal Communications. Environmental Supervisor, Luscar Sterco (1977) Ltd., Edson, Alberta.
- Newson, T., Fujiyasu, Y., and Fahey, M., 1996. A Field Study of the Consolidation Behavior of Saline Gold Tailings. Proceedings of the Tailings and Mine Waste'96 Conference, Fort Collins, Colorado, January 16-19, pgs. 179-188.
- Ravina, I., 1983. The Influence of Vegetation on Moisture and Volume Changes. *Geotechnique*, **33**:151-157.
- Sego, D.C., 1990. Use of Freeze-Thaw to Assist in Reclamation of a Coal Tailings Pond. Submitted to Luscar Sterco (1977) Ltd., 27 pgs.
- Sego, D.C., Burns, R., Dawson, R., Dereniwski, T., Johnson, R., and Lowe, L., 1993a. Dewatering of Fine Tails Utilizing Freeze-Thaw Processes. Fine Tailings Symposium, Proceedings of the Oil Sands - Our Petroleum Future, April 4-7, 1993, Edmonton, Alberta, Paper F17, 25 pgs.
- Sego, D.C., Proskin, S.A., and Burns, R., 1993b. Enhancement of Solids Content of Oil Sand Fine Tails by Chemical Treatment and Freeze-Thaw. Proceedings of the 46th Canadian Geotechnical Conference, Saskatoon, Saskatchewan, pgs. 293-300.
- Swarbrick, G.E., 1992. Transient Unsaturated Consolidation In Desiccated Mine Tailings. Unpublished Ph.D. Thesis, School of Civil Engineering, New South Wales, Australia.
- Swarbrick, G., and Fell, R., 1991. Prediction of the Improvement of Tailings Properties by Desiccation. Proceedings of the Ninth Pan American Conference on Soil Mechanics and Foundation Engineering, Chile, pgs. 995-1008.
- Tratch, D.J., Wilson, G.W., and Fredlund, D.G., 1995. An Introduction to Analytical Modelling of Plant Transpiration for Geotechnical Engineers. Proceedings, 48th Canadian Geotechnical Conference, Vancouver, B.C., pgs. 771-789.
- Williams, A.A.B., and Pidgeon, J.T., 1983. Evapo-transpiration and Heaving Clays in South Africa. *Geotechnique* **33**:141-150.
- Wilson, G.W., Fredlund, D.G., and Barbour, S.L., 1994. Coupled Soil Atmosphere Modelling for Soil Evaporation. *Canadian Geotechnical Journal*, **31**(2):151-161.

Chapter 9

Summary And Conclusions

9.1. SUMMARY AND CONCLUSIONS

Two tailings deposits exhibiting contrasting geotechnical properties were investigated as part of this research. The first deposit which represents the product of a segregating tailings stream and experienced hydraulic sorting during deposition in the Coal Valley tailings facility. The initiation of reclamation activities in 1989 provided opportunity to chronologically investigate the increase in geotechnical surface stability as a result of natural surface enhancement processes. Investigations were conducted in various regions of the impoundment from 1989 through 1996.

The second deposit investigated which represented the product of an engineered nonsegregating tailings stream was the Suncor NST Cell facility. Mature fine tailings, the final product of the segregating oil sands tailings stream, was combined with a portion of the tailings stream and coagulating agents to produce a nonsegregating mix. The deposit was comparatively less mature than the Coal Valley facility, with deposition occurring in 1993 only one year previous to the investigations.

The investigations required the development of light weight geotechnical testing apparatuses which could be effectively mobilized, using human effort, to the very weak tailings sites. The equipment developed included firstly a Plate Load Test (PLT) apparatus to evaluate the punching

shear load-deformation behavior of the surficial tailings. A Cone Penetration Test (CPT) apparatus was developed to define material behavior type and predict geotechnical properties. And lastly, Spectral Analysis of Surface Waves (SASW) techniques were used to develop shear wave velocity and subsequent small strain shear modulus profiles. The investigations conducted using this equipment provided increased understanding of the behavior and *insitu* conditions of these tailings deposits, and also facilitated chronological monitoring of dry landscape reclamation progress.

Based on the site investigation activities and subsequent analysis presented in the chapters and successive appendices, the following selective conclusions are presented.

- The segregating tailings within the Coal Valley tailings impoundment underwent hydraulic sorting resulting in a decreased mean grain size, D_{50} , and an increase in fines $F\%$, with distance from the discharge point. Depositional dynamics also created significant horizontal and vertical heterogeneity. In contrast, the Suncor NST facility maintained its desired design qualities, exhibiting relative homogeneity.
- The PLT results along the beach portion of the Coal Valley tailings impoundment illustrated that the bearing capacities decreased with increased distance from the discharge location. Bearing capacities recorded at the surface were considerably greater than those at depth, and significant increases in capacity were realized from 1991 to 1994. The factors which contributed individually and combined to these findings are water table proximity, matric suctions through evaporation and evapotranspiration dewatering, and fibre reinforcement effects of vegetative root systems.
- The PLT's conducted at Coal Valley and the Suncor NST facility both exhibited punching shear failure mechanism, however contrasting pressures-settlement relationships were experienced. The ultimate bearing pressures within regions of the Coal Valley tailings impoundment approached 1 order of magnitude greater than within the Suncor NST Cells.

- The CPT, SASW, and field vane shear test results within the Suncor NST Cells indicate the presence of a strengthened crust. This crust, the result of matric suction development from evaporation, was of limited strength, however, provided sufficient serviceability to facilitate the geotechnical investigations.
- Cyclic freeze-thaw consolidation resulting from seasonal temperature variations, coupled with selfweight induced moisture migration and consolidation have considerably enhanced the shear strength of the saturated silt and clay within the pond region of the Coal Valley tailings impoundment.
- Existing *insitu* pore water pressures existed within the Suncor NST Cells at the time of investigations. The *insitu* pore pressures and stress conditions are critical for evaluation of soil behavior type and geotechnical properties using the cone penetration test. Pore pressure dissipation tests within the NST Cells using the cone showed promise in predicting consolidation properties.
- A fibre reinforcing model was developed to analyze the plate load test results conducted on root permeated compressible tailings. The model, which is contingent on a variety of soil-fibre interaction variables, showed considerable promise in predicting the increase in bearing capacity of the Coal Valley tailings from 1991 to 1994.
- The range of geotechnical investigation techniques provided opportunity to investigate select correlations established in the literature. Cone correlation factors for tip and pore pressure showed promise in predicting field vane shear strengths in these weak deposits. A new factor for the cone tip to predict the bearing capacity of root reinforced soils was formulated.
- The PLT and CPT apparatuses provided the greatest information concerning geotechnical material properties and *insitu* behavior. In light of the confirmed and developed correlations, enhanced portability and information gathered, the portable CPT system is the preferred and perhaps quintessential investigation instrument to evaluate weak tailings

deposits and gauge reclamation performance. An important link is established between the CPT, and seismic techniques to establish shear wave velocity and shear modulus profiles. However, some difficulties were obtained using SASW techniques on the weak tailings deposits investigated. Although these difficulties may result from the authors limited field experience with the technique, possibly simpler methods of discrete shear wave velocity measurement including the seismic CPT techniques are worth exploring.

The definition of what constitutes a dry landscape from a geotechnical perspective is undefined in a regulatory sense. This is due in part to the range of geotechnical integrity and diversity encountered in dry landscapes found in natural undisturbed environments. The level of geotechnical stability of reclaimed facilities must satisfy the end land use requirements and operate harmoniously with the regional landscape conditions. The level of desired ultimate geotechnical stability may range from recreational grasslands to productive forest conditions. Recognizing that the duration of reclamation activities may vary from several years to 10's of 100's of years, engineering of natural surface enhancement processes is a cost effective vehicle to help achieve these goals.

9.2. SUGGESTED FUTURE RESEARCH

During the course of this relatively broad research initiative and subsequent analysis, several exciting issues were encountered which possibly deserve further investigation. Some of these issues are presented below.

- Extension of the simplified root reinforcing model to more accurately model the soil-fibre stress-strain behavior beneath a loaded footing. Considerations could be extended to the range of vegetative root and soil systems encountered in natural and reclaimed environments.

- Development of predictive capabilities/correlations to forecast the increase in bearing capacity resulting from vegetative root systems based on simple surface tests. In addition to the soil-fibre interaction variables, issues to consider are vegetation type and maturity.
- Utilize existing evaporation/evapotranspiration models on a regional scale to predict the dewatering, matric suction and shear strength development of tailings facilities undergoing reclamation.
- Develop a more sensitive cone or seismic cone to investigate weak tailings facilities. Dimensional modifications may be advantageous to facilitate increased portability and sounding ability.
- Verify the encouraging consolidation properties predicted with the cone pore pressure dissipation tests within Coal Valley tailings and more importantly the Suncor NST material. Acknowledging the importance of penetration and dissipation pore pressure in soft clay (slurry) deposits, develop dimensionally correct, possibly enlarged cone devices equipped solely with pore pressure transducers to investigate *insitu* strength and consolidation properties of saturated high void ratio fine tailings.
- The structural enhancement through dewatering and fibre reinforcement offered by vegetative root system highlighted herein was significant. These benefits should not, however, be restricted to surficial soils. Investigations into aggressive, deeply penetrating root systems warrants further study. In addition to enhancing surficial stability, the hydro-mechanical contributions of deeply rooting systems provide enhanced subsurface dewatering and reinforcement. This dewatering and reinforcing effects, contributing to increased shear resistance and internal confining stress, not only amplify serviceability with respect to static loading conditions, but may foster reduced liquefaction potential and/or cyclic mobility of weak deposits subjected to seismic loading.
- In addition to structurally enhancing existing impoundments undergoing reclamation, research into robust vegetative species which withstand periodic inundation of the stems

with tailings in active impoundments, resulting from sequential deposition, is an attractive research focus. Vegetative responses to partial tailings inundation, including vertical growth and lateral root development have far reaching effects. In addition to the structural reinforcement, the ongoing vegetative development and transpiration dewater the tailings and encourage consolidation and strength gain. Furthermore, migration pathways along active and expired root cavities may enhance drainage and consolidation under selfweight loading.

- As a course of scope limitation, reference to tailings contaminants and remediation was excluded from this thesis. However, the author maintains interest in a variety of remediation technologies including the application of phytoremediation: *the use of vegetation to clean up pollution*. In addition to the hydromechanical component offered through vegetation, enzymes and organic carbons secreted into the soil by select species can help break down contaminants and trigger bacteria to initiate different degradation processes. In addition, pollutants adsorbed through the root systems and distributed throughout the vegetation may ultimately be removed from the environment through harvesting. This cost effective and efficient remediation technology deserves consideration in dry landscape reclamation of tailings.

Appendix A

Index And Vane Shear Testing At Coal Valley And Suncor NST Cells

A.1. INTRODUCTION

The following index and vane shear information, which has been partially presented in the chapters of the thesis, is included in entirety in this appendix. The information contained herein has also been utilized for geotechnical analysis as discussed in later appendices. The following provides a brief summary of the tables and figures included herein. Additional laboratory information including sedimentation behavior and freeze-thaw consolidation tests (Sego 1990) on the Coal Valley tailings have been omitted from this thesis for brevity.

A.2. INDEX TABLES

Table A1 includes a summary of the *insitu* density measurements conducted along the beach portion of the Coal Valley tailings impoundment in 1992 using an *insitu* freezing technique utilizing dry ice. The coarser samples were subsequently subjected to relative density measurements as illustrated in Table A2. Both samples had very low relative densities which support the punching shear failure mechanism observed with the field plate load tests. Table A3 details the results of the large *insitu* sampling conducted in 1995 at Sites 1 through 4. The samples, obtained using a modified volumeter technique, were dissected in the laboratory to

determine the Root Area Ratios (*RAR*) and facilitate analysis of the potential contribution of the roots to bearing capacity as discussed in Appendix E. Selected samples from Table A3 and recent investigations within the pond portion of the Coal Valley impoundment were analyzed for ash content determination and ash specific gravity measurements. These results are summarized in Table A4

Table A5 includes a summary of the Atterberg limit data obtained on the thickener underflow material and pond material illustrated previously in Chapters 2 and 3 respectively, with Figure A6 summarizing the grain size distributions of these materials. Lastly, Table A6 includes Atterberg limit data obtained on selected samples from the Suncor NST Cells 3, 4 and 5.

A.3. GRAIN SIZE DISTRIBUTIONS

To compliment the shallow subsurface stratigraphy illustrations in Chapter 2, Figures A1 through A4 include grain size distributions from Sites 1 through 4 along the beach portion of the Coal Valley tailings impoundment, which were obtained during the 1995 investigations. To contrast the figures in Chapter 1 which only include grain sizes greater than 0.074 μm (# 200 sieve), these grain size distributions include hydrometer results conducted on the material passing the # 200 sieve. Figure A5 includes the grain size distribution of several samples obtained from Sites 1, 2, and 3 within the pond portion of the Coal Valley impoundment. As observed with the figures in Chapter 2, and Figures A1 to A4, considerable heterogeneity also exists within the pond. As comparison, the constructed average of the grain size distribution within the pond is combined with the two Coal Valley tailings waste streams as illustrated in Figure A6.

The grain size distribution of several samples obtained in 1994 from the NST Cells 3, 4, and 5 are illustrated in Figures A7, A8, and A9.

A.4. MOISTURE AND SOLIDS CONTENTS

Frozen and unfrozen samples were obtained from Sites 1, 2, and 3 within the pond portion of the Coal Valley impoundment. The frozen core samples obtained in 1995 were sliced into disks for analysis. Some of the consolidated soil “peds” (Chapter 3) were removed at various stages prior to, and during thaw to investigate their consolidated solids content prior to moisture reabsorption during thaw of the complete segregated frozen structure. The consolidated soil “ped” solids contents are compared with the frozen, unfrozen, and thawed solids contents at Sites 1, 2, and 3 in Figure A10 to A12.

Samples were obtained at 0.15 m intervals at the Suncor NST Cells 3, 4, and 5 in 1994 with the computed moisture and solids contents illustrated in Figures A13 and A14. The NST Cells have a relatively uniform moisture content below the surface, with Cells 3 and 4 illustrating a reduced moisture content in the upper 0 to 0.4 m indicating slight desiccation as a result of evaporation. Soil desiccation in Cell 5 was eliminated due to the relatively thin, maintained water cap.

A.5. FIELD VANE SHEAR STRENGTH PROFILES

Shear strength measurements were conducted using a Field Vane Shear Test (FVST) apparatus along the beach and pond portion of the Coal Valley tailings impoundment, and within the NST Cells. The FVST results at Sites 1 to 5 in 1991 and 1 to 4 in 1994 and 1995 along the beach portion of the Coal Valley impoundment are included in Figures A15 to A17 respectively. The FVST results within the pond portion of the Coal Valley tailings impoundment from 1989 to 1996 are included in Figures A18 to A25, with a summary of the average shear strengths included in Figure A26. The shear strength results from the NST Cells are included in Figure A27.

It is important to note that the *Genor* FVST employed to determine shear strength profiles does not include a slip coupling device to facilitate direct measurement and subtraction of the torque associated with rod friction from the total torque including rod friction and vane shear. The

torque required to overcome rod friction is determined by replacing the vane with a pin device and essentially repeating the profile without the vane. The soil disturbance and resulting stress conditions associated with the vane and rods compared with the pin and rods are different, and the measured torque associated with pin and rod friction may not represent (over predict) the actual value mobilized during vane measurements. This cautionary statement is of minor concern when investigating very soft soils at shallow depths where a large vane is used and the volume of soil sheared with the vane and rods is large compared to that sheared by the pin and rods alone. Such is the case with the vane shear profiles determined within the pond portion of the Coal Valley impoundment and within the NST Cells. This is not the case, however, during shear strength profiling along the beach portion of the Coal Valley impoundment. In stiffer soils which necessitated using a smaller vane, the reduced ratio of soil disturbed by vane and rods compared with rods alone limits confidence in the computed shear strength values determined at depth. Recognizing this problem, torque measurements with the pin and rods were conducted down the same hole created by the vane and rods. Limited success was achieved with this technique, however, some uncertainty still remains regarding the actual vane shear strength computed at depth.

A.6. REFERENCES

- Sego, D.C., 1990. Use of Freeze-Thaw to Assist in Reclamation of a Coal Tailings Pond. Submitted to Luscar Sterco (1977) Ltd., 27 pgs.
- Suthaker, N.N., 1995. Geotechniques of Oil Sand Fine Tailings. Unpublished Ph.D. Thesis, Department of Civil Engineering, The University of Alberta, 223 pgs.

Table A1 **Summary of 1992 Density Measurements at Coal Valley**

Samples Obtained by Surface Insitu Freezing

Site	Depth (cm)	Bulk Density Soil (gm/cm ³)	Dry Density Soil (gm/cm ³)	Dry Density Soil (gm/cm ³)	Specific Gravity
1	14-34	1.37	1.15	1.15	2.14
1	14-34	1.44	1.80	1.80	2.05
1	35-55	1.42	0.98	0.98	2.10
1	35-55	1.41	0.98	0.98	2.05
2	10-30	1.44	1.19	1.19	
2	10-30	1.35	1.07	1.07	
3	10-30	1.37	0.97	0.97	2.02
3	10-30	1.35	0.95	0.95	2.10
3	30-50	1.33	0.93	0.93	2.06

Table A2 **Summary of Relative Density Measurements on 1992 Samples**

Site	Depth (cm)	Maximum Density (gm/cm ³)	Minimum Density (gm/cm ³)	Average Insitu Density (gm/cm ³)	Relative Density (<i>D_r</i>)
1	35	1.306	0.979	1.164	0.64
2	30	1.386	1.041	1.132	0.32

Table A3 **Summary of 1995 Density and Root Area Ratio Measurements at Coal Valley**

Samples Obtained Using Field "Large Sample" Volumeter Technique

Site	Sample	Depth (cm)	Bulk Density Soil + Roots (gm/cm ³)	Bulk Density Soil (gm/cm ³)	Dry Density Soil (gm/cm ³)	A _R /A RAR	Specific Gravity
1	A1	0-4	1.34	1.37	0.92	7.6%	1.94
1	A2	4-8	1.44	1.44	1.05	1.2%	
1	A3	8-12	1.48	1.48	1.00	0.3%	
1	A4	12-15	1.44	1.44	1.02	0.1%	
1	B	15-32	1.44	1.44	0.91	0.2%	
1	C	32-53	1.55	1.55	1.05	0.1%	
2	A1	0-4	1.28	1.31	0.83	12.8%	1.68
2	A2	4-8	1.43	1.44	1.01	0.7%	as above
2	A3	8-12	1.37	1.37	0.94	0.2%	as above
2	A4	12-15	1.40	1.41	0.79	0.3%	as above
2	B	22-36	1.52	1.51	1.04	0.3%	1.86
2	C	36-54	1.47	1.46	1.04	0.1%	
3	A1	0-4	1.33	1.36	0.85	5.6%	1.69
3	A2	4-8	1.40	1.41	0.99	0.7%	as above
3	A3	8-12	1.40	1.40	0.92	0.2%	1.95
3	A4	12-15	1.27	1.27	0.80	0.2%	as above
3	B	22-35	1.41	1.40	0.79	0.2%	1.76
4	A1	0-4	1.24	1.27	0.75	8.9%	1.66
4	A2	4-8	1.27	1.27	0.81	0.5%	as above
4	A3	8-12	1.35	1.35	0.80	0.7%	as above
4	B	>12*	1.32	1.32	0.80	0.1%	1.72

Notes:

(1) Soil + Root and Soil Densities determined using laboratory volume displacement method.

(2) RAR determined based on mass measurements, assuming density of unsaturated roots (partially dried) = 0.7 g/cm³.

Table A4 **Ash Content and Ash Specific Gravity of Selected 1995/96 Samples at Coal Valley**

Sample	Ash Content (%)	Specific Gravity of Ash
Site 1C	63.2	2.61
Site 2C	60.0	2.62
Site 3B	52.7	2.57
Site 4B	37.9	2.66
1996 Pond Sample	55.2	2.49

Table A5 Summary of Atterberg Limit Data From Coal Valley

Description	Liquid Limit (%)	Plastic Limit (%)	Plasticity Index (%)	Specific Gravity
Fine Saturated Slurried Tailings	37.2	25.1	12.1	1.87
(Thickener Underflow)				
1992 Pond Sample	70.0	34.8	35.2	1.89

Table A6 Summary of Atterberg Limit Data From Suncor NST Cells

Location	Depth (m)	Liquid Limit (%)	Plastic Limit (%)	Plasticity Index (%)
NST 3	0.7-0.8	12.1	10.6	1.5
NST 4	1.3-1.4	12.6	10.4	2.2
NST 5	2.4-2.5	14.1	11.0	3.1

Test Results Supplied By AGRA Earth and Environmental Ltd., Edmonton, Alberta.

**Note : Suncor Mature Fine Tails (Liquid Limit = 41%; Plastic Limit = 21%; Plasticity Index = 20 %) Suthaker (1995).*

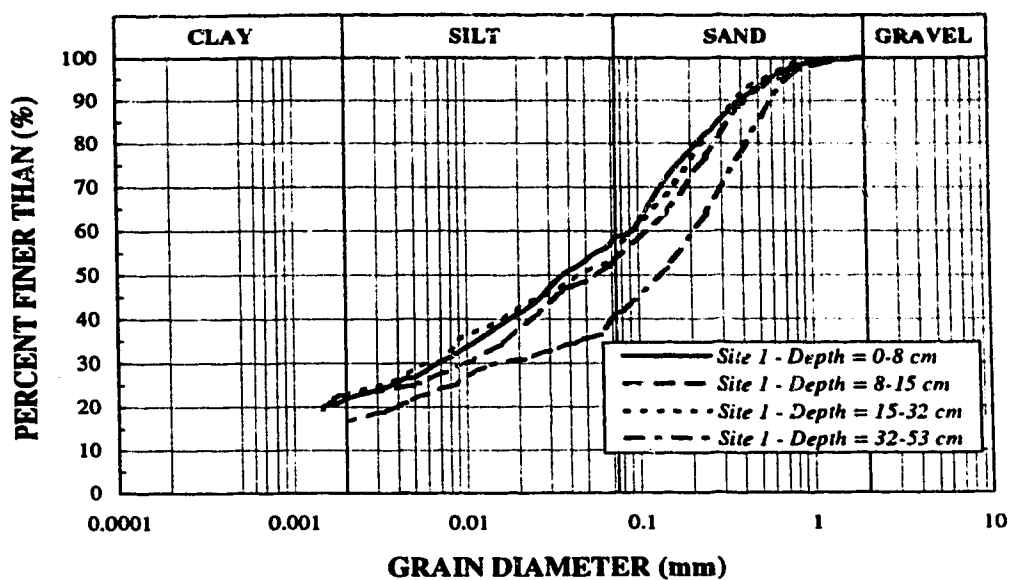


Figure A1 1995 Grain Size Distributions Along Coal Valley Tailings Beach - Site 1

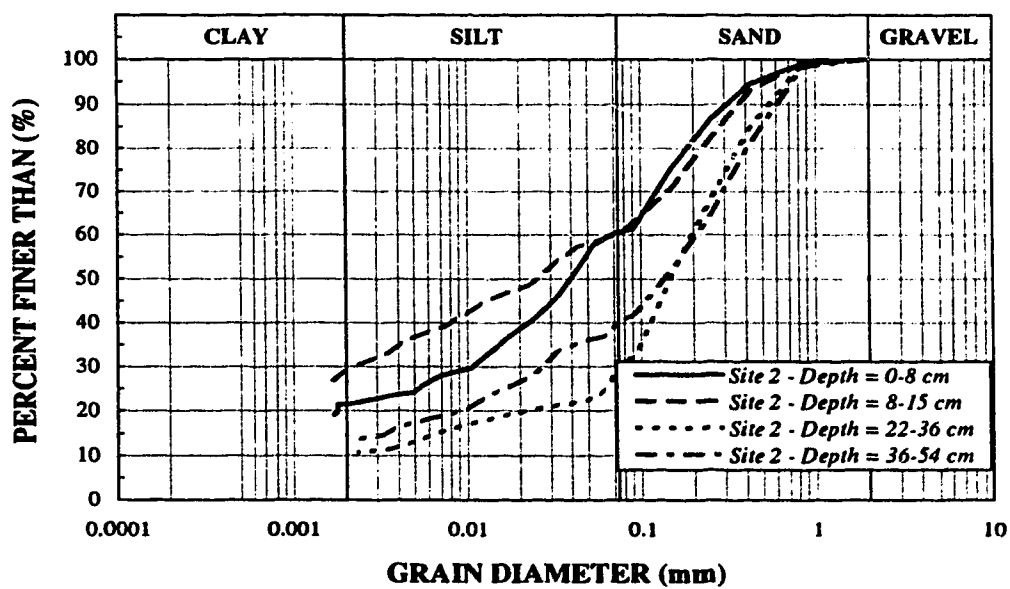


Figure A2 1995 Grain Size Distributions Along Coal Valley Tailings Beach - Site 2

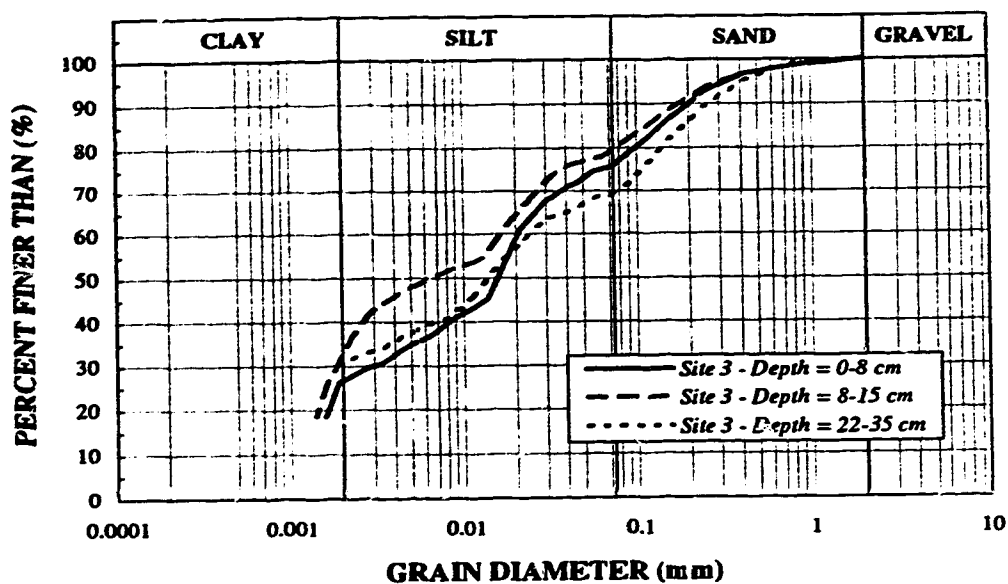


Figure A3 1995 Grain Size Distributions Along Coal Valley Tailings Beach - Site 3

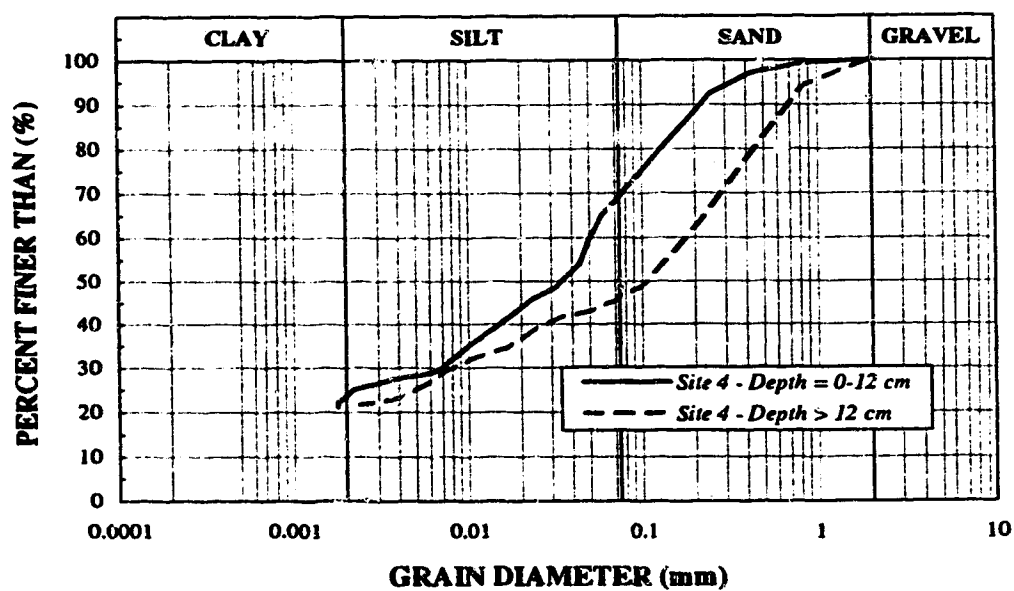


Figure A4 1995 Grain Size Distributions Along Coal Valley Tailings Beach - Site 4

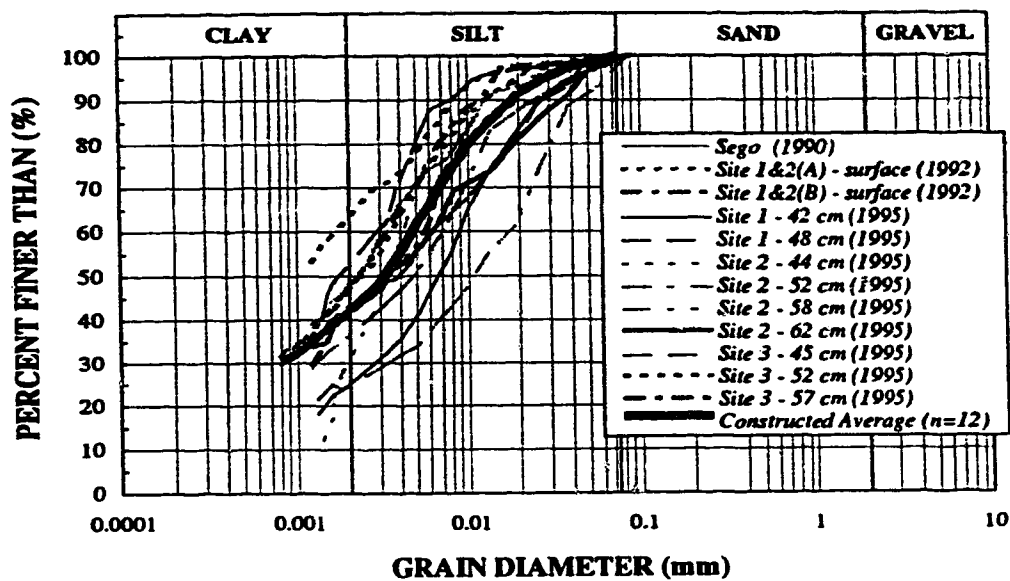


Figure A5 Grain Size Distributions Within Coal Valley Tailings Pond

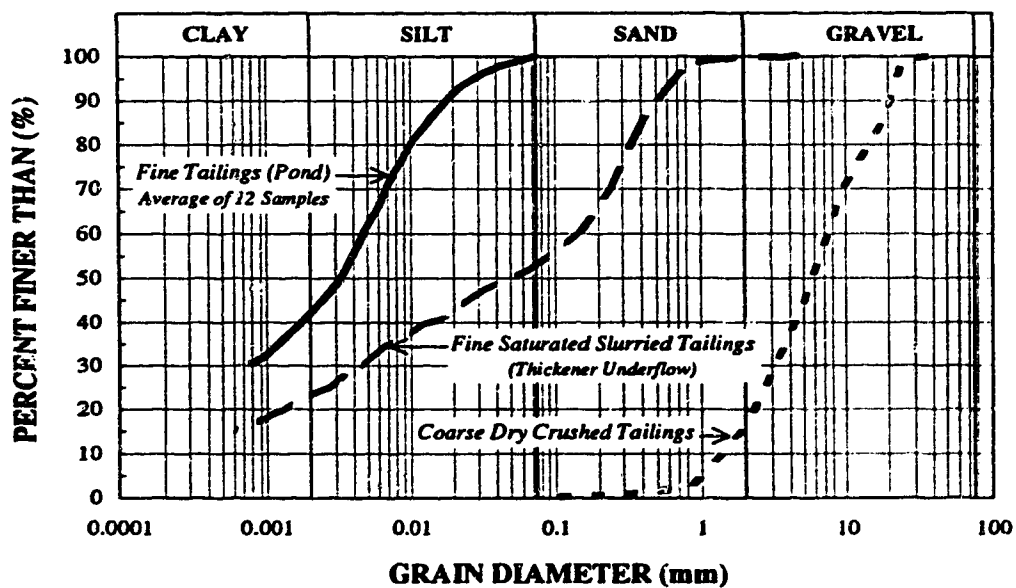


Figure A6 Grain Size Distributions of Coal Valley Wastes Streams and Constructed Pond Average

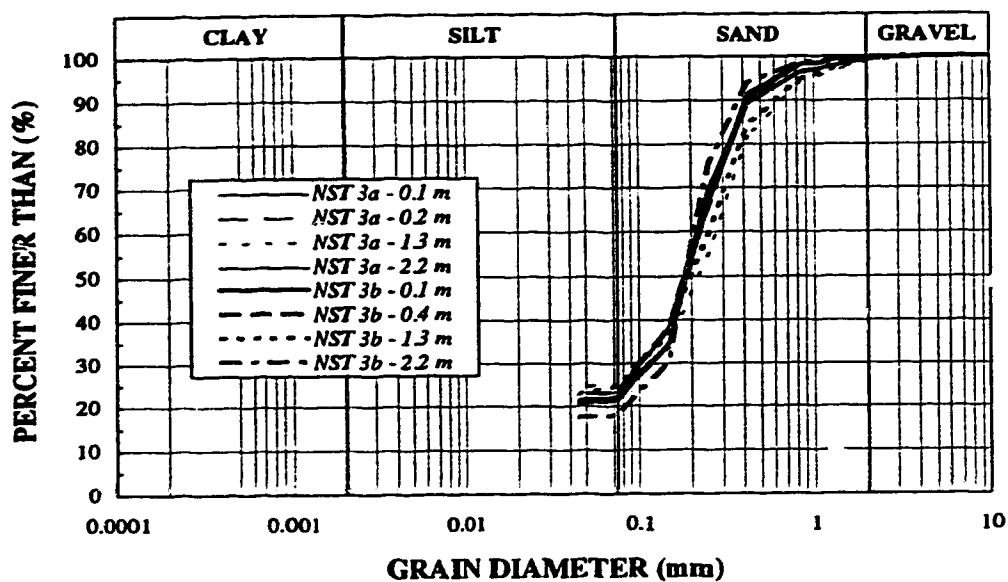


Figure A7 1994 Grain Size Distributions Within Suncor NST Cell 3

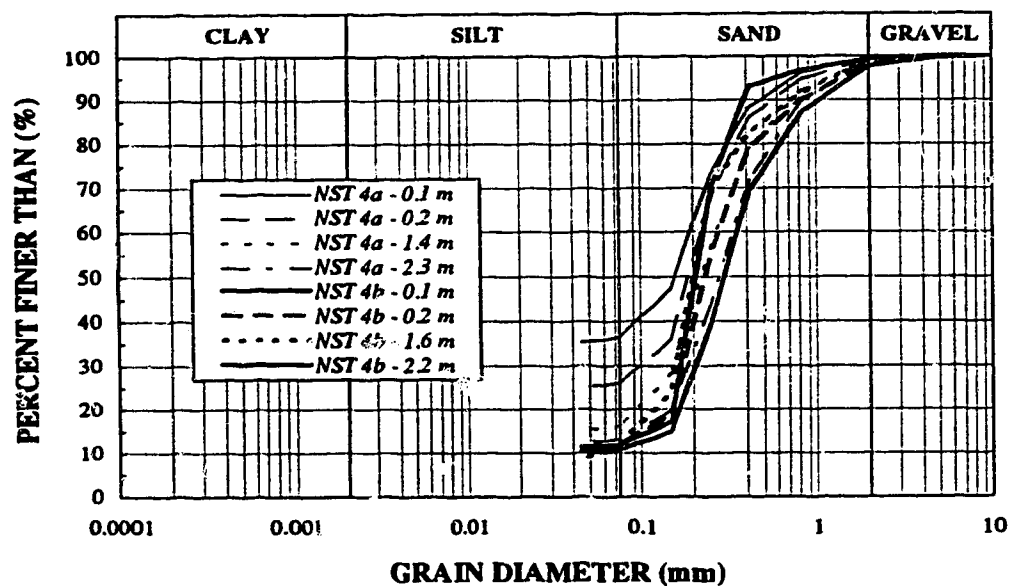


Figure A8 1994 Grain Size Distributions Within Suncor NST Cell 4

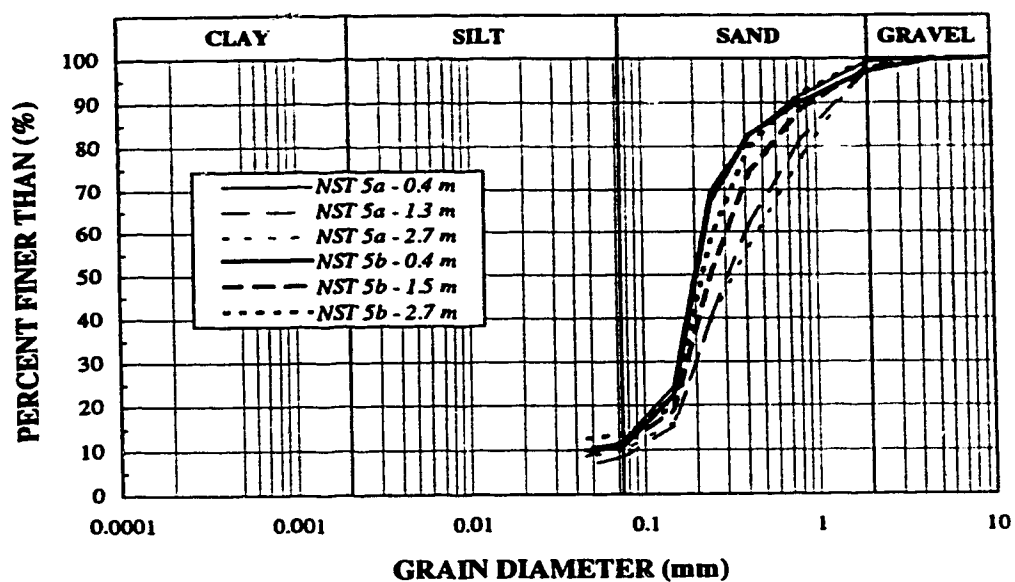


Figure A9 1994 Grain Size Distributions Within Suncor NST Cell 5

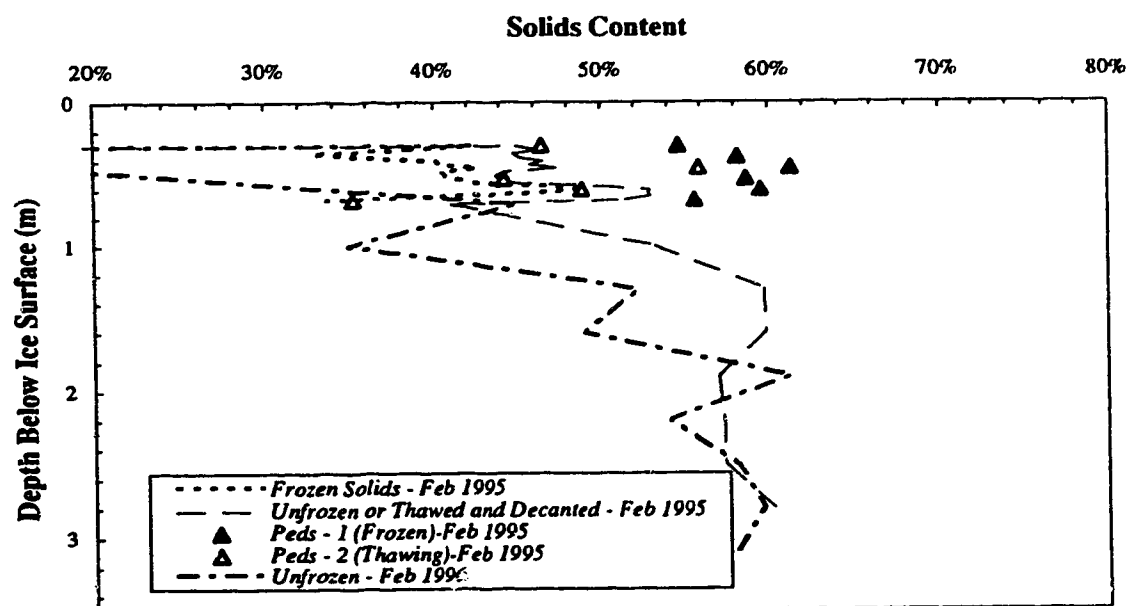


Figure A10 Solids Contents Within Coal Valley Pond - Site 1

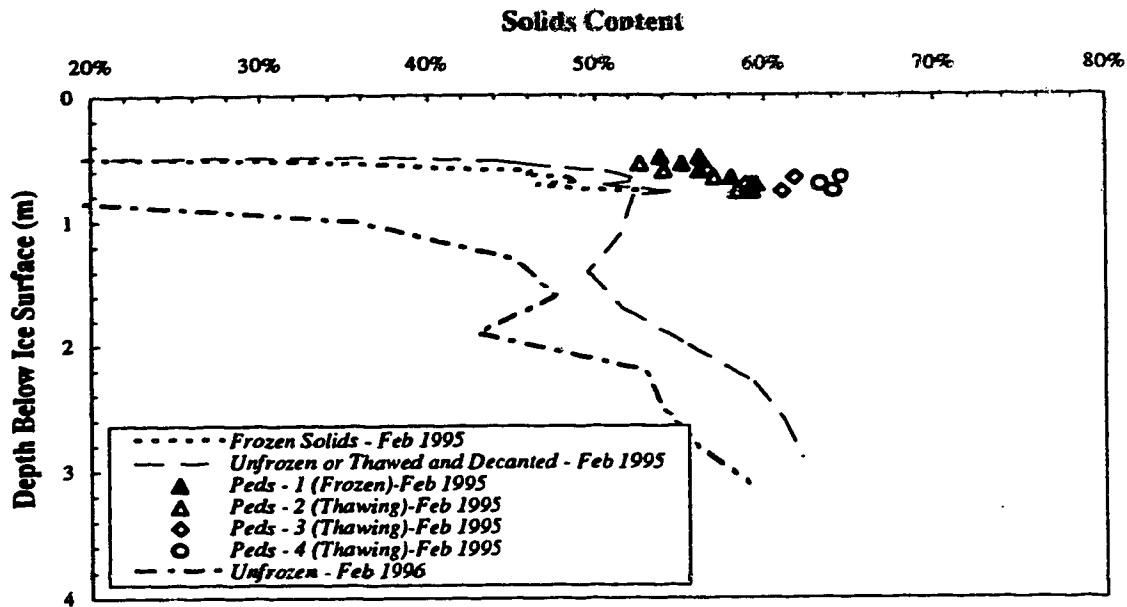


Figure A11 Solids Contents Within Coal Valley Pond - Site 2

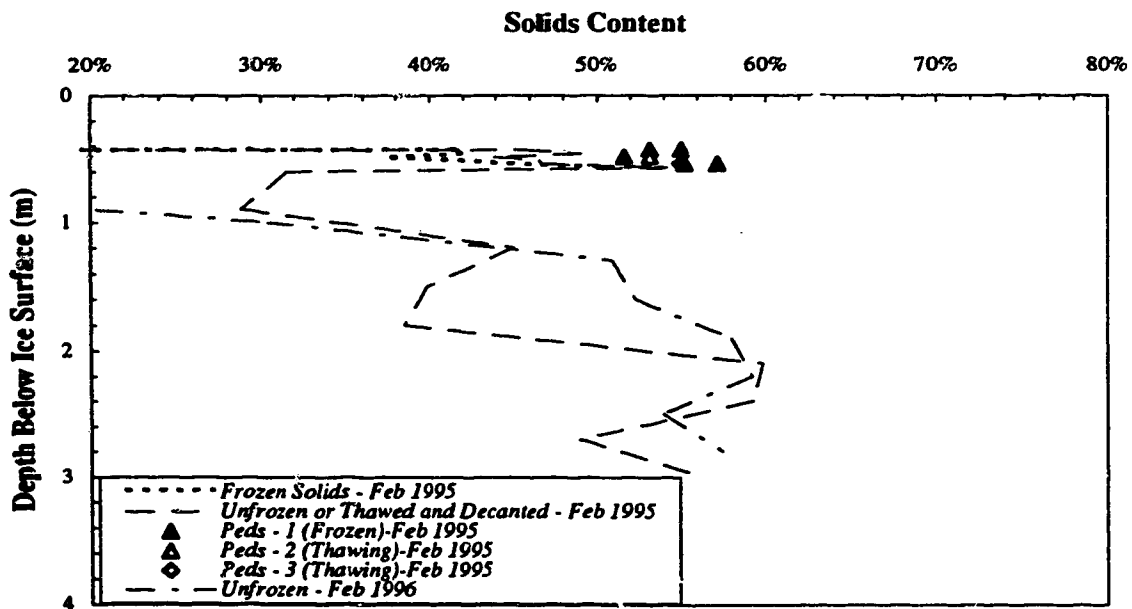


Figure A12 Solids Contents Within Coal Valley Pond - Site 3

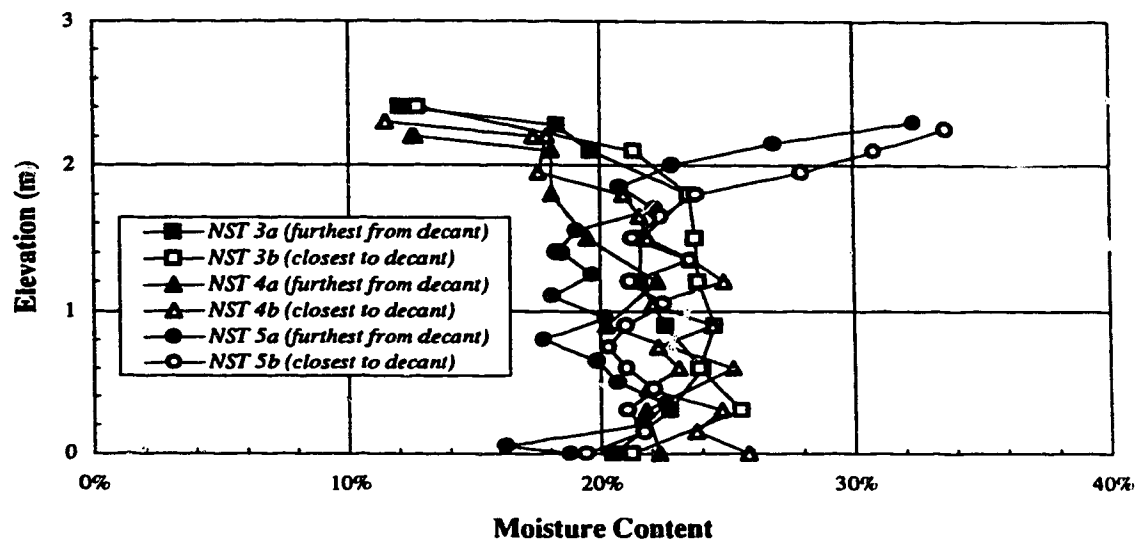


Figure A13 1994 Moisture Contents Within Suncor NST Cells

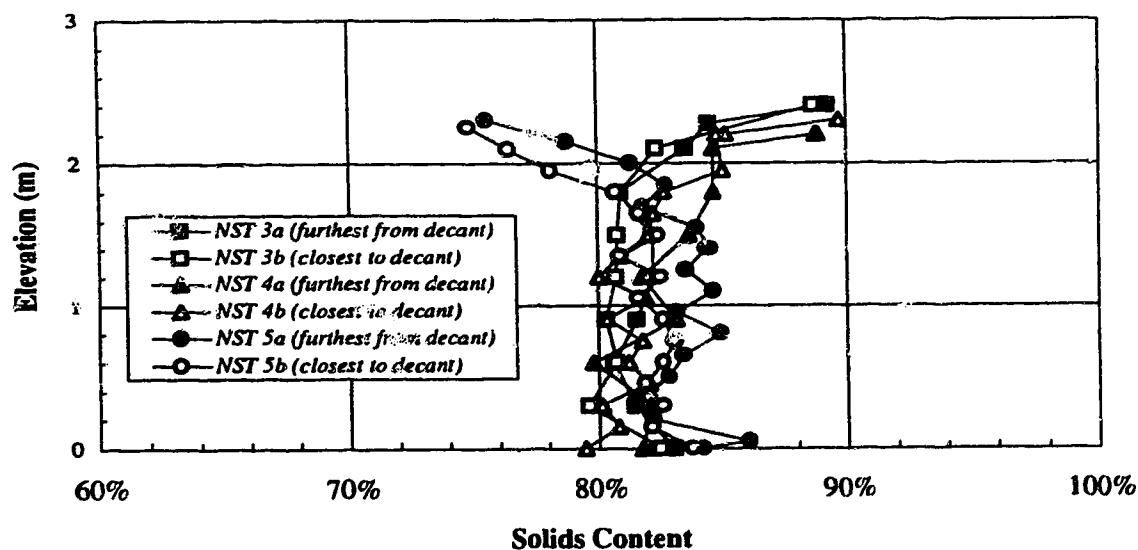


Figure A14 1994 Solids Contents Within Suncor NST Cell

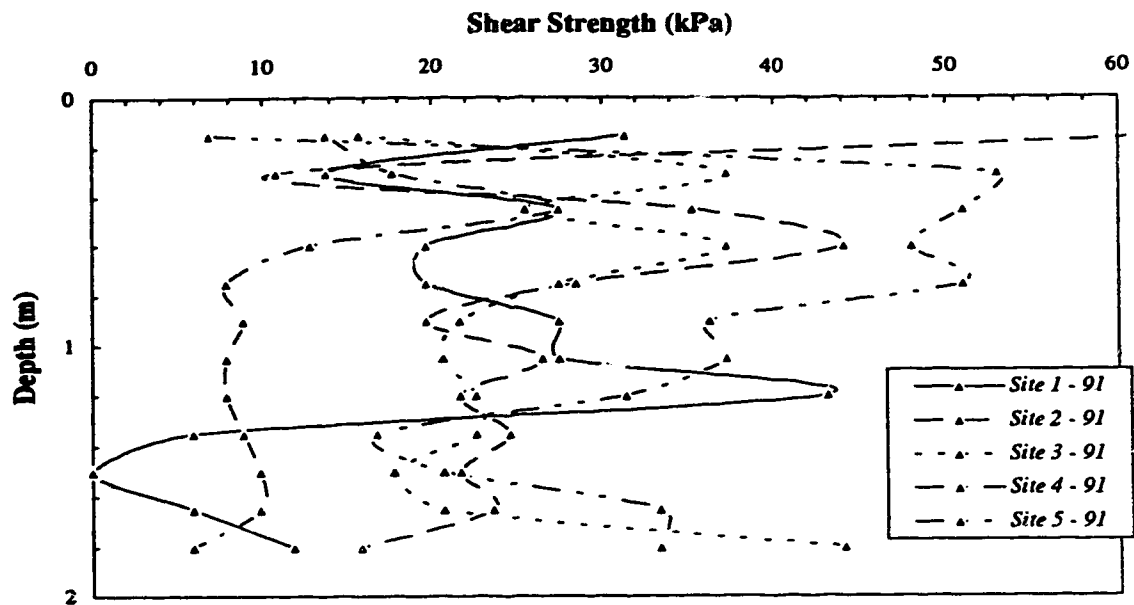


Figure A15 1991 Field Vane Shear Results Along Coal Valley Tailings Beach

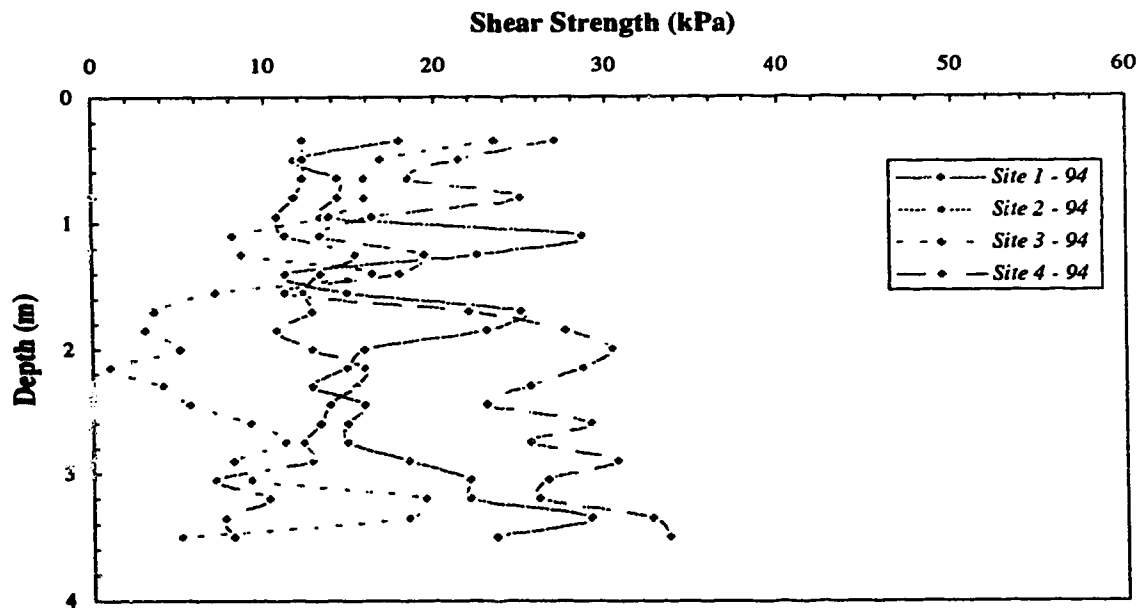


Figure A16 1994 Field Vane Shear Results Along Coal Valley Tailings Beach

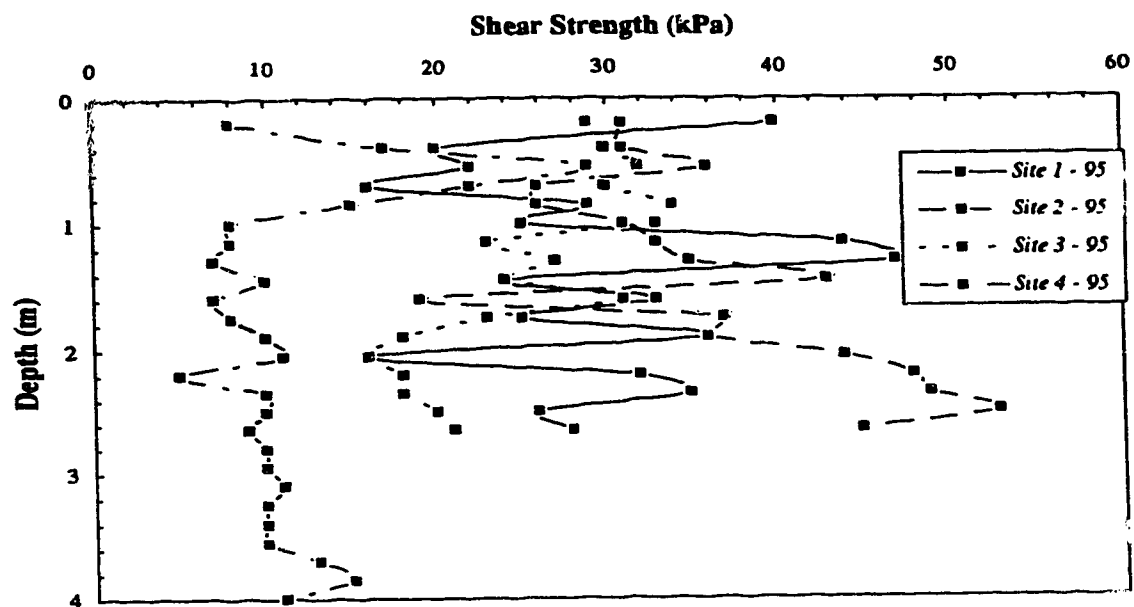


Figure A17 1995 Field Vane Shear Results Along Coal Valley Tailings Beach

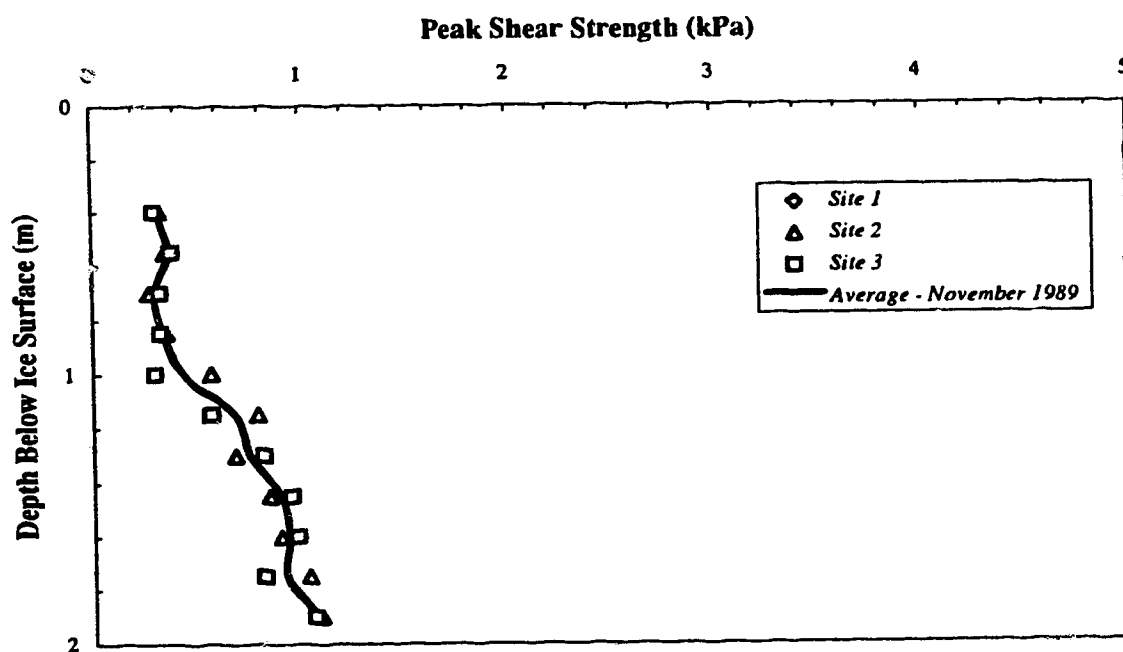


Figure A18 1989 (Nov) Field Vane Shear Results Within Coal Valley Tailings Pond

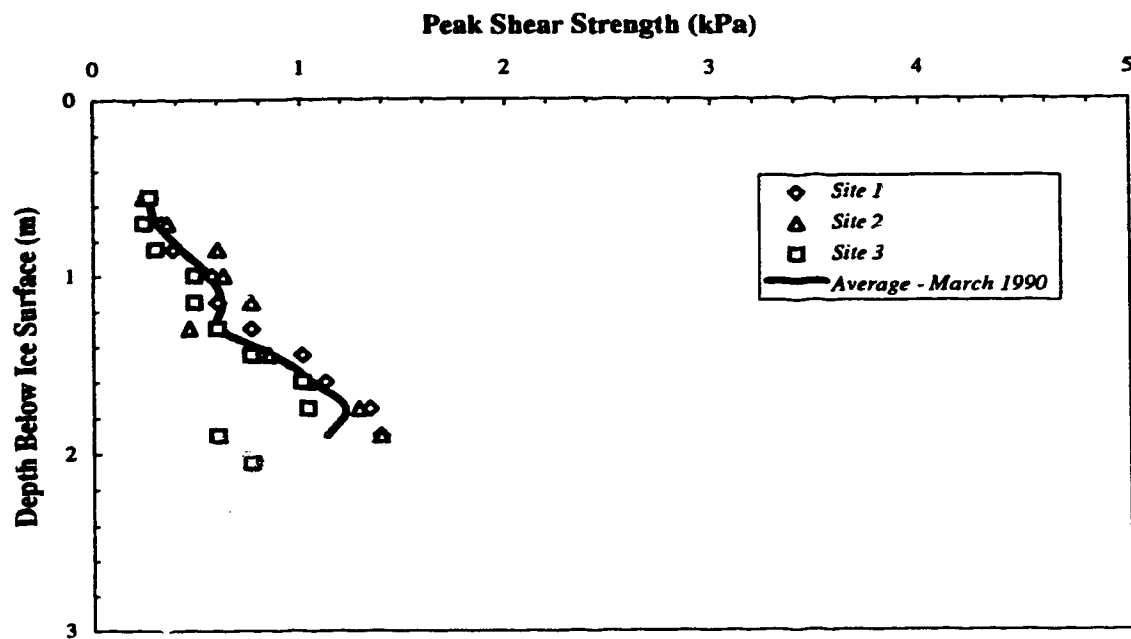


Figure A19 1990 (Mar) Field Vane Shear Results Within Coal Valley Tailings Pond

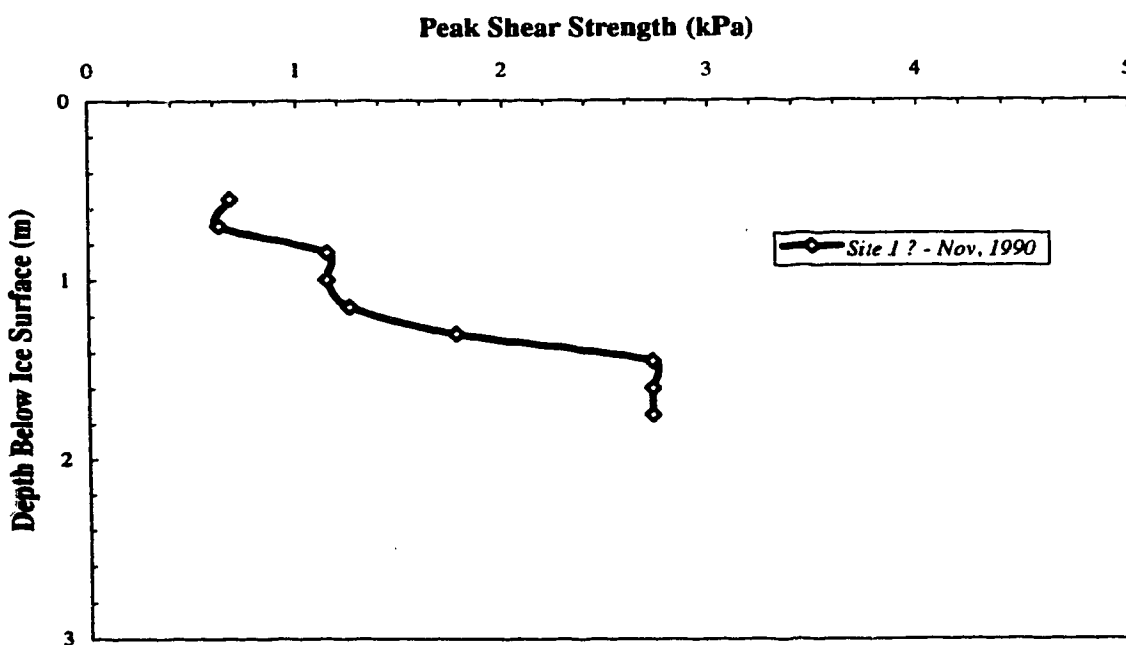


Figure A20 1990 (Nov) Field Vane Shear Results Within Coal Valley Tailings Pond

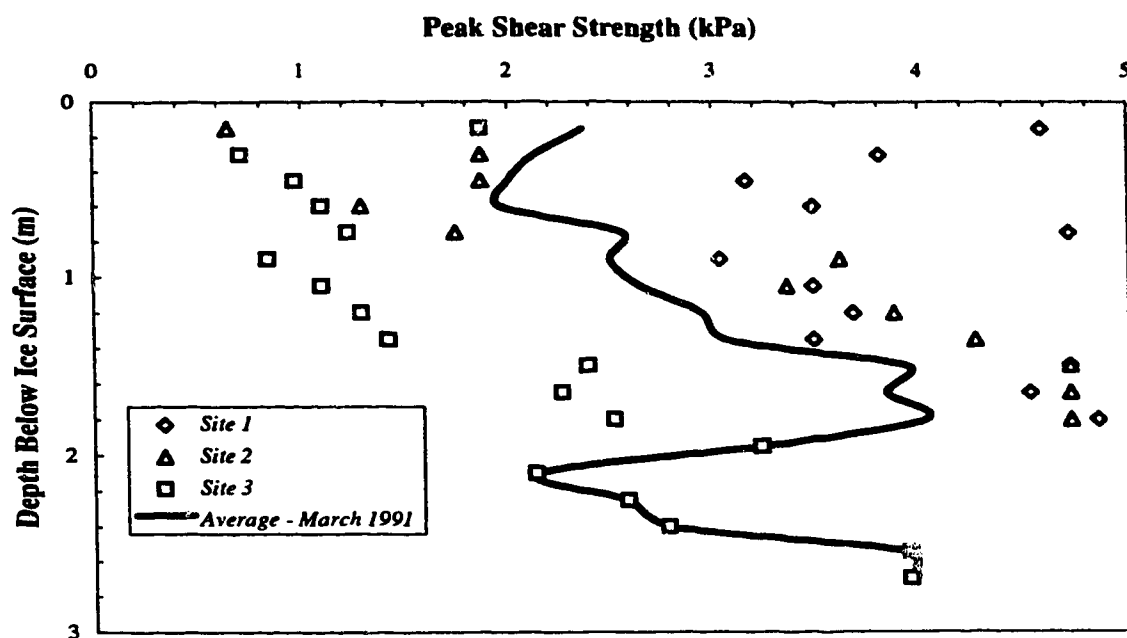


Figure A21 1991 (Mar) Field Vane Shear Results Within Coal Valley Tailings Pond

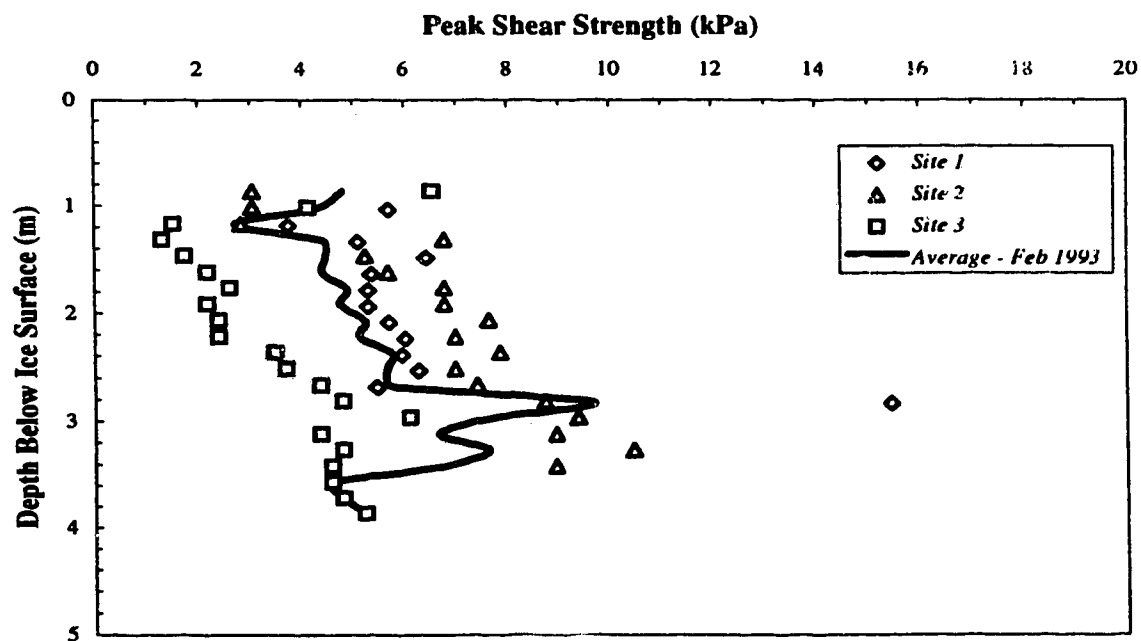


Figure A22 1993 (Feb) Field Vane Shear Results Within Coal Valley Tailings Pond

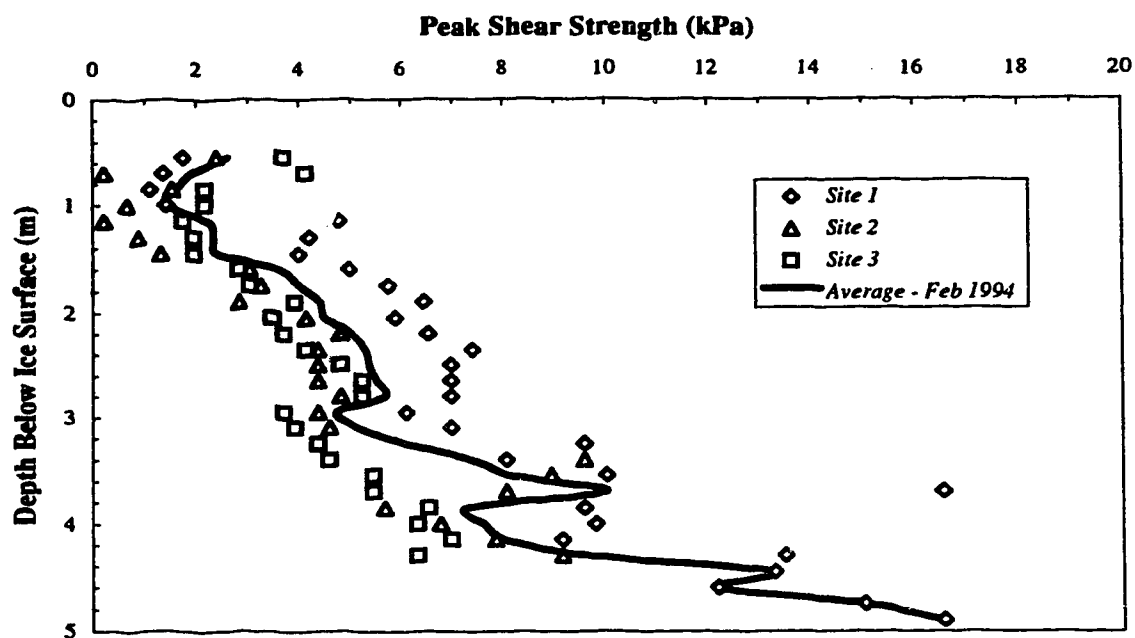


Figure A23 1994 (Feb) Field Vane Shear Results Within Coal Valley Tailings Pond

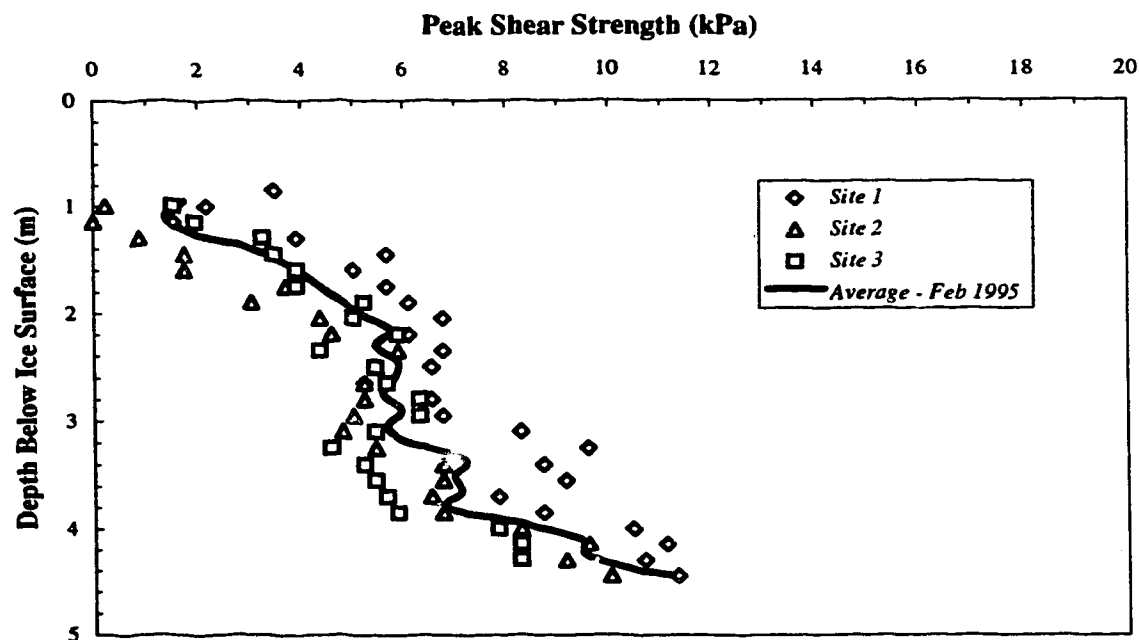


Figure A24 1995 (Feb) Field Vane Shear Results Within Coal Valley Tailings Pond

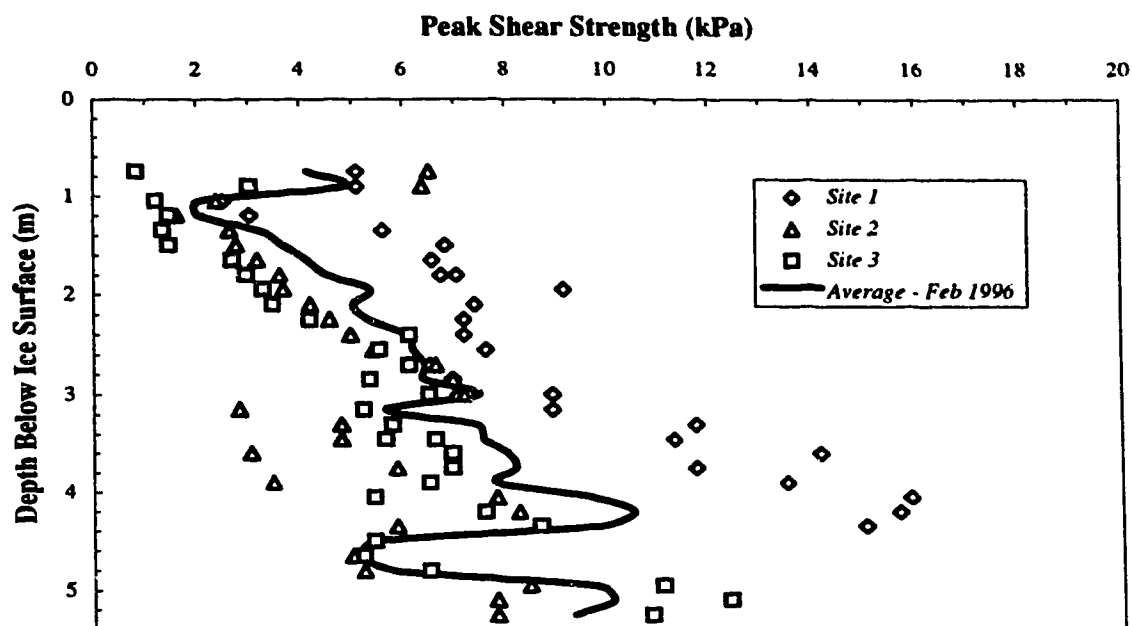


Figure A25 1996 (Feb) Field Vane Shear Results Within Coal Valley Tailings Pond

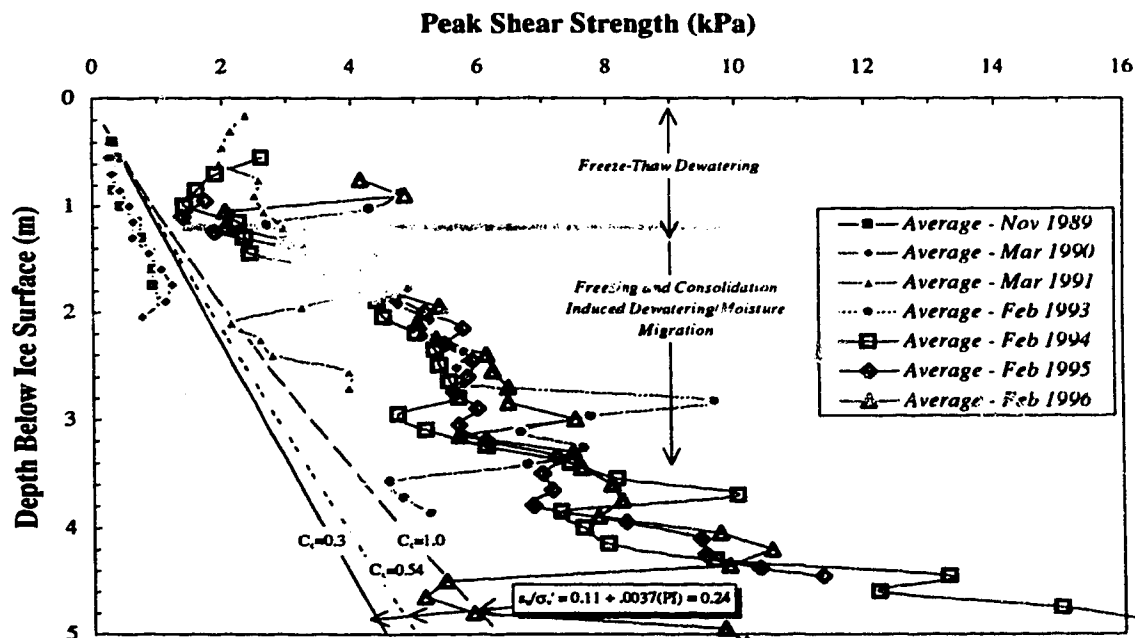


Figure A26 Average Field Vane Shear Results Within Coal Valley Tailings Pond

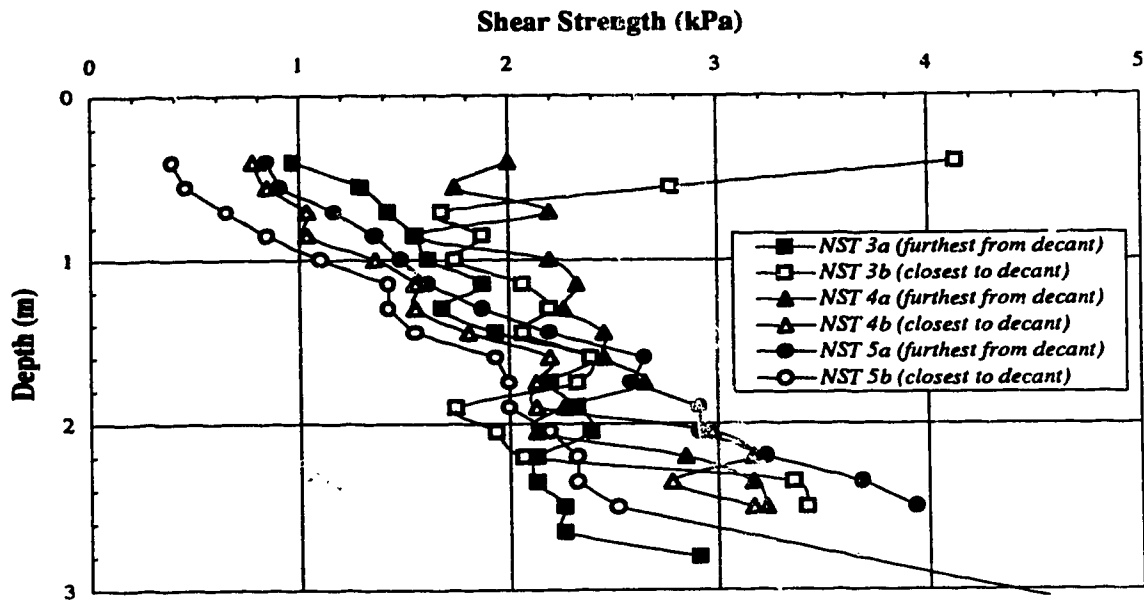


Figure A27 **1994 Field Vane Shear Results Within Suncor NST Cells**

Appendix B

Plate Load Test Results At Coal Valley And Suncor NST Cells

B.1. BACKGROUND

Plate Load Tests (PLT) were conducted along the beach portion of the Coal Valley impoundment in June 1991 and August 1994. The PLT locations, designated as Sites 1,2,3,4, and 5 are illustrated in Chapter 2. In 1991, PLT's were conducted at all five sites, however, time constraints experienced in 1994 prevented complete testing at all sites and only Sites 1, 2 and 4 were selected for investigation. Plate load tests were also conducted within the Suncor NST Cells 3 and 4 in October, 1994. The NST facility detailing the site investigation locations is illustrated in Chapter 4.

A brief description of the plate load test apparatus is included in Chapter 2. This chapter also provides a brief discussion of bearing capacity theory for shallow foundations. The traditional bearing capacity formulations are restricted to incompressible soils or the general shear failure mode as discussed in Chapter 2. These formulations cannot be suitably applied to analyze the punching shear failure mechanism exhibited by the compressible tailings without account for compressibility. Factors to incorporate within the bearing capacity formulation which attempt to account for compressibility are discussed by Terzaghi and Peck (1967), Vesic (1973), and Ismael and Vesic (1981). To compliment the early description of the PLT apparatus presented in Chapter 2, Chapters 4 and 6 discuss the system in greater detail highlighting the design

constraints, terminology employed to describe the following results, and the various boundary conditions investigated.

B.2. PLATE LOAD TEST RESULTS

The PLT results obtained from Coal Valley in 1991 are included in Figures B1 through B5, and the 1994 results are included in Figures B6 to B8. Figures B9 and B10 include the 1994 PLT results from the Suncor NST Cells 3 and 4. These figures include plots of pressure versus settlement presented on both arithmetic and logarithmic scale, as well as pressure versus relative settlement on logarithmic scale. As described by Vesic (1973), first failure in a PLT is only clearly defined in the general shear failure mechanism, with difficulty realized in establishing failure with tests experiencing local or punching shear failure. Hence, a common method of selecting the point of failure on PLT's conducted compressible soils is to select the "point of break" of the pressure versus relative settlement relationship portrayed on logarithmic scale. Presentation of the PLT results in this format was valuable for previous studies, which included determination of the effective mobilized shear strength considering the compressibility factors mentioned above. The PLT information is presented in this format herein, however, only to illustrate and compare the pressure-deformation behavior trends of the various deposits.

In addition to evaluating the ultimate bearing capacity of soils, the PLT results may provide an indication of the *insitu* modulus properties of the soil. As discussed by Jamiolkowski *et al.* (1985), the plate load test may be interpreted using formulae from the theory of elasticity. The immediate settlement, s , of a circular rigid plate at the surface of a semi infinite isotropic, homogeneous elastic half space is given as (Craig 1983):

$$s = \frac{\Delta Q D_p}{E} (1 - \nu^2) \frac{\pi}{4} \quad [B1]$$

where ΔQ is the applied pressure to the plate, D_p is the plate diameter, E is the elastic modulus over the loading range, and ν is the Poisson's ratio. As outlined by Jamiolkowski *et al.* (1985),

[B1] may be rearranged as shown below to predict the shear modulus, G , of a relative large volume of soil stressed beneath the PLT conducted at the surface.

$$G = \frac{\Delta Q D_p}{s} (1 - \nu) \frac{\pi}{8} \quad [B2]$$

It is acknowledged that the assumptions made to arrive at this formulation (ie. isotropic, homogeneous, elastic) are not valid for the tailings deposits investigated (compressible, nonlinear stress-strain behavior), particularly the extremely heterogeneous Coal Valley tailings facility. However, this formulation provides some insight regarding the stiffness of the surficial tailings at the sites investigated, and presents a comparison between the shear modulus response of the tailings measured at small settlements, and the maximum shear modulus, G_o , determined through shear wave velocity measurements using the Spectral Analysis of Surface Waves (SASW) technique presented in Appendix D. The SASW technique is briefly discussed in Chapter 4, with the predicted shear wave velocities and computed small strain shear modulus, G_o , values presented in Appendix D. The shear modulus determined using the PLT results and [B2] are subsequently compared at the various sites through a relative pressure relationship, Q/Q_{max} , where Q_{max} is the maximum bearing pressure sustained by the tailings within the settlement range investigated. Figures B11 through B15 and B16 through B18 include the 1991 and 1994 results at Coal Valley, and B19 and B20 include the 1994 results at the Suncor NST Cells.

The key observation forwarded comparing Figures B11 through B18 is the rate of attenuation of shear modulus in the 1991 results compared with the 1994 results. The shear modulus appears to attenuate more rapidly with Q/Q_{max} in 1991 than in 1994. As discussed in Appendix E, fibres or roots try to resist deformation through development of increased internal shear strength and internal confining stress within the stressed soil. These effects likely restricts the shear modulus attenuation as observed with the 1994 PLT results.

The shear modulus values determined from the PLT results were employed to help predict the approximate rigidity index, I_r , of the tailings as discussed in Appendix F. The rigidity index, defined as the shear modulus divided by shear strength ($I_r = G/s_u$), was used for a variety of

analysis purposes including prediction of cone tip factor, N_{ti} (Chapter 5) for shear strength prediction from the CPT profiles.

A comprehensive summary of the plate load test results at Coal Valley in 1991 and 1994 is presented in Chapter 6. Figure 6.8 from this chapter summarizes the PLT results comparing the bearing pressures at the sites in terms of 10% and 20% relative settlement, and the maximum recorded bearing pressure. This figure has been reproduced in this appendix as Figure B21.

Mathematical relationships were derived from the pressure versus settlement results obtained from Coal Valley in 1991 and 1994. These “averaged” relationships facilitated flexible portrayal and comparison of the results from the two years. The products of this exercise are summarized in Figures B22 and B23. Figure B22 includes the bearing pressure increase versus settlement from 1991 to 1994, comparing the various boundary conditions. Figure B23 includes the percentage of bearing pressure increase versus settlement of the 1994 results compared with those in 1991. It is interesting to note that the percentage increase in bearing capacities in Figure B23 generally occurs very rapidly, within the first 10 mm of settlement. This early percentage increase is subsequently maintained within continued settlement. Also, as previously illustrated in Figure B21, significant increases in capacity are observed at Sites 1 and 4 with less of a relative increase observed at Site 2.

B.3. MATRIC SUCTIONS AND BEARING CAPACITY

The chapters of this thesis discussed the contribution of matric suction, resulting from evaporation and evapotranspiration processes, on the increased bearing capacity experienced at the surface of the tailings compared to the capacities determined at depth. Although matric suctions were not recorded in the field, visual observations indicated that an excessive evaporation profile (Chapter 6) was present in the field. Although the following was not presented in the main chapters of the thesis due to lack of supporting physical data, it is instructive, “conceptually”, to relate the effect of matric suction on bearing capacity.

The impact of matric suction in a clay on the ultimate bearing capacity of a footing was illustrated by Fredlund and Rahardjo (1993). Considering a total stress approach using undrained shear strengths, the initial (prior to matric suction changes) ultimate bearing capacity of an unsaturated soil may be written as:

$$q_{fu} = N_c S_{uo} \approx N_c \overbrace{\{ c' + (\sigma_f - u_a)_f \tan \phi' + (u_a - u_w)_f \tan \phi^b \}}^{\text{Shear Strength of Unsaturated Soils}} \quad [\text{B3}]$$

The variables included in shear strength and bearing capacity formulation of unsaturated soils are defined in Chapter 6.

A change in matric suction from changing climatic conditions or varying footing elevations, result in a change in bearing capacity as given by:

$$\Delta q_f = N_c \Delta S_{uo} = N_c \Delta(u_a - u_w)_f \tan \phi^b \quad [\text{B4}]$$

By dividing [B3] by [B4], the percent change in bearing capacity versus percent change in matric suction can be evaluated for various ϕ^b values as illustrated in Figure B24. This figure illustrates the effect of evaporation and resulting matric suction development ($\Delta(u_a - u_w)/S_{uo} (\%) \rightarrow$) on increased bearing capacity for a range of ϕ^b values. Conversely, this figure also highlights the decrease in bearing capacity through a reduction in matric suction ($\Delta(u_a - u_w)/S_{uo} (\%) \leftarrow$) sponsored by precipitation or a rising water table. As illustrated in the inset matric suction profiles in Figure B24, matric suctions may also vary spatially, particularly with depth. Once again emphasizing that matric suctions were not recorded and only visual observations provide support, the decrease in bearing capacity observed below the tailings surface (compared to the tailings surface) in 1994 and particularly in 1991 is likely the result of decreasing matric suction with depth. Emphasis is placed on the 1991 PLT results since the 1994 likely had a coupled effect of reduced matric suction and reduced vegetative root reinforcement.

Although the previous discussion conceptualizes the effect of matric suction on bearing capacity, it simplifies the actual stress-strain matric suction changes as the unsaturated compressible tailings undergo compression and shear following load application.

B.4. REFERENCES

- Craig, R.F., 1983. **Soil Mechanics. (Third Edition)**, Van Nostrand Reinhold (UK) Co. Ltd., Berkshire, England, 419 pgs.
- Fredlund, D.G., Rahardjo, H., 1993. **Soil Mechanics For Unsaturated Soils**. John Wiley & Sons, Inc. New York., 517 pp.
- Ismael, N.F., and Vesic, A.S., 1981. Compressibility and Bearing Capacity. *ASCE Journal of Geotechnical Engineering* GT. 12:1677-1691.
- Jamiolkowski, M., Ladd, C.C., Germaine, J.T., and Lancellotta, R., 1985. New Developments in Field and laboratory Testing of Soils. *Proceedings of the 11th Conference on Soil Mechanics and Foundation Engineering*, San Francisco, California, August 12-16, Vol. 1, pgs. 57-153.
- Terzaghi, K., and Peck, R.B., 1967. **Soil Mechanics in Engineering Practice. (Second Edition)**, John Wiley and Sons, New York, New York, 729pgs.
- Vesic, A.S., 1973. Analysis of Ultimate Loads of Shallow Foundations. *ASCE Journal of Soil Mechanics and Foundation Division*, 99(1):45-73.

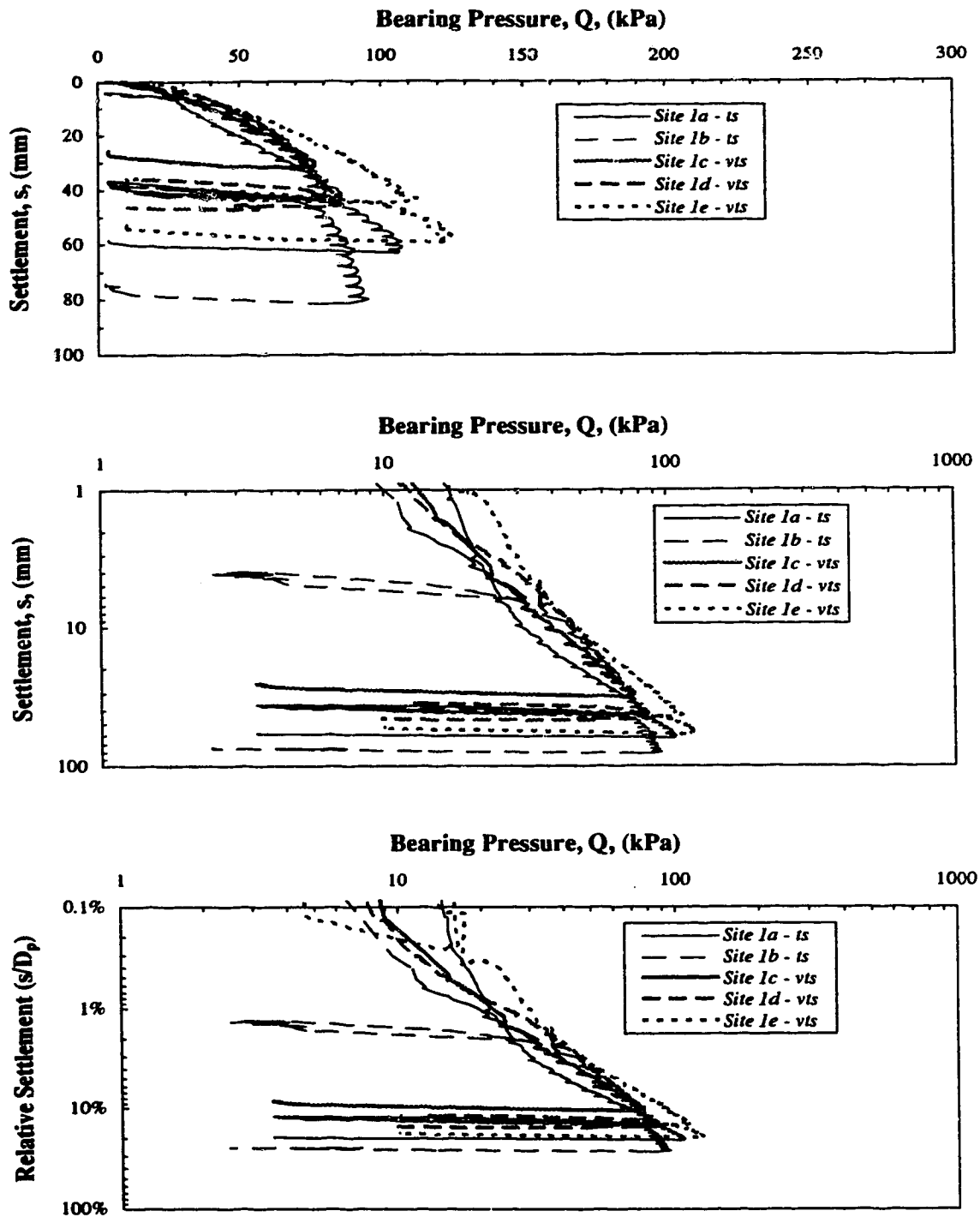


Figure B1 1991 PLT Results Along Coal Valley Tailings Beach - Site 1

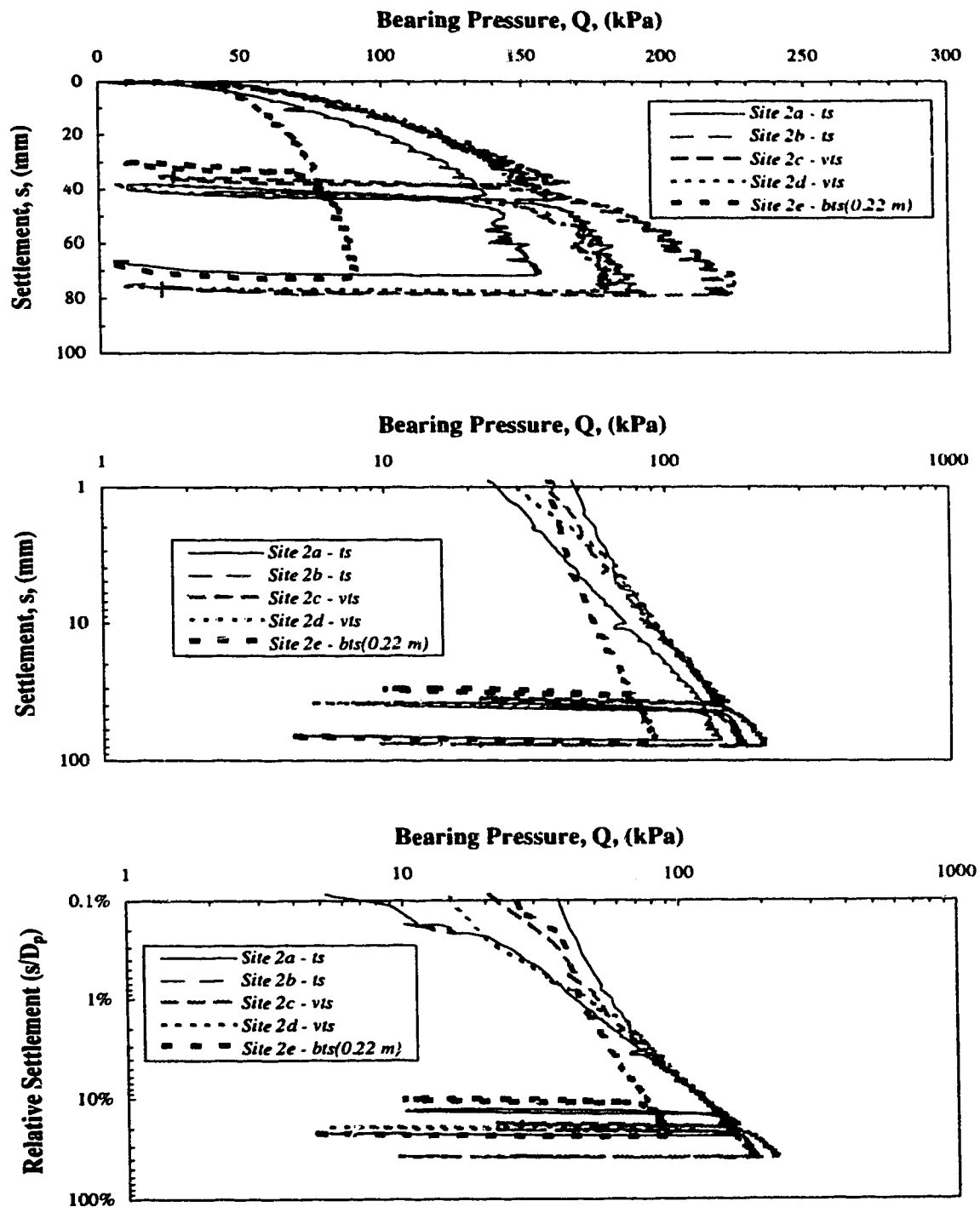


Figure B2

1991 PLT Results Along Coal Valley Tailings Beach - Site 2

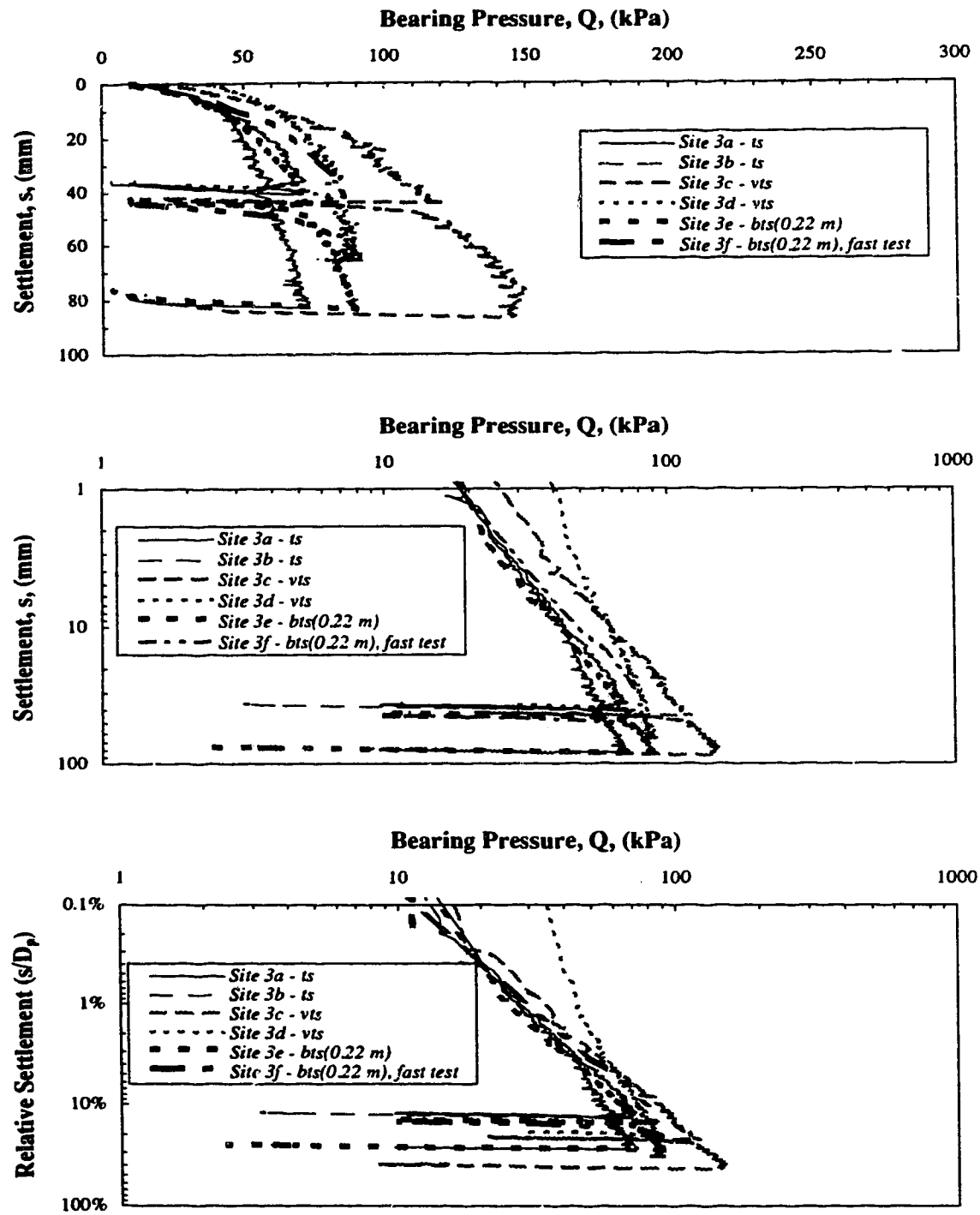


Figure B3 1991 PLT Results Along Coal Valley Tailings Beach - Site 3

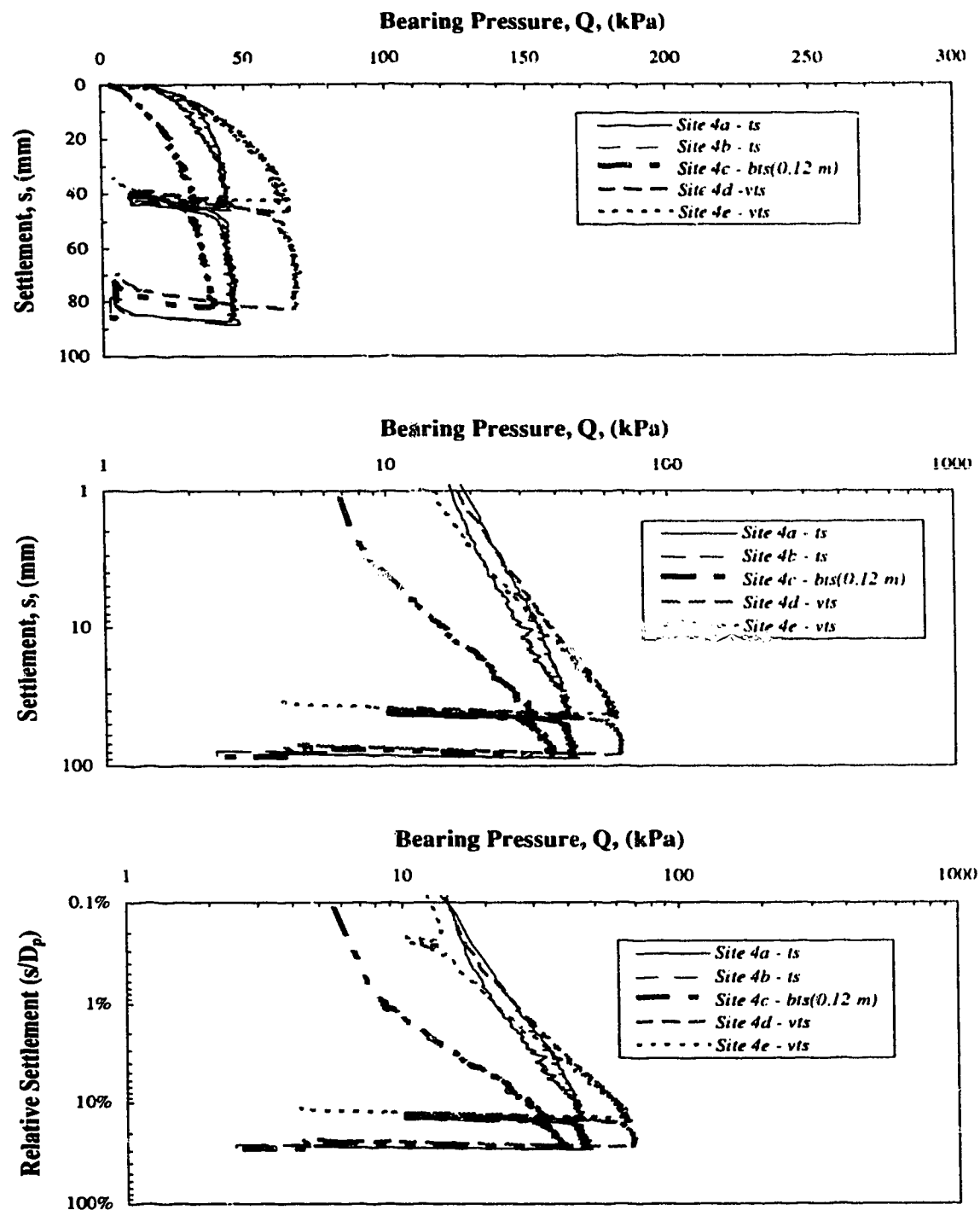


Figure B4 1991 PLT Results Along Coal Valley Tailings Beach - Site 4

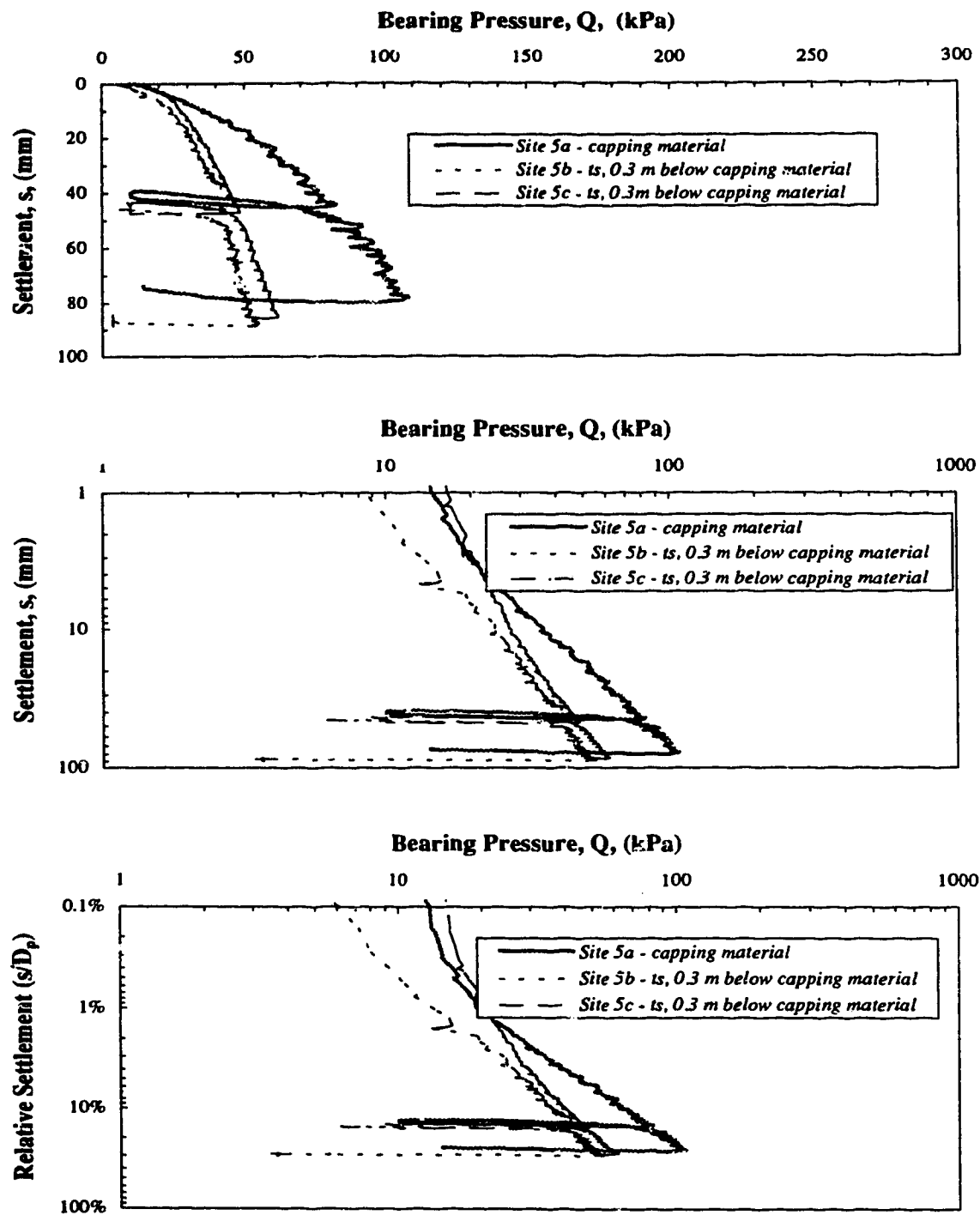


Figure B5 **1991 PLT Results Along Coal Valley Tailings Beach - Site 5**

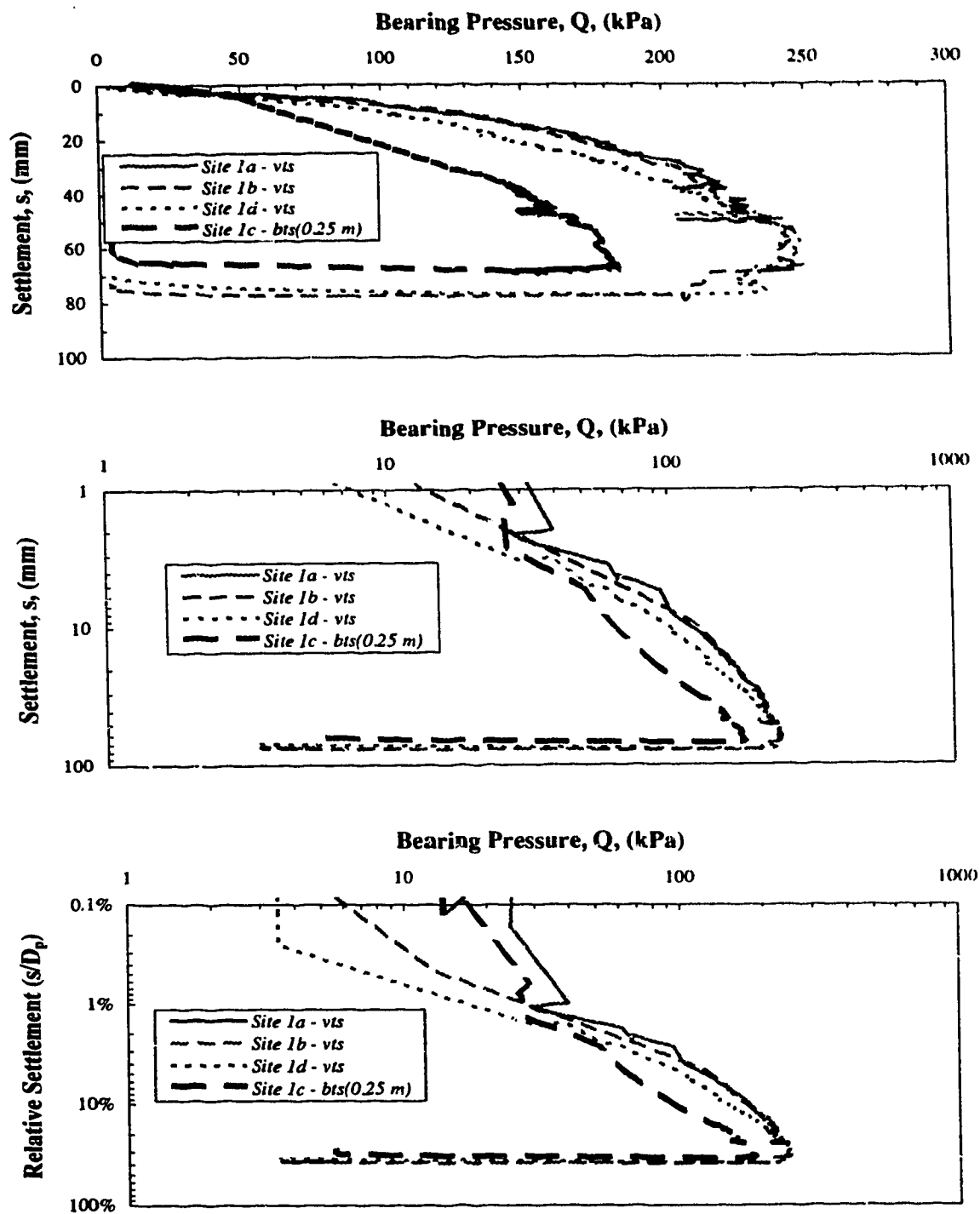


Figure B6

1994 PLT Results Along Coal Valley Tailings Beach - Site 1

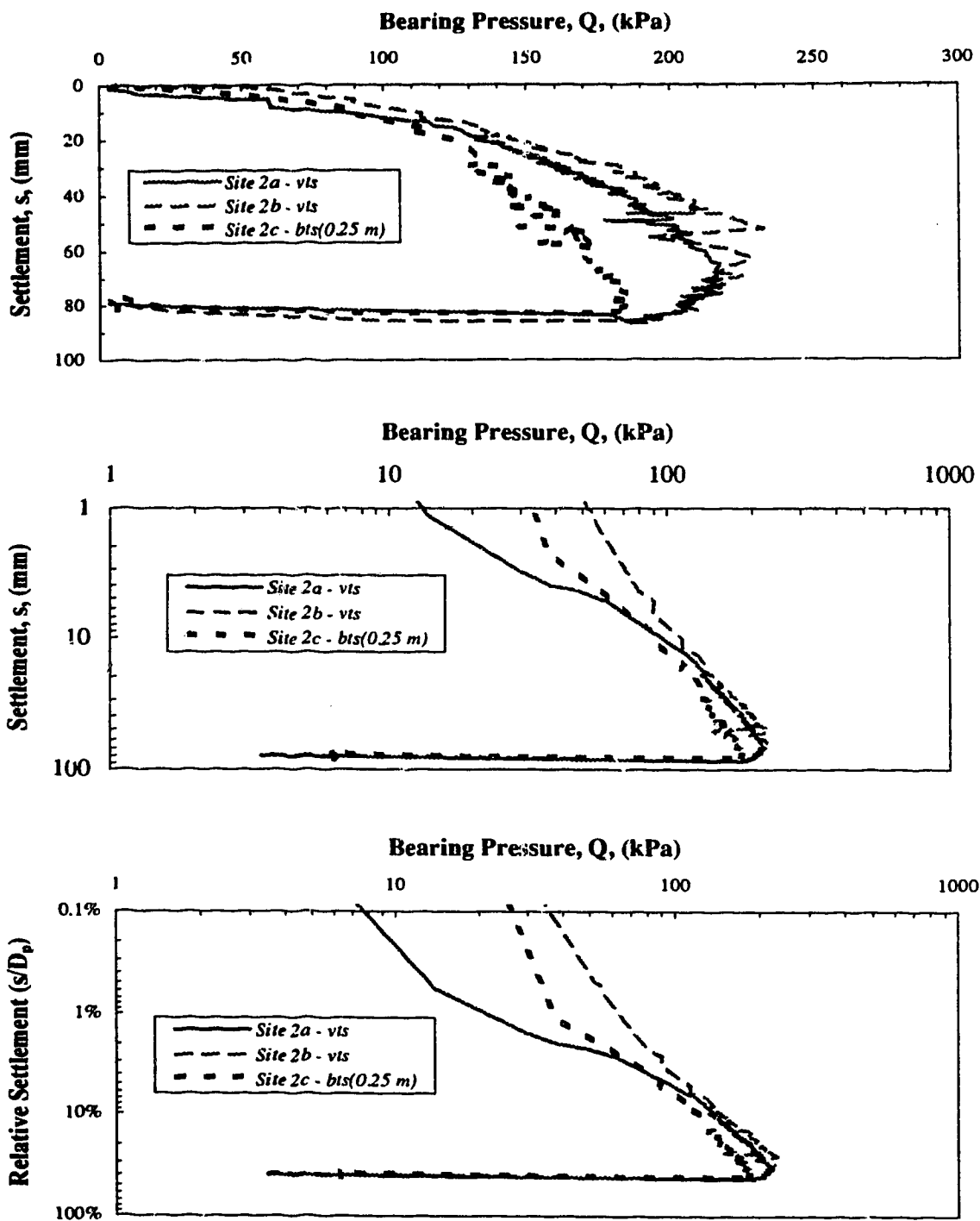


Figure B7 **1994 PLT Results Along Coal Valley Tailings Beach - Site 2**

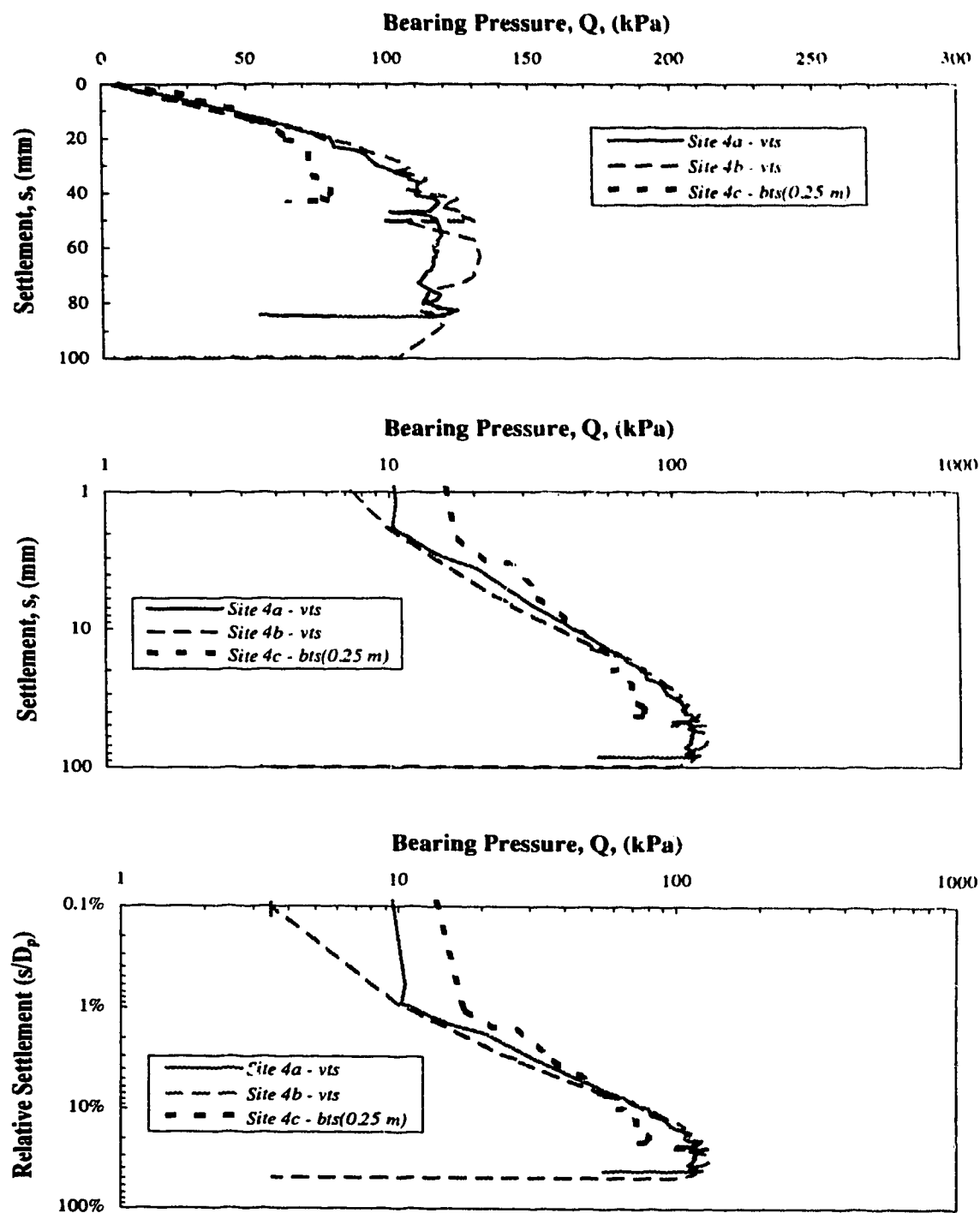


Figure B8 1994 PLT Results Along Coal Valley Tailings Beach - Site 4

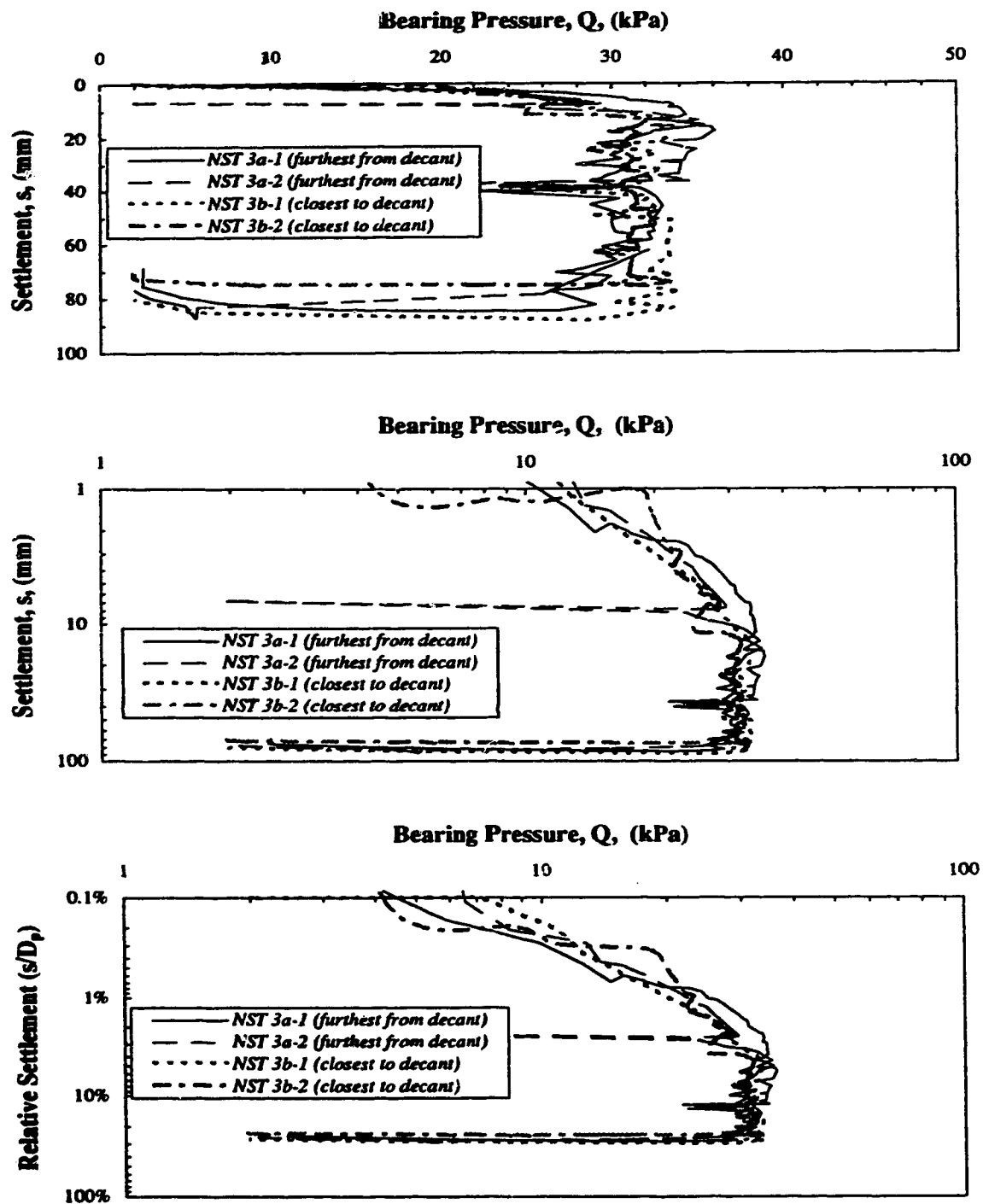


Figure B9 **1994 PLT Results Within Suncor NST Cell 3**

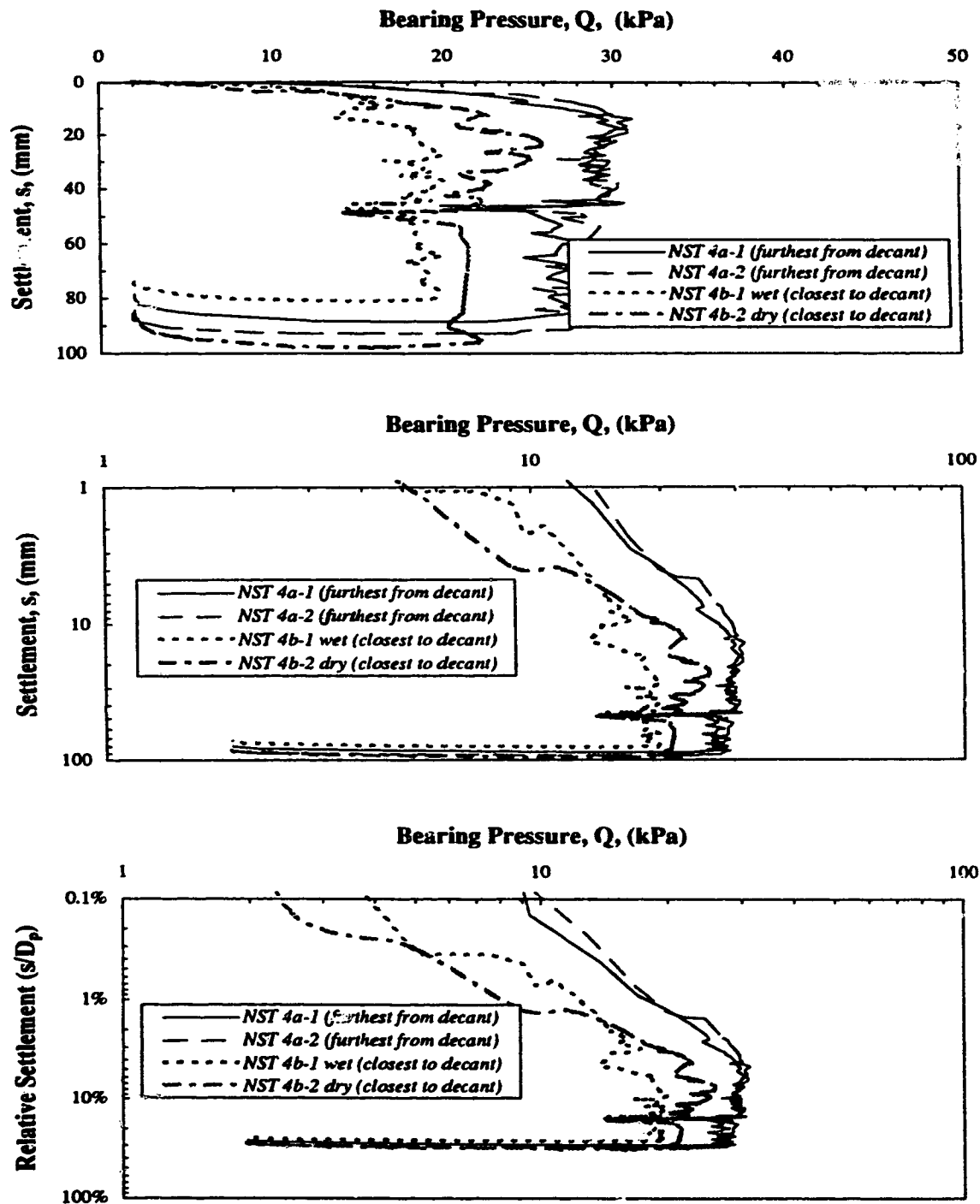


Figure B10 1994 PLT Results Within Suncor NST Cell 4

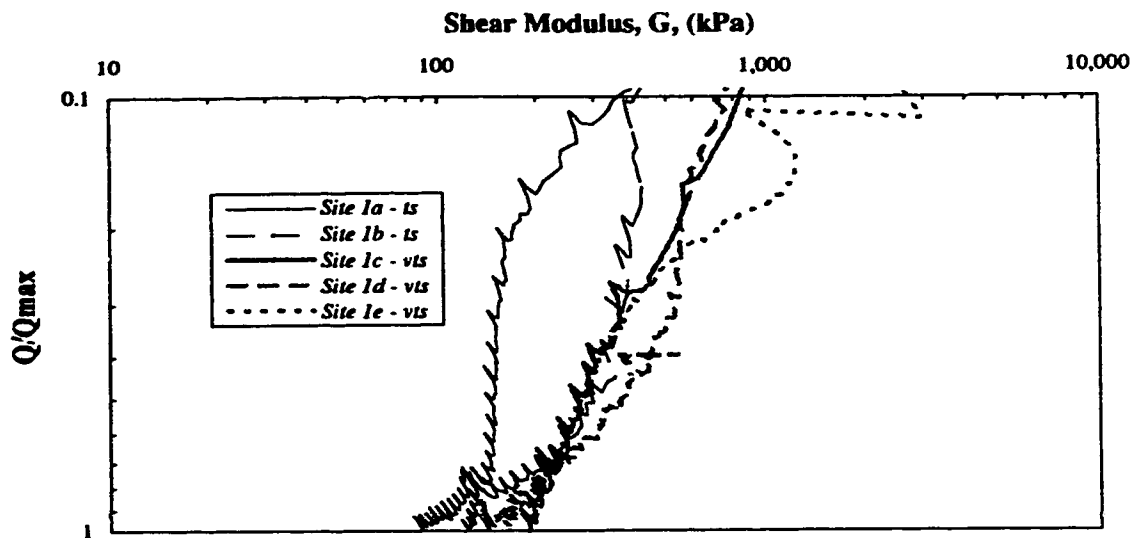


Figure B11 Shear Modulus Relationships from 1991 PLT Results Along Coal Valley Tailings Beach - Site 1

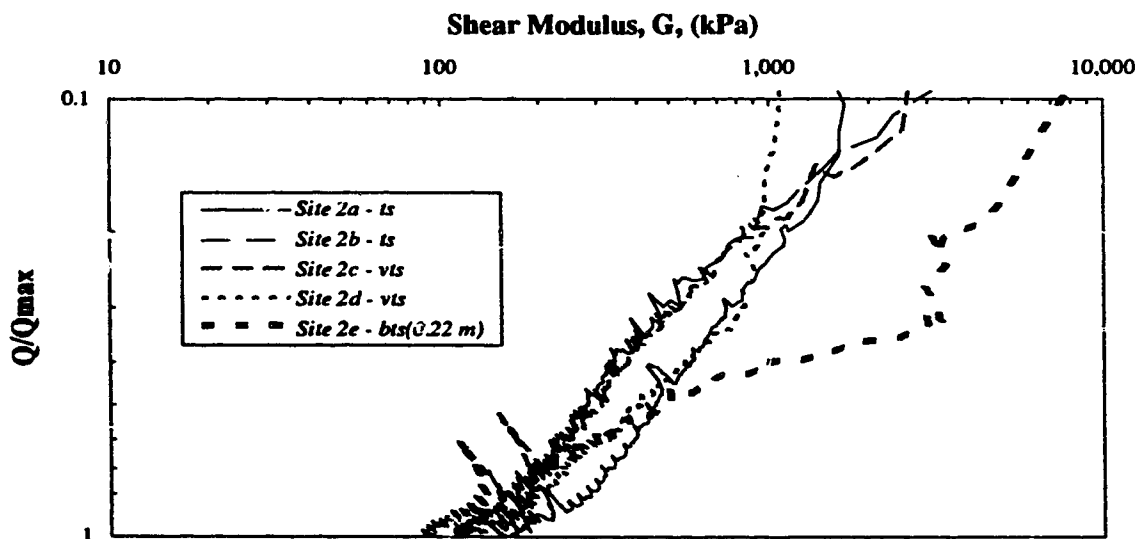


Figure B12 Shear Modulus Relationships from 1991 PLT Results Along Coal Valley Tailings Beach - Site 2

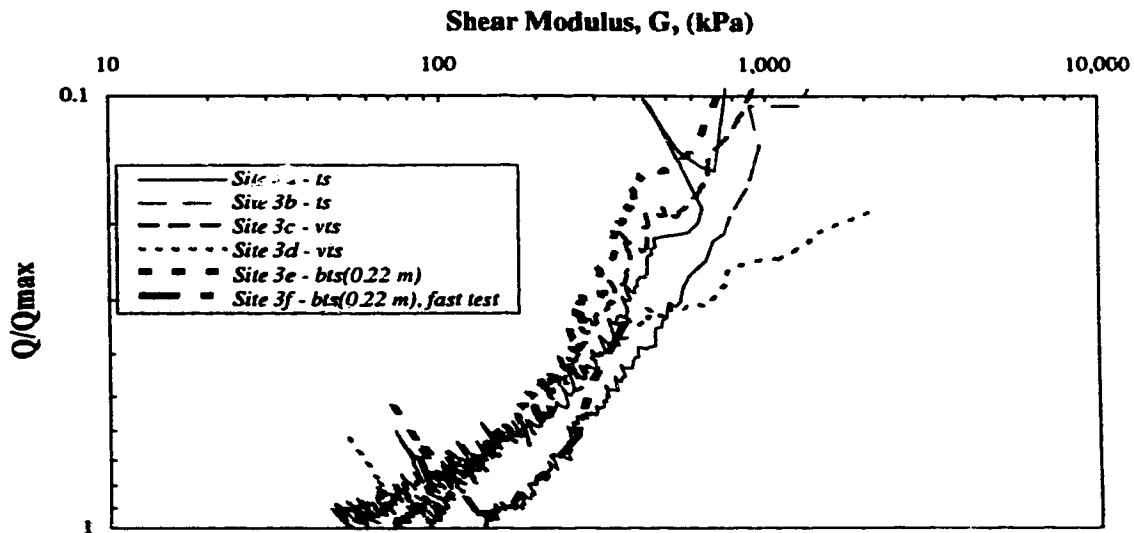


Figure B13 Shear Modulus Relationships from 1991 PLT Results Along Coal Valley Tailings Beach - Site 3

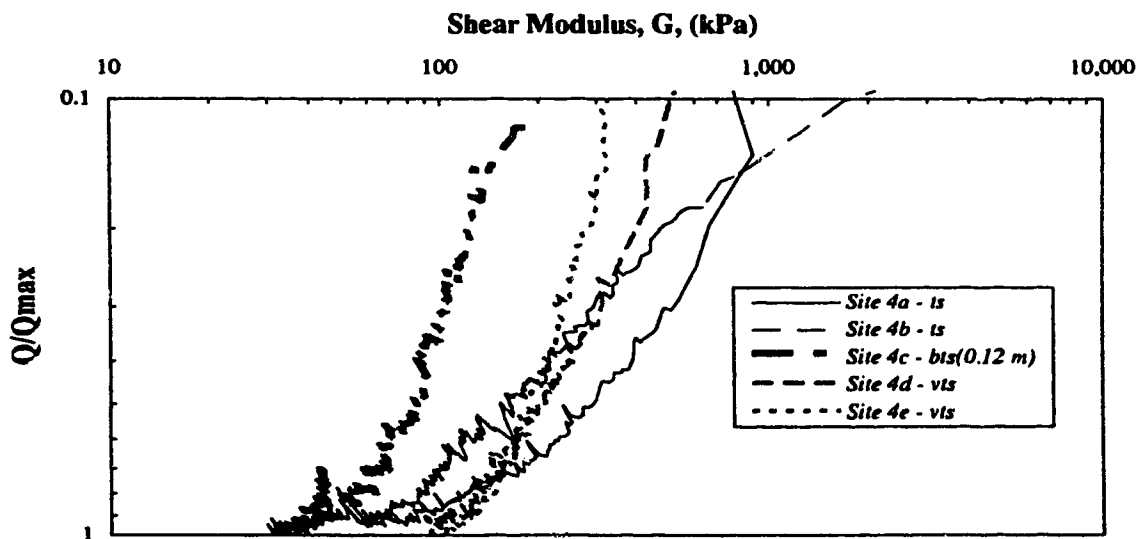


Figure B14 Shear Modulus Relationships from 1991 PLT Results Along Coal Valley Tailings Beach - Site 4

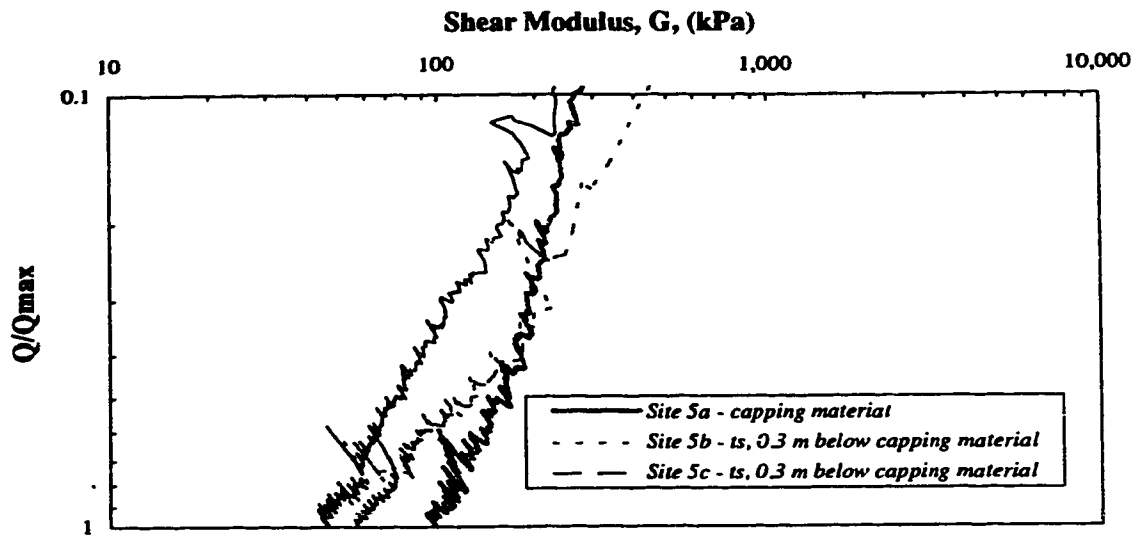


Figure B15 Shear Modulus Relationships from 1991 PLT Results Along Coal Valley Tailings Beach - Site 5

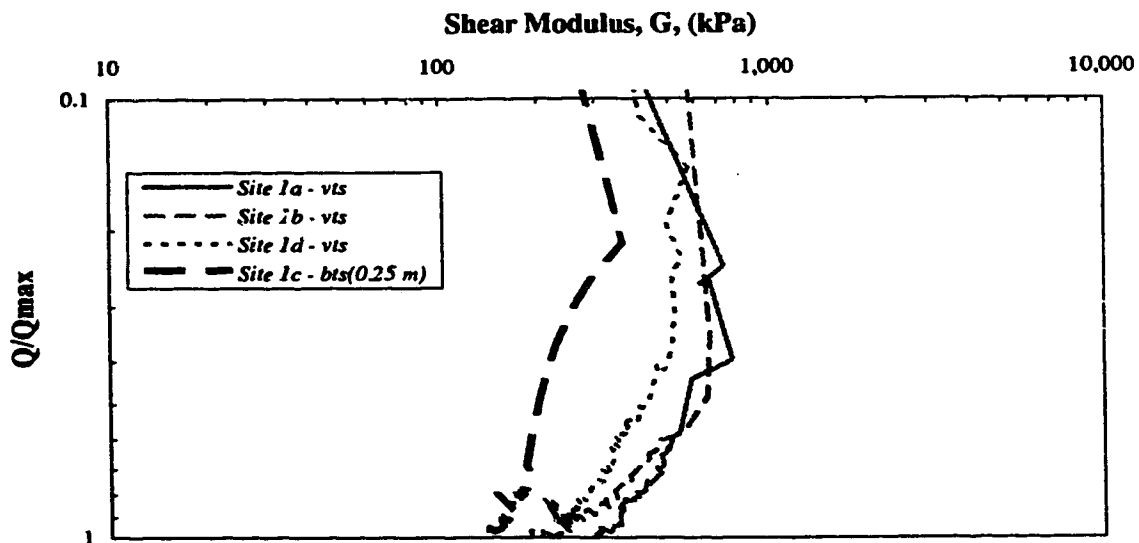


Figure B16 Shear Modulus Relationships from 1994 PLT Results Along Coal Valley Tailings Beach - Site 1

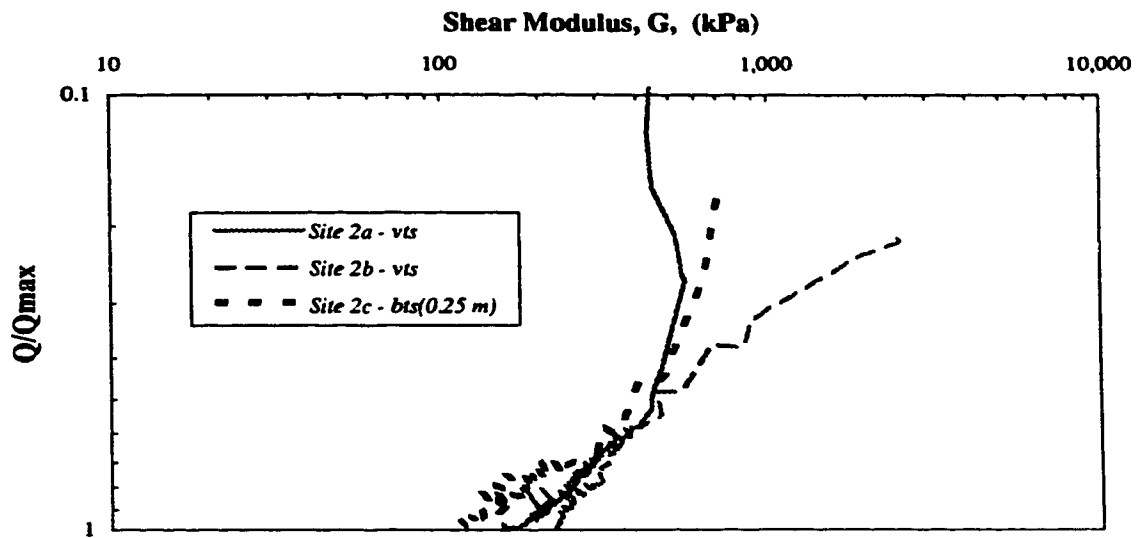


Figure B17 Shear Modulus Relationships from 1994 PLT Results Along Coal Valley Tailings Beach - Site 2

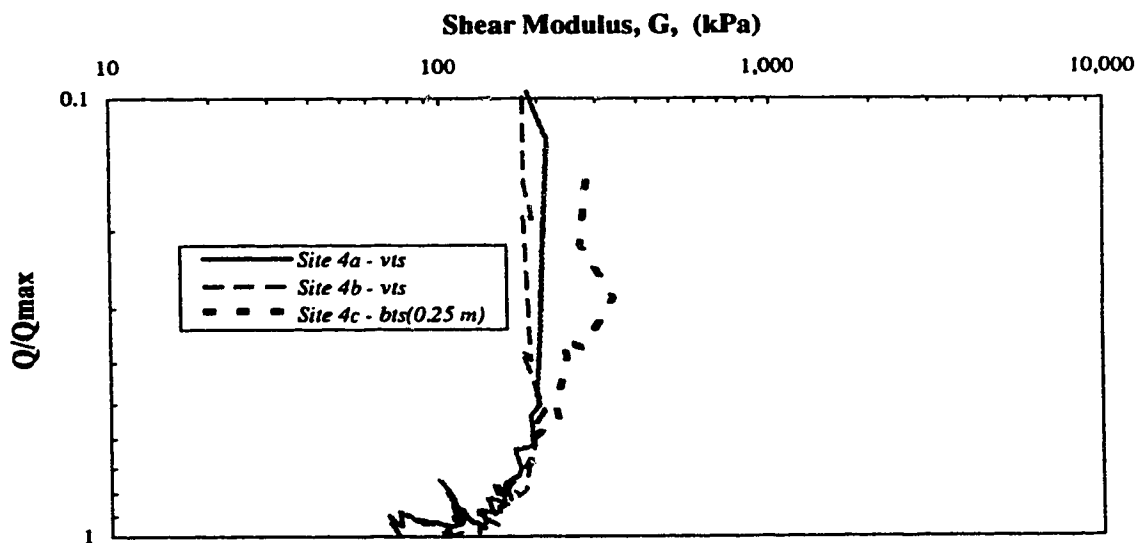


Figure B18 Shear Modulus Relationships from 1994 PLT Results Along Coal Valley Tailings Beach - Site 4

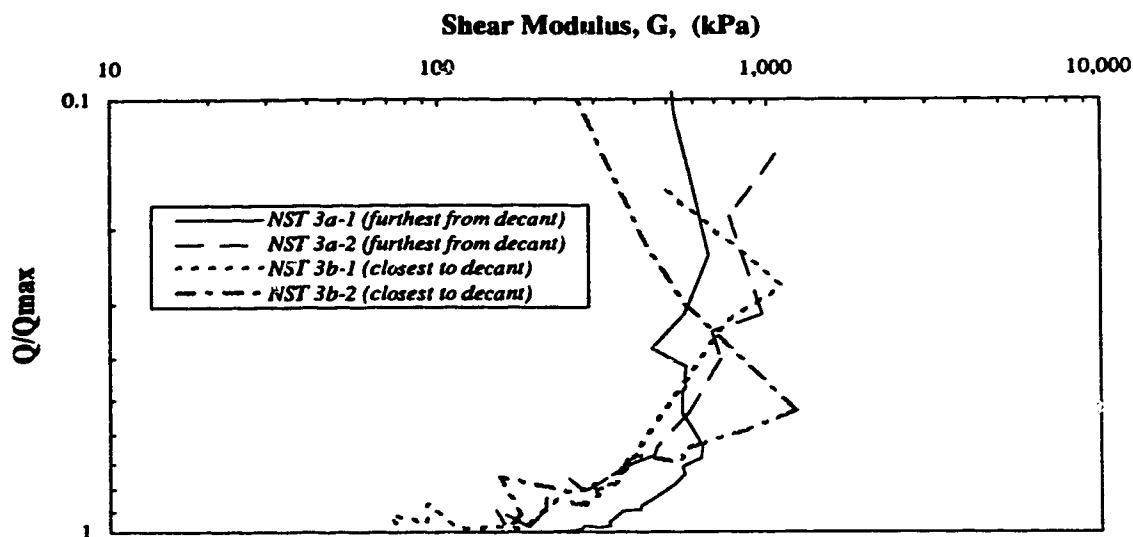


Figure B19 Shear Modulus Relationships from 1994 PLT Results Within Suncor NST Cell 3

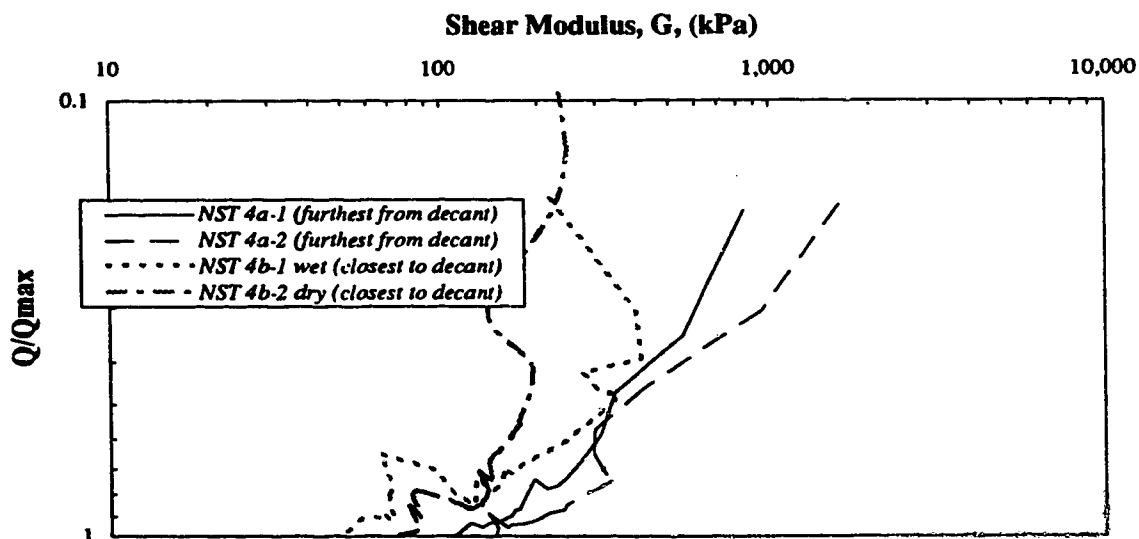


Figure B20 Shear Modulus Relationships from 1994 PLT Results Within Suncor NST Cell 4

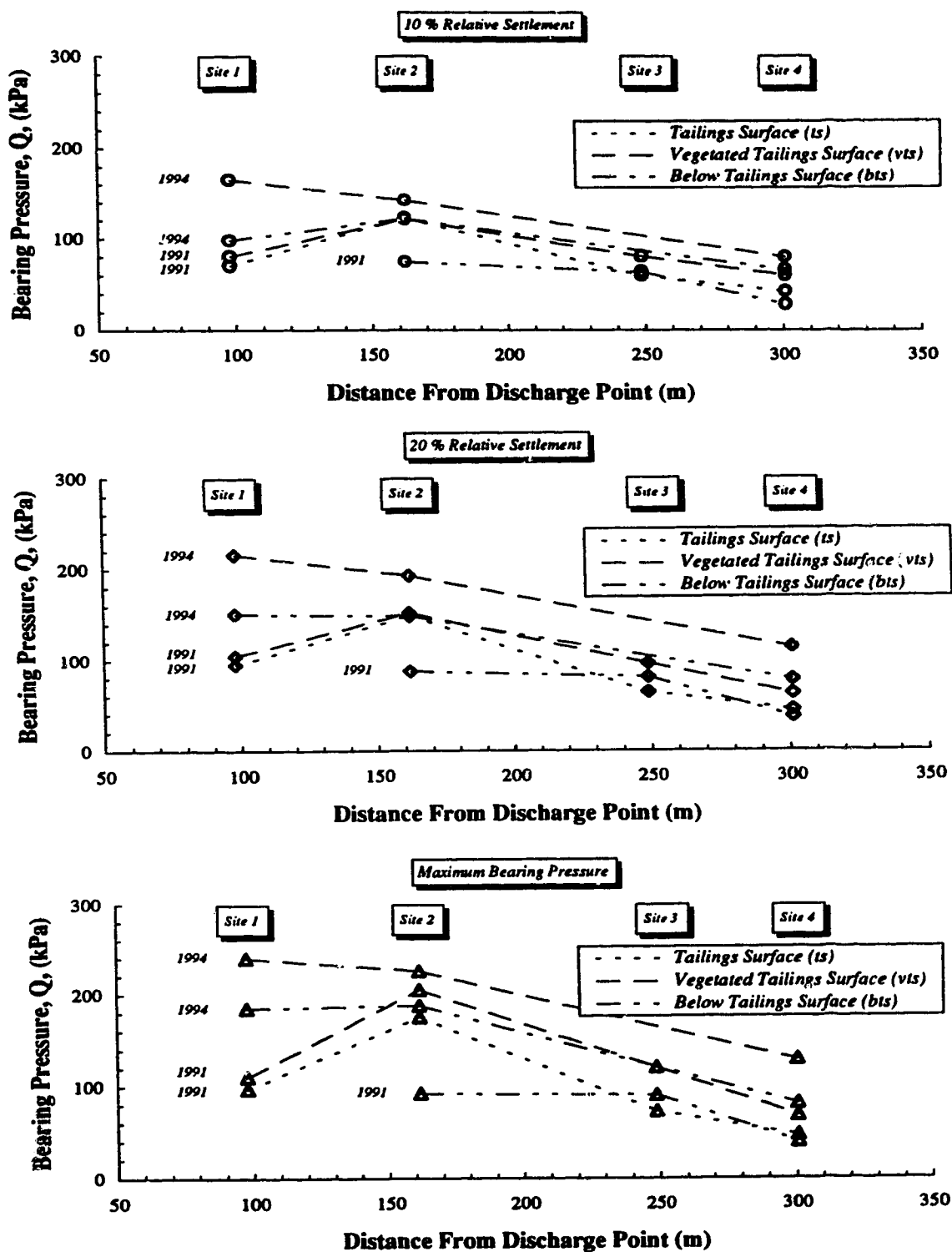


Figure B21 Summary of 1991 and 1994 Plate Load Test Results Along Coal Valley Tailings Beach - Sites 1 to 4

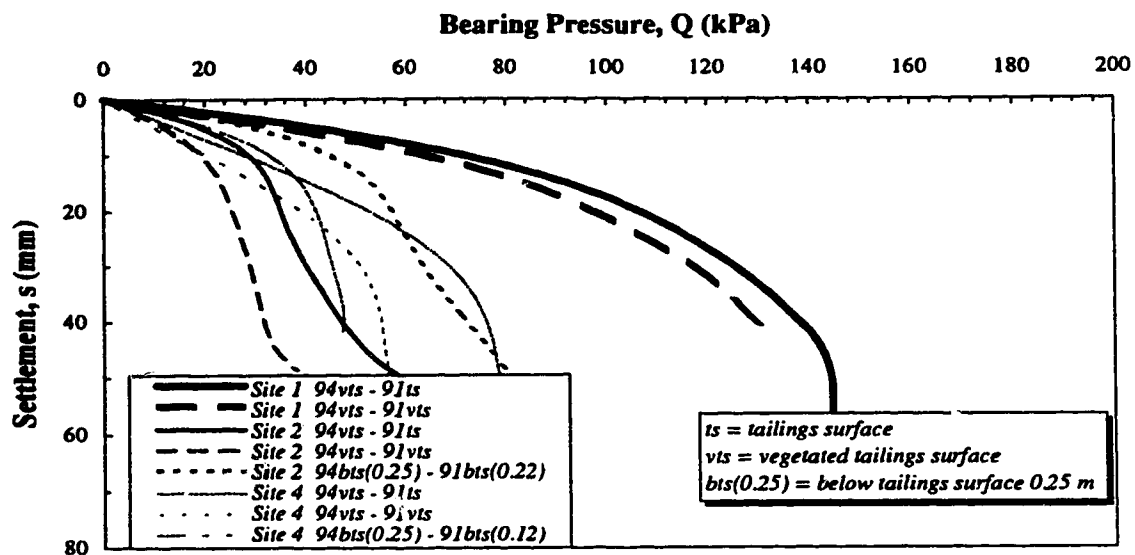


Figure B22 **Bearing Pressure Increase From 1991 to 1994 Along Coal Valley Tailings Beach**

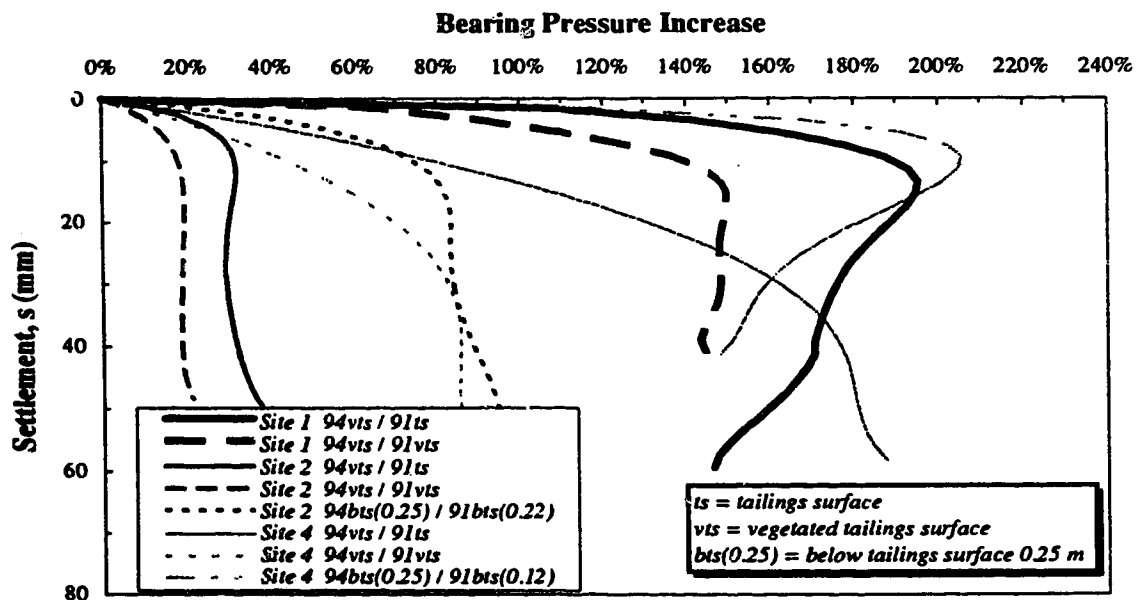


Figure B23 **Percent Bearing Pressure Increase From 1991 to 1994 Along Coal Valley Tailings Beach**

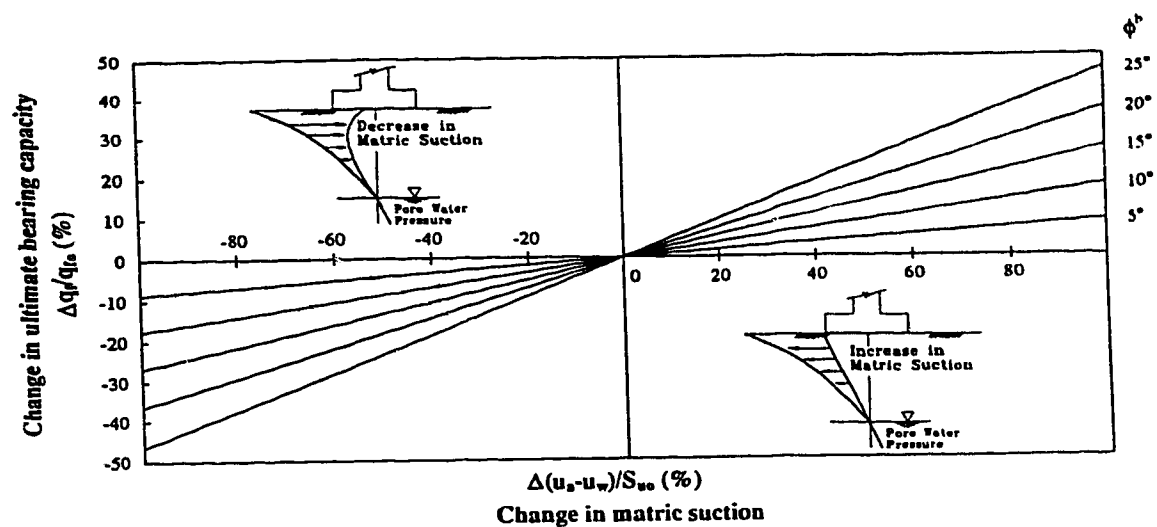


Figure B24 Variation in Ultimate Bearing Capacity with Variation in Matric Suction
(modified from Fredlund and Rahardjo, 1993)

Appendix C

Cone Penetration Tests At Coal Valley And Suncor NST Cells

C.1. BACKGROUND AND SOUNDING RESULTS

Cone Penetration Test (CPT) soundings were conducted at Sites 1 through 4 along the beach portion of the Coal Valley tailings impoundment in August, 1994. Soundings were also conducted within the Suncor NST Cells 3 and 4 in October, 1994. The locations of the soundings and a brief description of the CPT apparatus developed to investigate these weak deposits is briefly outlined in Chapter 4. The cone used for the investigations, provided by ConeTec Investigations Ltd. of Vancouver, B.C., was a standard "low capacity" 2.5 ton cone with a 10 cm² cone tip area, 150 cm² friction sleeve area, and pore pressure sensor located directly behind the cone tip. The cone was pushed into the ground at the standard rate of penetration of 2 cm/sec.

A variety of soil classification charts have been developed in the past to provide an indication of the soil behavior type (Robertson and Campanella 1983, Robertson *et al.* 1986, Robertson and Van Impe 1987). Perhaps the most recent and comprehensive technique which is employed by consultants and *insitu* contractors was presented by Robertson (1990, 1991). These latest soil behavior type charts were coded into a microcomputer spreadsheet program to interpret the CPT soundings obtained as part of this research.

The CPT soundings are summarized in this appendix in the following sequence. Each sounding includes 3 figures with the first figure detailing the direct CPT data, profiling versus depth the total cone bearing resistance, q_t , friction sleeve resistance, f_s , pore pressure during penetration, u , and friction ratio, R_f . The initial cone resistance, q_c , is corrected for unequal end areas to estimate q_t using (Robertson 1990):

$$q_t = q_c + (1 - a)u \quad [C1]$$

where a is the net area ratio, equal to approximately 0.85 for the cone used in these investigations. As defined in the first figure of the soundings, the friction ratio is defined as:

$$R_f = \frac{f_s}{q_t} \times 100\% \quad [C2]$$

The second figure of the soundings includes presentation of the normalized data on the soil classification charts outlined in Robertson (1990, 1991). The data was normalized using the following parameters:

$$\text{Normalized Cone Resistance} = Q_i = \frac{q_t - \sigma_{vo}}{\sigma_{vo}} \quad [C3]$$

$$\text{Normalized Friction Ratio} = F_R = \frac{f_s}{q_t - \sigma_{vo}} \times 100\% \quad [C4]$$

and

$$\text{Pore Pressure Ratio} = B_q = \frac{u - u_0}{q_t - \sigma_{vo}} \quad [C5]$$

These charts represent a three dimensional classification system which includes all the components of the CPT data. Details of the various regions within the charts is outlined by Robertson (1990) and the reader is encouraged to review this information. It is stressed that these charts are global in nature and should be used as a guide defining soil behavior type. A variety of factors including changes in stress history, *insitu* stresses, sensitivity, stiffness, macrofabric, and void ratio will influence the classification (Robertson 1990).

The third and final figure of each sounding includes profiling of the normalized data versus depth. This representation assisted the interpretation of the subsurface stratigraphy encountered within the CPT soundings.

The CPT soundings along the beach portion of the Coal Valley tailings impoundment, Sites 1 through 4, which include the three sets of figures at each site, are included in Figures C1 through C12.

The CPT soundings from the Suncor NST Cells 3 and 4 required considerably more interpretation and analysis than those at Coal Valley due to the lower *insitu* strength and stress conditions during the investigations. Although the NST material was deposited almost 1 year prior to the investigation period, excess pore pressures were still present. The *insitu* pore pressures, recorded using pneumatic piezometers installed along vertical posts within the cells (locations shown in Chapter 4), were recorded up to 5 months (May, 1994) prior to the October 1994 investigation period and are included in Scott and Caughill (1994). These pore pressure profiles indicated that very little effective stress had developed within the NST material. Furthermore, the pore pressures profiles indicated the seal at the post-liner interface was ineffective and localized bottom drainage was occurring. The range of estimated¹ pore pressures profiles determined from the May 1994 pore pressure readings at the posts are illustrated in the shaded regions in Figures C13 and C14. The shaded region within these figures illustrate the range of excess pore pressures within the NST Cells, as well as the elbow in pore pressure profiles supporting the concept of an ineffective seal and subsequent drainage at the post-liner interface.

¹ Pore pressure profiles determined 5 months prior to CPT investigation were reduced by about 10 % assuming single drainage and infinitesimal strain consolidation theory.

Since the CPT soundings were conducted several meters away from the posts (and their associated localized bottom drainage condition), these measured pore pressure profiles could not be used to accurately analyze the CPT soundings. Furthermore, insitu static pore water pressure profiles could not be constructed from the pore pressure dissipation tests due to insufficient test duration and incomplete dissipation. Consequently, a reverse approach of estimating the pore pressure profiles from the vane shear results was adopted. Linear relationships from the vane shear strength profiles (Appendix A) were established, and these profiles were merged with typical shear strength ratio relationships presented in the literature as considered in Chapter 3 and summarized in [C6].

$$\frac{S_u}{\sigma_v} = 0.2 \rightarrow 0.3 \{0.25 \text{ chosen}\} \quad [C6]$$

The shear strength is defined as S_u , and σ_v' is the vertical effective stress.

The results of the *insitu* pore pressure prediction within the Cells constructed from the vane shear strength profiles and [C6] are illustrated in Figure C13. These predicted pore pressure profiles are designated globally for future reference as PWP 1. These profiles are encouraging since they closely resemble the magnitude and slope of estimated profiles from the posts, and exclude the elbow associated with bottom drainage.

To complicate the pore pressure prediction within the NST Cells, Liu *et al.* (1994) highlight from laboratory tests that the shear strength ratio at a fines content greater than 20 % equals:

$$\frac{S_u}{\sigma_c} = 0.15 \quad [C7]$$

where σ_c' is the effective consolidation stress. This equation approximately converts to

$$\frac{S_u}{\sigma_v} = 0.14 \quad [C8]$$

The pore pressure profiles estimated using [C8] are designated as PWP 2 condition and are illustrated in Figure C14. These profiles are considerably less than those predicted in Figure C13 and are approaching or less than hydrostatic conditions. Due to the similarities and contrast in PWP 1 and PWP 2 with respect to the post profiles respectively, PWP 1 conditions were selected for subsequent analysis. Due to strategic and commitment changes, pore pressures have not (to the authors knowledge) been recorded within the NST cells since May, 1994. Although considerable time has elapsed, recording exiting pore pressures today would be very valuable and may possibly providing insight or confirmation on the estimated October, 1994 profiles. The author is currently investigating the possibility of "post" May 1994 readings to assist analysis.

The CPT soundings from the NST Cells 3 and 4, considering the pore pressure profiles in Figure C13 (PWP 1), are included in Figures C15 to C26. The CPT soundings have also been analyzed considering the PWP 2 conditions, however the detailed figures have not been included in this appendix. The impact of the reduced pore pressure condition of PWP 2, compared to PWP 1, is to reduce the computed normalized cone tip resistance, Q_c . Comparison of the charts indicates that this reduction in Q_c is minor and only accounts for small shifts in the soil behavior type classification. As illustrated in Appendix F, however, the *insitu* pore pressure influences the predicted shear strength correlation's determined from the CPT.

To summarize and extend the above pore pressure discussion, it is emphasized that correct interpretation of soil behavior type and estimation of mechanical properties requires a sufficient understanding of the *insitu* total vertical stresses and pore pressures. The importance of understanding the *insitu* pore pressures was critical, in particular, for evaluation of the CPT results within the Suncor NST Cells. Prediction of soil behavior type and geotechnical properties requires this understanding and appreciation.

C.2. INTERPRETATION OF SOIL BEHAVIOR TYPE

Grain size distribution curves of shallow subsurface samples obtained (to a maximum depth of about 0.6 m) at Sites 1 through 4 along the beach portion of the Coal Valley tailings impoundments are included in Chapter 2 and Appendix A. The grain size description at the four sites based on the detailed grain size distributions in Appendix A, and estimated from the limited grain size distribution data contained in Chapter 2 is summarized in Table C1. This table also includes the key soil behavior type classifications estimated from the CPT normalized soil behavior type contained within Figures C1 through C12.

Based on the CPT soil behavior type classifications, the following general points are presented:

- The Q_t vs F_r chart generally grouped more of the data points in the finer regions than the Q_t vs B_q chart. This is likely the result of the relatively high compressibility of the tailings which would likely effect both Q_t and F_r , but would likely provide less influence to B_q .
- The charts predict that the material behaves as (3) Clay - Clay to Silty Clay to a (5) Sand Mixture - Silty Sand to Sandy Silt. Some data, particularly the surficial, higher Q_t data is plotted in regions (6) Sands - Clean Sand to Silty Sand and (7) Gravelly Sand to Sand.
- The tailings are normally consolidated, and the charts acknowledge this by plotting much of the data within the "Normally Consolidated" region of the Q_t vs F_r chart.
- The high Q_t values obtained in the upper surficial material are generally represented on the Q_t vs F_r chart in region (6) in the area of increasing "OCR, Age or Cementation". This is encouraging since the surficial material has likely undergone consolidation through matric suction development sponsored through evaporation and evapotranspiration processes.
- Lastly, assuming that the stratigraphic range experienced in the samples is indicative of the material at depth, the global CPT classification charts satisfactorily predicted the range of soils encountered within the surficial material.

The grain size distribution plots from the NST Cells included in Appendix A were also compared to the soil behavior type classification (assuming PWP 1) as summarized in Table C2.

Table C2 clearly emphasizes the importance of recognizing the designation of "*Soil Behavior Type Classification*" in the Q_t , F_r , and B_q charts. Although the grain size distributions represent the NST material as a sand with a trace to some silt and clay, the behavior predicted from the

CPT soundings is much different. The charts generally predict the material to behave as a (3) clay to a (4) silt mixture to a (1) sensitive fine grained soil. As with the Coal Valley soil behavior classifications, a slight trend was noticed with the predictions based on comparison of the Q_t vs F_r , and Q_t vs B_q charts. The Q_t vs F_r charts represented the majority of the data within the (1) sensitive fine grained region, whereas the companion Q_t vs B_q charts represented the majority of the data within the (3) clay region. This trend is likely the result of the very low sleeve friction (and resulting F_r) values recorded during penetration which resulted in migration of the Q_t vs F_r data into the (1) sensitive fine grained region.

A valuable observation and lesson is gathered from this comparison. Armed solely with the grain size distribution of the NST material, one may over predict the geotechnical properties (strength, compressibility, hydraulic conductivity). Since soil behavior controls design and performance, the valuable information gathered from the CPT is paramount. The behavior predicted by the CPT is confirmed by the other *insitu* tests presented in Appendix A and B.

C.3. SOUNDING AND ANALYSIS COMMENTS

A variety of issues were faced during the investigation and interpretation of the CPT soundings conducted at these weak tailings facilities. One of the first issues deals with sensitivity. As discussed by Robertson *et al.* (1986), the cone tip load cell may be required to record loads less than 1% of rated capacity with an inaccuracy of up to 50 % of the measured value. For the 2.5 ton "low capacity" cone employed during the investigations, the 1 % \pm 50 % translates to a total cone tip resistance of 25 kPa \pm 13 kPa. Although this is negligible in stiff or dense soils, this sensitivity is significant in these investigations particularly in the NST Cells. Fortunately, the pore pressures generated during penetration in soft clays are very high and accurate and provide a valuable link in stratigraphic determination and estimation of geotechnical properties. For example, penetration pore pressures were utilized for shear strength estimation as discussed in Appendix F.

In addition to sensitivity, thermally induced baseline shifts in cone tip resistance, friction sleeve, and pore pressure required significant consideration in these soft tailings deposits. Although extreme care was exercised trying to maintain thermal stability with the cone between and during soundings, small temperature changes following soil penetration and intersection with the water table resulted in (relatively) significant baseline shifts. Baselines values were typically recorded prior to, during, and following completion of penetration, with the resulting shifts effectively factored into the CPT values. Many of these shifts and resulting corrections occurred at depths which included pore pressure dissipation tests (discussed below). Within the NST Cells, these corrections at depth reduced the tip resistance below the value of recorded penetration pore pressure. Since the tip resistance must at least equal the penetration pore pressure, the algorithm developed to analyze the data conditionally maintained the tip resistance at or above the recorded pore pressure. The conditional arguments resulted in equivallency between tip and pore pressure values beyond a depth of about 0.7 m and 1.5 m in Cells 3 and 4 respectively.

C.4. PORE PRESSURE DISSIPATION TESTS

The pore pressure information gathered during continual penetration of the cone is extremely valuable in determining soil stratigraphy, behavior type, and select mechanical properties. Monitoring of pore pressure following interruption of the penetration processes (Pore Pressure Dissipation *PPD* test) compliments the information gathered during steady penetration by assisting stratigraphic interpretation, and providing valuable information on hydraulic properties including permeability and coefficient of consolidation.

Pore pressure dissipation tests were conducted at Coal Valley and Suncor NST at various depths to determine horizontal coefficients of consolidation, c_h , and possibly gather additional information on the *insitu* pore water pressure conditions. The *PPD* process and a brief discussion of the theory and early formulations are provided in Robertson and Van Impe (1987).

The methodology employed to determine the horizontal coefficient of consolidation from pore pressure dissipation results is outlined in Teh and Houlsby (1991). Based on model simulations

using the Terzaghi-Rendulic uncoupled consolidation theory, Teh and Houlsby (1991) proposed the use of a modified time factor, T^* , for evaluation of PPD information. This factor is defined as:

$$T^* = \frac{c_h t}{a^2 \sqrt{I_r}} \quad [C9]$$

where c_h is the coefficient of consolidation in the horizontal direction, a is the cone radius, t is the time, and I_r is the rigidity index. The rigidity index is defined as the ratio of shear modulus to shear strength ($I_r = G/s_u$). Teh and Houlsby (1991) discuss that dissipation calculations conducted considering isotropic soils are generally similar and that if $c_h > c_v$, the consolidation behavior is dominated by c_h with c_v having negligible effect. The dissipation results considering the pore pressure sensor located behind the cone tip for rigidity indices ranging from 25 to 500 are illustrated in Figure C27.

For short dissipation records which do not establish the extended dissipation curve, Teh and Houlsby (1991) highlight an alternate method to determine c_h which incorporates the initial portion of the pore pressure dissipation record. When the pore pressure dissipation information is plotted against $\sqrt{T^*}$, the initial portion of the computed dissipation curves have been found linear. The gradients of these curves considering various pore pressure element locations along the cone are presented by Teh and Houlsby (1991). The slope of the initial portion of the $\Delta u/\Delta u_i$ versus $\sqrt{T^*}$ considering the pore pressure location behind the cone tip is defined as 1.15. The results which define the slope are valid for I_r in the range of 50 to 500.

Equation [C9] may subsequently be rewritten considering the initial slope portion of 1.15 as:

$$c_h = \left[1 - \frac{\Delta u}{\Delta u_i} \right]^2 \frac{a^2 \sqrt{I_r}}{(1.15)^2 t} \quad [C10]$$

This equation allows one to plot the pore pressure dissipation information versus \sqrt{t} to establish the early portion of the curve. Appropriate selections of $\Delta u/\Delta u_i$ and \sqrt{t} from this plot are inserted into [C10] to compute c_h .

Figure C28 illustrates two *PPD* records obtained at Coal Valley, and schematically outlines the methodology employed to obtain $\Delta u/\Delta u_i$ and \sqrt{t} . This figure is instructive since firstly it includes *PPD* information from one of the more permeable layers (Site 2) and less permeable layers (Site 4) which were encountered at Coal Valley. In addition, these plots illustrate that the pore pressure reaches a maximum some time after dissipation has proceeded. As discussed in Robertson and Van Impe (1987) and analytically observed by Teh and Houlsby (1991), the pore pressure behind the cone tip may initially increase following penetration interruption as a result of local pore pressure redistribution from the high pore pressure region at the tip.

The results of the pore pressure dissipation data from Coal Valley and Suncor NST are outlined in Tables C3 and C4. The c_h and t_{50} values estimated in Table C4 are based on the estimated pore pressure profiles (PWP 1) illustrated in Figure C13.

It is interesting to note that the estimated c_h values in Table C4 are very close and within the same order of magnitude, however, the extrapolated t_{50} 's indicate a slightly greater range. Utilizing [C10] and assuming the slope of the pore pressure dissipation curve is approximately constant up to t_{50} , the t_{50} values in Table C4 produce c_h values in the range of 1.0 E^{-3} to $3.6 \text{ E}^{-3} \text{ cm}^2/\text{s}$ with a higher value of $1.4 \text{ E}^{-2} \text{ cm}^2/\text{s}$ associated with the t_{50} of 4.9 minutes. These results are in general very similar to the c_h values reported in Table C4.

As outlined in [C9] and [C10], computation of c_h requires an estimate of the appropriate rigidity index. Since the theory does not prescribe the appropriate shear modulus, a average shear modulus, G_{50} was approximately chosen. A supporting comparison is provided by Luke (1995) who selected the E_{50} from the triaxial test to establish the rigidity index for determination of an appropriate N_{kt} factor. The N_{kt} factor fostered comparison of undrained strengths from field CPT results with anisotropic consolidated triaxial tests.

Estimation of G_{50} was obtained using the elastic solutions for the plate load tests outlined in Appendix B, and selecting the shear modulus associated with $Q/Q_{max} = 50\%$. Although the shortcomings of estimating G from these plate load test results were briefly discussed in Appendix B, the method provides a usable approximation. The shear strength, which is the denominator of the rigidity index relationship, was determined from vane shear results and correlation's with the CPT tip resistance and penetration pore pressure as discussed in Appendix F and Chapter 5. The computed rigidity indices for both Coal Valley and Suncor NST were about 50, and this value was used in [C10] to calculate the values in Tables C3 and C4. It is noted that computation of c_h using [C10] is relatively insensitive to the selection of I_r , increasing by only a factor of 3.2 from $I_r = 50 \rightarrow 500$. This is encouraging considering that c_h (and hydraulic conductivity) may vary by several orders of magnitude (Robertson and Van Impe 1987).

To compliment the horizontal coefficient of consolidation values determined from the *PPD* using the CPT, Table C5 includes a summary of the laboratory consolidation tests results conducted on Coal Valley coal tailings by Thurber Engineering (Thurber, 1992). It is observed firstly that the coefficients of consolidation are approximately within the same order of magnitude. Secondly, the c_h values in Table C3 range from 10^{-2} to 10^{-3} cm²/s, and the c_v values in Table C5 range from 10^{-3} to 10^{-4} cm²/s. Neglecting the dissimilar loading conditions, different materials tested, and theoretical assumptions and taking the numbers at face value, the data suggests possible material anisotropy with coefficients of consolidation and possibly hydraulic conductivities greater in the horizontal than vertical direction.

A comparison may also be conducted with the *PPD* results on NST material shown in Table C4. Figure C29 includes the results of the large strain consolidation results reported by Liu *et al.* (1994). Superimposed on this figure are the field results determined from the CPT pore pressure dissipation tests illustrated in Table C4. The shaded region represents the range of vertical effective stress and c_h values predicted *insitu*. Although difficult to draw hard conclusions without consideration of potential anisotropy, the results are encouraging and deserve further investigation.

C.5. REFERENCES

- Jefferies, M.G., and Davies, M.P., 1991. Soil Classification by the Cone Penetration Test: Discussion. *Canadian Geotechnical Journal* **28**:173-176.
- Liu, Y., Caughill, D., Scott, J.D., and Burns, R., 1994. Consolidation of Suncor Non Segregating Tailings. 47th Canadian Geotechnical Conference, September 21-23, 1994. Halifax, Nova Scotia, pgs 504-513.
- Luke, K., 1995. The use of c_u from the Danish Triaxial Tests to Calculate the Cone Factor. Proceedings of the International Symposium on Cone Penetration Testing, "CPT'95", Linköping, Sweden, October 4-5, pgs 209-214.
- Robertson, P.K., 1990. Soil Classification Using the Cone Penetration Test. *Canadian Geotechnical Journal* **27**:151-158.
- Robertson, P.K., 1991. Soil Classification Using the Cone Penetration Test: Reply. *Canadian Geotechnical Journal* **28**:176-178.
- Robertson, P.K., and Campanella, R.G., 1983a. Interpretation of Cone Penetration Tests. Part I: Sand. *Canadian Geotechnical Journal* **20**:718-733.
- Robertson, P.K., and Campanella, R.G., 1983b. Interpretation of Cone Penetration Tests. Part II: Clay. *Canadian Geotechnical Journal* **20**:734-745.
- Robertson, P.K., and Van Impe, W.F., 1987. Cone Penetration With Pore Pressure Measurement. Belgisch Comité voor Ingenieursgeologie, B.C.I.G., Belgium, Dec. 1987, 60 pgs.
- Robertson, P.K., Campanella, D., Gillespie, D., and Greig, J., 1986. Proceedings of the ASCE Specialty Conference "IN-SITU 86", Use of In-situ Testing in Geotechnical Engineering, June, pgs 1263-1280.
- Robertson, P.R., Sully, J.P., Woeller, D.J., Lunne, T., Powell, J.J.M., and Gillespie, D.G., 1992. Estimating Coefficient of Consolidation from Piezocone Tests. *Canadian Geotechnical Journal* **29**:539-550.
- Scott, J.D., and Caughill, D.L., 1994. Suncor Nonsegregating Tailings Summer 1993 Field Experiment - Geotechnical Analysis Report for the Tank and Cell Filling Program. Presented to Suncor Inc., Oil Sands Group.
- Teh, C.I., and Houlsby, G.T., 1991. An Analytical Study of the Cone Penetration Test in Clay. *Geotechnique*, **41**(1):17-34.
- Thurber Engineering Ltd., 1992. Coal Valley Mine Site Tailings Reclamation Research Project Geotechnical Report. Submitted to Luscar Sterco (1977) Ltd. 80 pgs.

Table C1 Comparison of Soil Description and Soil Behavior Type at Coal Valley

Site	Grain Sizes - <i>Appendix A</i>	Grain Sizes - <i>Chapter 2</i>	CPT Soil Behavior Type Classification
1	Sand, silty with some clay → Sand, silty, clayey	Sand, some silt → Silt, sandy, clayey	(Qt vs Fr): Generally (3) Clays → (4) Silt Mixtures, <i>some (5) Sand Mixtures & (6) Sands</i> (Qt vs Bq): Generally (3) Clays → (5) Sand Mixtures → (4) Silt Mixtures, <i>some (6) Sands & (7) Gravelly Sand to Sand</i>
2	Sand, some silt, trace clay → Sand and Silt, clayey	Sand, silty, trace clay → Silt and Sand, some clay	(Qt vs Fr): Generally (4) Silt Mixtures → (5) Sand Mixtures, <i>some (6) Sands</i> (Qt vs Bq): Generally (4) Silt Mixtures → (5) Sand Mixtures, <i>some (6) Sands & (7) Gravelly Sand to Sand</i>
3	Silt, sandy, clayey → Silt and Clay, sandy	Sand, some silt, trace clay → Silt, sandy	(Qt vs Fr): Generally (4) Silt Mixtures → (5) Sand Mixtures, <i>some (3) Clays & (6) Sands</i> (Qt vs Bq): Generally (4) Silt Mixtures → (5) Sand Mixtures, <i>some (3) Clays & (6) Sands & (7) Gravelly Sand to Sand</i>
4	Sand, silty, clayey → Silt, sandy, clayey	Sand, silty, trace clay → Silt and Clay, sandy	(Qt vs Fr): Generally (3) Clays → (4) Silt Mixtures → (5) Sand Mixtures, <i>some (6) Sands</i> (Qt vs Bq): Generally (3) Clays → (4) Silt Mixtures → (5) Sand Mixtures <i>some (6) Sands & (7) Gravelly Sand to Sand</i>

Table C2 Comparison of Soil Description and Soil Behavior Type at Suncor NST

NST Cell	Grain Sizes - <i>Appendix A</i>	CPT Soil Behavior Type Classification
3	Sand, some silt and clay → Sand, some silt, trace clay	<u>3A</u> (Qt vs Fr): Generally (1) Sensitive, Fine Grained → (4) Silt Mixtures, <i>some (3) Clays, (5) Sand Mixtures, and (6) Sands</i> (Qt vs Bq): Generally (3) Clays <i>some (1) Sensitive, Fine Grained, (4) Silt Mixtures, (5) Sand Mixtures & (6) Sands</i> <u>3B</u> (Qt vs Fr): Generally (3) Clays (Qt vs Bq): Generally (3) Clays → (4) Silt Mixtures <i>some (5) Sand Mixtures & (6) Sands</i>
4	Sand, trace silt and clay → Sand, some silt and clay	<u>4A</u> (Qt vs Fr): Generally (1) Sensitive, Fine Grained → (5) Sand Mixtures, <i>some (3) Clays & (4) Silt Mixtures</i> (Qt vs Bq): Generally (3) Clays, <i>some (1) Sensitive, Fine Grained, (4) Silt Mixtures, & (5) Sand Mixtures</i> <u>4B</u> (Qt vs Fr): Generally (3) Clays, <i>some (1) Sensitive, Fine Grained, (2) Organic Soils, (4) Silt Mixtures, & (5) Sand Mixtures</i> (Qt vs Bq): Generally (3) Clays, <i>some (1) Sensitive, Fine Grained, (2) Organic Soils, (4) Silt Mixtures, & (5) Sand Mixtures</i>

Table C3 Summary of Pore Pressure Dissipation Test Results at Coal Valley

SITE	DEPTH (m)	Estimated t_{50} ¹ (min)	Estimated c_h ² (cm²/s)
1	2.6	17.0	4.2 E-3
1	3.6	0.9	7.8 E-2
1	4.7	35.3	2.0 E-3
2	0.6	1.1	6.4 E-2
2	1.6	8.1	8.7 E-3
2	2.6	2.0	3.5 E-2
2	3.6	10.4	6.8 E-3
2	4.6	12.2	5.8 E-3
2	5.6	22.8	3.1 E-3
2	5.7	24.0	2.9 E-3
4	3.8	17.1	4.1 E-3
4	5.8	26.7	2.6 E-3

(1) t_{50} = time for 50% dissipation in excess pore pressure(2) c_h = horizontal coefficient of consolidation**Table C4 Summary of Pore Pressure Dissipation Test Results at Suncor NST**

SITE	DEPTH (m)	Estimated t_{50} ¹ (min)	Estimated c_h ² (cm²/s)
NST 3A	2.3	19.5	4.5 E-3
NST 3B	2.7	25.6	4.1 E-3
NST 4A	2.5	68.3	2.6 E-3
NST 4B	2.6	4.9	8.7 E-3

(1) t_{50} = time for 50% dissipation in excess pore pressure, extrapolated from PPD curve(2) c_h = horizontal coefficient of consolidation, estimated from initial slope of PPD curveNote: Both t_{50} and c_h subject to estimation of initial u_o

Table C5 **Summary of Laboratory Consolidation Data Conducted By Thurber (1992)**

<i>Site</i>	<i>Sample</i>	<i>Depth (m)</i>	<i>Description</i>	<i>c_v (cm²/s) ¹</i>	<i>m_v (cm²/g) ²</i>	<i>k_v (cm/s) ³</i>
TH90-1	SA#1	0.8-1.1	"coarse"	4.3 E-3	5.6 E-5	2.4 E-7
TH90-1	SA#4	2.3-2.6	"coarse"	3.9 E-3	5.3 E-5	2.1 E-7
TH90-4	SA#1	0.6-1.0	"fine"	4.2 E-4	8.6 E-5	3.6 E-8
TH90-4	SA#3	2.6-2.9	"fine"	8.6 E-4	7.1 E-5	6.1 E-8
TH89-4	SA#2	1.5-2.2	"fine"	2.1 E-3	5.9 E-5	1.2 E-7

(1) *c_v* = vertical coefficient of consolidation

(2) *m_v* = vertical coefficient of volume change

(3) *k_v* = vertical hydraulic conductivity

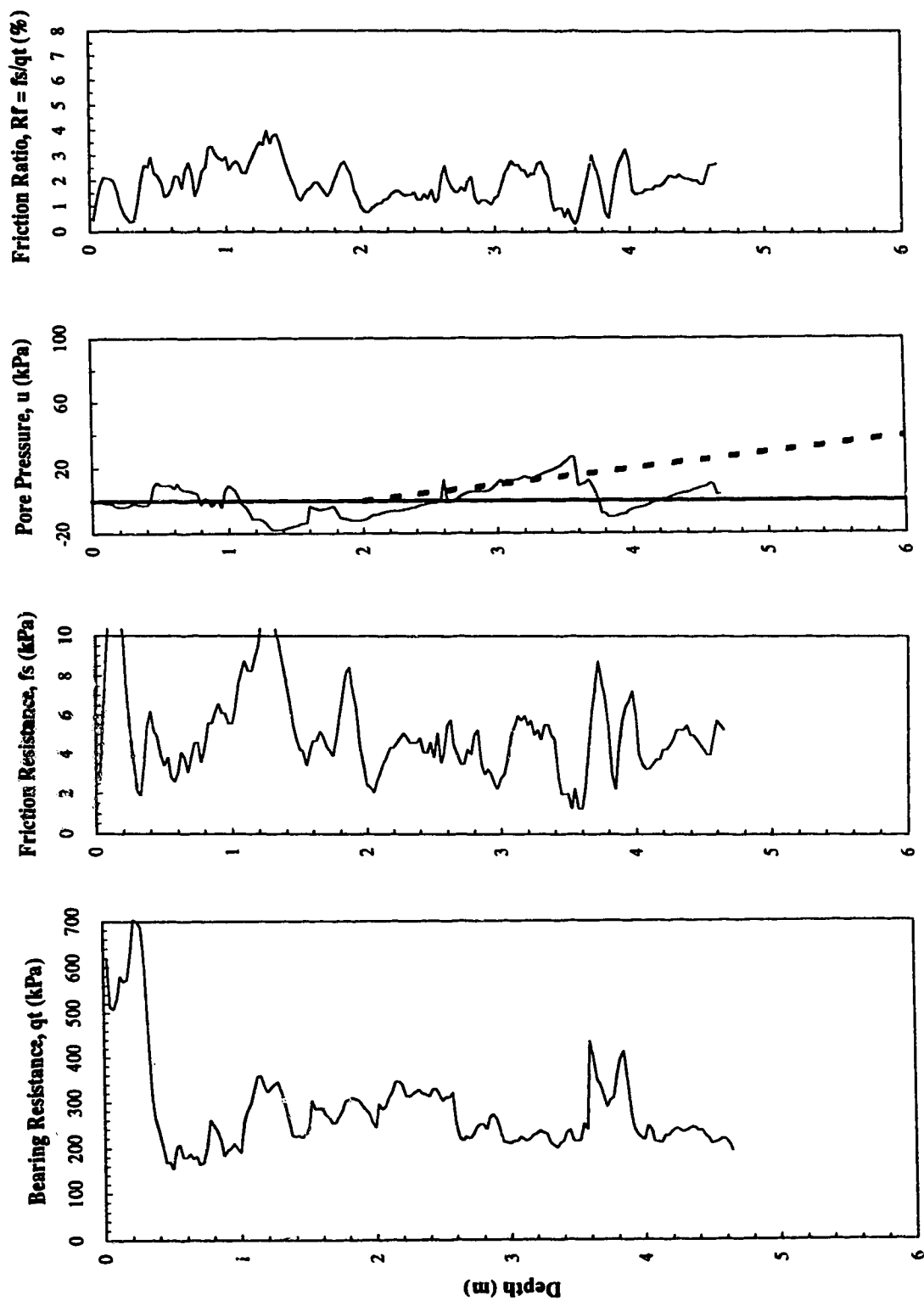
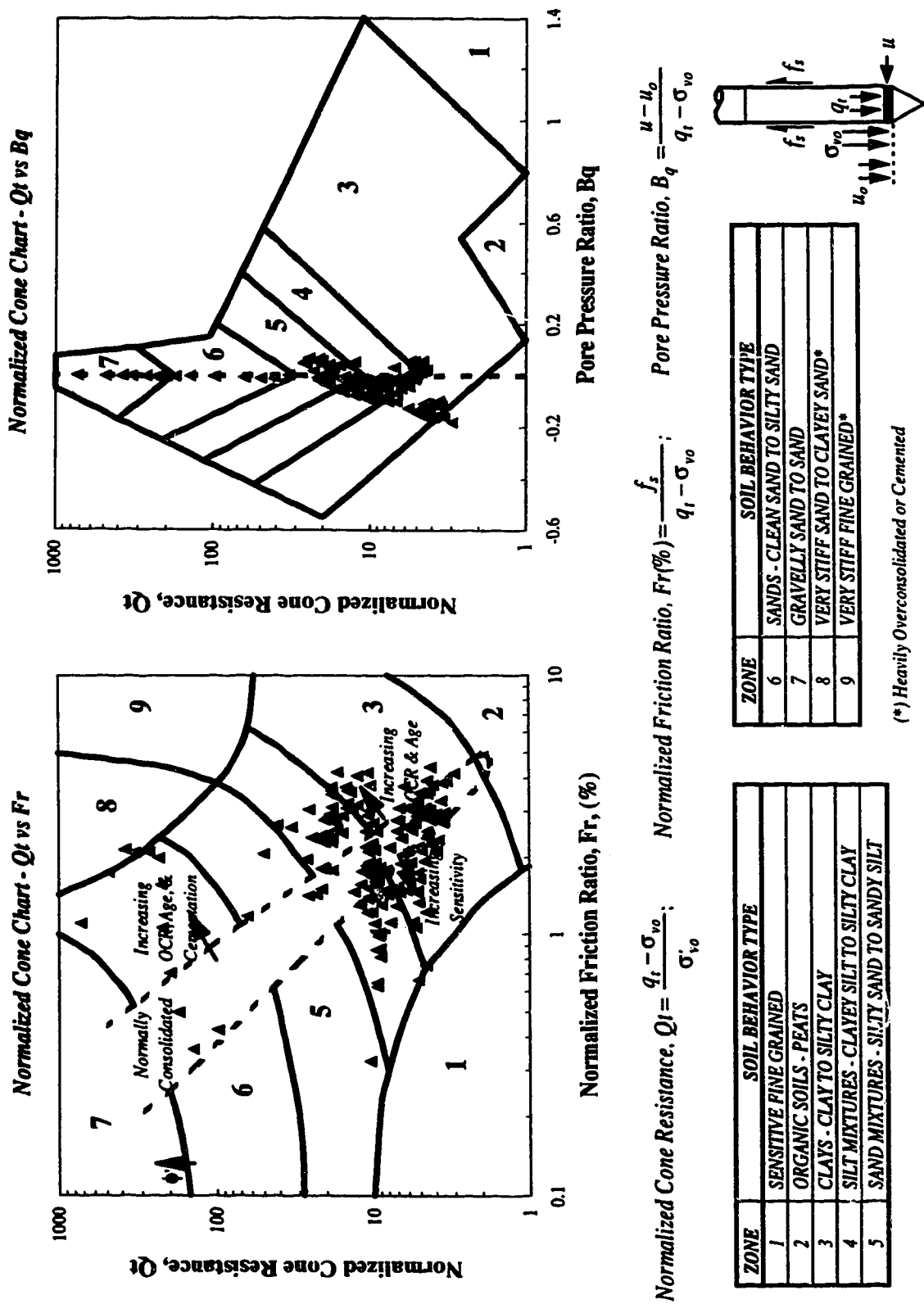


Figure C1 CPT Profiles - Coal Valley Tailings Beach - Site 1



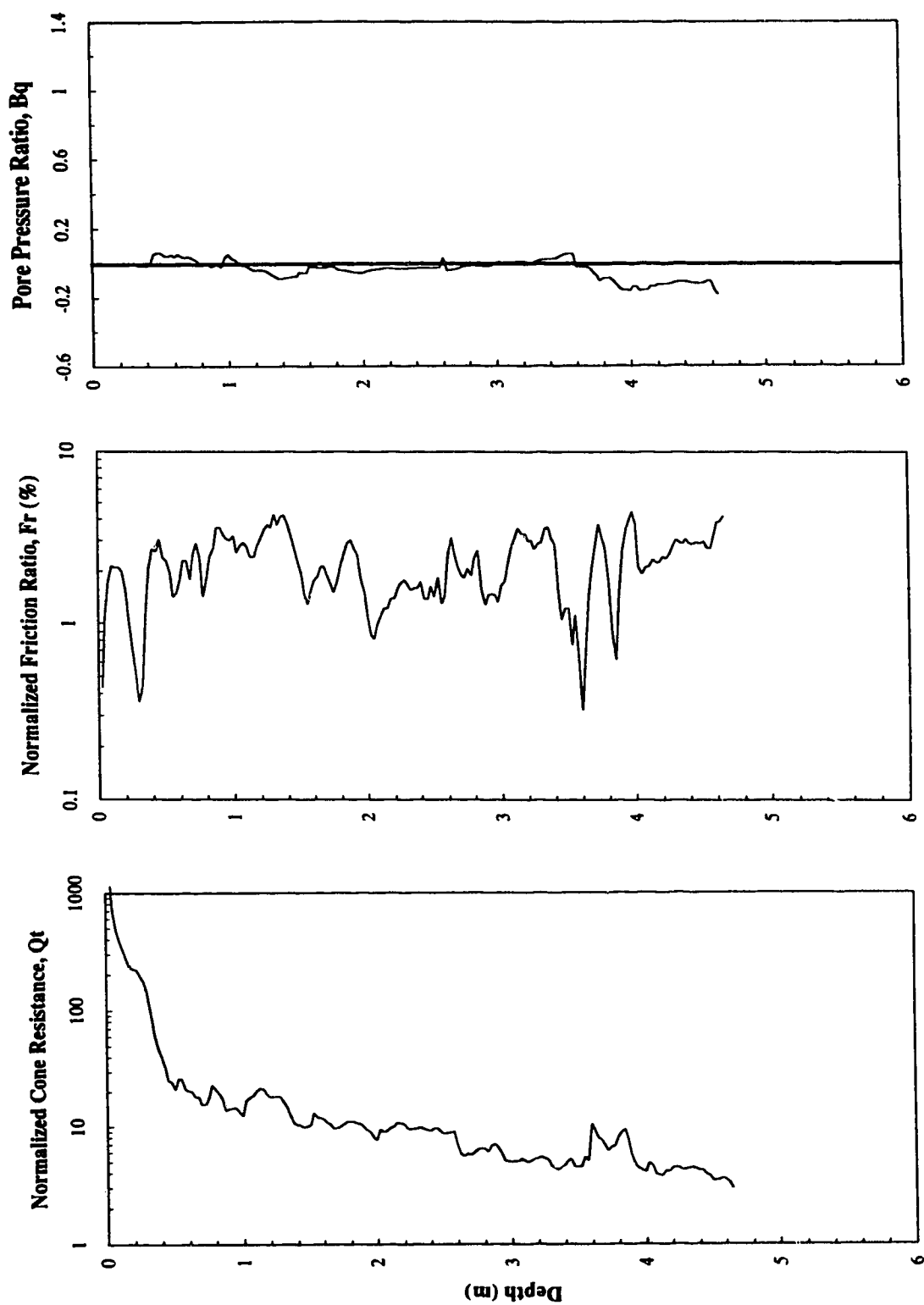


Figure C3 Normalized CPT Data Profiles - Coal Valley Tailings Beach - Site 1

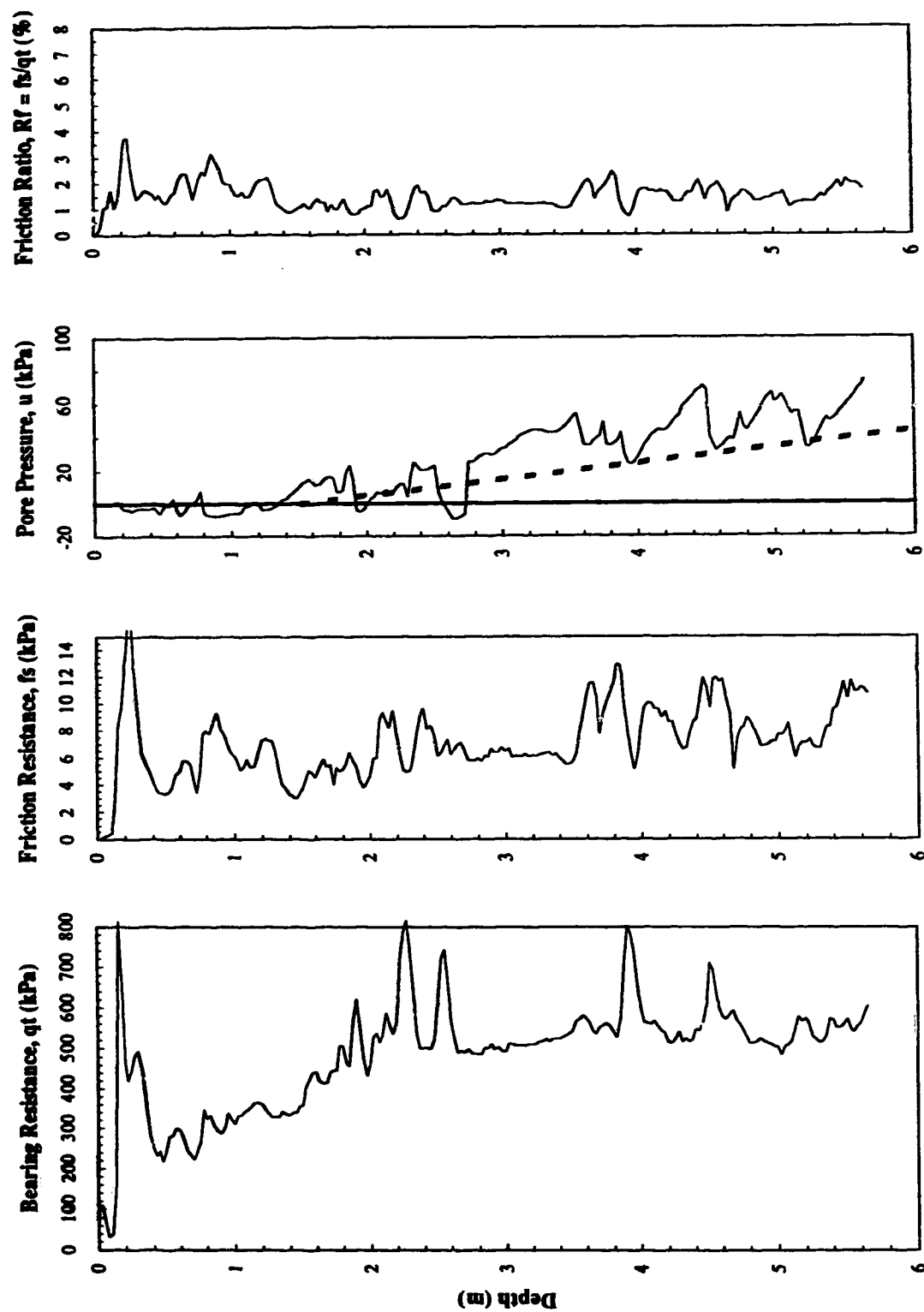


Figure C4 CPT Profiles - Coal Valley Tailings Beach - Site 2

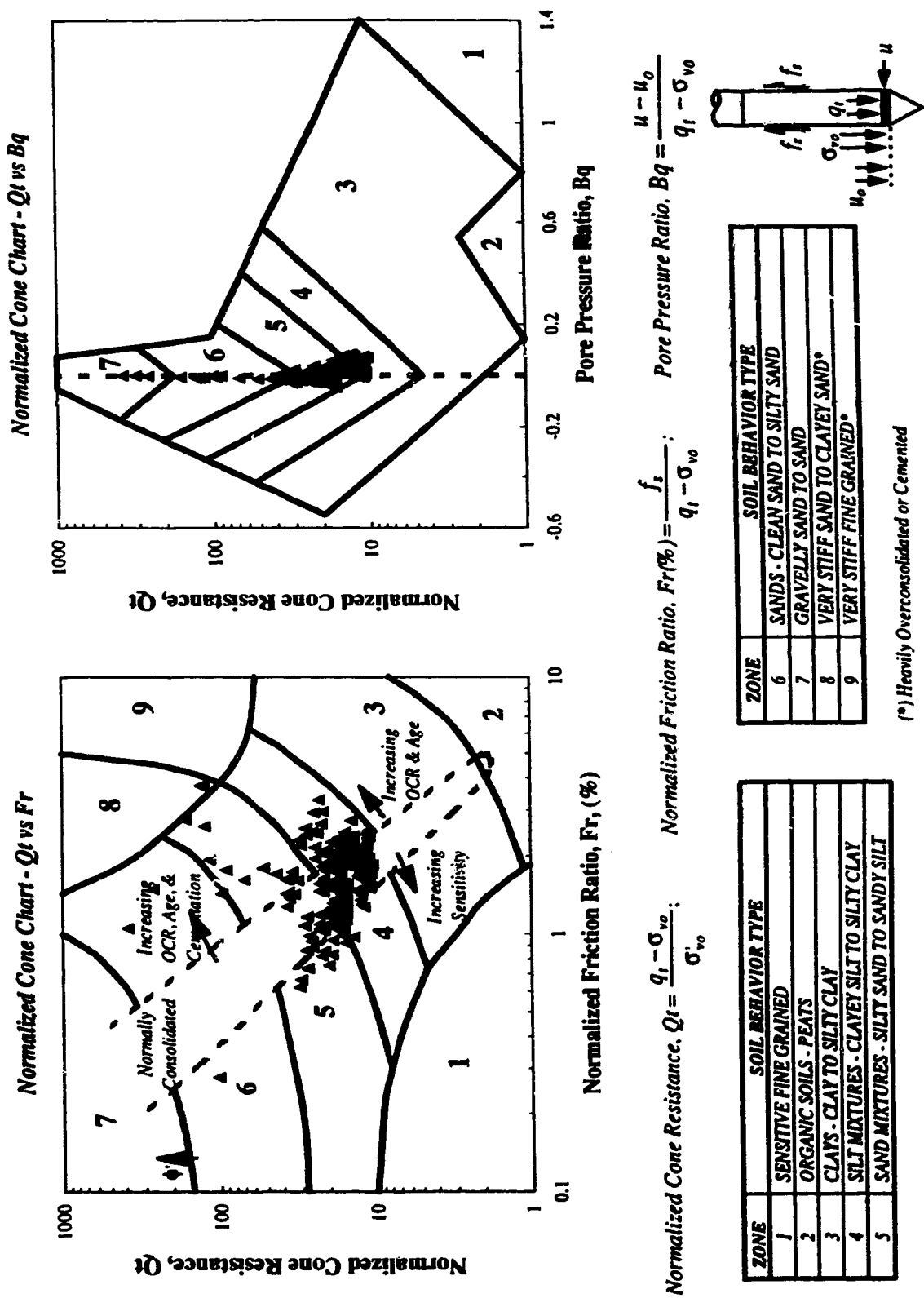


Figure C5 Normalized CPT Data Presented on Soil Behavior Type Charts - Coal Valley Tailings Beach - Site 2

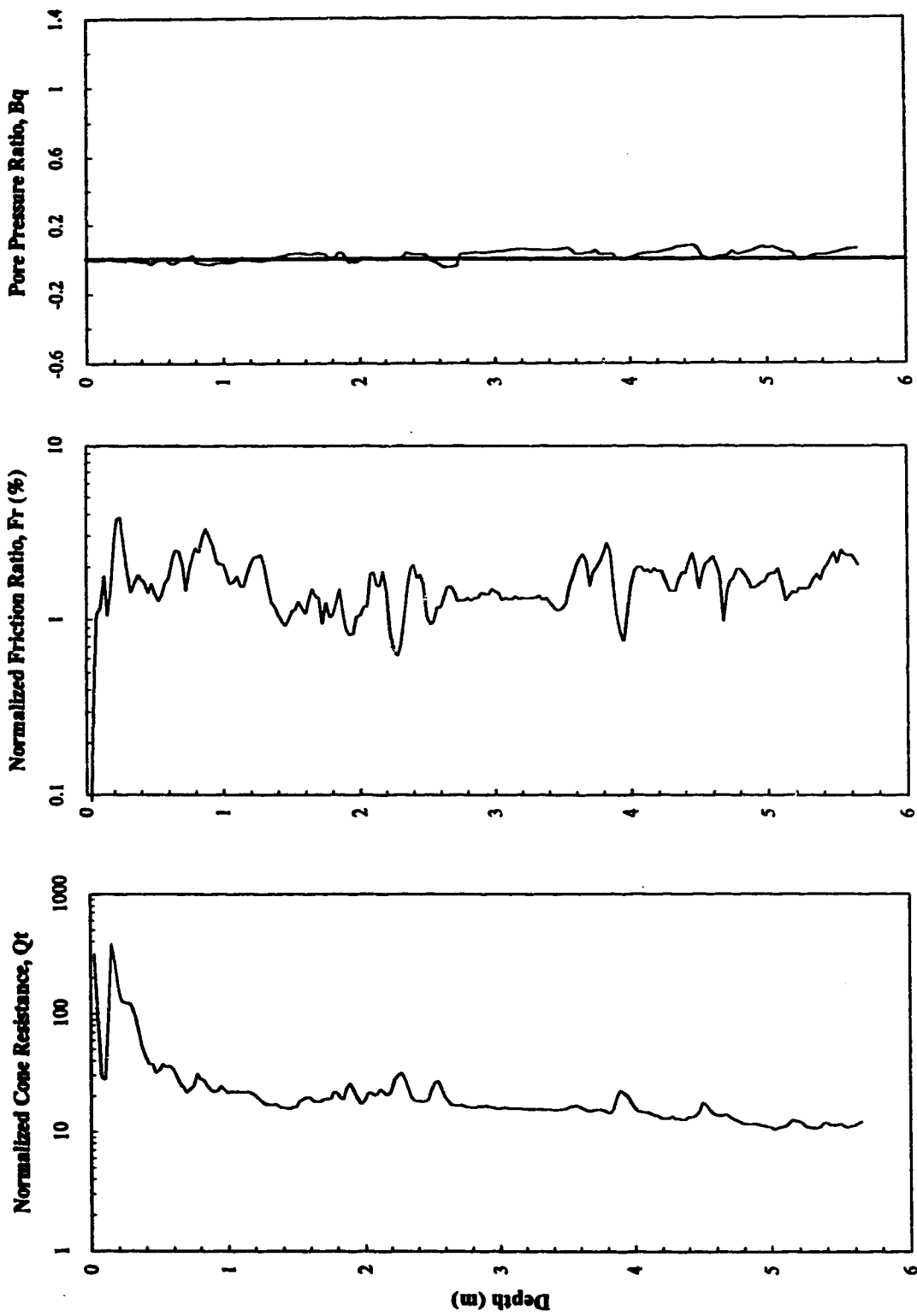


Figure C6 Normalized CPT Data Profiles - Coal Valley Tailings Beach - Site 2

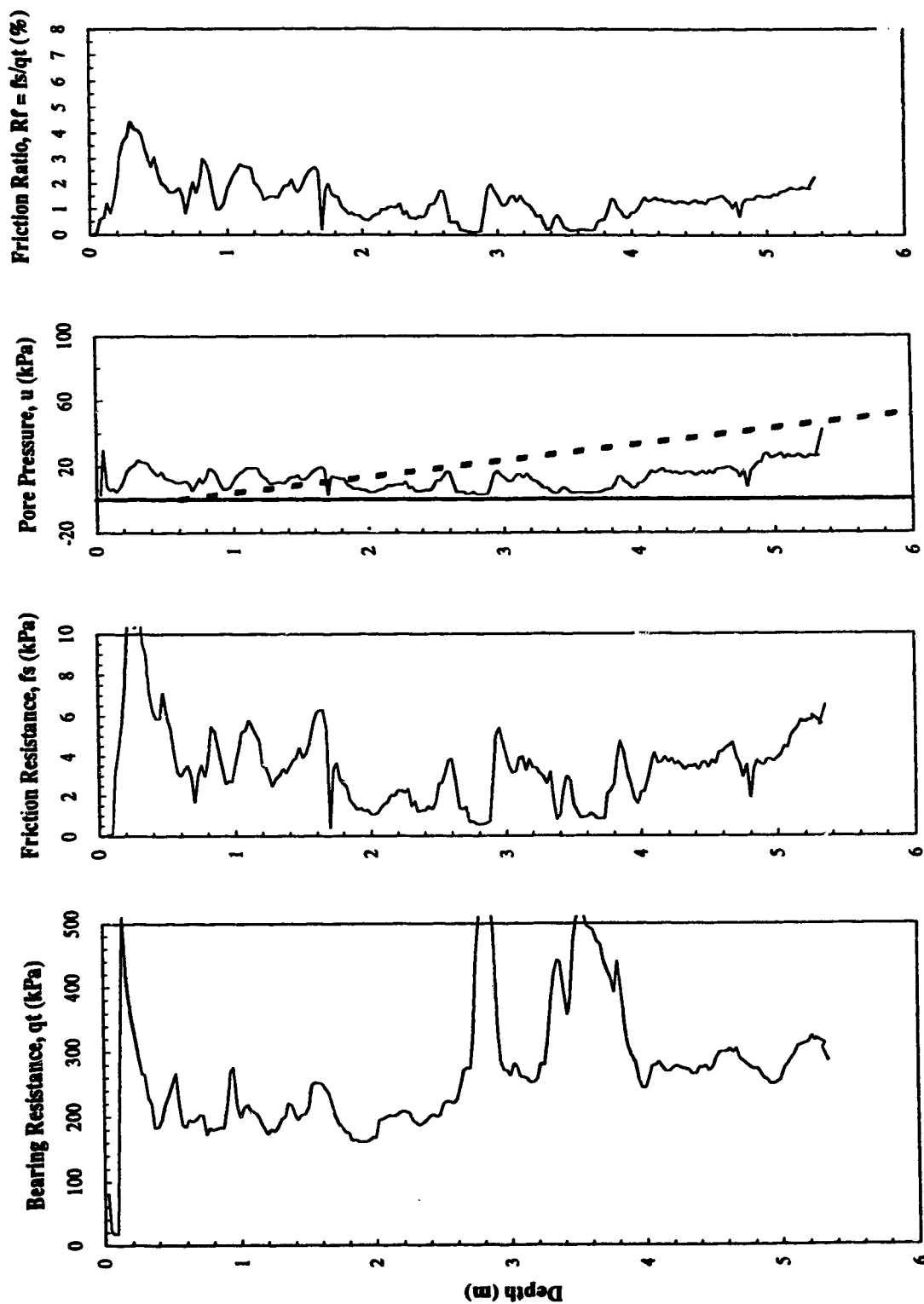


Figure C7 CPT Profiles - Coal Valley Tailings Beach - Site 3

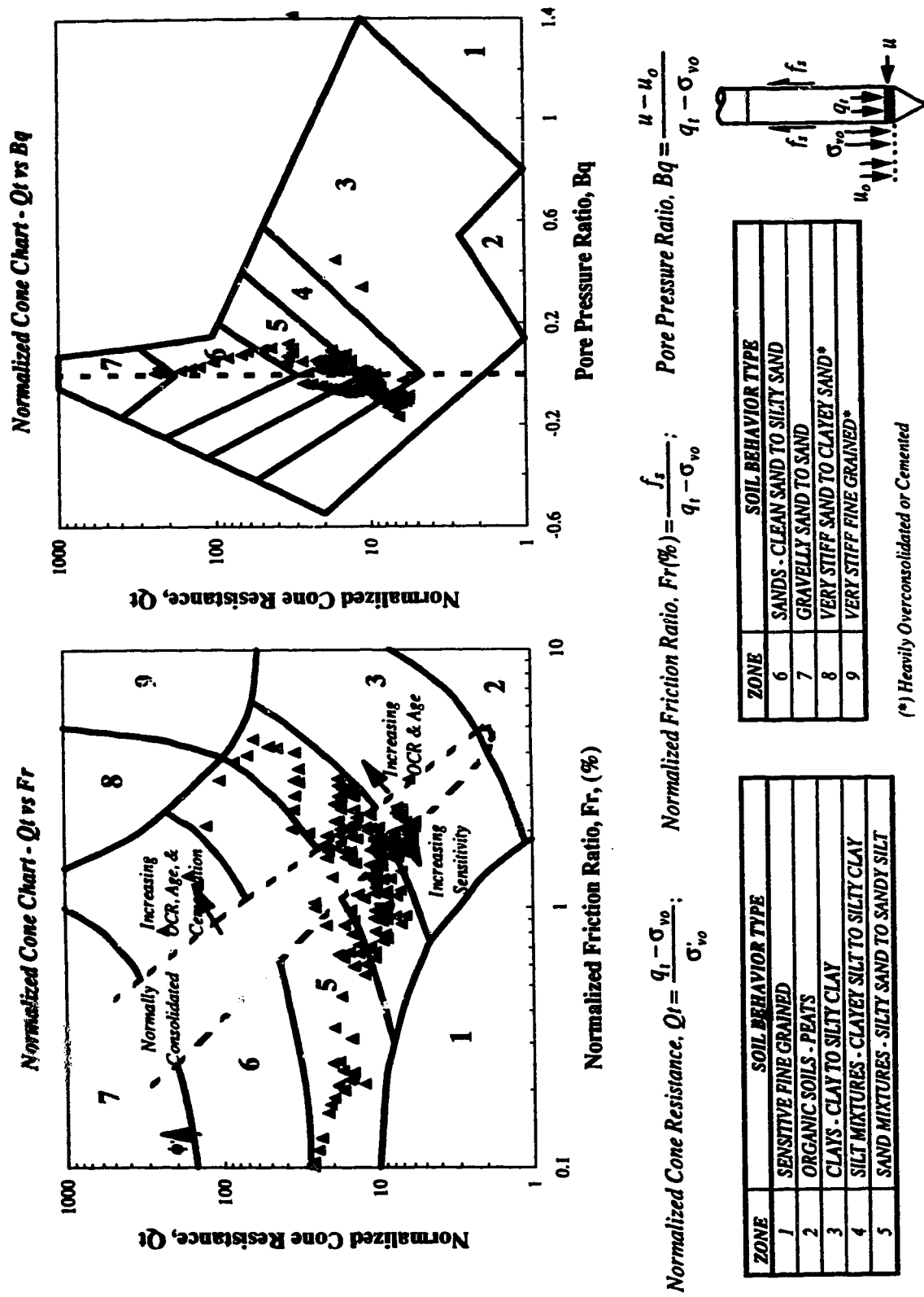


Figure C8 Normalized CPT Data Presented on Soil Behavior Type Charts - Coal Valley Tailings Beach - Site 3

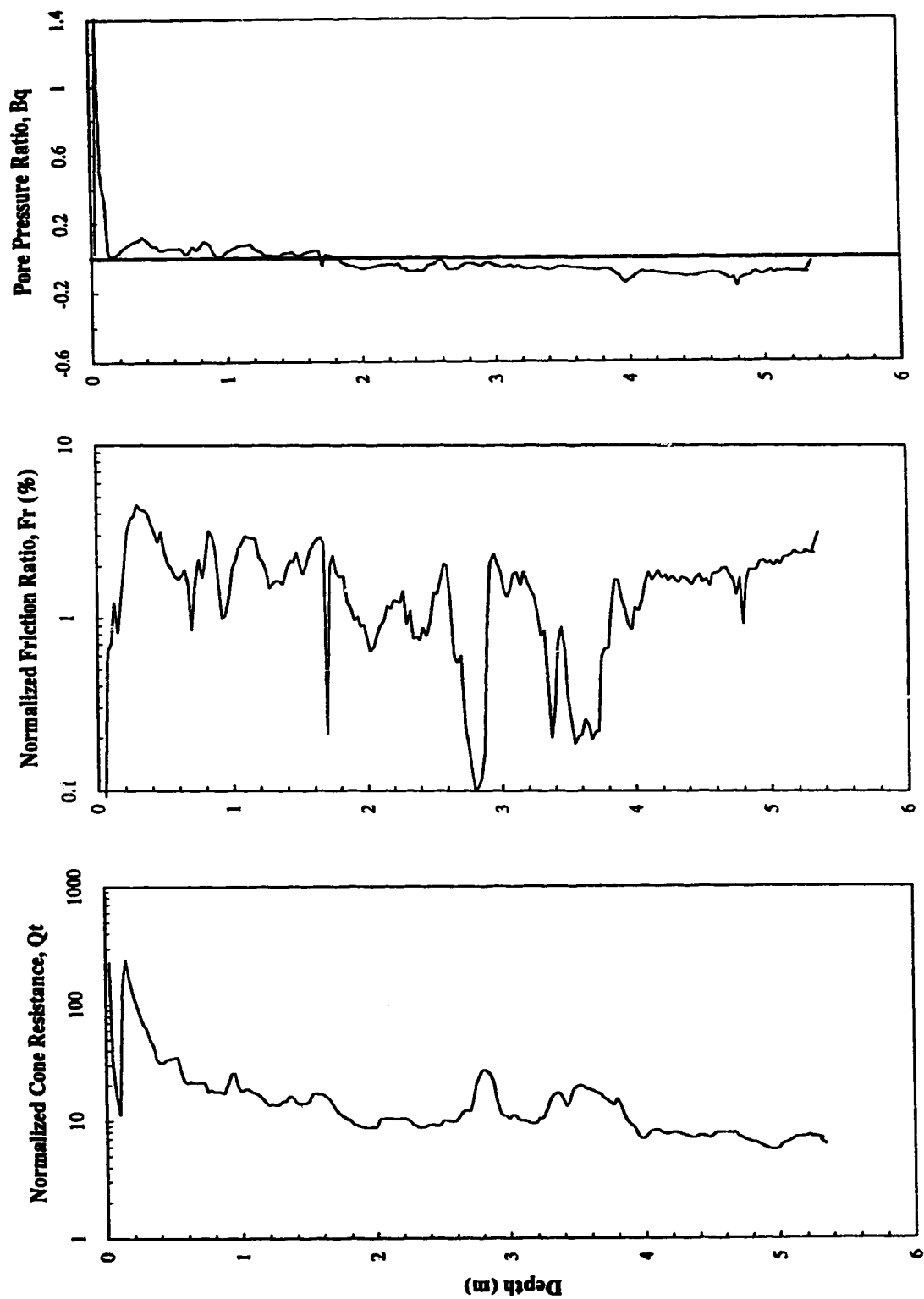


Figure C9 Normalized CPT Data Profiles - Coal Valley Tailings Beach - Site 3

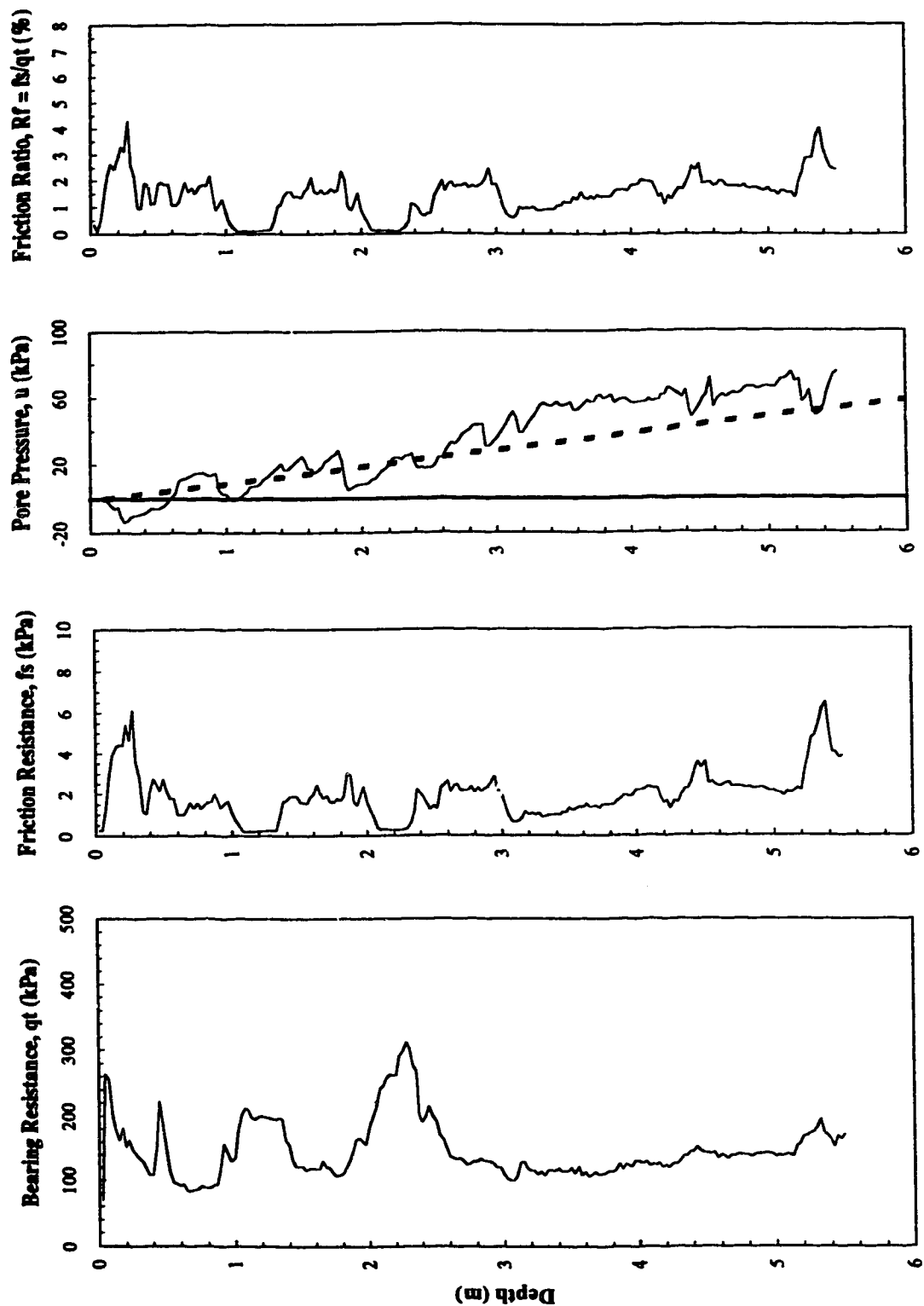


Figure C10 CPT Profiles - Coal Valley Tailings Beach - Site 4

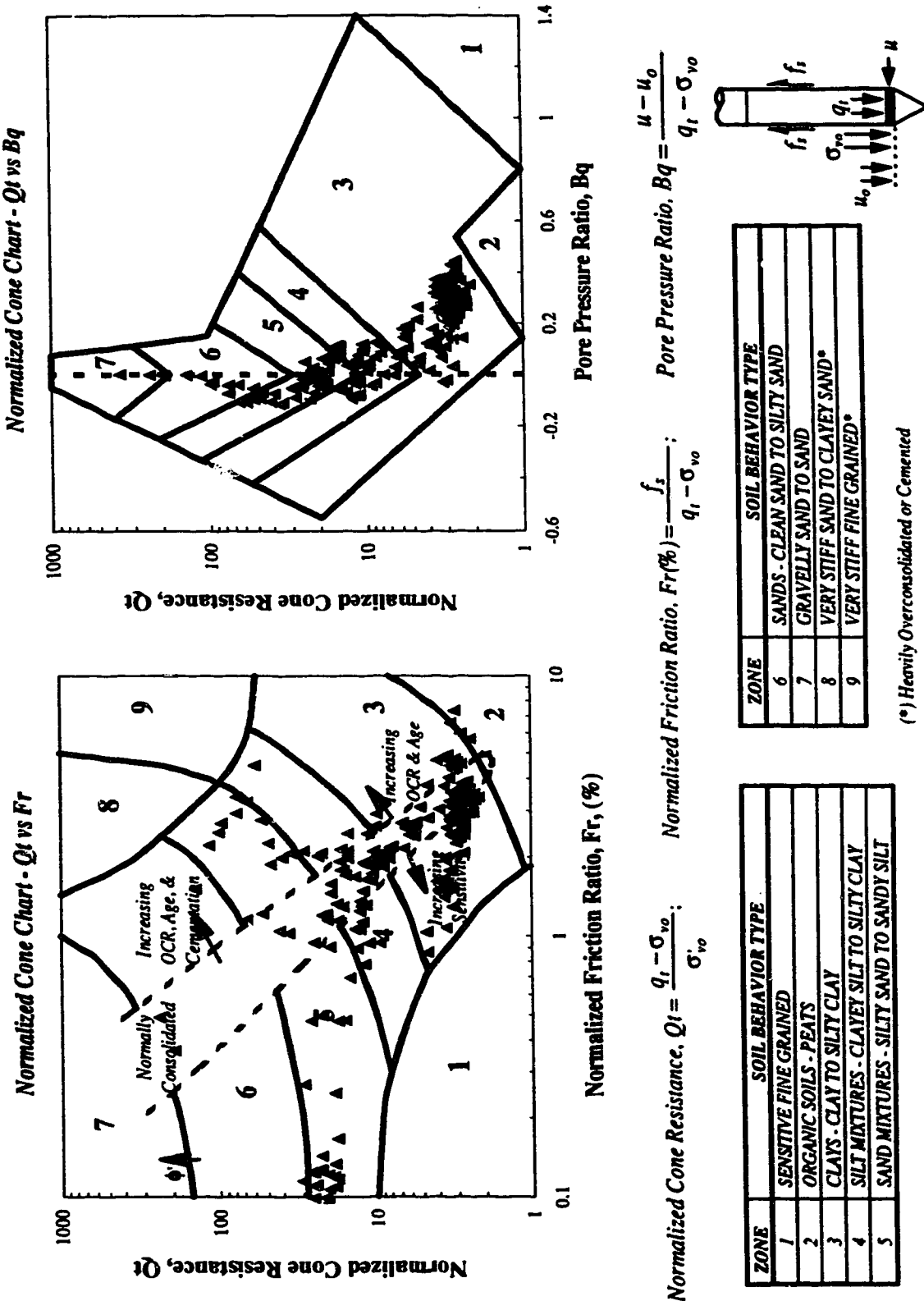


Figure C11 Normalized CPT Data Presented on Soil Behavior Type Charts - Coal Valley Tailings Beach - Site 4

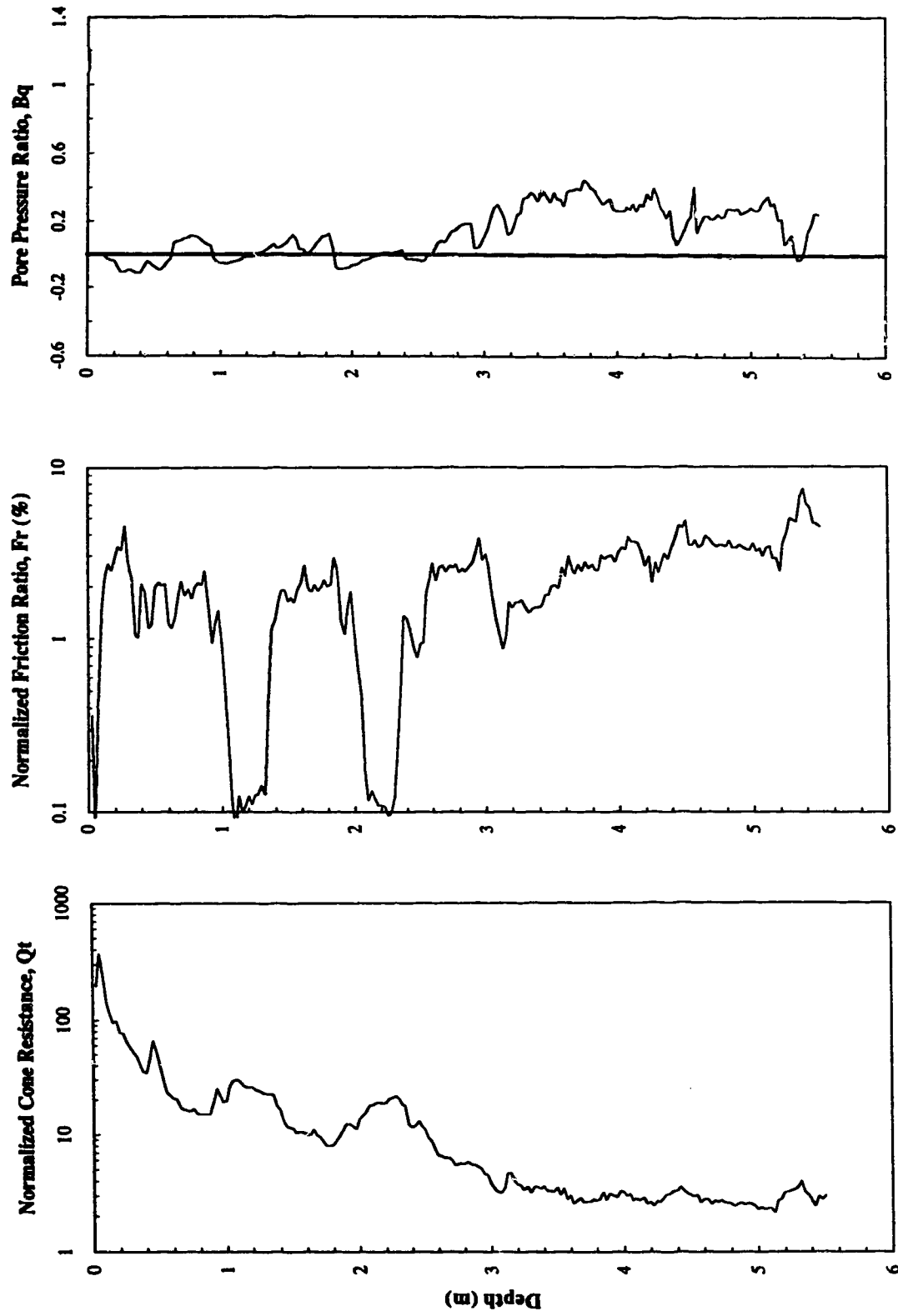


Figure C12 Normalized CPT Data Profiles - Coal Valley Tailings Beach - Site 4

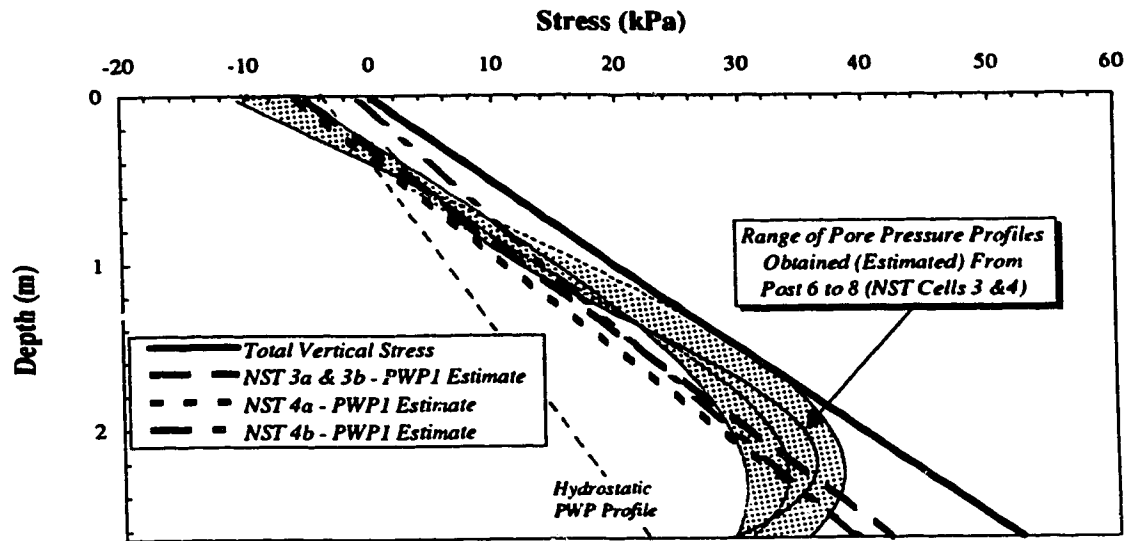


Figure C13 Estimated PWP (PWP 1) Profiles in Suncor NST Cells 3 and 4

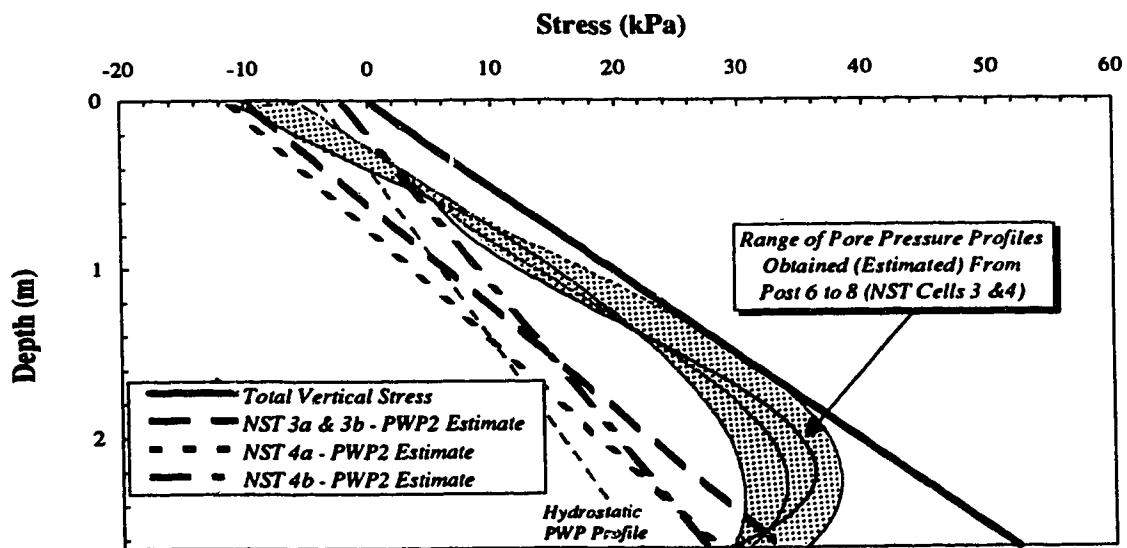


Figure C14 Estimated PWP (PWP 2) Profiles in Suncor NST Cells 3 and 4

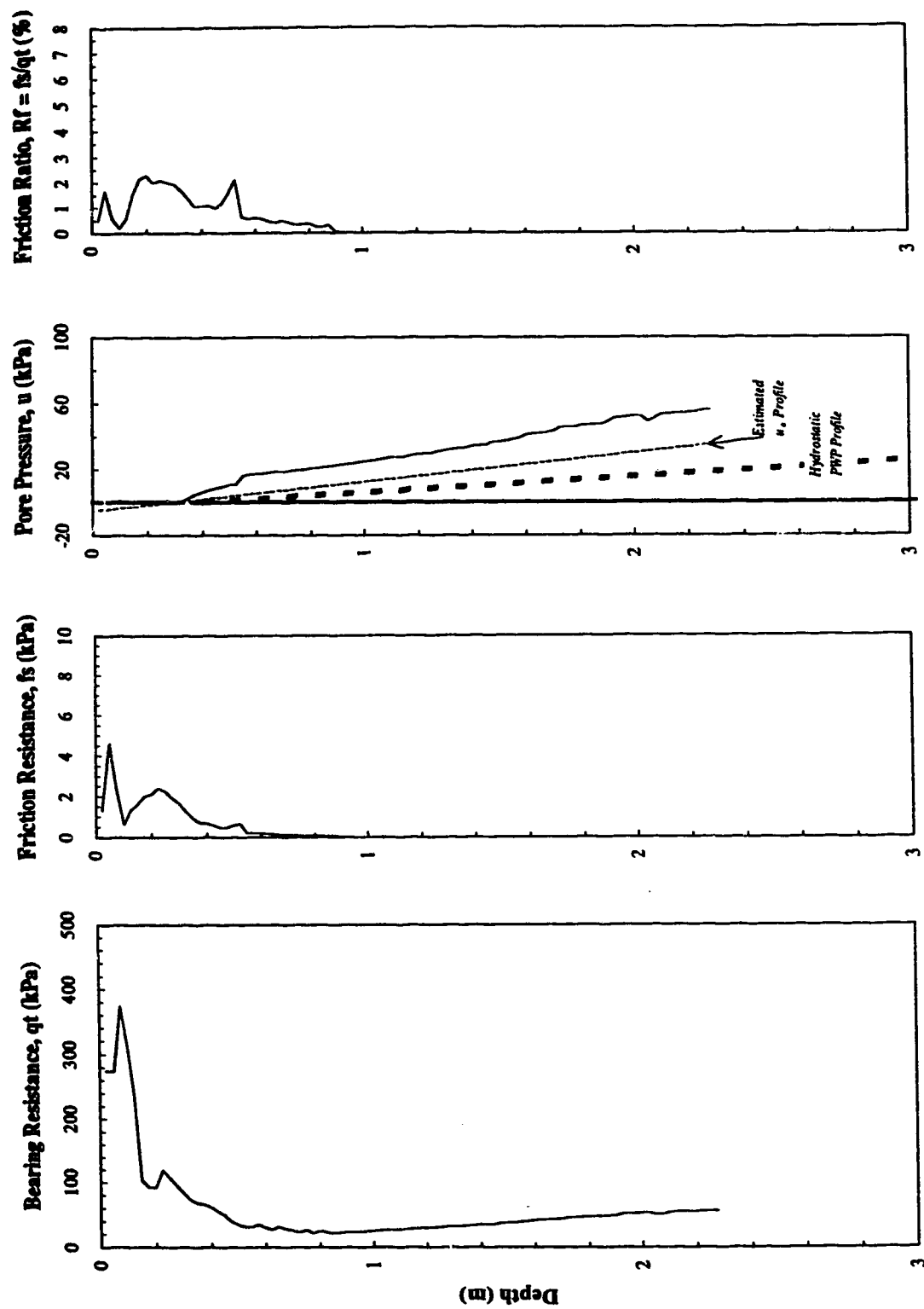


Figure C15 CPT Profiles - Suncor NST Cells - Site 3a

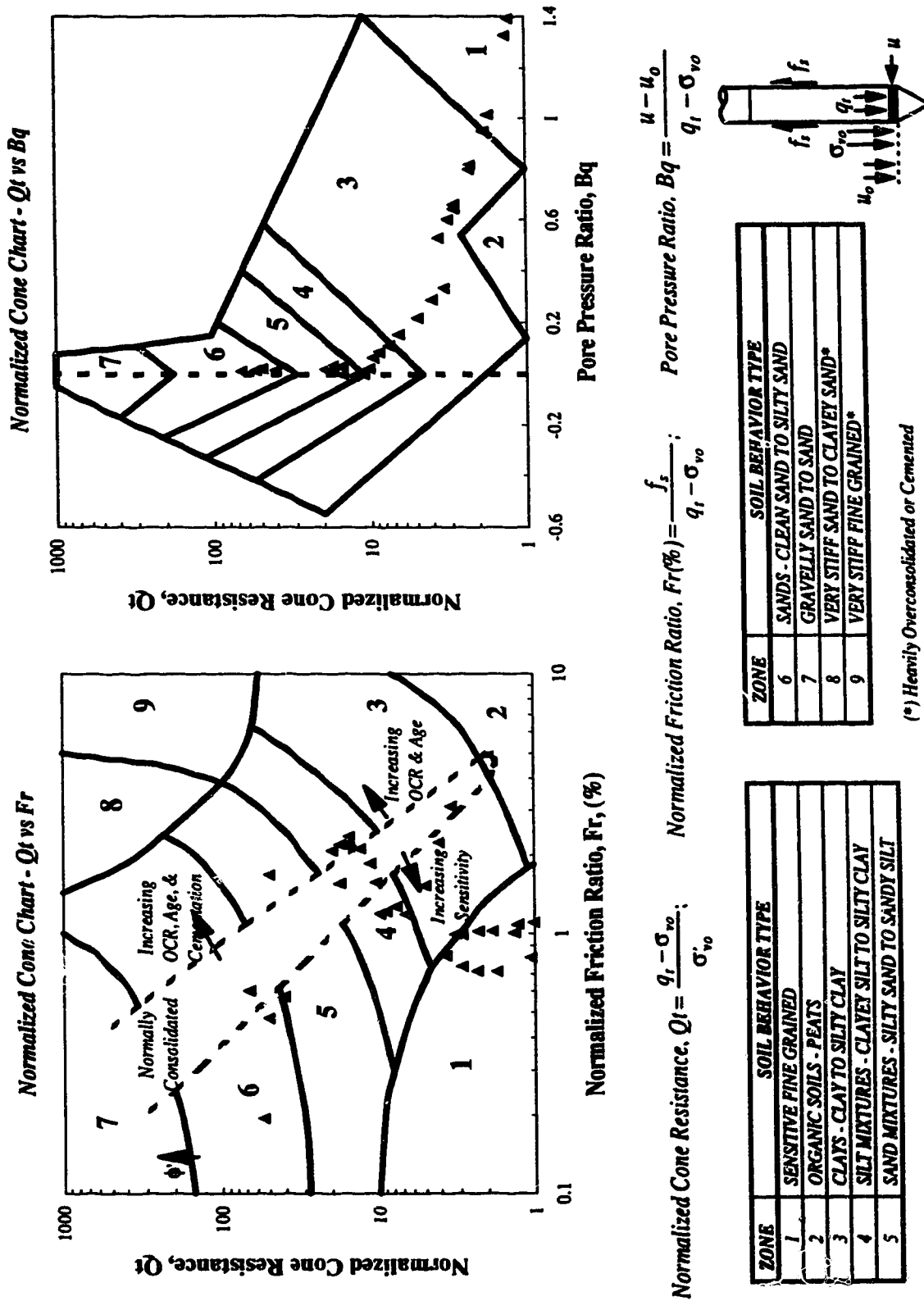


Figure C16 Normalized CPT Data Presented on Soil Behavior Type Charts - Suncor NST Cells - Site 3a

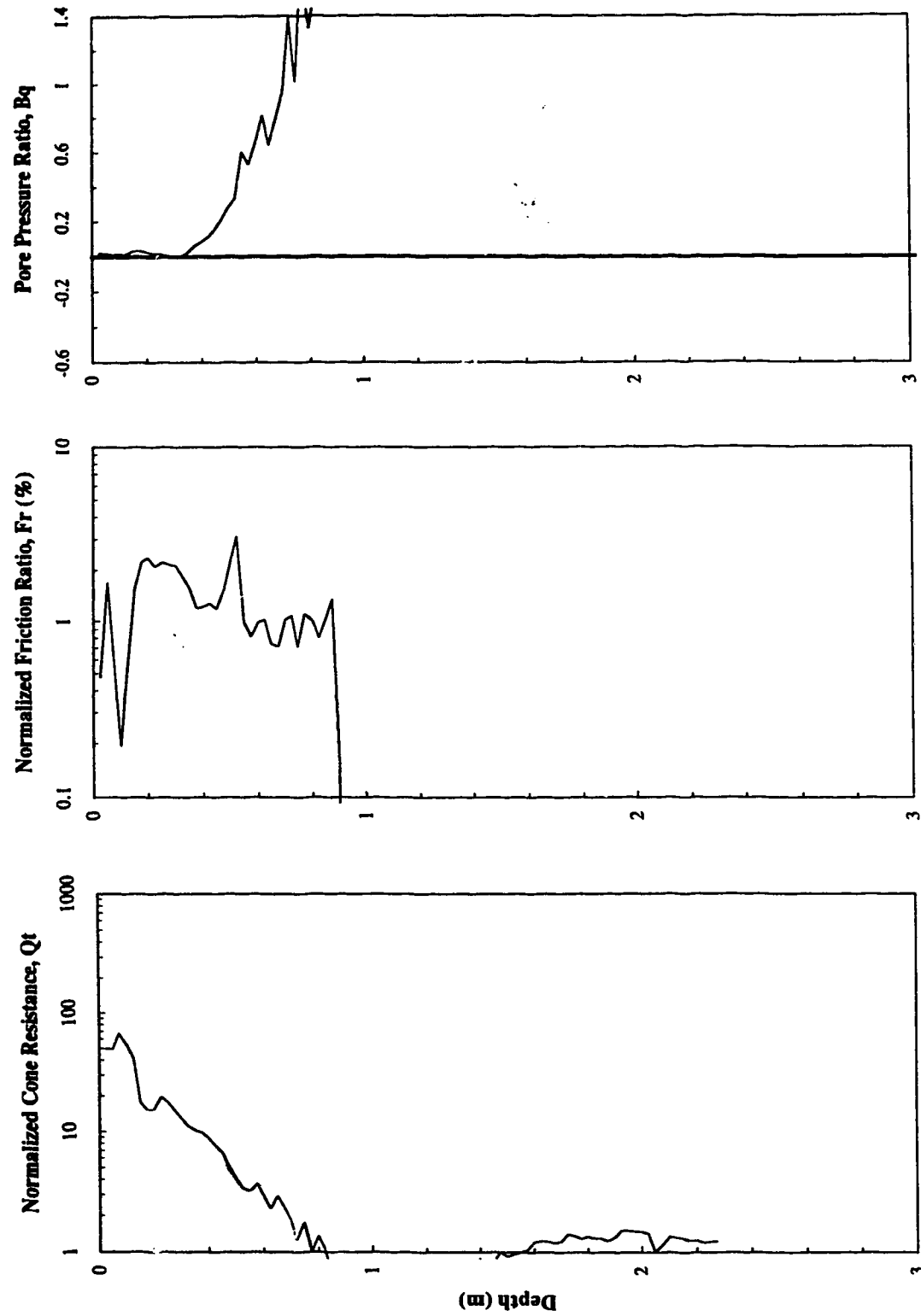


Figure C17 Normalized CPT Data Profiles - Suncor NST Cells - Site 3a

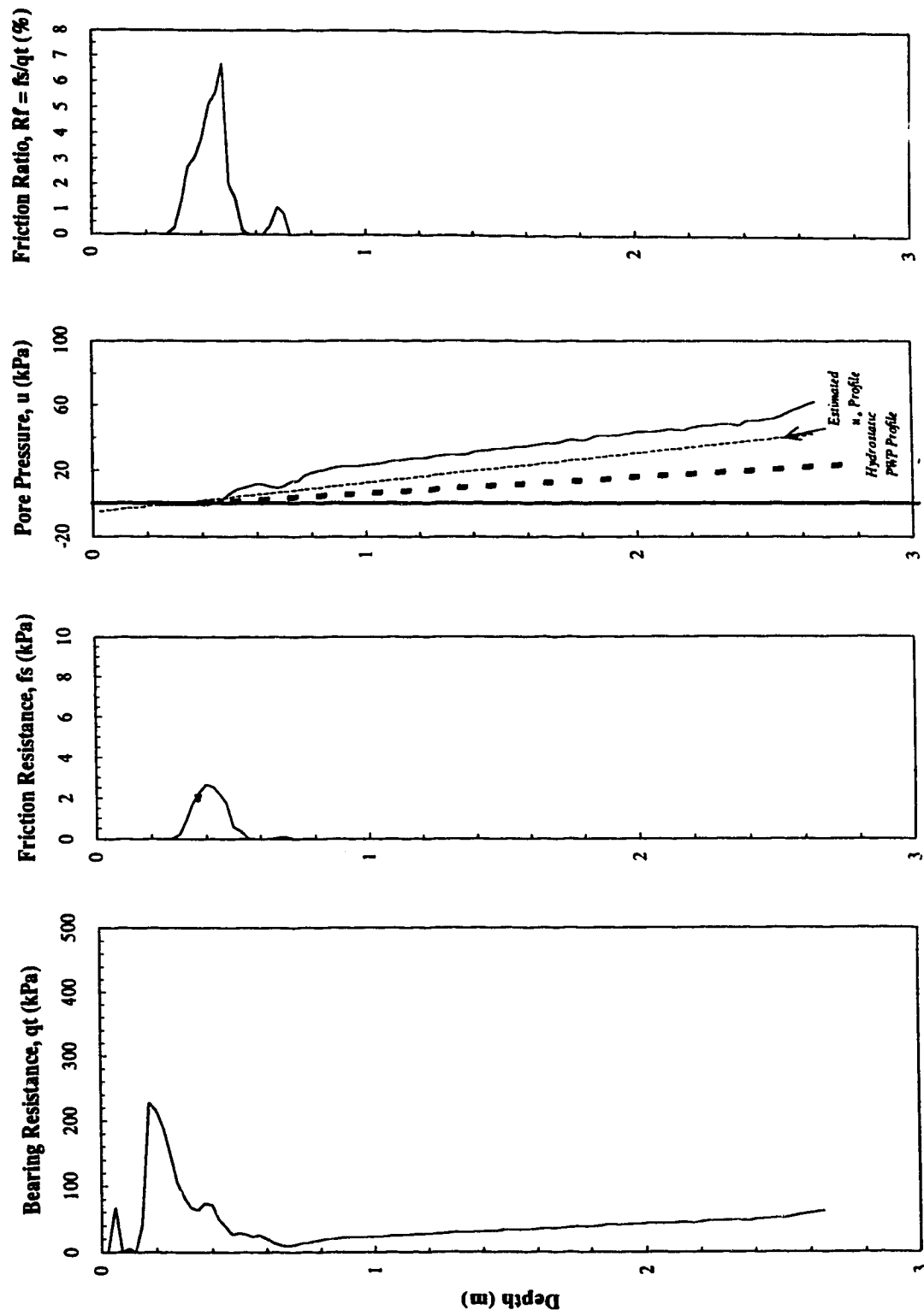


Figure C18 CPT Profiles - Suncor NST Cells - Site 3b

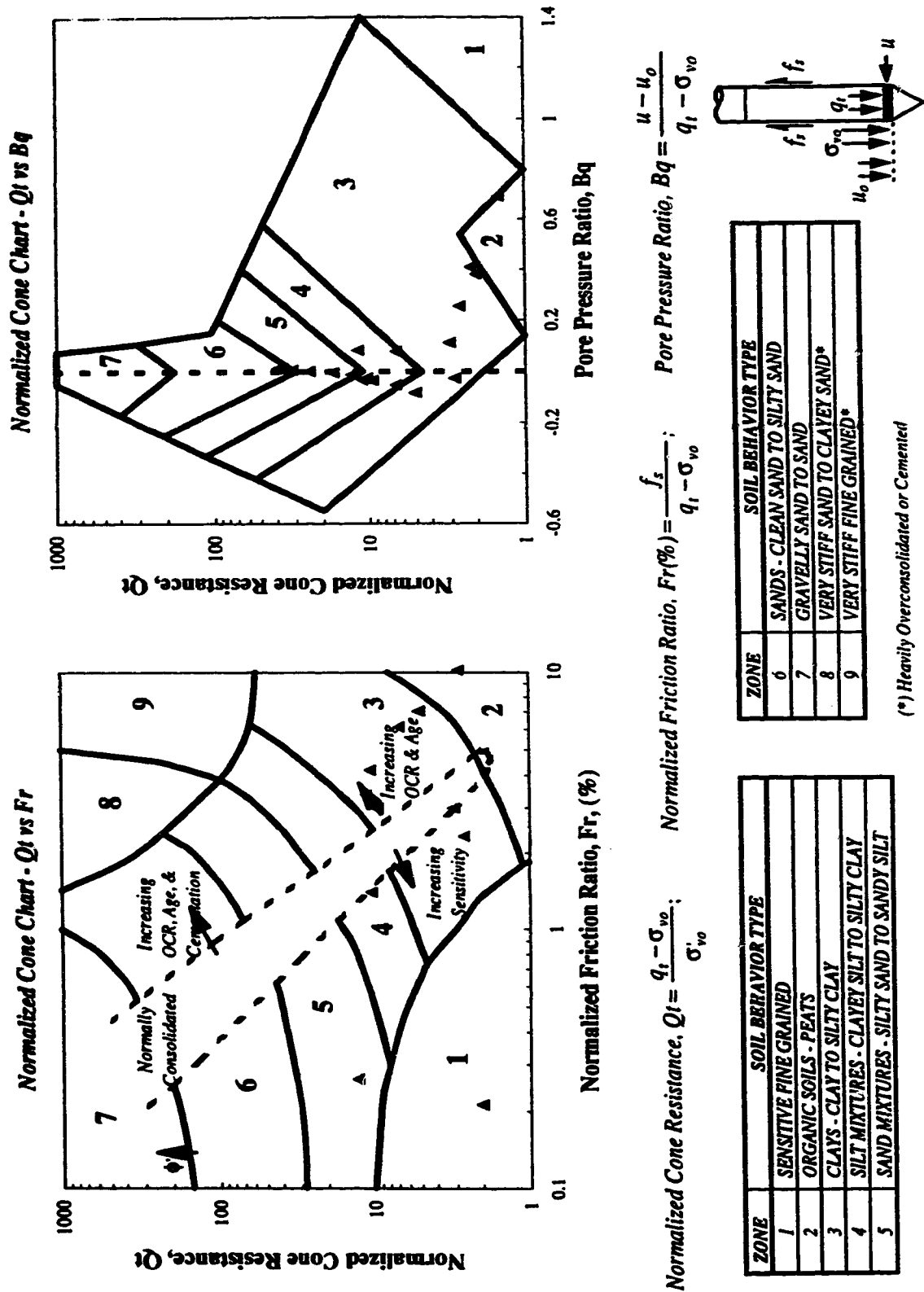


Figure C19 Normalized CPT Data Presented on Soil Behavior Type Charts - Suncor NST Cells - Site 3b

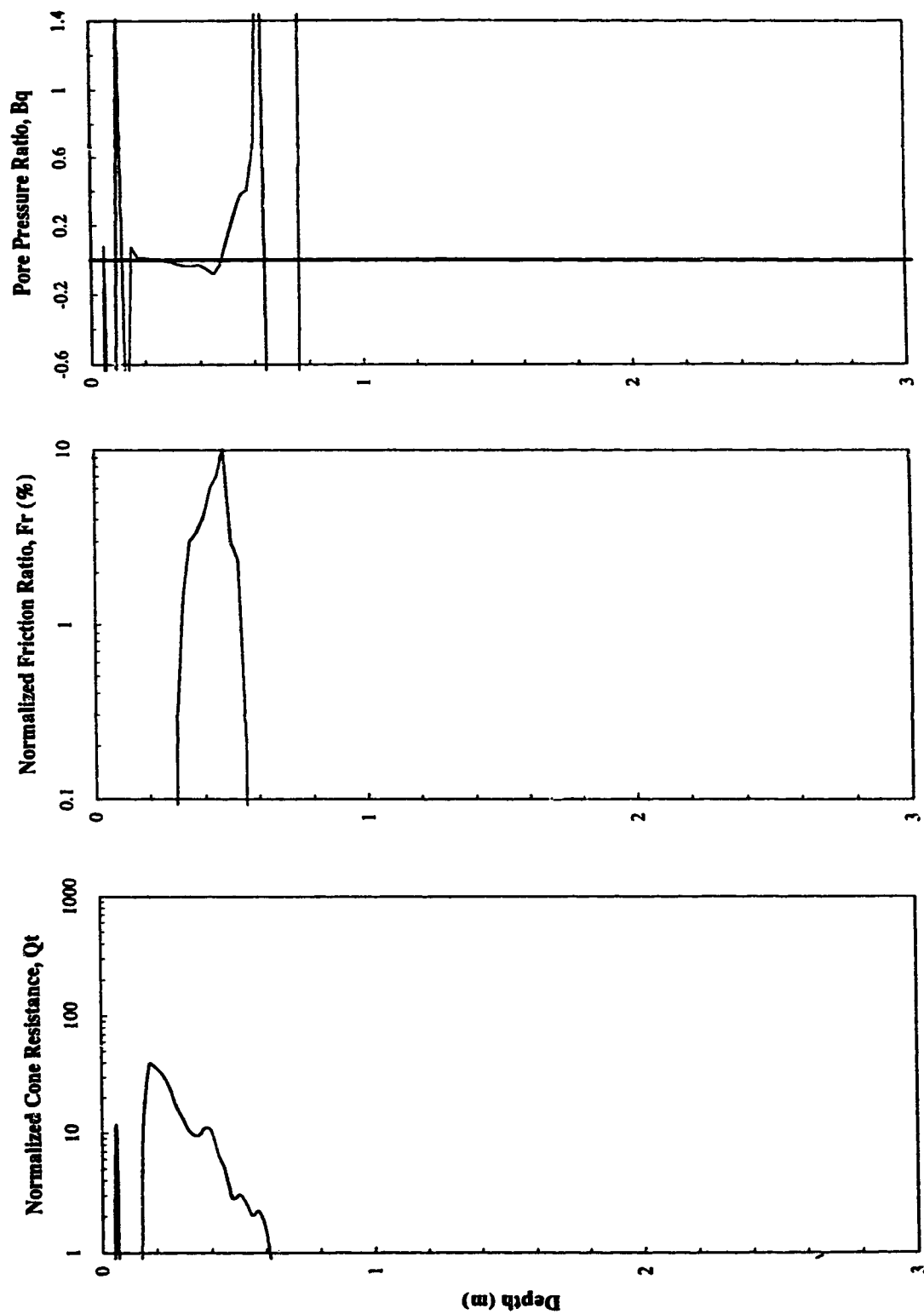


Figure C20 Normalized CPT Data Profiles - Suncor NST Cells - Site 3b

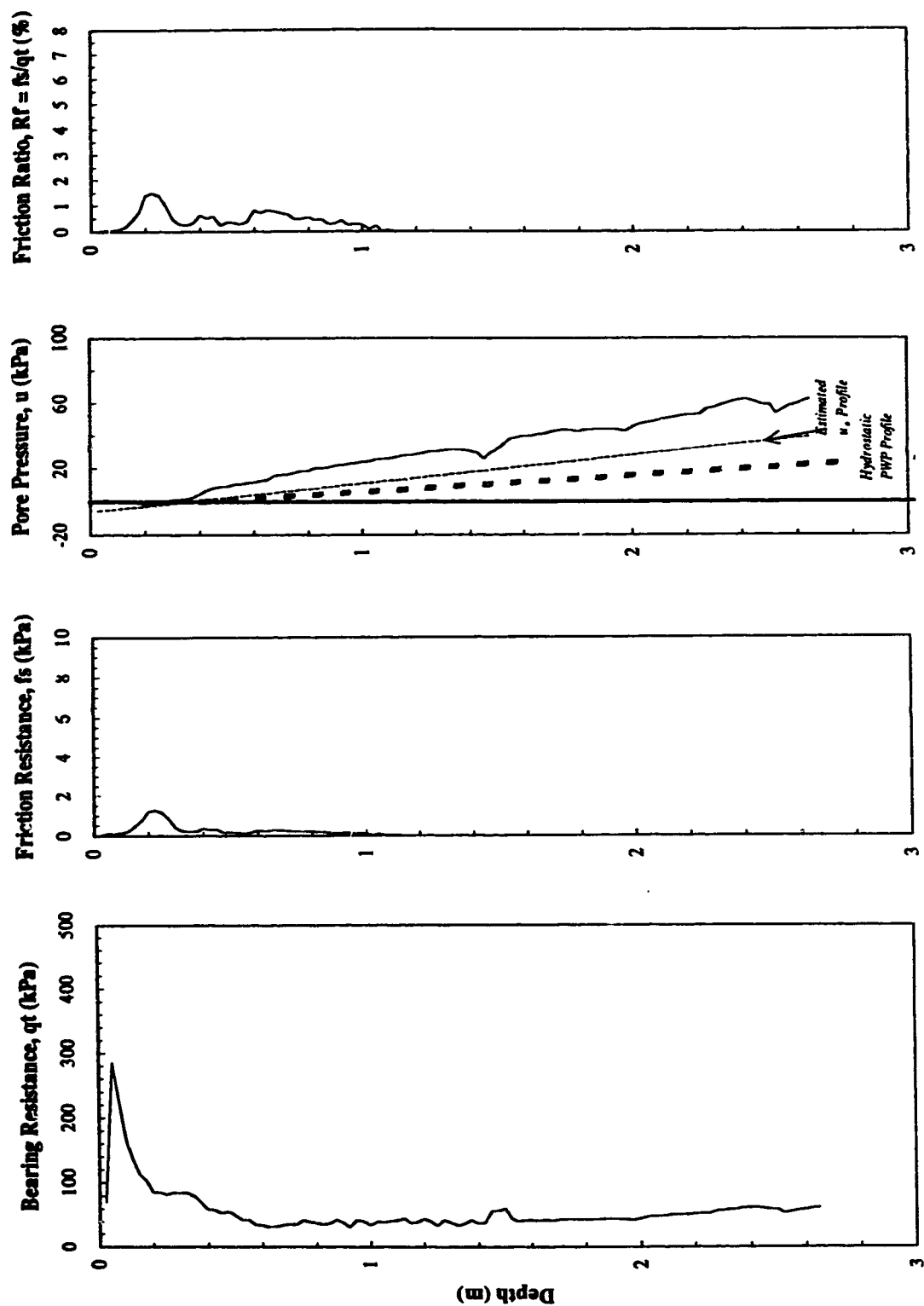


Figure C21 CPT Profiles - Suncor NST Cells - Site 4a

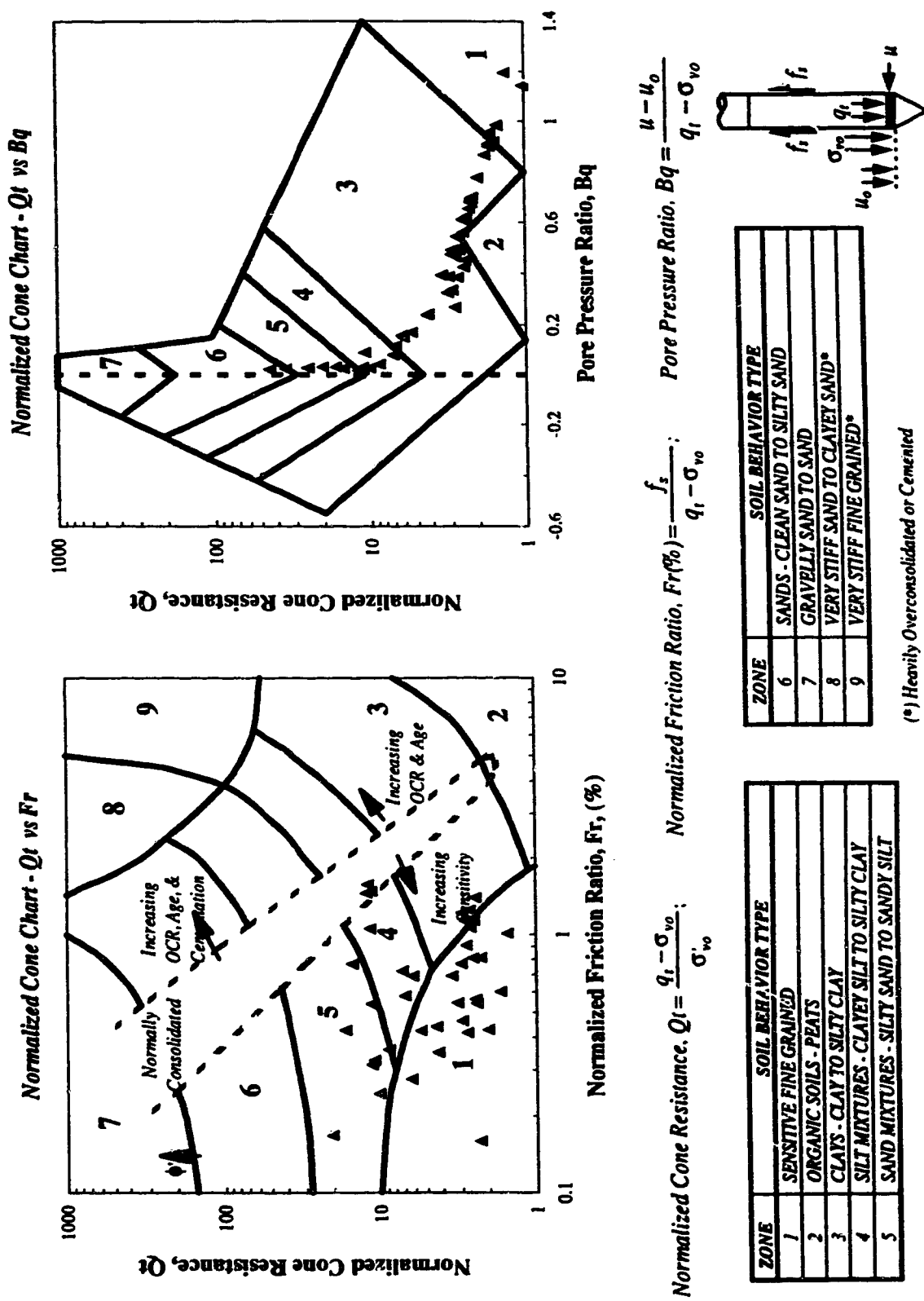


Figure C22 Normalized CPT Data Presented on Soil Behavior Type Charts - Suncor NST Cells - Site 4a

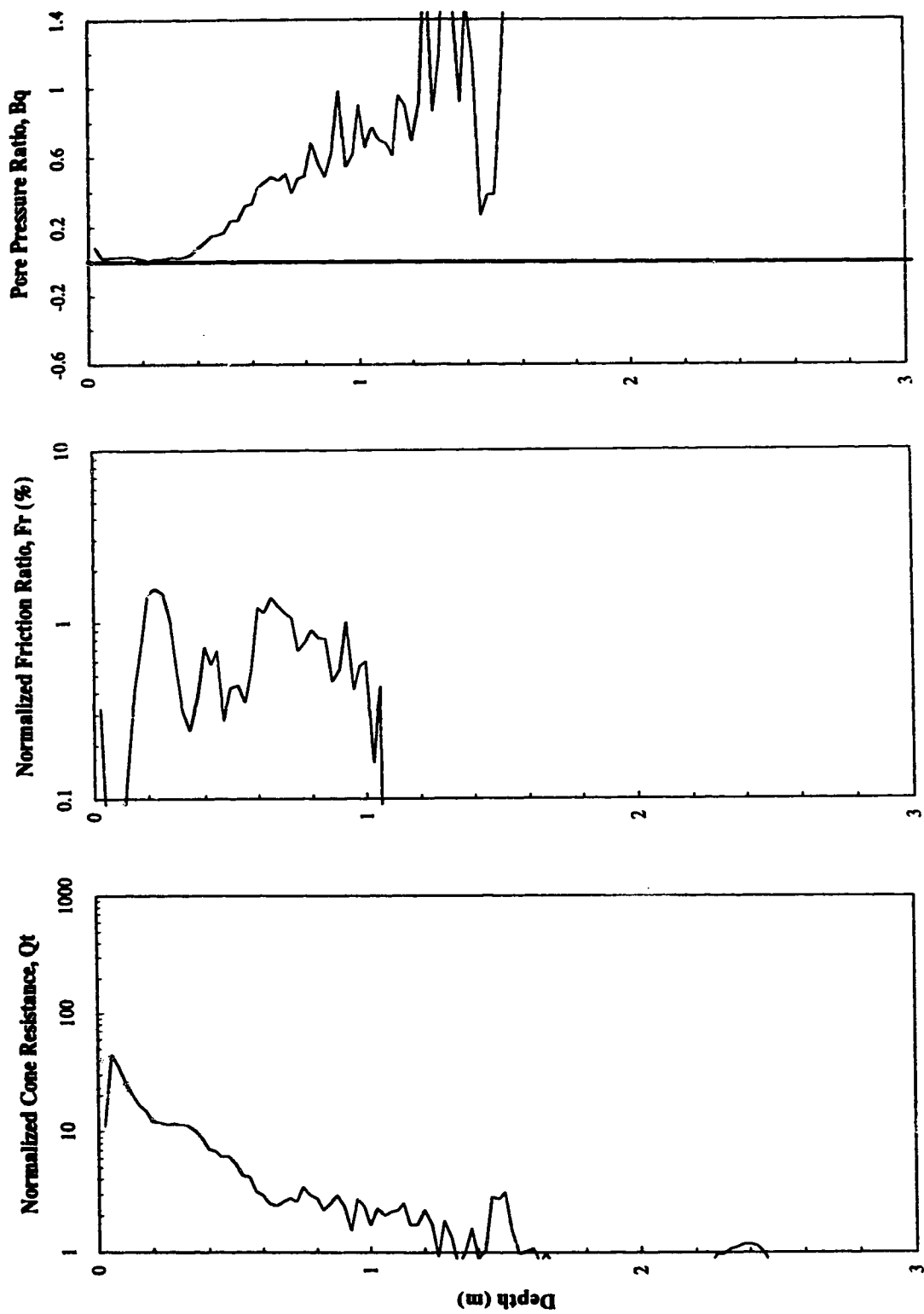


Figure C23 Normalized CPT Data Profiles - Suncor NST Cells - Site 4a

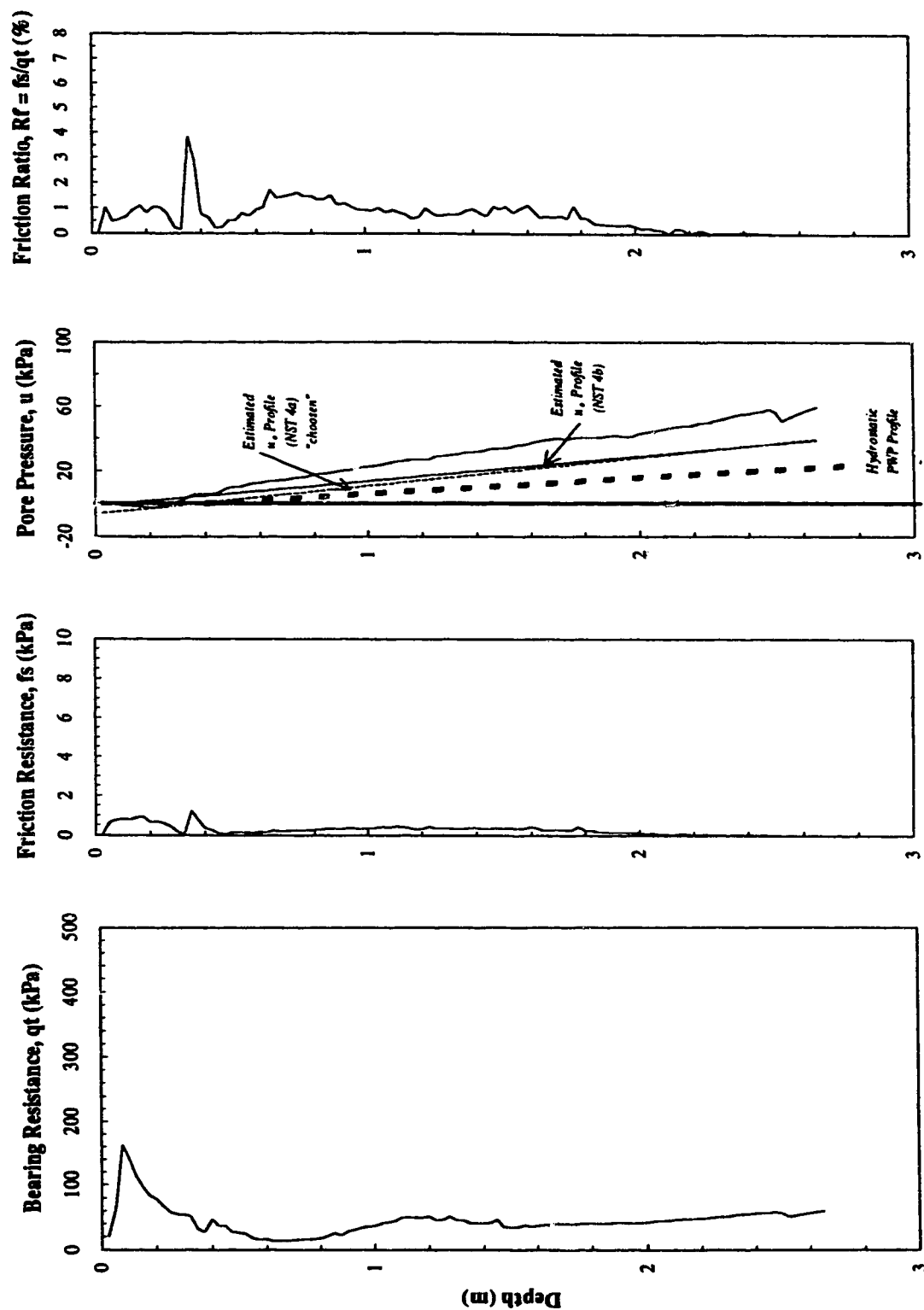


Figure C24 CPT Profiles - Suncor NST Cells - Site 4b

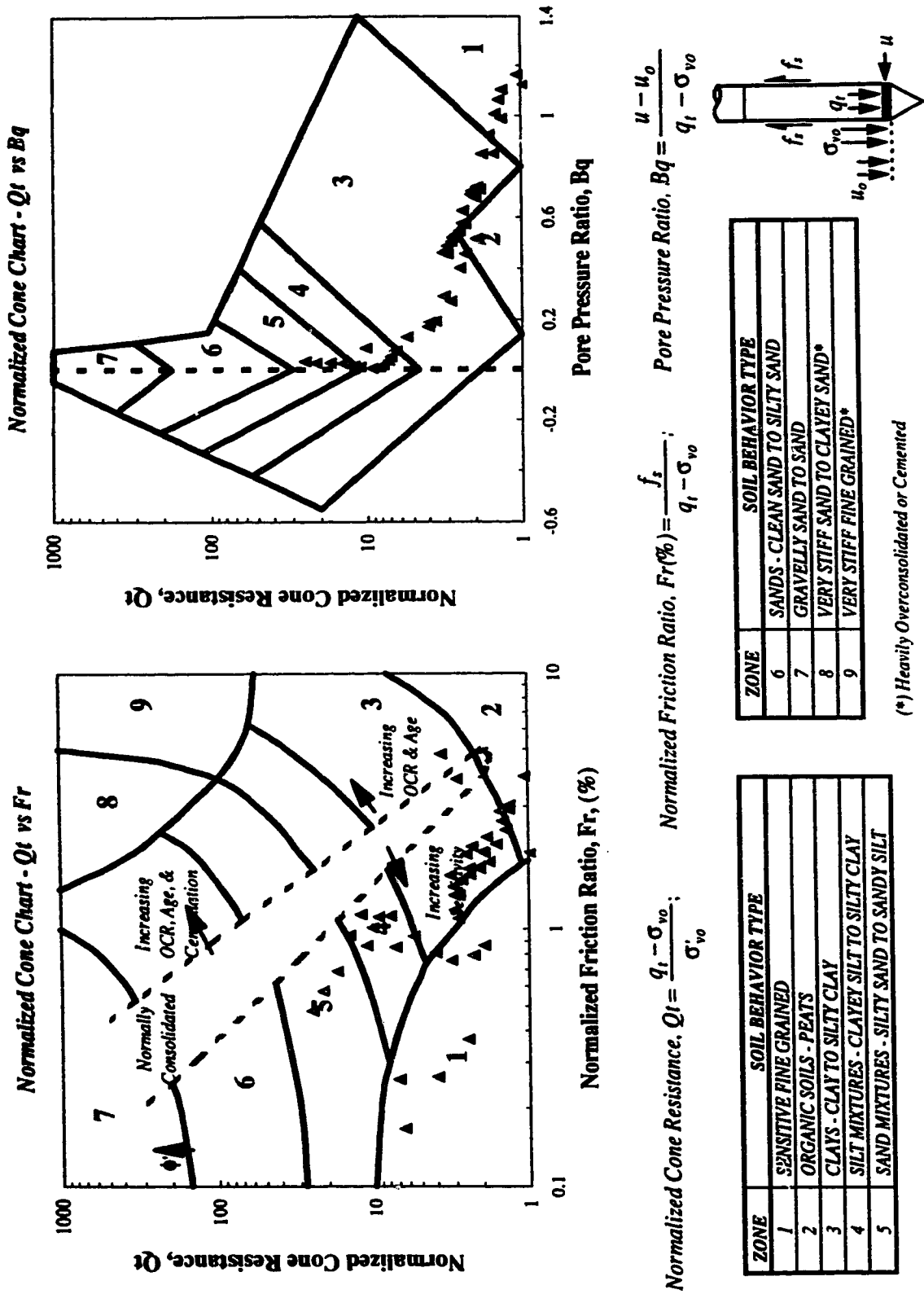


Figure C25 Normalized CPT Data Presented on Soil Behavior Type Charts - Suncor NST Cells - Site 4b

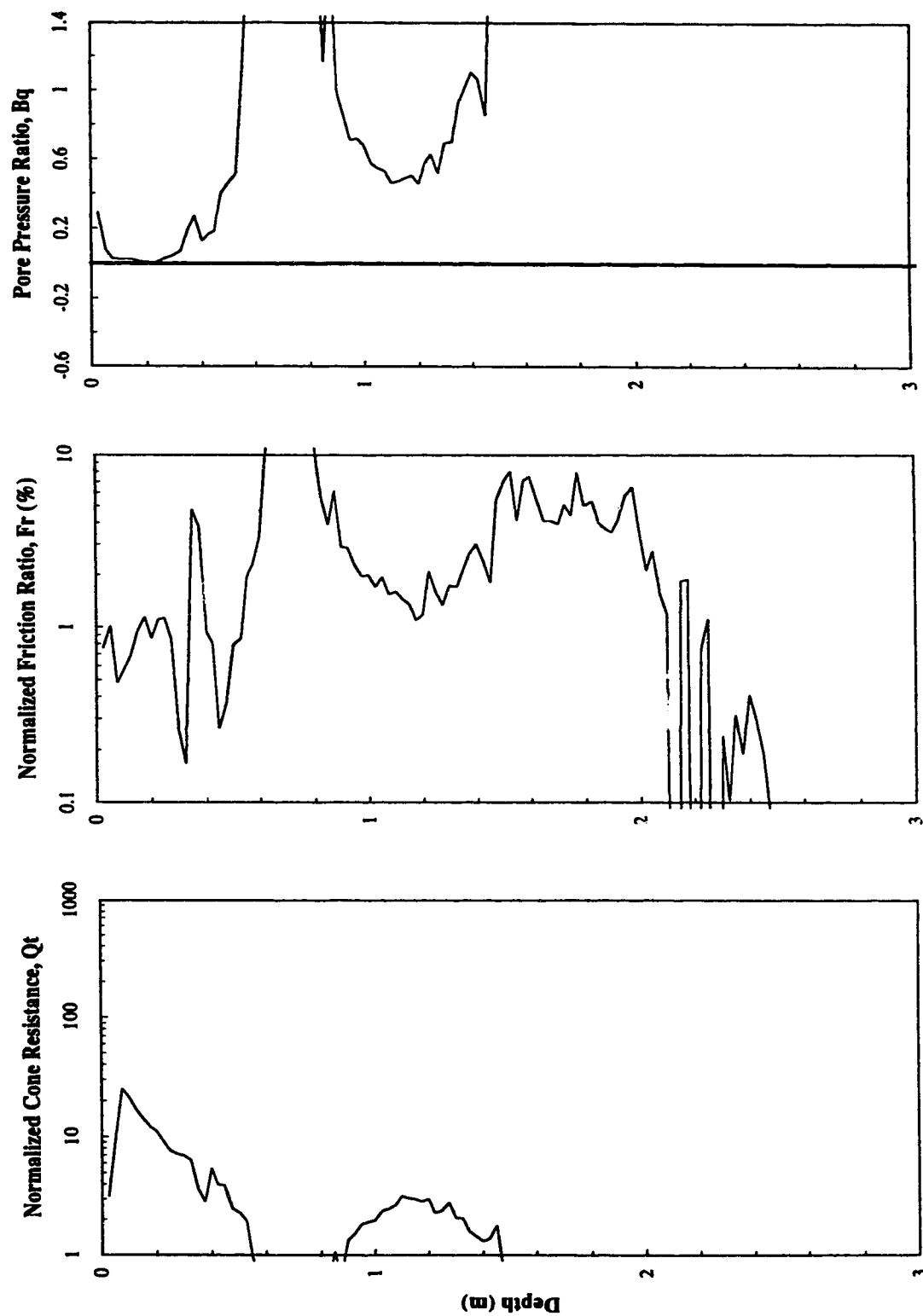


Figure C26 Normalized CPT Data Profiles - Suncor NST Cells - Site 4b

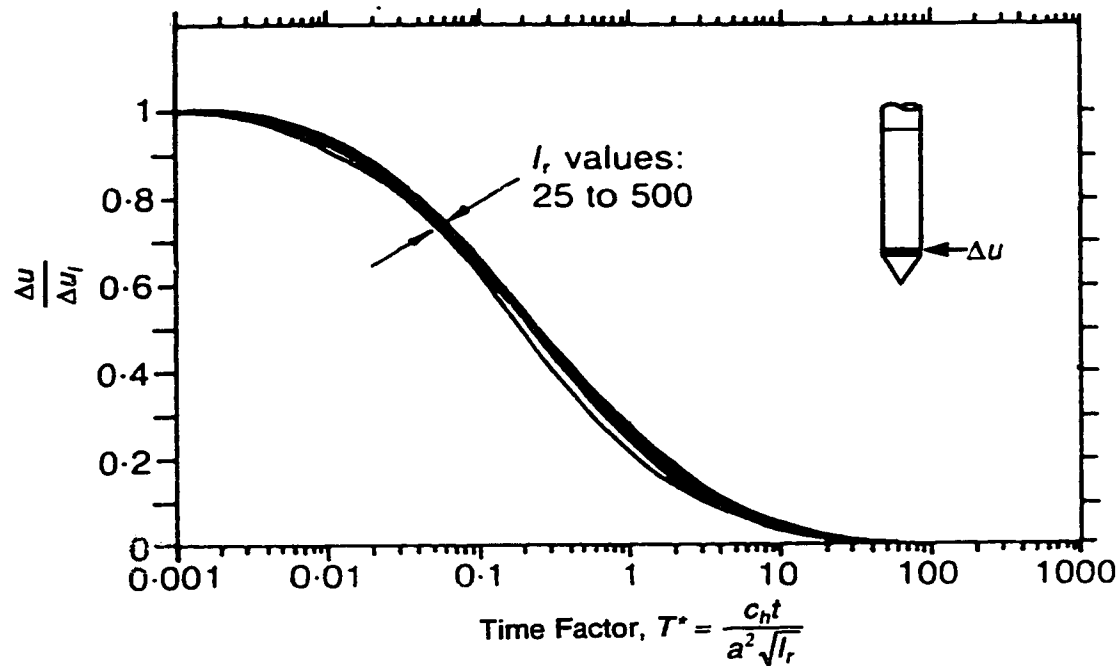


Figure C27 Excess Pore Pressure Dissipation Against Modified Time Factor (T^*)
(modified from Teh and Houlsby, 1991)

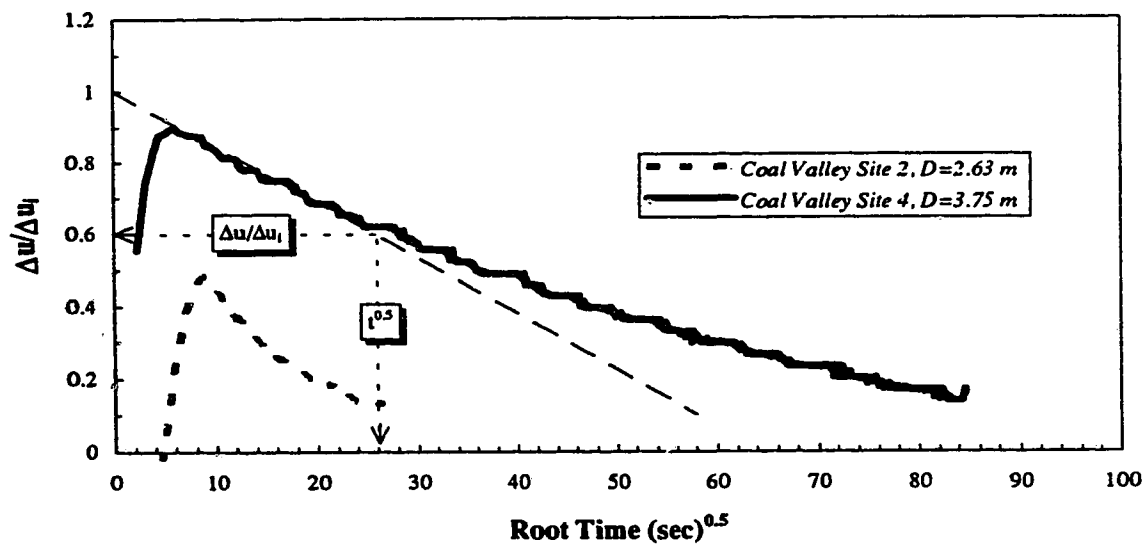


Figure C28 Selected Pore Pressure Dissipation Results From Coal Valley Tailings Beach

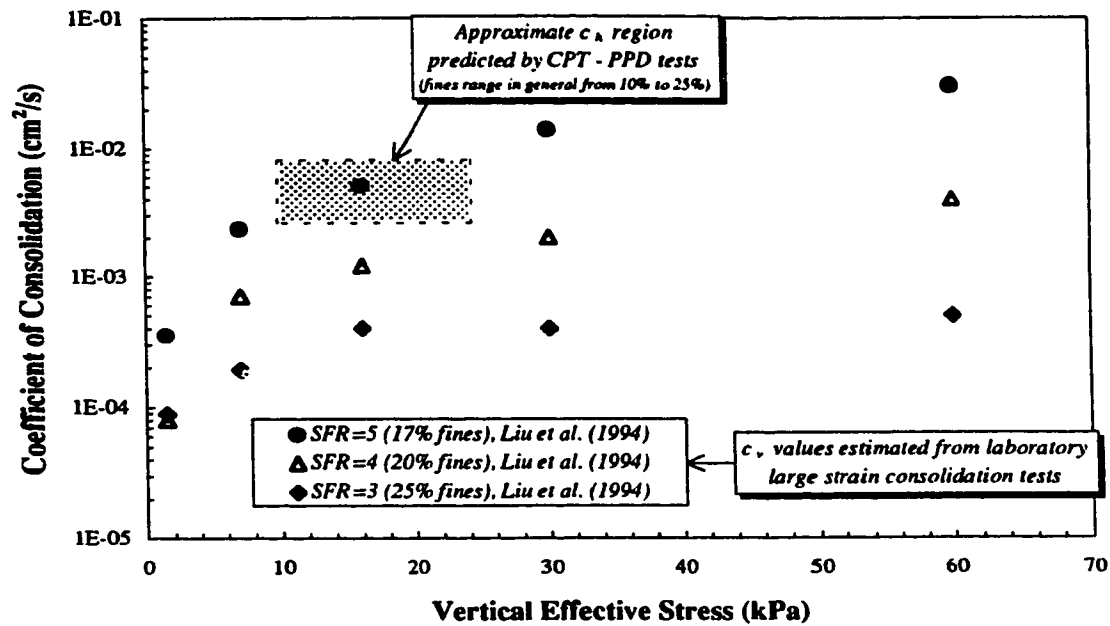


Figure C29 Comparison Between Laboratory and Field Coefficient of Consolidation Values of Suncor NST

Appendix D

Spectral Analysis Of Surface Waves Investigations At Coal Valley And Suncor NST Cells

D.1. INTRODUCTION

This appendix includes the results of the Spectral Analysis of Surface Waves (SASW) technique employed to determine the shear wave velocity profiles at the two tailings deposits investigated. SASW investigations were conducted in June, 1992 and August, 1994 at Sites 1 through 4 along the beach portion of the Coal Valley tailings impoundment, and in October, 1994 within the Suncor NST Cells. The results contained herein exclude the June, 1992 results for reasons described below. As with the PLT and CPT investigations described in the two previous appendices, Chapter 4 illustrates the equipment and sounding locations for these investigations. The following includes a complimentary discussion of the SASW technique included in Chapter 4, presentation of the results, and summary of the key issues faced.

D.2. SASW DESCRIPTION

Prior to the 1970's the very time consuming steady state Rayleigh-wave technique incorporating a steady state vibrator with adjustable frequencies was used to obtain the dispersion curve and subsequent shear wave velocity profile at a site (Stokoe *et al.* 1994). Recent software and hardware developments facilitated the use of impulse, swept-sinusoidal or random noise load

applied at the surface of the soil with two or more vertical receivers located on the surface to monitor the passage of waves generated at the source. The digitized signals from the receivers are recorded and transformed to the frequency domain using a Fast Fourier Transform algorithm, with the phase velocity, $\phi(f)$, between the receiver signals calculated for each frequency. The travel time, $t(f)$, between receivers can then be obtained for each frequency by:

$$t(f) = \frac{\phi(f)}{2\pi f} \quad [D1]$$

where the phase difference, $\phi(f)$, for each frequency is in radians and the frequency, f is in cycles per second. Since the distance between receivers ($d_2 - d_1$) is known, Rayleigh wave velocity, V_R is calculated using:

$$V_R = \frac{d_2 - d_1}{t(f)} \quad [D2]$$

The corresponding Rayleigh surface wavelength, λ_R , is determined using:

$$\lambda_R = \frac{V_R}{f} \quad [D3]$$

The formulations above may be implemented at each frequency with the results combined to form a field dispersion curve illustrating the variation of Rayleigh surface wave velocity with wavelength. The concept of dispersion recognizes that surface waves of different wavelengths propagate at different phase velocities in non-ideal media. Generally, longer wavelengths travel through greater depths with shorter wavelengths sampling the near surface materials.

Establishing the field dispersion curve requires step wise incremental spacing of receivers and source to sample the desired wavelength and depth spectrum. The wave sampling and data acquisition at the site was conducted using the common receiver midpoint geometry technique as shown in Das (1994) where a common center is maintained for all receiver spacings and the source is alternated to propagate forward and reverse wave signals.

The process of determining the shear wave velocity profile from the *insitu* surface wave dispersion curve is called forward modelling. As described in Chapter 4, the forward modelling process is an iterative procedure where an initial soil model of a multi-layered system is proposed and a theoretical dispersion curve is produced. The soil model parameters (shear wave velocity, bulk density, Poisson's ratio, and layer thickness) are then varied until the theoretical dispersion curve matches the experimental dispersion curve. Since this is a modeling procedure, the results of the method cannot be exact as discrete shear wave velocity measurements between fixed points within the ground. However, previous experimental comparisons have shown that shear wave velocity profiles determined by forward modeling of SASW results versus those determined by direct *insitu* measurement have been within 10 to 15 percent of each other (Stokoe and Nazarian, 1985)

Of the available surface waves, the Rayleigh wave is used in SASW testing for soil and pavement structures. This is because of its relative ease of generation and detection. The algorithm used to forward model the Rayleigh wave dispersion curve is based on well accepted procedure developed at the University of Texas. The formulations included in this Windows based forward modelling program named WinSASW are discussed in Stokoe *et al.* (1994). The analysis is not biased by the user in that the answer is constrained by the fact that the theoretical and dispersion curves match. Two of the input parameters, Poisson's ratio, ν , and bulk density, ρ , only weakly influence Rayleigh wave velocity, thus leaving only the shear wave velocity, V_s , and the layer thickness as the main variables.

Following the forward modelling procedure, the key input parameters which modelled the field dispersion curve (namely shear wave velocity and layer thickness) are used to develop profiles of soil small strain shear modulus with depth. The small strain shear modulus, G_o , may be computed using:

$$G_o = \rho V_s^2 \quad [D4]$$

D.3. RESULTS

The 1994 SASW results from Sites 1 through 4 at Coal Valley are summarized in Figures D1 through D8. Figures D1, D3, D5 and D7 include the screened field dispersion profiles and constructed theoretical dispersion profiles at each of the sites, with Figures D2, D4, D6, and D8 presenting the resulting shear wave velocity profiles. Figures D9 through D16 include the SASW results obtained within the NST Cells 3 and 4, with the field and constructed dispersion curve(s) similarly preceding the shear wave velocity profile(s). As indicated above and illustrated in Figures D9 through D16, more than one theoretical dispersion curve and resulting shear wave velocity profile was constructed at each site. The profiles represent the scatter of field dispersion data obtained within the surficial soils. Enhanced screening of the data indicated the possibility of two distinct profiles within the shallow surficial materials. These profiles are designated as “*With Crust*” and “*Without Crust*”. The former profile attempts to model the possible presence of a surficial crust, developed through evaporation dewatering and matric suction development.

Based on the shear wave velocity profiles in the previously described figures, the small strain shear modulus, G_o , profiles were constructed using [D4]. These profiles are included for Coal Valley in Figure D17, and for the NST Cells in D18 and D19. Figure D18 and Figure D19 includes the results from the “*With Crust*” and “*Without Crust*” modelling considerations.

As illustrated in Appendix B with the presentation of the PLT data in G vs Q/Q_{max} space, the shear modulus is strain dependent. To illustrate this dependency further, Figure D20 conceptually relates the computed small strain shear modulus, G_o , illustrated above, with the shear modulus values illustrated in Appendix B. As discussed by Viggiani and Atkinson (1995), at very small strains the shear modulus reaches a nearly constant value of G_o . The stiffness begins to decrease for reconstituted soils at about 0.001% for low plastic soils and 0.01% for plastic soils. Vucetic and Dobry (1991) presented graphically this plasticity dependent shear modulus attenuation initiation location soils with plasticity indices ranging from 0 to 200%. Beyond a strain of 1%, the stiffness is approximately 1 order of magnitude less than G_o , with continual reduction as failure is approached (Viggiani and Atkinson 1995). Based on the relationship presented by Stroud (1988) the average shear strains estimated from the 1991 plate

load test results at $Q/Q_{max} = 25\%$ and 50% are 1.5% and 3.6% respectively. As presented by Burland (1989) in a variety of case histories and examples, strains recorded in the field beneath and adjacent structures founded on stiff soils are typically within the range small and very small strain regions noted in Figure D20.

D.4. INVESTIGATION AND ANALYSIS COMMENTS

A few procedural issues were encountered through the implementation of SASW technology at these tailings sites. These issues are believed to be a coupled results in the authors limited expertise in application of this technology, and the generally weak nature of the soils investigated. The key issue which was never completely resolved included the clarity and magnitude of the source. Significant impact energies were usually required in order for adequate signal detection. Due to the weak nature of these soils, these energies would successively force the striking plate into the soil with sequential impacts. Limited success was achieved by varying the plate dimensions and material type. Although unconfirmed, this gradually changing source boundary condition may have influenced the results.

Upon detailed analysis of the “apparently” screened field results, some scatter was observed with the field dispersion data. Coherence values usually in excess of 0.98 were required in order to construct possible profiles. An indication of this scatter is illustrated in the dispersion and shear wave velocity profiles for Coal Valley Site 3 presented in Figures D5 and D6. The cluster of high coherence data at small wavelength's, resulting in the construction of *Dispersion Curve (1)* is questionable. Although considerable scatter (←authors classification of some field data) was observed in the field dispersion data which required enhanced time consuming filtering, this scatter resembles that produced in Das (1994).

The beginning of this appendix highlighted that SASW measurements were conducted in 1992 at Coal Valley but were not included herein. These 1992 results were analyzed and produced shear wave velocity profiles significantly greater than those determined in 1994. Although careful screening of the signals in the field was conducted by others in 1992, the relative complexity

associated with SASW investigations on these compressible soils likely contributed to error. Acknowledging the authors (and others) early assent of the procedural learning curve at the time of the investigations, this problem may have been resolved through continued experience. Considerable breadth of experience with the SASW system on a variety of soils has been developed in industry with *insitu* contractors, namely ConeTec Investigations Ltd. of Vancouver, B.C..

The SASW technique is a robust non intrusive technique for determining the shear wave velocity profile at a site. Although the *insitu* profiles at Coal Valley and the Suncor NST Cells were one of the most difficult to evaluate (ie. stiff desiccated crust overlying weaker material which continually increases in stiffness with depth), the author is reasonably confident with the final computed shear wave velocities. However, is light of some of the procedural issues/problems faced and acknowledging the tremendous information gathered from the CPT, future investigations such as these should consider utilization of seismic CPT (SCPT) techniques. The SCPT not only furnishes valuable CPT information, but facilitates direct shear wave velocity measurement. Although unprecedented, SCPT investigations using the lightweight CPT frame discussed in Chapter 4 may deserve future research considerations.

D.5. REFERENCES

- Addo, K., and Robertson, P.K., 1992. Shear Wave Velocity Measurement of Soils Using Rayleigh Waves. *Canadian Geotechnical Journal* 29:558-568.
- Burland, J.B., 1989. Small is Beautiful: The Stiffness of Soils at Small Strains. *Canadian Geotechnical Journal*, 26:499-516.
- Das, D. 1994. Application of SASW for Evaluation of Pavement-Like Structures. Unpublished Ph.D. Thesis, Department of Civil Engineering, The University of Alberta.
- Stokoe, K.H., and Nazarian, S., 1985. Use of Rayleigh Waves in Liquefaction Studies. ASCE proceedings of Measurement and Use of Shear Wave Velocity for Evaluating Dynamic Soil Properties. pp. 1-17.

- Stokoe, K.H., Wright, S.G., Bay, J.A., and Roesset, J.M., 1994. Characterization of Geotechnical Sites By SASW Method. Geophysical Characterization of Sites, 13th ICSMFE, New Delhi, India, pgs. 15-25.
- Stroud, M.A., 1988. The Standard Penetration Test - Its Application and Interpretation. Proceedings of the Conference on Penetration Testing in the UK., Birmingham, England, July 6-8, 1988, pgs. 29-49.
- Viggiani, G., and Atkinson, J.H., 1995. Stiffness of Fine-Grained Soil at Very Small Strains. *Geotechnique* **45**(2):249-265.
- Vucetic, M., and Dobry, R., 1991. Effect of Soil Plasticity on Cyclic Response. *ASCE Journal of Geotechnical Engineering*, **117**(1):89-107.

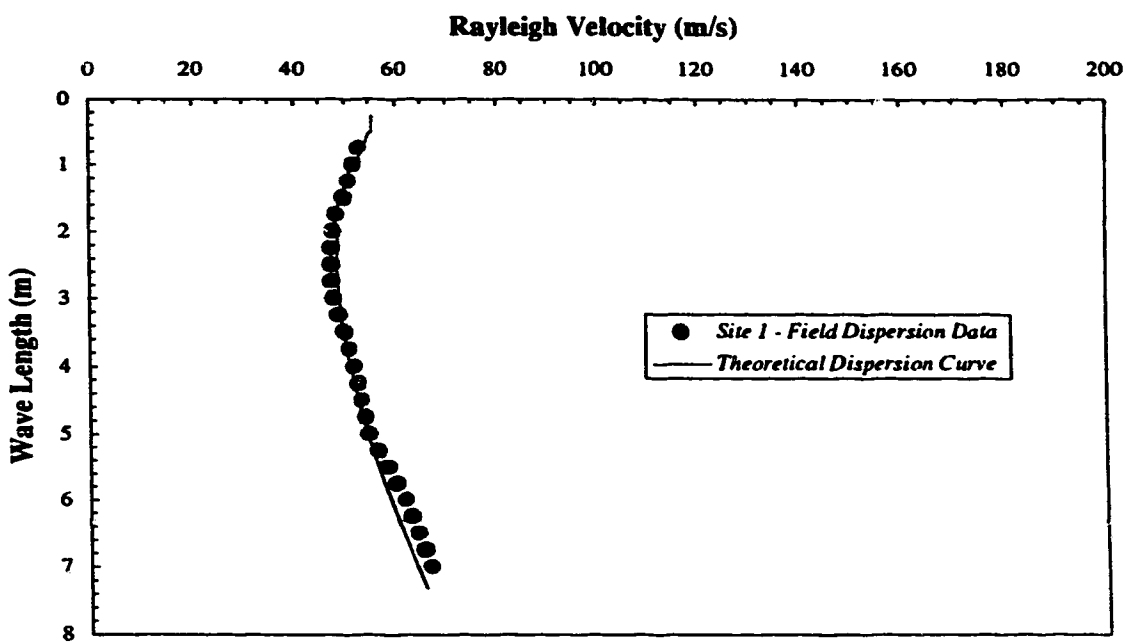


Figure D1 SASW Field and Theoretical Dispersion Curves - Coal Valley Tailings Beach - Site 1

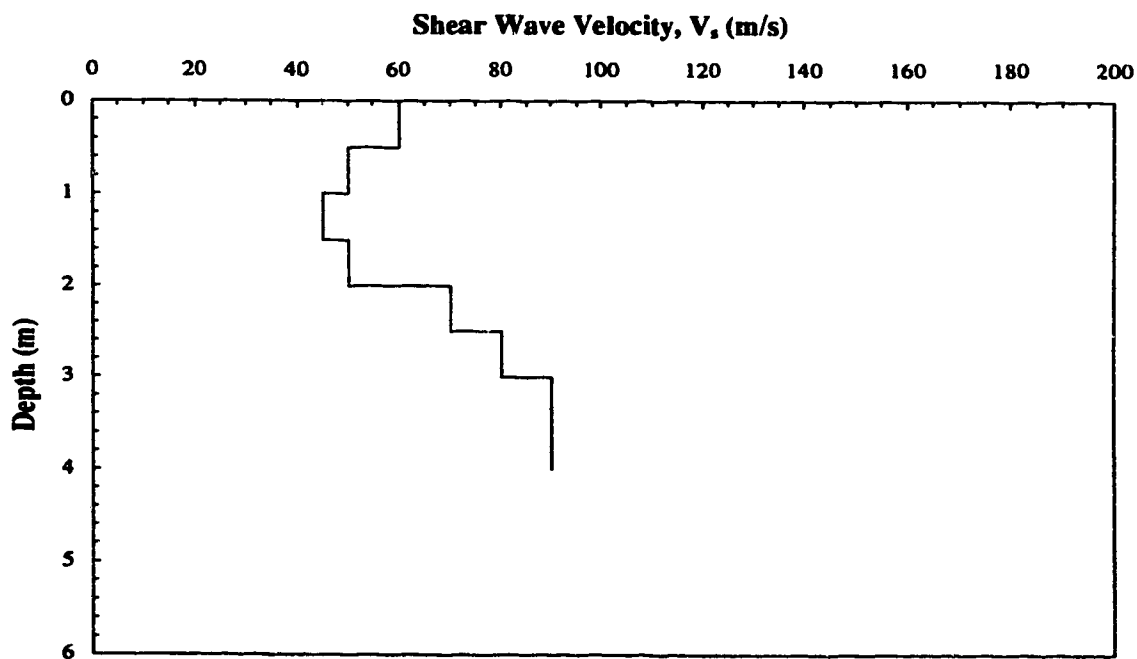


Figure D2 SASW Estimated Shear Wave Velocity Profile - Coal Valley Tailings Beach - Site 1

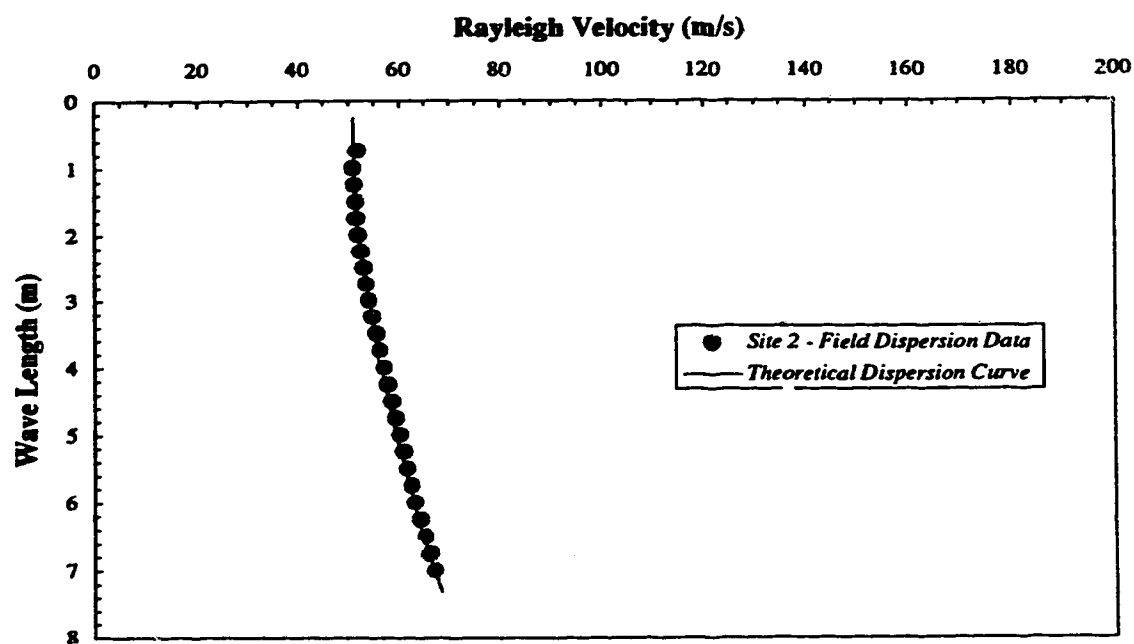


Figure D3 SASW Field and Theoretical Dispersion Curves - Coal Valley Tailings Beach - Site 2

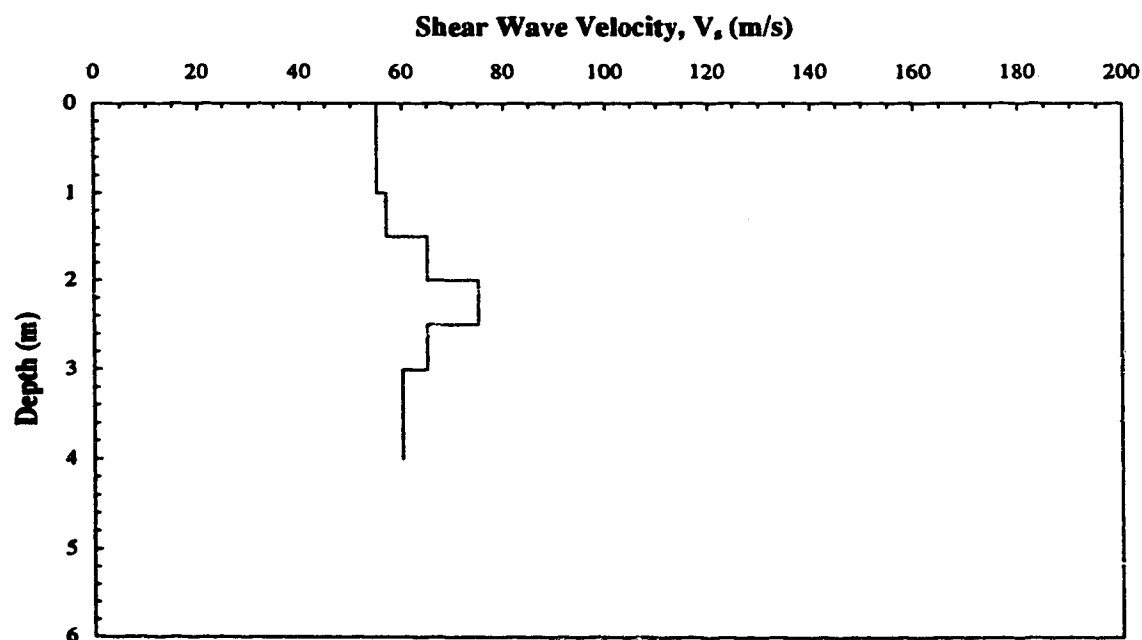


Figure D4 SASW Estimated Shear Wave Velocity Profile - Coal Valley Tailings Beach - Site 2

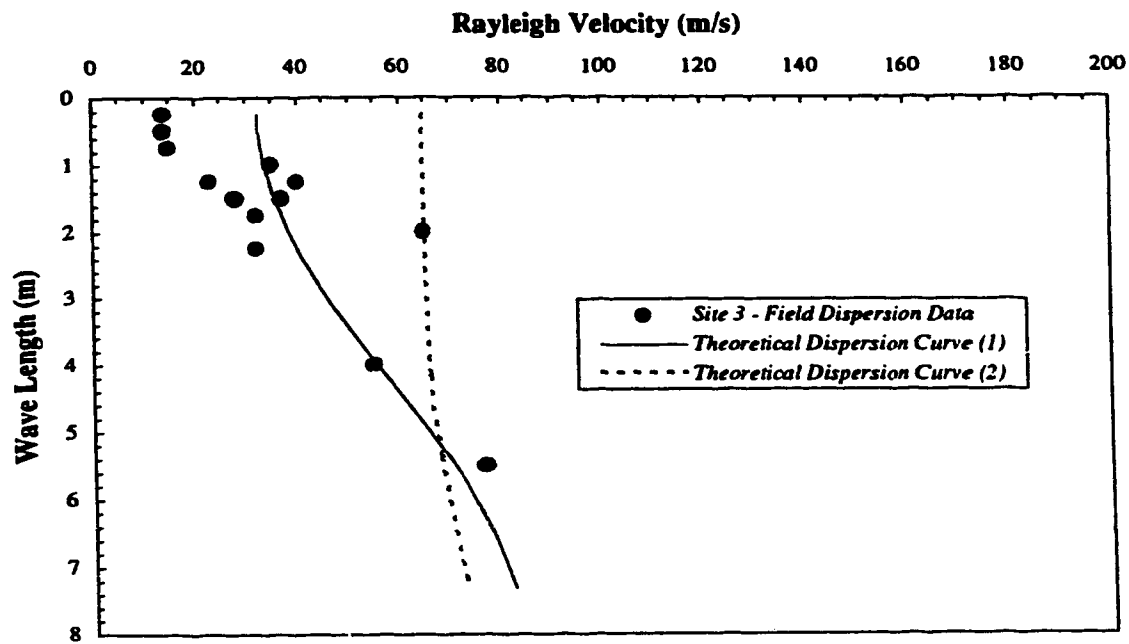


Figure D5 SASW Field and Theoretical Dispersion Curves - Coal Valley Tailings Beach - Site 3

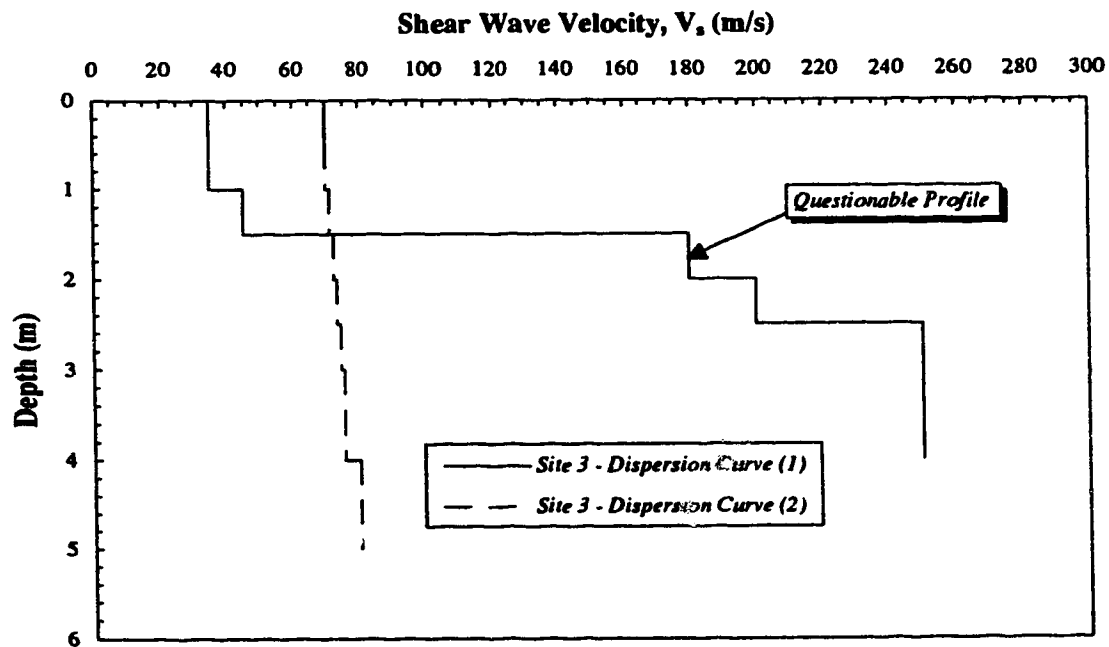


Figure D6 SASW Estimated Shear Wave Velocity Profiles - Coal Valley Tailings Beach - Site 3

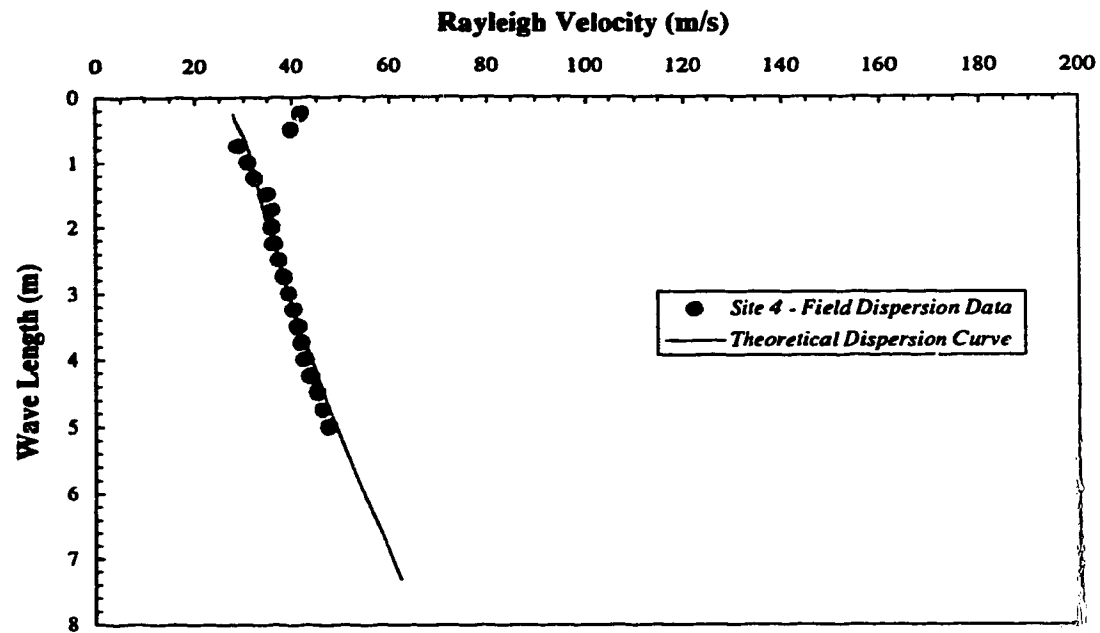


Figure D7 SASW Field and Theoretical Dispersion Curves - Coal Valley Tailings Beach - Site 4

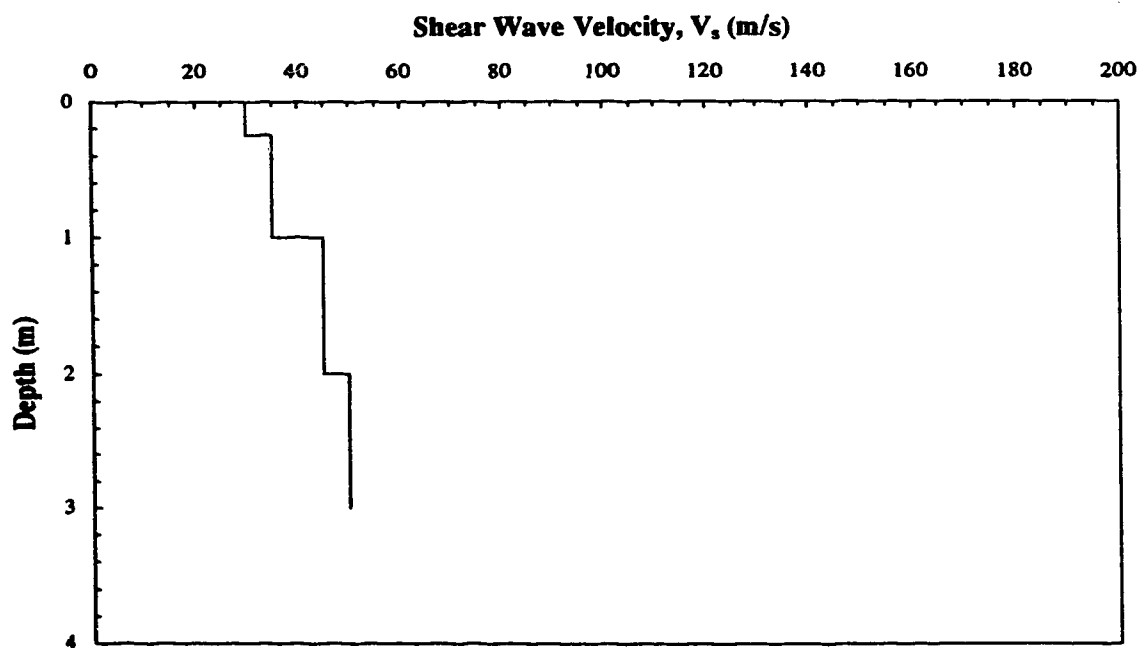


Figure D8 SASW Estimated Shear Wave Velocity Profile - Coal Valley Tailings Beach - Site 4

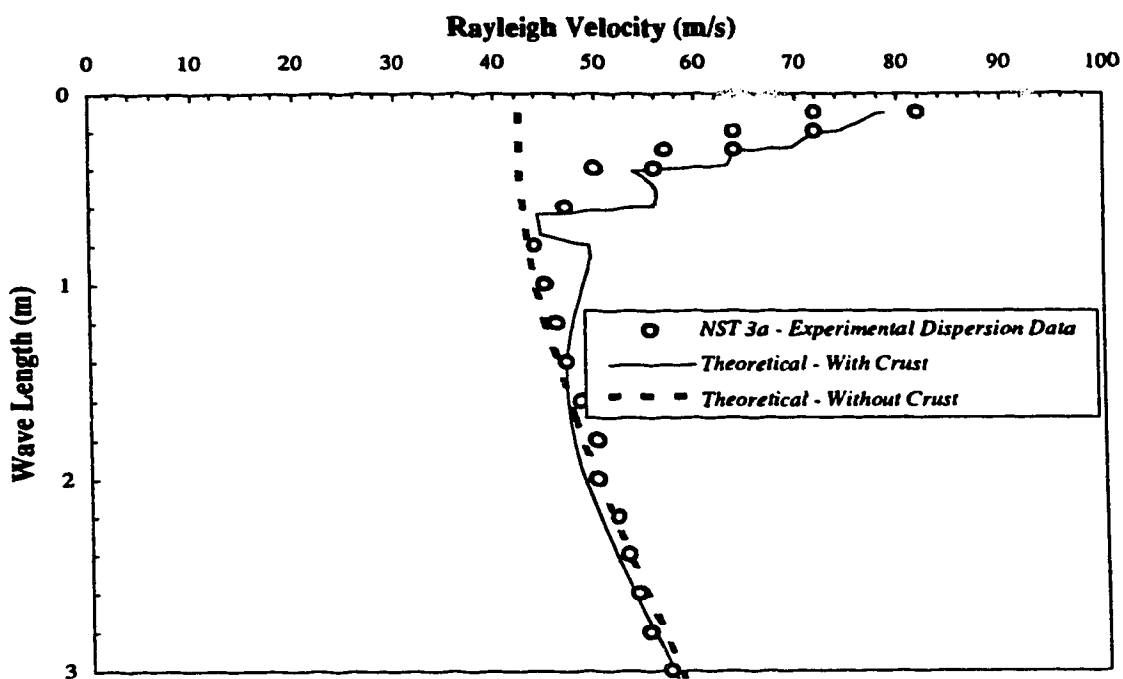


Figure D9 SASW Field and Theoretical Dispersion Curves - Suncor NST Cell 3a

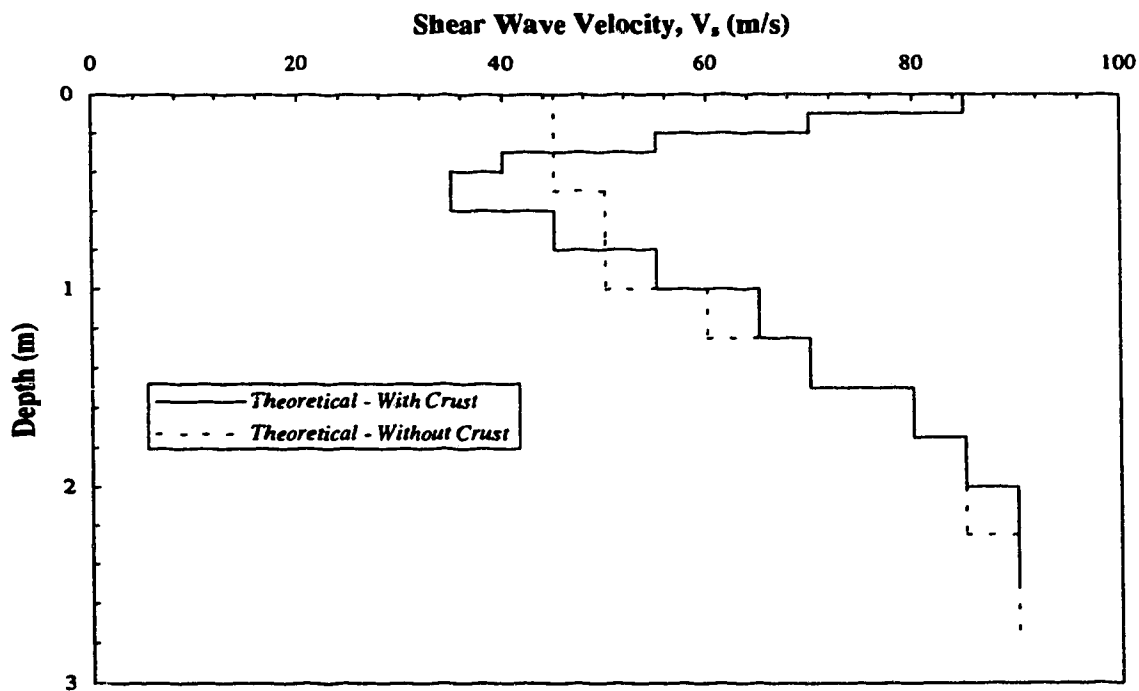


Figure D10 SASW Estimated Shear Wave Velocity Profiles - Suncor NST Cell 3a

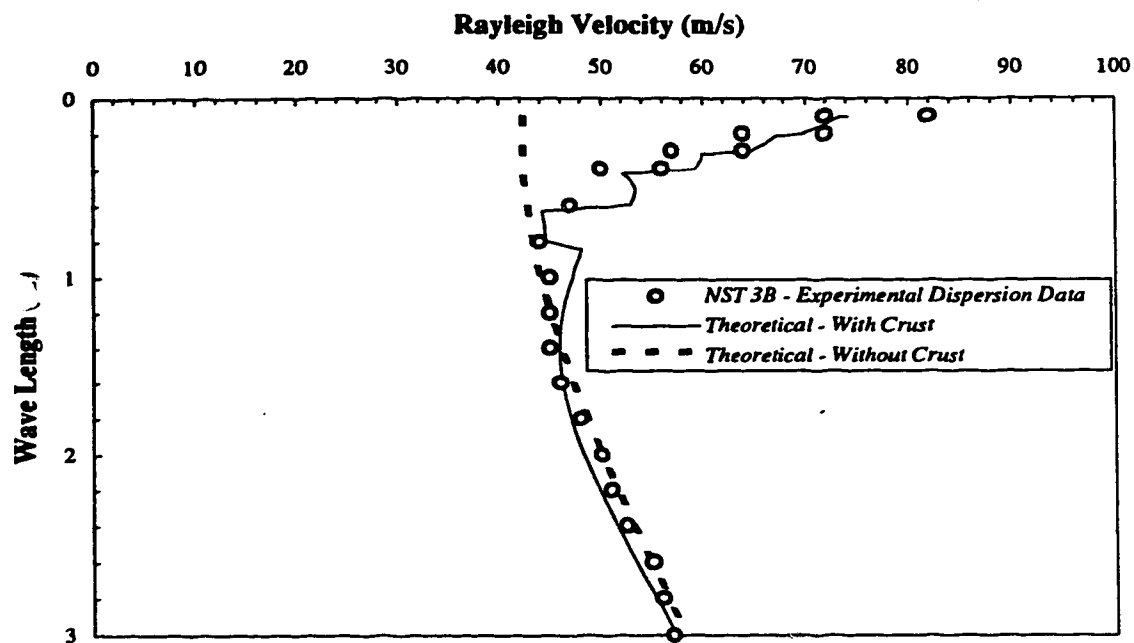


Figure D11 SASW Field and Theoretical Dispersion Curves - Suncor NST Cell 3b

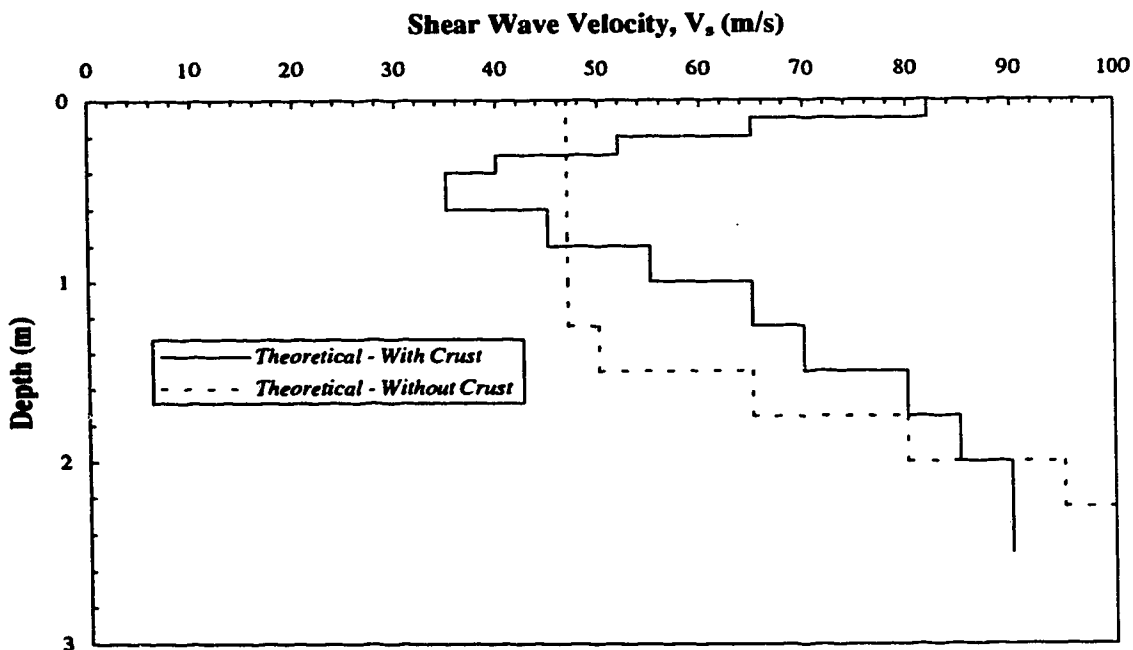


Figure D12 SASW Estimated Shear Wave Velocity Profiles - Suncor NST Cell 3b

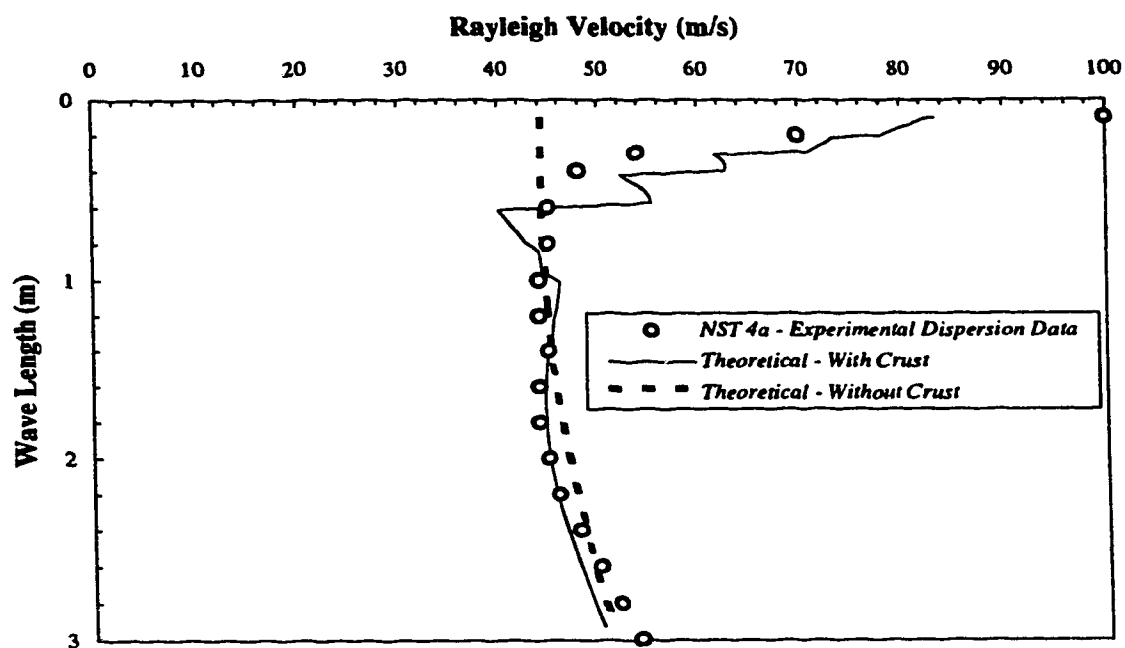


Figure D13 SASW Field and Theoretical Dispersion Curves - Suncor NST Cell 4a

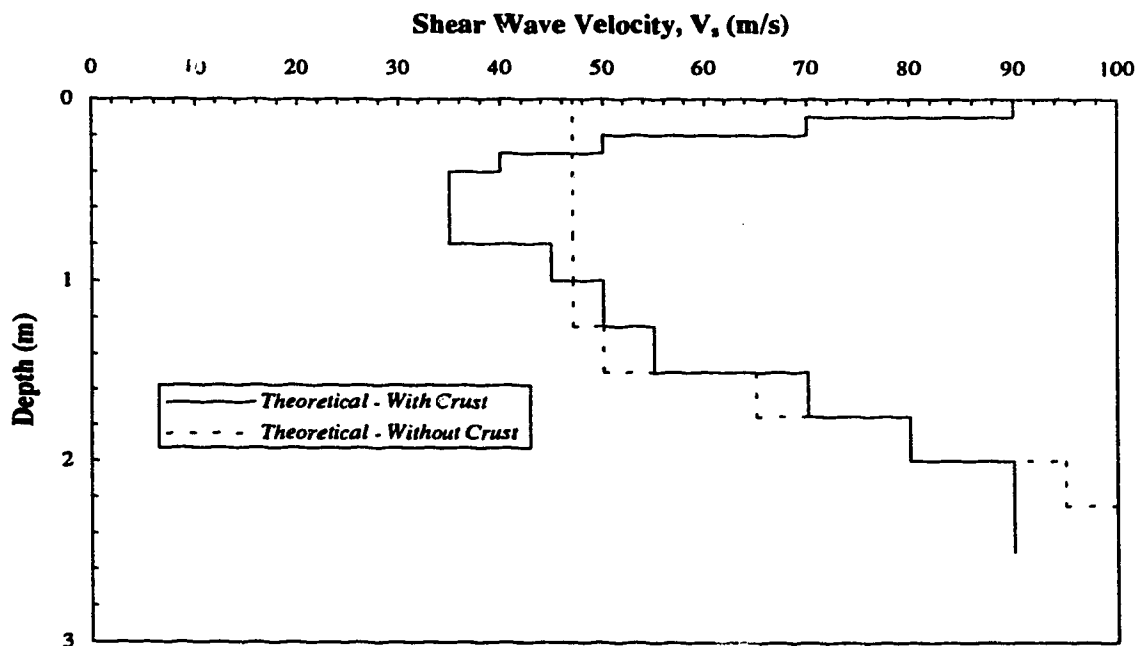


Figure D14 SASW Estimated Shear Wave Velocity Profiles - Suncor NST Cell 4a

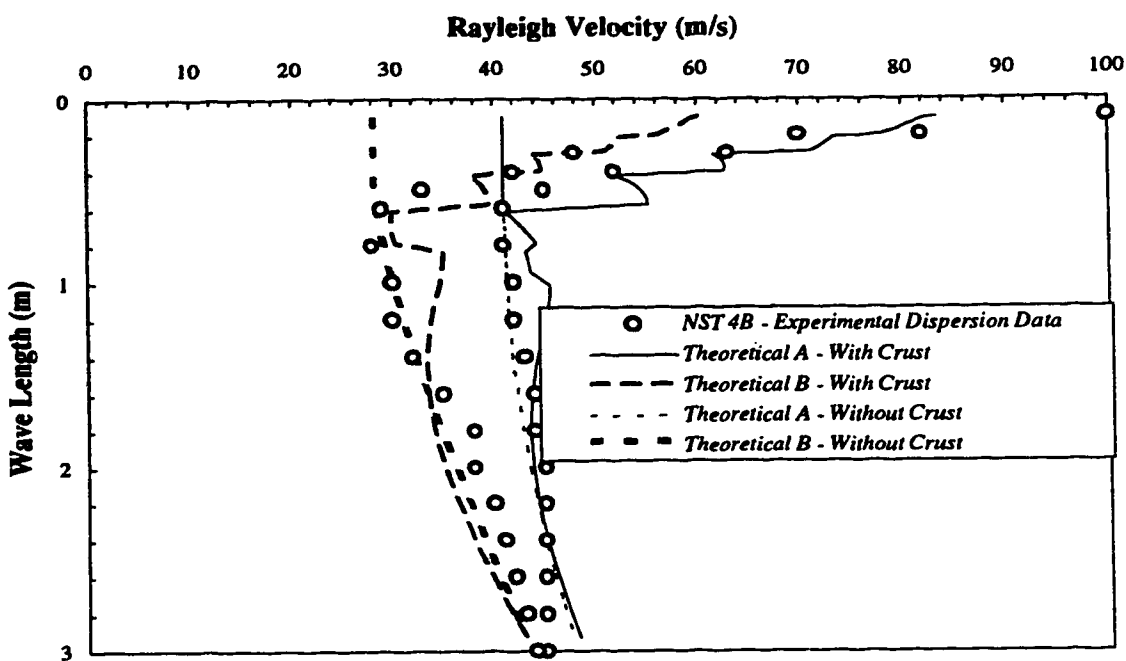


Figure D15 SASW Field and Theoretical Dispersion Curves - Suncor NST Cell 4b

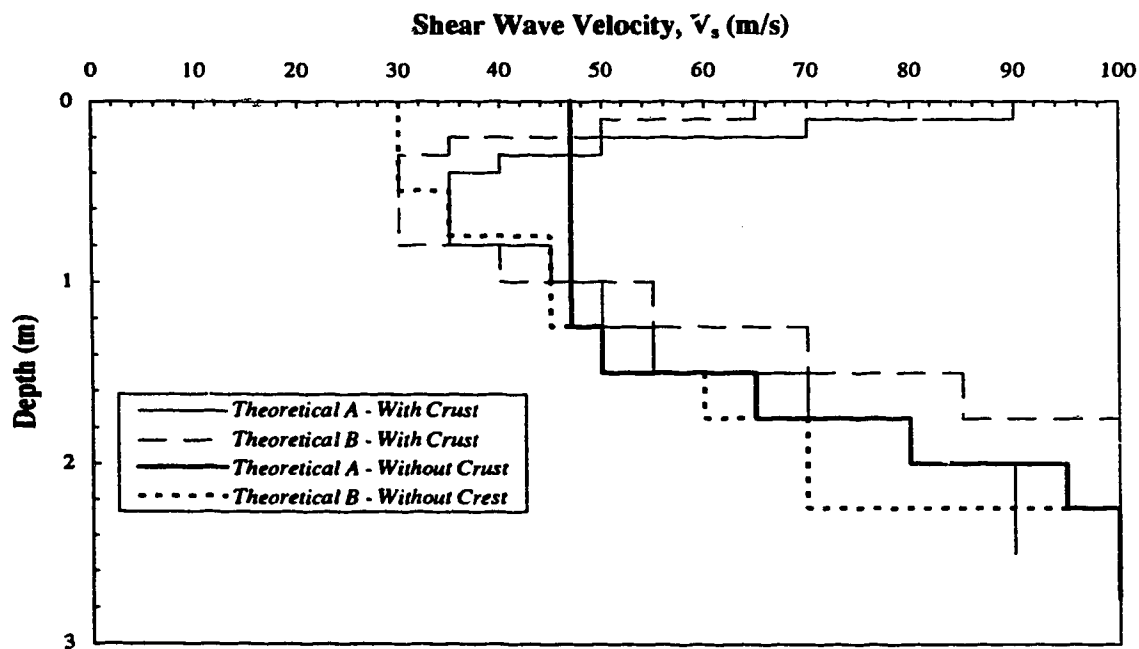


Figure D16 SASW Estimated Shear Wave Velocity Profiles - Suncor NST Cell 4b

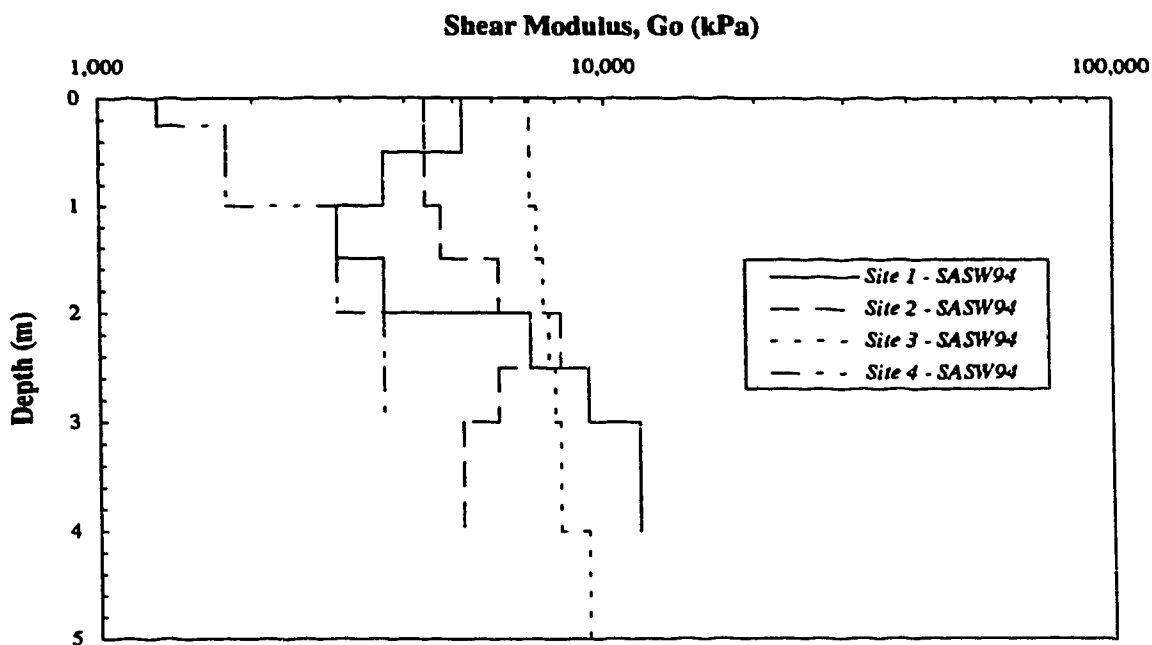


Figure D17 Small Strain Shear Modulus Profiles Along Coal Valley Tailings Beach

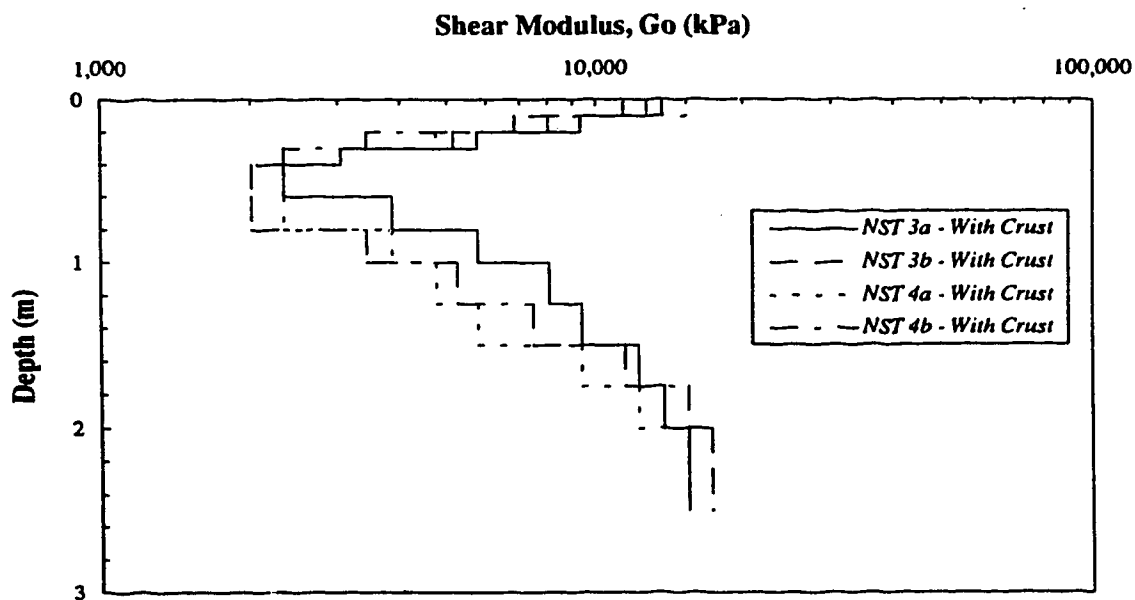


Figure D18 Small Strain Shear Modulus Profiles Within Suncor NST Cells (With Crust)

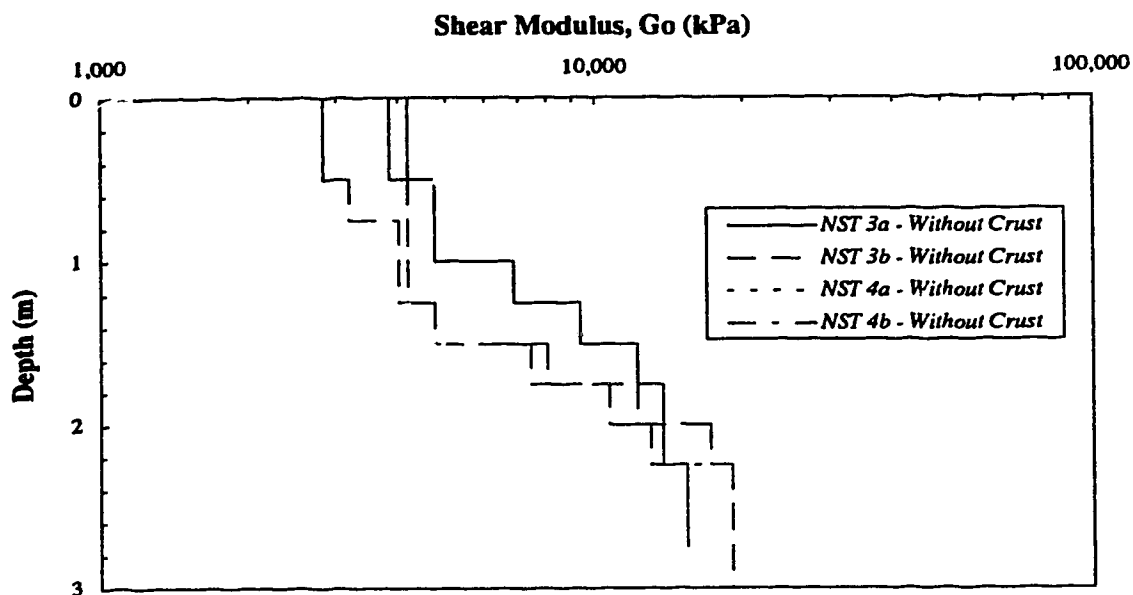


Figure D19 Small Strain Shear Modulus Profiles Within Suncor NST Cells (Without Crust)

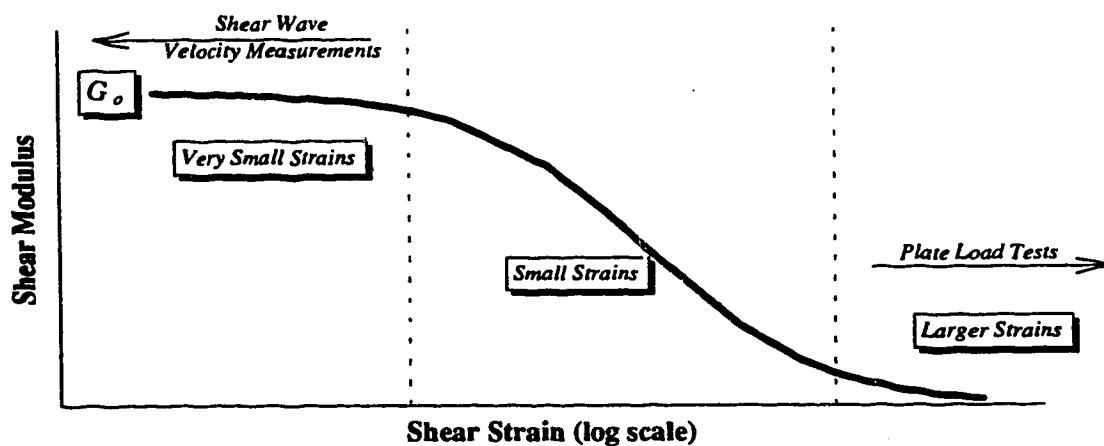


Figure D20 Schematic of Typical Shear Modulus Attenuation Curve (modified from Viggiani and Atkinson 1995)

Appendix E

Increased Shear Strength And Bearing Capacity From Vegetative Root Systems

E.1. SHEAR STRENGTH FORMULATIONS

The effects of fibre reinforcement on the increased shear strength of soils has been discussed extensively in the literature (Waldron 1977, Waldron and Dakessian 1981, Ziemer 1981, Gray and Ohashi 1983, Gray and Al-Refeai 1986, , Maher 1988, Sotir and Gray 1989, Maher and Gray 1990, Al-Rafeai 1991, Terwilliger and Waldron 1991, Day 1993). The focus of much of the literature is directed towards the effect of natural vegetation root systems or artificially placed natural, metal or synthetic fibres on the increase in stability of natural or constructed slopes or embankments.

Based on the stress-strain response of fibre reinforced soils, the effect of roots is to provide an increase in the effective cohesion of the soil with no affect on the internal angle of friction (Gray and Ohashi 1983, Sotir and Gray 1989, Day 1993). Several simplistic empirical formations are presented in the literature which attempt to predict the increase in shear strength of root permeated soils. Sotir and Gray (1989) quote from the literature the shear strength increase of root permeated sands (ΔS_R) based on field and laboratory shear tests between 7.4 to 8.7 psi/lb of root/cf soil. Assuming a root density of 0.8 g/cm³, this increase in soil shear strength from roots translates to:

$$\Delta S_R \{kPa\} = 2550 \left(\frac{A_R}{A} \right) \Rightarrow 3000 \left(\frac{A_R}{A} \right) \quad [E1]$$

where A_R is the cross-sectional area of the roots within the shear zone and A is the total cross-sectional area of the shear zone. The ratio of A_R/A is defined as the Root Area Ratio (RAR) and is assumed in [E1] to equal:

$$RAR = \frac{A_R}{A} = \frac{V_R}{V} \quad [E2]$$

where V_R and V correspond to the volume of roots and total volume of roots and soil within the shear zone respectively.

Waldron (1977) conducted a series of laboratory direct shear tests (following elimination of matric suction within the soil) on soil columns germinated with alfalfa, barley, and yellow pine species. The soil columns included layered combinations of silty clay loam, loamy sand, and sandy gravel. Based on the results, Waldron (1977) devised the following theoretical formulations for the increase in shear strength due to barley roots for lateral displacements of 5 and 25 mm.

$$\Delta S_{R(5mm)} \{kPa\} = 10,800 RAR \Rightarrow \Delta S_{R(25mm)} \{kPa\} = 31,400 RAR \quad [E3]$$

Ziemer (1981) conducted *insitu* direct shear tests on coastal sands containing mature *pinus contorta*. The shear resistance of the root permeated soil was determined along two parallel planes of a partially excavated block sample. After subtracting the shear resistance of the severed soil-root plane cut with a knife, the shear strength based on the dry weight of live roots (root diameter < 17 mm) is reported as:

$$Strength \{kPa\} = 3.13 + 3.31 \times Biomass \{kg/m^3\} \quad [E4]$$

Although specific details regarding the shear test root morphology, and shear strength calculations were not presented, it is assumed that [E4] may in fact represent the increase in shear strength ΔS_R rather than strength as reported by Ziemer (1981). Once again, assuming a dry root density of 0.5 gm/cm^3 , and assuming [E2] as valid, [E4] may be rewritten as:

$$\Delta S_R \{kPa\} = 3.13 + 1660 RAR \quad [E5]$$

Equations [E1], [E3], and [E5] illustrate simplified formulations which predict the increase in shear strength of soil resulting from vegetative root reinforcement. Although these equations illustrate similar trends with respect to RAR , they unfortunately represent different boundary conditions, loading condition, soil types, and root morphologies.

In addition to the empirical relationships above, force-equilibrium models have been developed to predict the strength increase from fibre reinforced soils. These models consider randomly distributed discrete fibers as well as multiple orientated fibre arrays within a soil matrix (Gray and Al-Refeai, 1986). Figure E1 shows the initial model illustrated by Gray and Al-Refeai (1986) which includes fibres orientated perpendicular and inclined within the shear zone, with the inclined fibres orientated in the direction of shearing ($i < 90^\circ$). This model was subsequently expanded as part of this research to reflect the random orientation of vegetative fibres within the soil, and includes fibres which are initially positioned in a compression orientation through the shear zone ($i > 90^\circ$). The model illustrating the two potential initial inclined fibre orientations with $i < 90^\circ$ and $i > 90^\circ$ is illustrated in Figure E2. As illustrated in this model, roots initially in a compression orientation do not contribute to shear strength until the deformation of the shear zone causes sufficient rotation of the roots to develop tensile stresses.

The application of shearing stresses results in deformations, the development of a shearing zone, and the mobilization of tensile resistance in the fibres through friction within the fibre-sand interface. Distortion and development of tensile stress in the fibres results in a tangential stress component which directly opposes shear, and a normal component which increases the confining stress on the failure plane. The predicted strength increase from regular arrays of multiple, orientated fibres is given by the following equations (Gray and Al-Refeai, 1986):

$$\text{Perpendicular Fibres: } \Delta S_R = t_R (\sin \theta + \cos \theta \tan \phi) \quad [E6]$$

$$\text{Inclined Fibres: } \Delta S_R = t_R [\sin(90 - \psi) + \cos(90 - \psi) \tan \phi] \quad [E7]$$

$$\text{where } \psi = \arctan \left[\frac{l}{k + (\tan i)^{-1}} \right] \quad [E8]$$

and t_R is the mobilized tensile strength of fibres (roots) per unit area of soil, ϕ is the angle of internal friction of the sand; θ is the angle of shear distortion; i is the initial orientation angle of the fibre with respect to the shear surface; k is the shear distortion ratio ($k = x/z$) with z being the thickness of the shear zone and x being the horizontal shear displacement. The mobilized tensile strength per unit area of soil is the product of the mobilized tensile stress in the fibre at the shear plane and the area ratio or concentration of fibres in the shear plane and is given as:

$$t_R = \left(\frac{A_R}{A} \right) \sigma_R \quad [E9]$$

The tensile stress developed in the fibres (roots) within the shear zone is defined as σ_R , with A_R and A as defined above.

Maher (1988) modified this tensile stress component in the above equation to include a pullout resistance factor which incorporates fibre skin friction, average confining stress in a triaxial chamber housing reinforced sand, soil properties, probability function defining average number of fibres intersecting a shear plane, fibre modulus, and maximum fibre tensile stress. Maher (1988) found that the modified model satisfactorily predicted the behavior of laboratory experiments up to an fibre length to diameter (L/d) ratio of 100.

E.1.1. Fibre Orientation Effects

Gray and Al-Refeai (1986) highlight that predictive models indicate the maximum strength increase occurs when reinforcements are oriented in the direction of maximum principal tensile strain. In the direct shear test, this translates to a 60° inclination of fibre reinforcement with respect to the shear zone using dry sand ($\phi = 30^\circ$). This statement is verified experimentally as shown by Gray and Al-Refeai (1986). For randomly orientated fibres, as may be the case in fibre reinforced fill, statistical analysis, confirmed by experimental results, support that the failure envelope for randomly distributed fibres virtually coincides with the envelope for perpendicular fibres as given in [E6].

E.2. THEORETICAL SHEAR STRENGTH AND BEARING CAPACITY PREDICTION

Several simplistic empirical formulations were presented above which attempt to predict the increase in shear strength of root permeated soils. As discussed above, these equations generally only require volume percentage of roots within the soil or area percentage of roots across a shear plane, and are based on specific boundary and loading conditions, soil types, and root morphology. The specifics of these formulations limits their applicability and prevents their confident utilization in prediction of the enhanced shear strength and bearing capacity of root permeated compressible tailings.

The theoretical prediction of the increase in shear strength and bearing capacity offered by natural root systems was determined using the force-equilibrium model illustrated in Figure E2. The stress-strain and deformation conditions beneath a plate load tests conducted on root permeated compressible soils is complex and requires several formative steps and assumptions to predict the increase in shear strength and bearing capacity using this model.

The theoretical approach, using equations [E7] through [E9], firstly requires determination of the *RAR* distribution in the subsurface, followed by consideration of the subsurface fibre orientation

and distribution within the shear zone, account for fibre strength, soil strength, and root pull out or rupture under excessive stress. The sequence of steps followed to determine the shear strength and bearing capacity of root reinforced soils is discussed below.

Large volumeter disturbed samples (Appendix A) of root permeated soil were obtained in July, 1995 from Sites 1 through 4 along the Coal Valley tailings impoundment. The samples were obtained using the ring volumeter technique. The volume of the roots per volume of soil were determined in the laboratory, and the corresponding cross-sectional area of roots per area of soil was determined using [E2].

The Root Area Ratio (*RAR*) versus depth for Sites 1 through 4 at Coal Valley are illustrated in Figure E3. This figure, which records the *RAR* on a logarithmic scale illustrates the exponential reduction of root area with depth at the four sites. It is expected that the step wise reduction in *RAR* is an artifact of the root measurement frequency technique of the otherwise expected continuous nonlinear decreasing profile.

Figure E4 illustrates conceptually the plate load test behavior on root reinforced compressible soils formulated and applied in this research. This conceptual shear zone development model is similar to that illustrated for compressible soils which fail in punching shear as illustrated in Figure E5, part (c). The circumferential shear zone assumed to develop beneath the plate is similar (orientated at 90°) to that shown in Figure E2. The idealized *fibre reinforced* shear zone deformation model shown in Figure E4 was employed to guide the stress-strain development formulation.

In accordance with the random orientation of natural vegetative fibres intersecting the shear zone, 50% of the fibres are assumed initially to be in a tension orientation, with the remaining 50% in a compression orientation. Following development of the shear zone through increasing settlement of the plate (increasing $k = x/z$), roots in compression would rotate within the shear zone and eventually develop tensile stress. Roots which are initially in a compression orientation do not contribute to shear strength until sufficient rotation transpires to achieve a tensile orientation and develop tensile stress.

The shear zone development and ensuing rotation of roots from compression to tension orientations is illustrated in Figure E6. The nondimensional ordinate, relating $\Delta S/t$, as defined in [E7], and the abscissa of initial orientation of the fibres, i , as illustrated in Figure E2, highlight through plate settlement and shear zone development the mobilization of an increasing proportion of roots. Reflection of this root rotation effect and resulting mobilization of an increasing percentage of fibres contributing to shear strength is observed in the empirical formulation presented in [E3].

The shear zone assumes to develop to a depth of $2D_p$ below the depth of the footing or plate (D_p = diameter of plate), with the shear zone displacement, k , decreasing linearly with depth from a maximum of $k=s/z$ at the surface (where s is the plate settlement and z is the shear zone thickness as illustrated in Figure E2 and assumed equal to 10 mm), to a minimum of zero at a depth $2D_p$. The thickness of the shear zone is difficult to estimate, and is likely not invariant as shear progresses (Waldron and Dakessian 1981). As illustrated by Waldron and Dakessian (1981), the effect of the estimated shear zone thickness on ΔS_R is most significant at small displacements (2 to 20 mm), with the estimated shear zone thickness showing little effect on the computed ΔS_R at larger displacements.

In addition to the shear zone development assumption, consideration was given to potential root slippage. The minimum length of root required to avoid slippage is given as (Waldron, 1972):

$$L_{min} = \frac{\sigma_R d}{4\tau_B} \quad [E10]$$

where L_{min} is the minimum root length, σ_R is the root tensile strength, d is the root diameter, and τ_B is the limiting bond stress between soil and root. Considering a σ_R of 20 kg/cm² (Schiechl 1980, Naeth 1995), an average d of 0.3 mm, and a τ_B of 25 g/cm², the L_{min} of 5 cm is computed. The average d of about 0.3 mm is based on laboratory measurements and visual estimations of the roots obtained from Coal Valley. Estimation of independent and accurate root tensile strengths is difficult; firstly because of gripping difficulties in laboratory experiments; and

secondly because of root morphological variables including growing environment, seasonal variations, diameter, and species (Anderson and Richards (1987)). The root tensile strengths reported in the literature (Schiechtl 1980, Anderson and Richards 1987) indicated variations of greater than one order of magnitude for specific vegetative species. Based on Schiechtl (1980) and Naeth (1995), a lower bound estimate of σ_R of 20 kg/cm² was chosen for the reed canary root systems present at Coal Valley. A lower bound rather than an average value was chosen in order to artificially account for potential root rupture beneath the sharp edges of the plunging plate load test.

The τ_B values reported in the literature are also extremely variable and depend on a variety of factors including *insitu* soil conditions and soil type, root tortuosity within the soil, root skin texture and presence of root hairs. Values of τ_B reported by Waldron and Dakessian (1981) range from 25 to 800 g/cm² for a variety of conditions. Based on model simulations, Waldron and Dakessian (1981) reported that saturated clay loam impregnated with barley and pine root systems indicated a τ_B of 25 g/cm², and this value was chosen for the analysis. Based on these assumptions and the resulting computed L_{min} of 5 cm, the ΔS_R in the upper 5 cm of was subsequently reduced to account for root slippage. Assuming an average inclined root orientation of 30° to the vertical, the resultant ΔS_R in the upper 5 cm of soil was reduced by 40%.

It is emphasized that the assumptions above are gross approximations attempting to account for the complex stress-strain distribution beneath a plate load test conduct on root reinforced compressible soils. Although the assumptions are unlikely completely correct, they follow a rational approach and are indicative of the expected general trend of behavior.

With the assumptions above, the *RAR* measurements in Figure E3, the theoretical increase in shear strength from vegetative root systems, the ΔS_R mobilized beneath the plate load test is computed as illustrated in Figures E7 to E10 for Sites 1 through 4 respectively at Coal Valley. These figures assume an average friction angle ϕ for the soil of 22°, and illustrate the influence of increasing plate load test settlement (increasing k) causing increased root rotation from compression to tension orientations within the shear zone.

The nonlinear ΔS_R profiles above were subsequently coupled with bearing capacity theory to predict the increase in bearing capacity resulting from root reinforcement. The increase in bearing capacity, ΔQ_{roots} , resulting from root reinforcement was determined using, as a framework, the cohesion component formulation of the general bearing capacity equation (Bowles 1988, Vesic 1973, Vesic 1975) shown as:

$$\Delta Q_{roots} = N_c s_c \Delta S_R \quad [E11]$$

where N_c is the bearing capacity factor for cohesion (5.14), s_c is the shape factor for a circular footing (1.2), and ΔS_R is the theoretical shear strength from root reinforcement as shown in Figures E7 through E10.

The theoretical contribution of vegetative root systems to increase bearing capacity at Sites 1 through 4 at Coal Valley using [E11] is illustrated in Figures E11 to E14 respectively. These figures illustrate the theoretical increase in bearing capacity from the vegetative root system, coupled with the 1991 tailings surface (*ts*) plate load test profiles. The plate load tests conducted in 1994 on the vegetated tailings surface (*vts*) are also illustrated. Since plate load tests were not conducted at Site 3 in 1994, no comparison could be provided in Figure E13. The bearing capacity contribution from root reinforcement considers root tensile strengths, σ_R , ranging from 2000 kPa to 3000 kPa (20 to 30 kg/cm²), which still reflect lower bound strength ranges and provide conservatism for potential root rupture as discussed above.

Although several preliminary assumptions and estimates were made to model the soil-root interaction mechanics beneath a *PLT* on compressible tails at Coal Valley, the predicted increase in bearing capacity at Sites 1 and 4 are within the same range as the 1994 vegetated tailings surface (*vts*) results. The comparison at Site 2 between the 1991 (*ts*) bearing capacities coupled with root reinforcement predictions and the 1994 (*vts*) results is less encouraging.

Several comments are forwarded to highlight the potential factors contributing to the discrepancies, particularly those observed at Site 2. In addition to the assumptions discussed above which may include some error, site heterogeneity may provide influences. As discussed in

Chapters 2, 5, and 6, the tailings are heterogeneous on the scale of millimeters to centimeters, with plate load test and sampling locations positioned 1 to 2 meters apart possibly experiencing slightly contrasting soil conditions. Secondly, the vegetative development at the various sites exhibited some surficial nonuniformity, with likely some root development and density contrasts present on a local scale. Hence, slightly dissimilar *RAR* profiles may have existed between sampling and PLT locations. Lastly, due to logistics and research development phase, the vegetative root measurements were conducted in the summer of 1995 rather than in 1994 when the plate load tests were conducted. Although the vegetation development appeared seemingly unchanged from 1994 to 1995, some minor changes are expected with vegetation maturity.

E.3. SOIL-FIBRE INTERACTION VARIABLES

Maher (1988) developed a theoretical model employing the shear strength equations defined above to investigate sand and fibre interactions. The works of Waldron (1972), Gray and Ohashi (1983), and Gray and Al-Refeai (1986) were used to formulate the mechanics of fibre contribution to “randomly distributed reinforced sand” composites as outlined in Maher (1988). In addition, several laboratory triaxial compression tests were conducted using different sands and associated granulometric properties, and several fibre types with varying strength, modulus, and skin friction properties. Based on the laboratory tests which were generally collaborated by the model, Tables E1 and E2 were prepared based on Maher’s (1988) findings. The strength increase of the soil-fibre composite material, σ_1 , (Tables E1 and E2) refers to the major principal stress defined in triaxial compression tests. The critical confining stress, σ_{crit} , defines the confining stress at which a transition or break occurs within the curved-linear or bilinear failure envelopes. Beyond the defined σ_{crit} , the reinforced soil failure envelope displays the same slope as the unreinforced soil envelope plotted in σ_1 and σ_3 stress space.

In addition to the summary provided above (which was in part collaborated by the earlier laboratory tests outlined by Gray and Ohashi (1983) and Gray and Al-Refeai (1986)) Gray and Ohashi (1983) report that fibres defined as ideally extensible which did not rupture, not only

contributed to peak strength, but also reduced the post peak reduction in shear strength of dense sands (Gray and Al-Refeai 1986). Furthermore, Gray and Al-Refeai (1986) report that rougher rather than stiffer fibres are more effective in increasing the strength of a fibre reinforced soil. Waldron and Dakessian (1981) supported this finding through extension of the initial soil root model to predict the amount of increase in soil reinforcement produced by stretching, slipping, and breaking roots. Based on model simulations and experiments considering various parameters including root length, shear zone thickness, and root strength, it was determined that the strength of the soil-root bond, τ_B , is the most important unmeasured parameter.

A variety of issues were presented above which may explain some of the discrepancies observed with the plate load test results illustrated in Figure E11 to E14. Although the focus of the information in this appendix is not to rationalize the differences, evidence is provided in Tables E1 and E2 which support the different theoretical capacities predicted at Site 4 and particularly Site 2. This evidence is coupled with the potential errors provided in the previous section namely soil heterogeneity, vegetation nonuniformity, and contrasting sampling and PLT investigation periods.

E.4. PARAMETRIC ANALYSIS OF THEORETICAL MODEL PREDICTIONS

A limited parametric study was conducted to evaluate the impact of the values discussed in Section E2., in computation of the theoretical increase in bearing capacity. The key variables which were evaluated include the soil friction angle, ϕ , the root tensile strength, σ_R and the level of shear zone development, k . These variables were evaluated for Sites 1 through 4 at Coal Valley considering the influence of footing size and the nonlinear decreasing shear strength profiles offered by the vegetative root systems shown in Figures E7 through E10. The theoretical increase in bearing capacities considering the parametric analysis is illustrated in Figures E15 through E18 for Coal Valley Sites 1 through 4 respectively. As illustrated in the figures, the decreasing trend of ΔQ_{roots} with increasing footing diameter is reflective of the decreasing RAR with increasing depth. This trend indicates that large footing areas (for example a wide pad

construction vehicle designed for weaker soils) would benefit less from the root reinforcement than smaller footing areas (for example human or animal traffic).

The parametric analysis also indicates that the selected friction angle of the soil has little effect on the theoretical increase in bearing capacity. However, the critical factors to consider include the tensile strength of the roots, σ_{roots} and the degree of shear zone development, k . Although this parametric analysis is not complete and a variety of other variables may be investigated, it nonetheless indicates the sensitivity and perhaps the complications with accurate determination of the increase in bearing capacity of root reinforced compressible tailings and perhaps provides a starting point for future studies.

E.5. REFERENCES

- Al-Refeai, T.O., 1991. Behavior of Granular Soils Reinforced with Discrete Randomly Orientated Inclusions. *Geotextiles and Geomembranes* **10**: 319-333.
- Anderson, M.G., and Richards, K.S., 1987. **Slope Stability: Geotechnical Engineering and Geomorphology** (Chapter 6), John Wiley and Sons, New York, New York.
- Bowles, J.E., 1988. **Foundation Analysis and Design**. McGraw-Hill, Inc., New York, New York, 1004 pgs.
- Craig, R.F., 1983. **Soil Mechanics**. (Third Edition), Van Nostrand Reinhold (UK) Co. Ltd., Berkshire, England, 419 pgs.
- Day, R.W., 1993. Surficial Slope Failure: A Case Study. *ASCE Journal of Performance of Constructed Facilities* **7**(4): 264-269.
- Gray, D.H., and Al-Refeai, T., 1986. Behavior of Fabric-Versus Fibre-Reinforced Sand. *ASCE Journal of Geotechnical Engineering*, **112**(8) 804-821.
- Gray, D.H., and Leiser, A.T., 1982. **Biotechnical Slope Protection and Erosion Control**. Van Nostrand Reinhold Company, New York, New York, 271 pgs.
- Gray, D.H., and Ohashi, H., 1983. Mechanics of Fibre Reinforcement in Sand. *ASCE Journal of Geotechnical Engineering* **109**(3): 335-353.
- Ismael, N.F. and Vesic, A.S., 1981. Compressibility and Bearing Capacity. *Journal of Geotechnical Engineering*, ASCE, No GT. 12, pp. 1677-1691

- Maher, M.H., 1988. Static and Dynamic Response of Sands Reinforced With Discrete, Randomly Distributed Fibres. Ph.D. Thesis, The University of Michigan.
- Maher, M.H., and Gray, D.H., 1990. Static Response of Sands Reinforced with Randomly Distributed Fibres. *ASCE Journal of Geotechnical Engineering* **116**(11): 1661-1677.
- Naeth, A., 1995. Personal Communications. Assistant Professor, Department of Renewable Resources, The University of Alberta, Edmonton, Alberta.
- Schiechtl, H., 1980. **Bioengineering for Land Reclamation and Conservation**. University of Alberta Press, Edmonton, Alberta, 400 pgs.
- Sotir, R.B., and Gray, D.H., 1989. Fill Slope Repair Using Soil Bioengineering Systems. *Journal of Public Works*, **120**(13): 37-40, 77.
- Terwilliger, V.J., and Waldron, L.J., 1991. Effects of Root Reinforcement on Soil-Slip Patterns in the Transverse Ranges of Southern California. *Geological Society of America Bulletin* **103**: 775-785.
- Vesic, A.S., 1973. Analysis of Ultimate Loads of Shallow Foundations. *Journal of Soil Mechanics and Foundation Division, ASCE*, **99**(1):45-73.
- Vesic, A.S., 1975. Chapter 3 of Winterkorn, H.F., and Fang, H.Y.. *Foundation Engineering Handbook*. Van Nostrand.
- Waldron, L.J. and Dakessian, S., 1981. Soil Reinforcement by Roots: Calculation of Increased Soil Shear Resistance From Root Properties. *Soil Science* **132**(6): 427-435.
- Waldron, L.J., 1977. The Shear Resistance of Root-Permeated Homogeneous and Stratified Soil. *Soil Science Society of America*, **41**: 843-849
- Ziemer, R.R., 1981. Roots and Stability of Forested Slopes. *International Association of Hydrological Sciences, Publication No. 132*: 343-361.

Table E1 **Influence of Soil Properties on Increased Strength and Increased Critical Confining Stress of Fibre Reinforced Soil** (*developed from Maher, 1988*).

Strength Increase ($\uparrow \sigma_1$), ($\uparrow \Delta S_R$)	Critical Confining Stress Increase ($\uparrow \sigma_{crit}$)
Decrease Sand Grain Size ($\downarrow D_{50}$)	Negligible Effect of Sand Grain Size
Increase Sand Angularity (\downarrow Sphericity Index)	Increase Sand Roundness (\uparrow Sphericity Index)
Decrease Sand Uniformity ($\uparrow C_u = D_{60}/D_{10}$)	Increase Sand Uniformity ($\downarrow C_u = D_{60}/D_{10}$)

Table E2 **Influence of Fibre Properties on Increased Strength and Increased Critical Confining Stress of Fibre Reinforced Soil** (*developed from Maher, 1988*).

Strength Increase ($\uparrow \sigma_1$), ($\uparrow \Delta S_R$)	Critical Confining Stress Increase ($\uparrow \sigma_{crit}$)
Increase Fibre Content (\uparrow % Fibres)	Negligible Effect of Fibre Content
Increase Length to Diameter Ratio ($\uparrow L/d$)	Decrease Length to Diameter Ratio ($\downarrow L/d$)
Increase Fibre Modulus ($\uparrow E$)	Increase Fibre Modulus ($\uparrow E$)

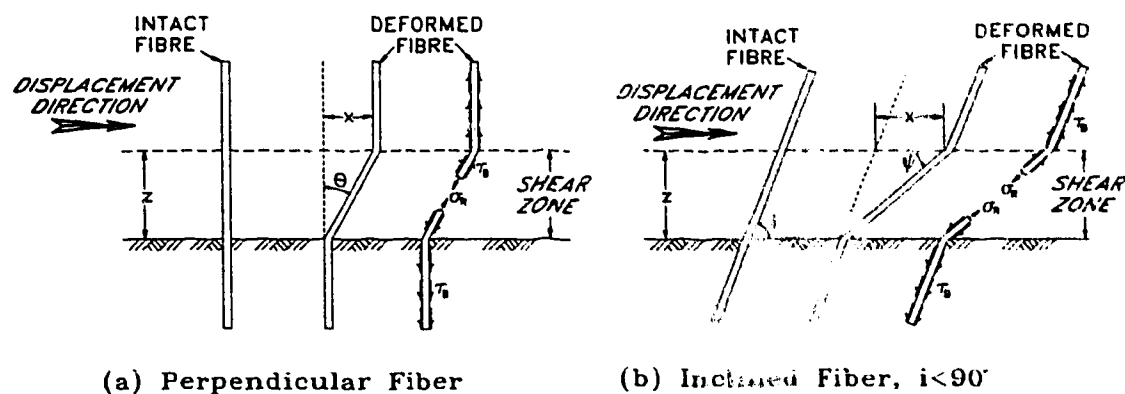


Figure E1 Fibre Reinforcing Model for Perpendicular and Inclined Fibres (modified from Gray and Al-Refeai, 1986)

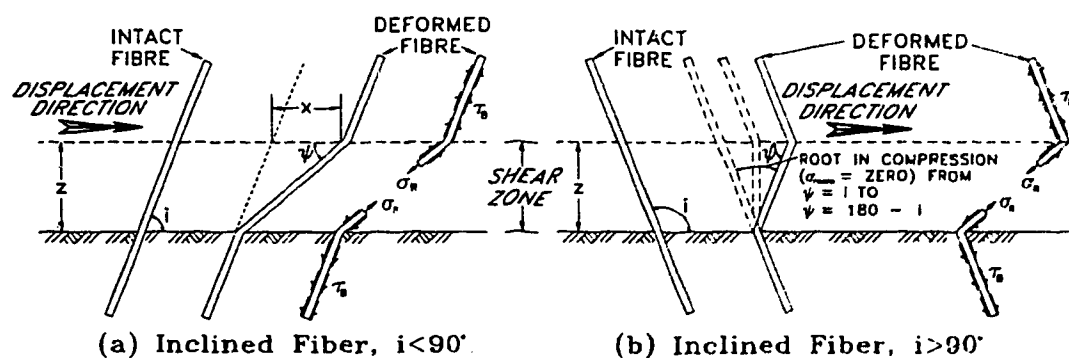


Figure E2 Fibre Reinforcing Model for Inclined Fibres

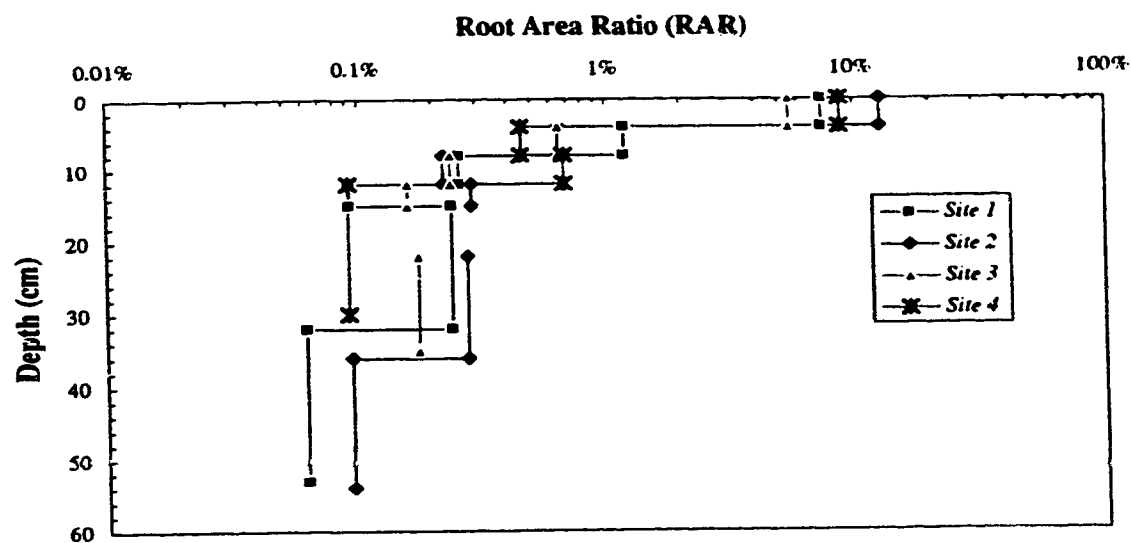


Figure E3 Root Area Ratio (RAR) Profiles Along Coal Valley Tailings Beach

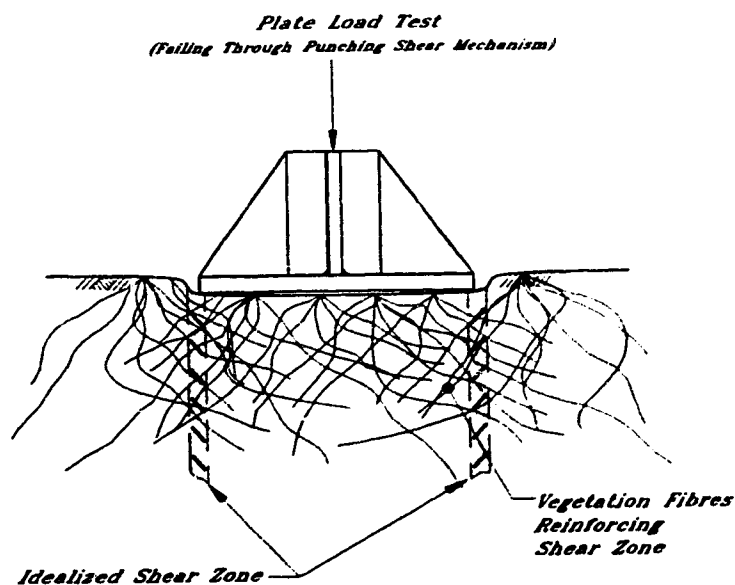


Figure E4 Conceptual Model of Shear Zone Development Beneath a PLT on Compressible Root Reinforced Soil

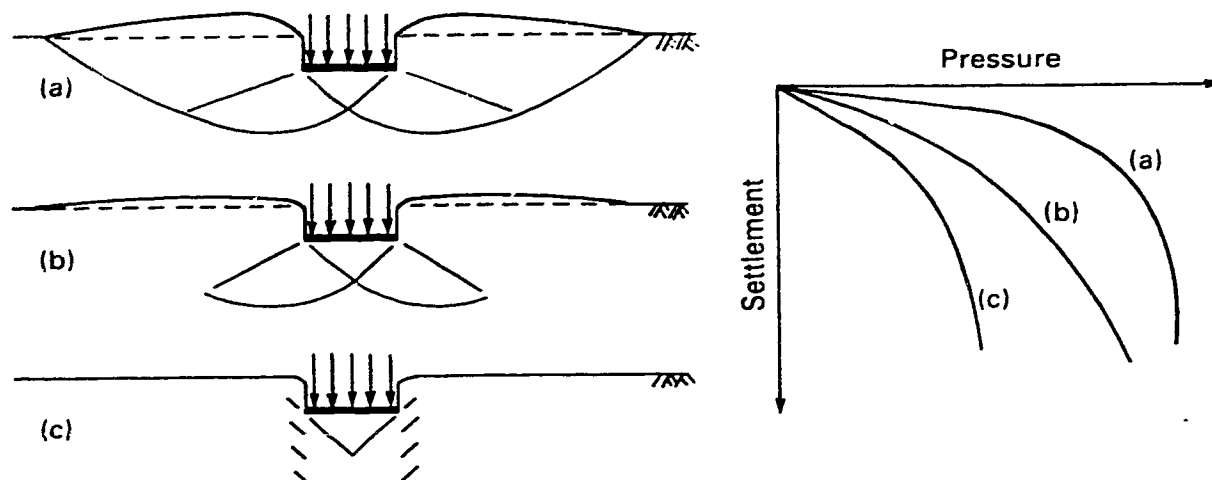


Figure E5 Modes of Bearing Capacity Failure: (a) General Shear, (b) Local Shear, (c) Punching Shear (from Craig 1983)

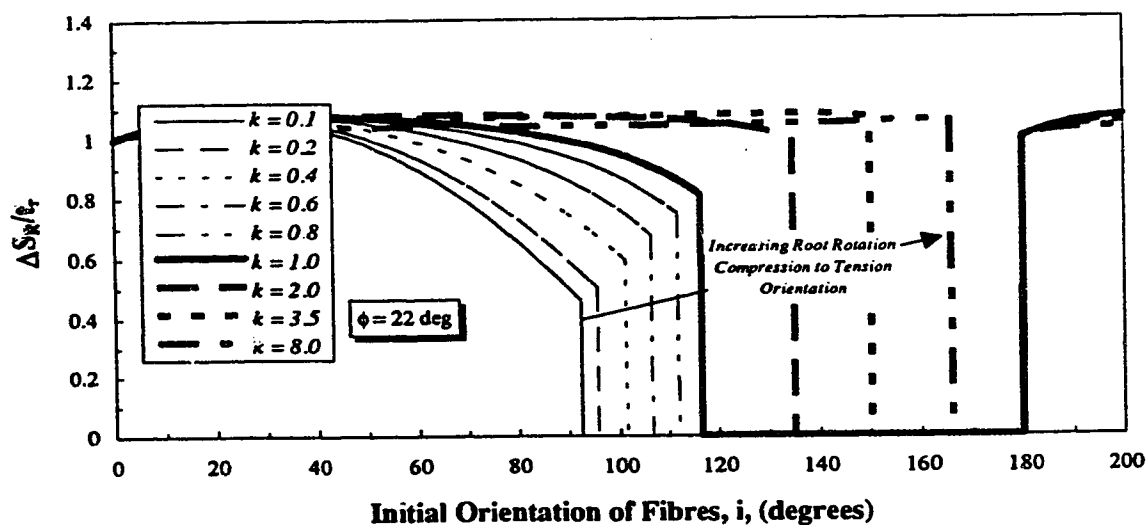


Figure E6 Effect of Shear Zone Displacement (k) and Initial Fibre Inclination (i) on Mobilized Strength Ratio ($\Delta S_R/t_r$)

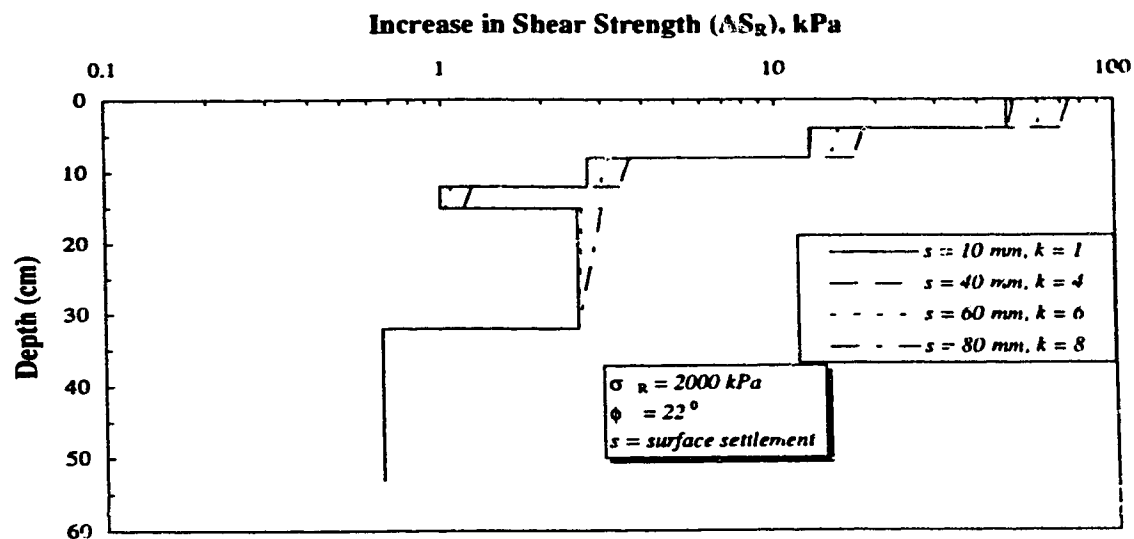


Figure E7 Theoretical Increase in Shear Strenght From Vegetative Root Systems - Coal Valley Tailings Beach - Site 1

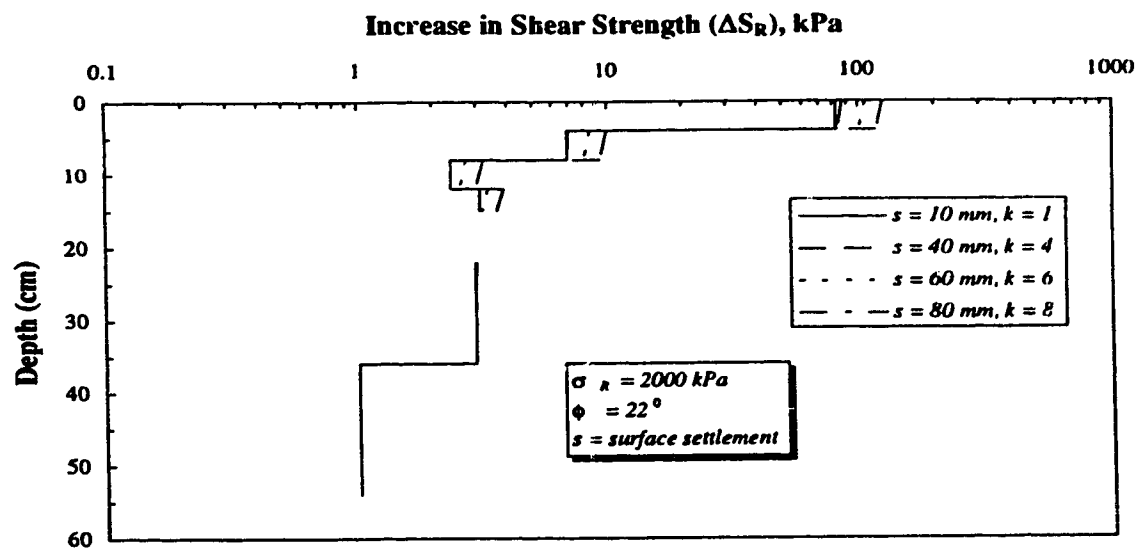


Figure E8 Theoretical Increase in Shear Strenght From Vegetative Root Systems - Coal Valley Tailings Beach - Site 2

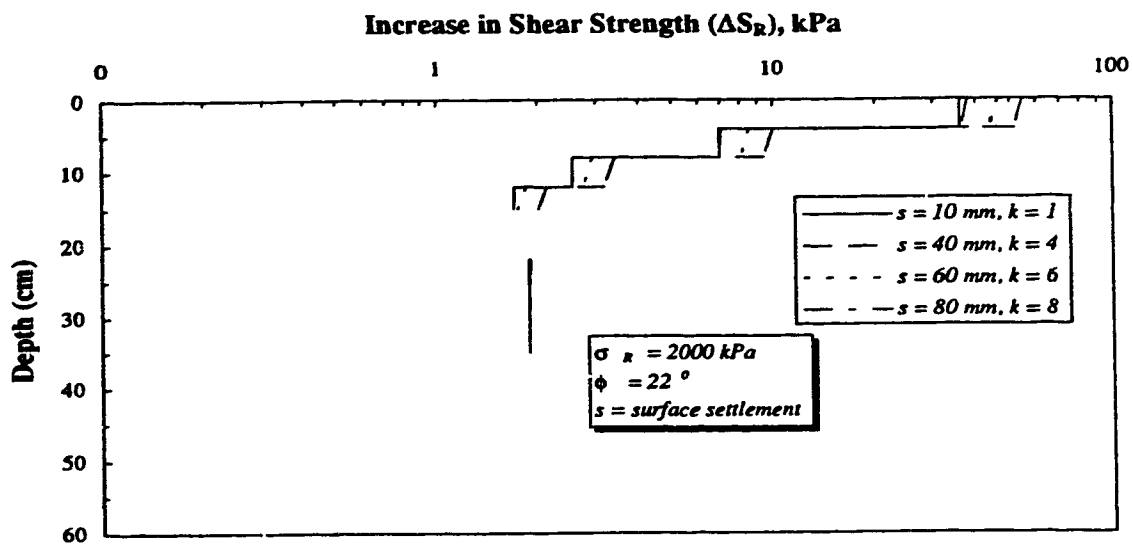


Figure E9 Theoretical Increase in Shear Strength From Vegetative Root Systems - Coal Valley Tailings Beach - Site 3

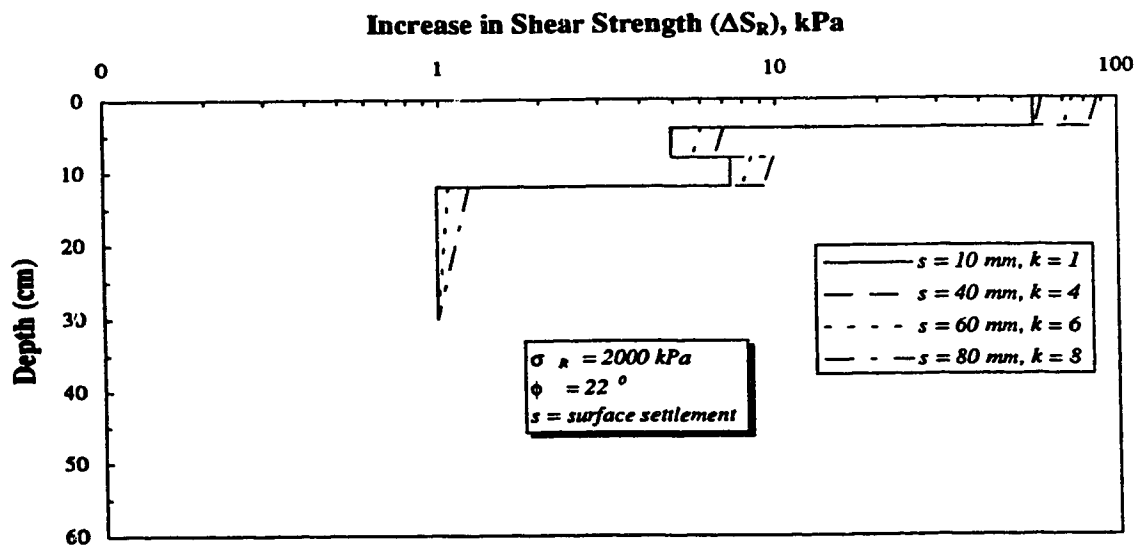


Figure E10 Theoretical Increase in Shear Strength From Vegetative Root Systems - Coal Valley Tailings Beach - Site 4

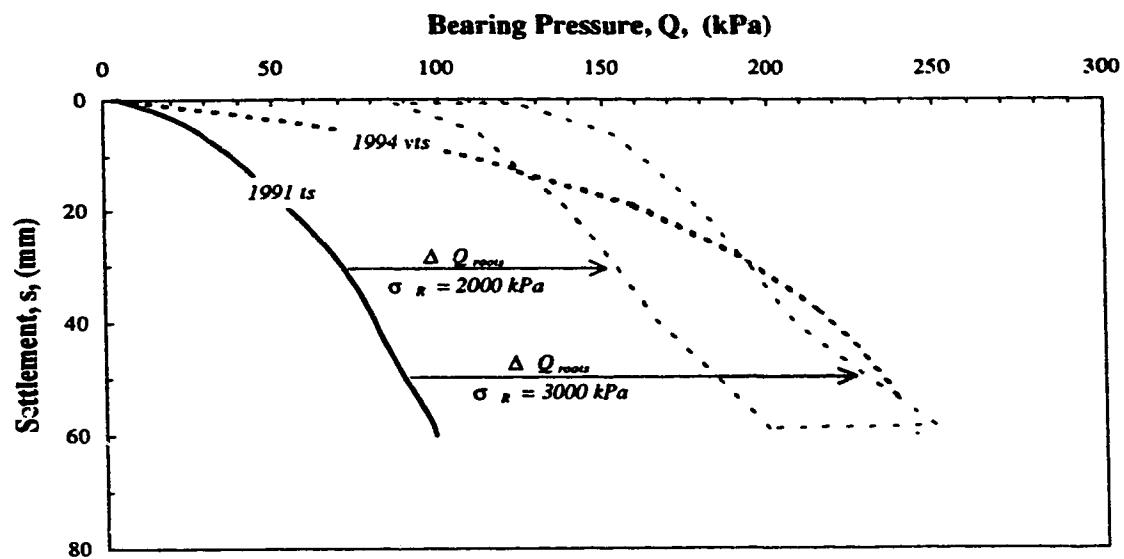


Figure E11 Theoretical Increase in Bearing Capacity From Vegetative Root Systems
- Coal Valley Tailings Beach - Site 1

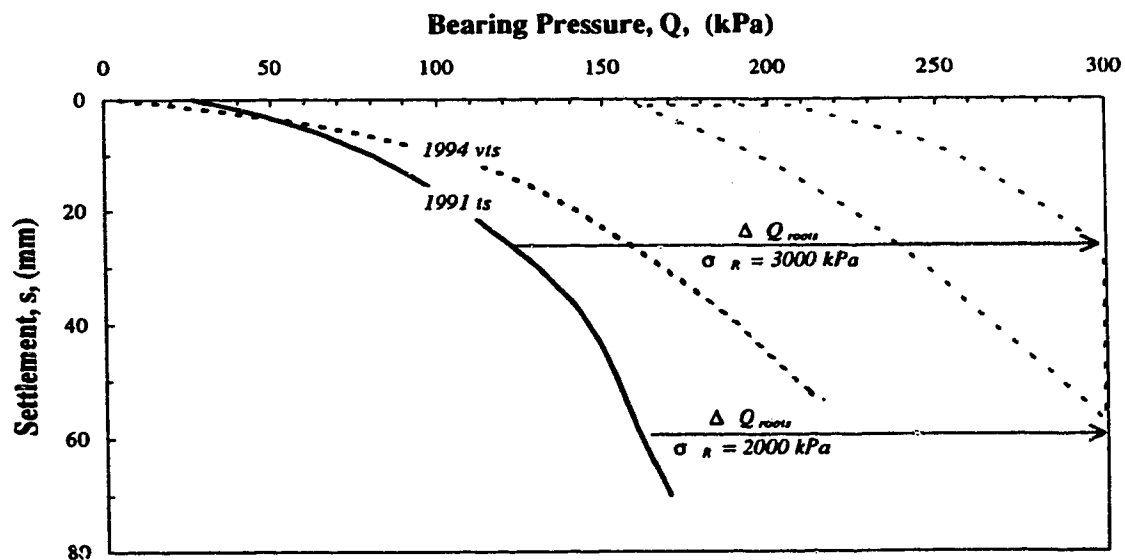


Figure E12 Theoretical Increase in Bearing Capacity From Vegetative Root Systems
- Coal Valley Tailings Beach - Site 2

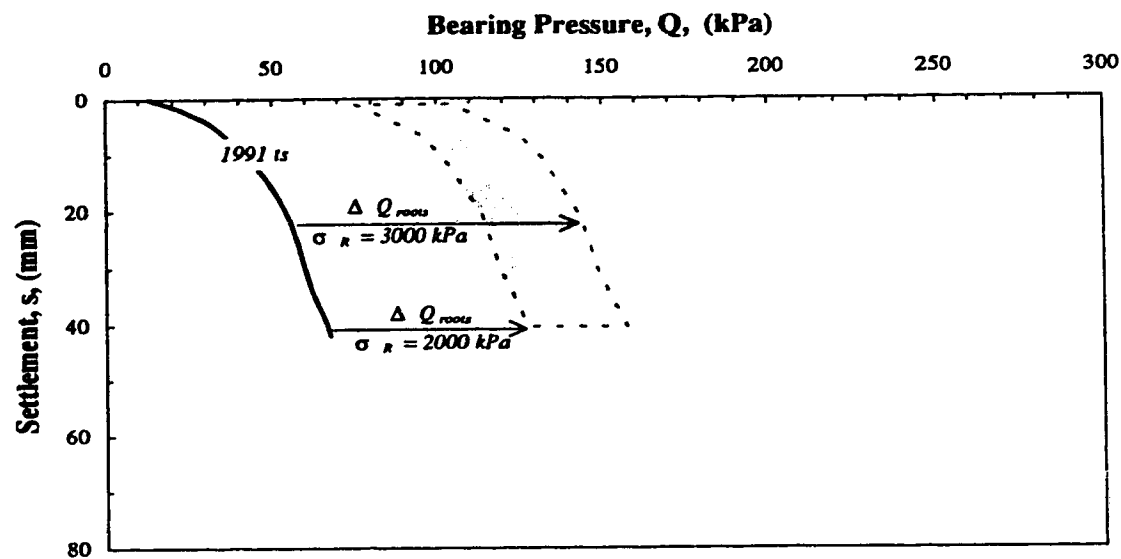


Figure E13 Theoretical Increase in Bearing Capacity From Vegetative Root Systems
- Coal Valley Tailings Beach - Site 3

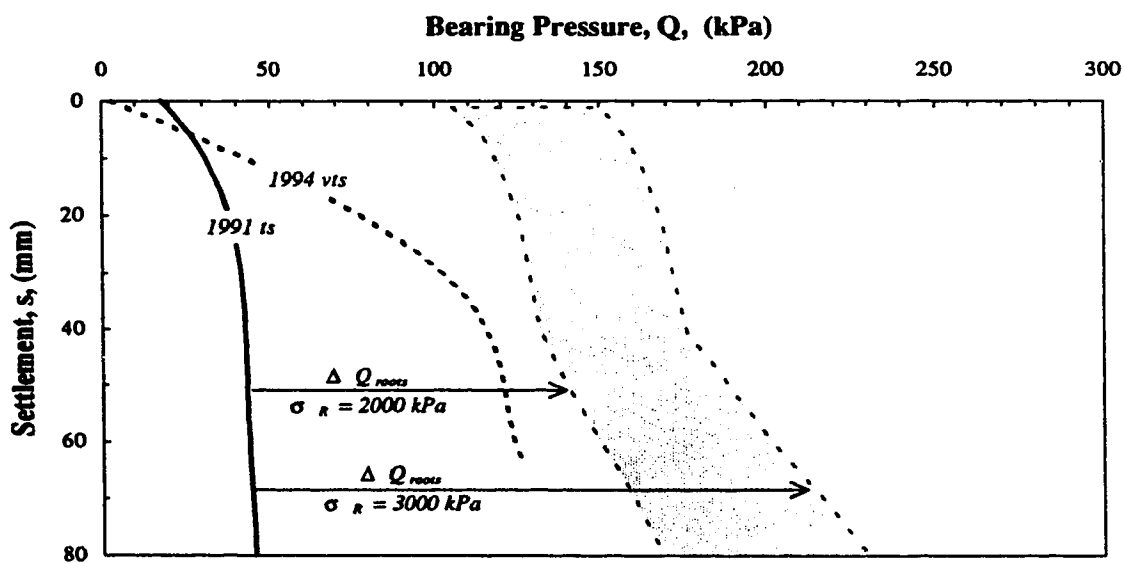


Figure E14 Theoretical Increase in Bearing Capacity From Vegetative Root Systems
- Coal Valley Tailings Beach - Site 4

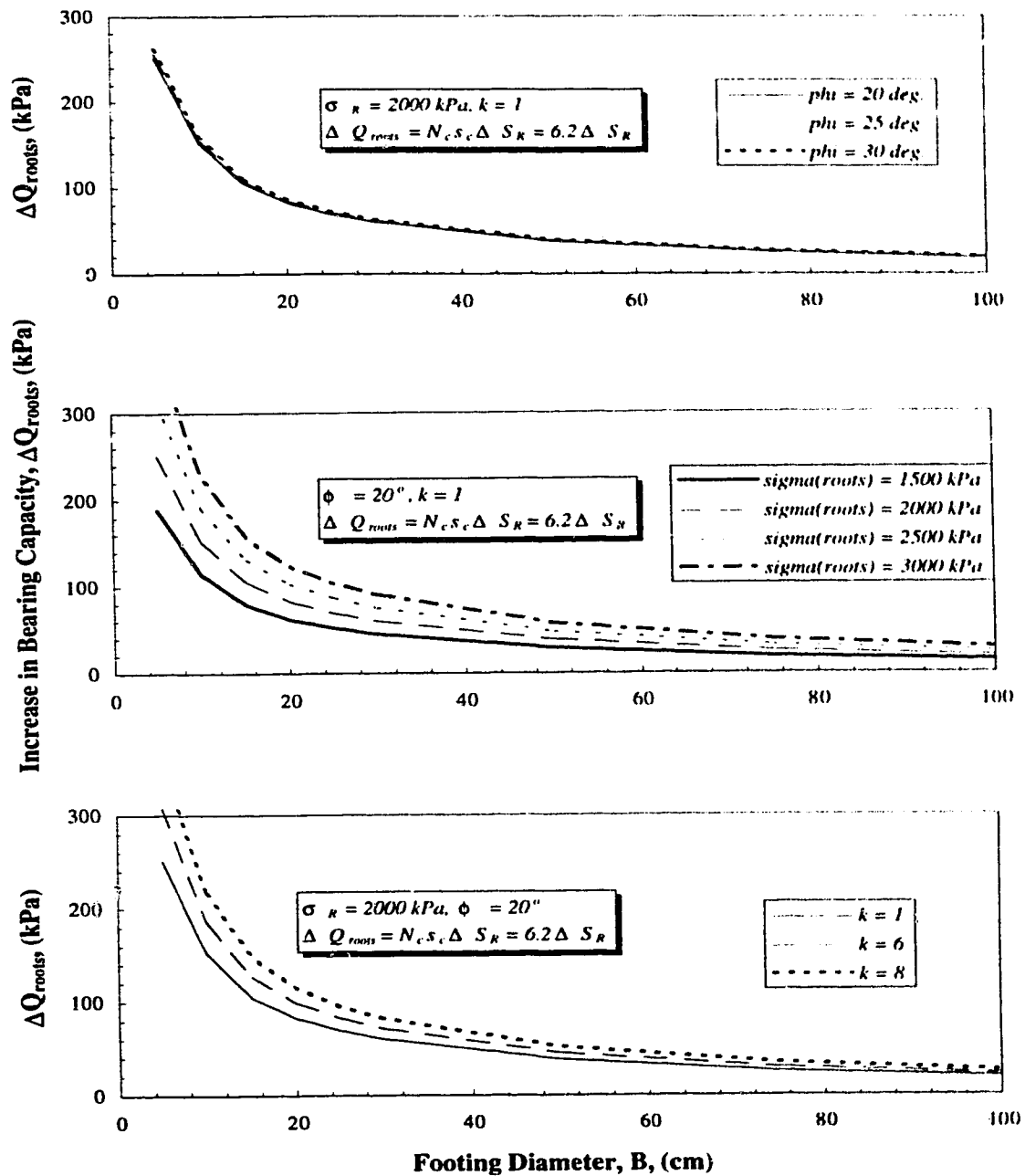
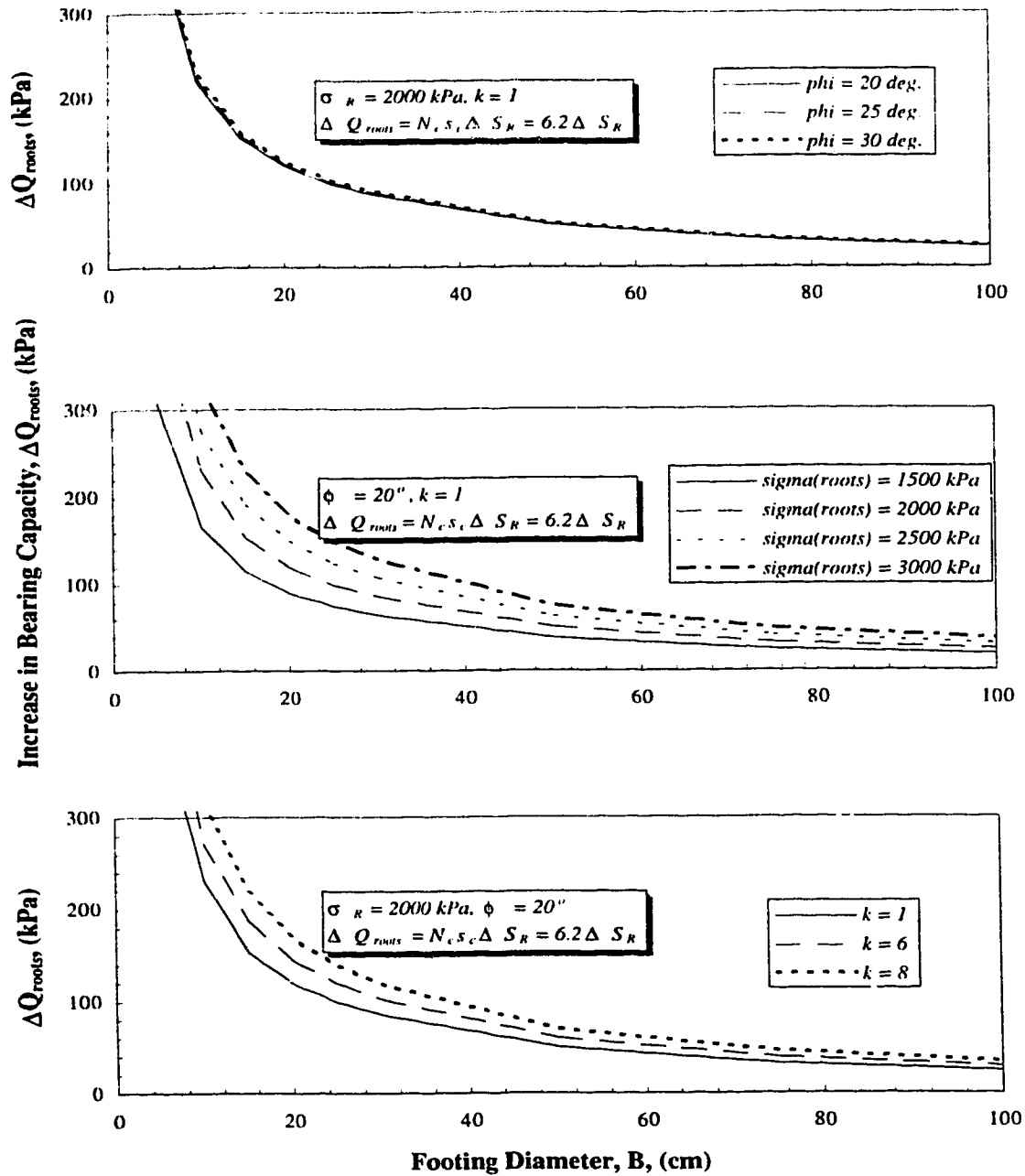


Figure E15

Parametric Analysis of Theoretical Increase in Bearing Capacity From Vegetative Root Systems - Coal Valley Tailings Beach - Site 1

**Figure E16**

Parametric Analysis of Theoretical Increase in Bearing Capacity From Vegetative Root Systems - Coal Valley Tailings Beach - Site 2

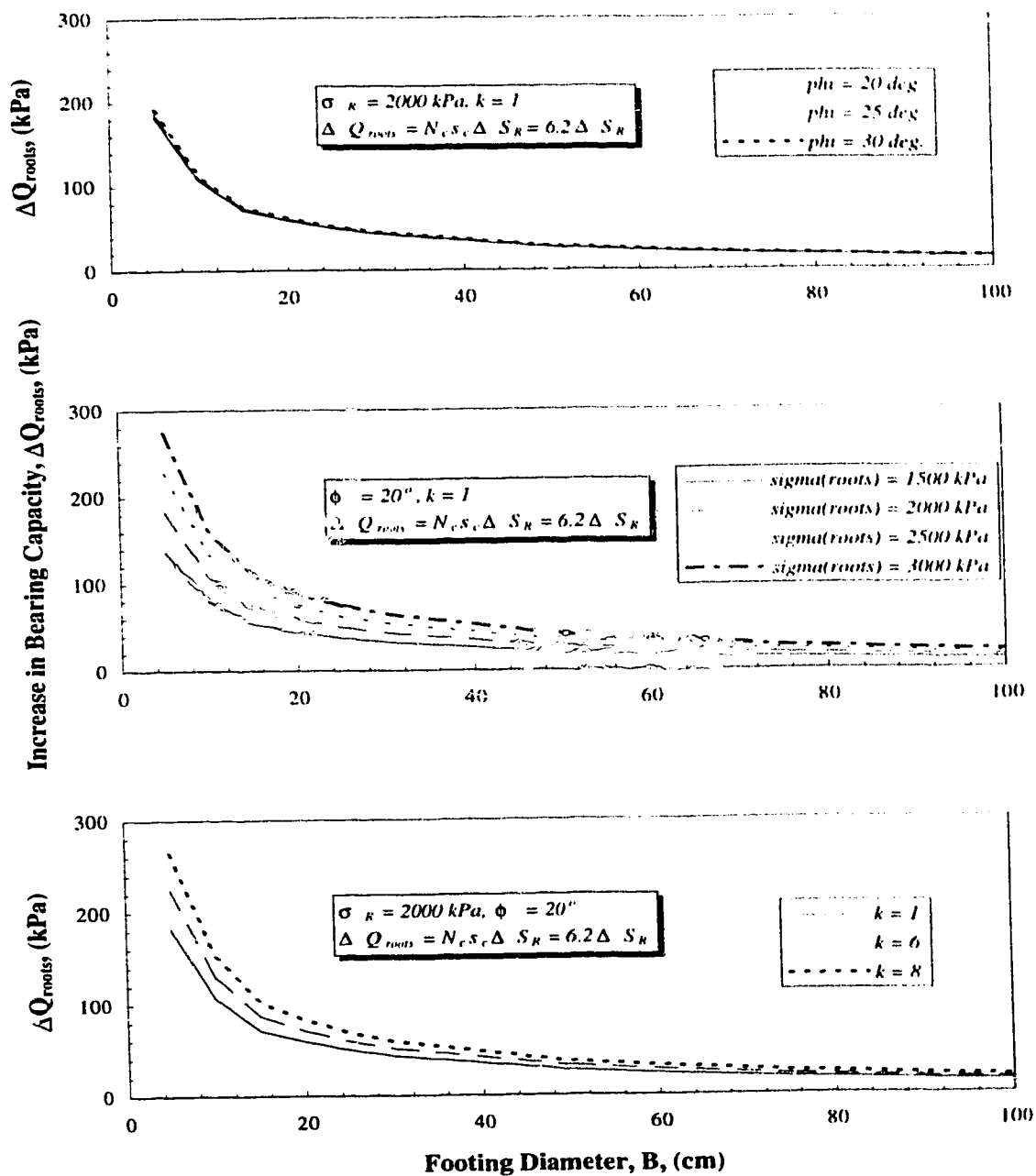
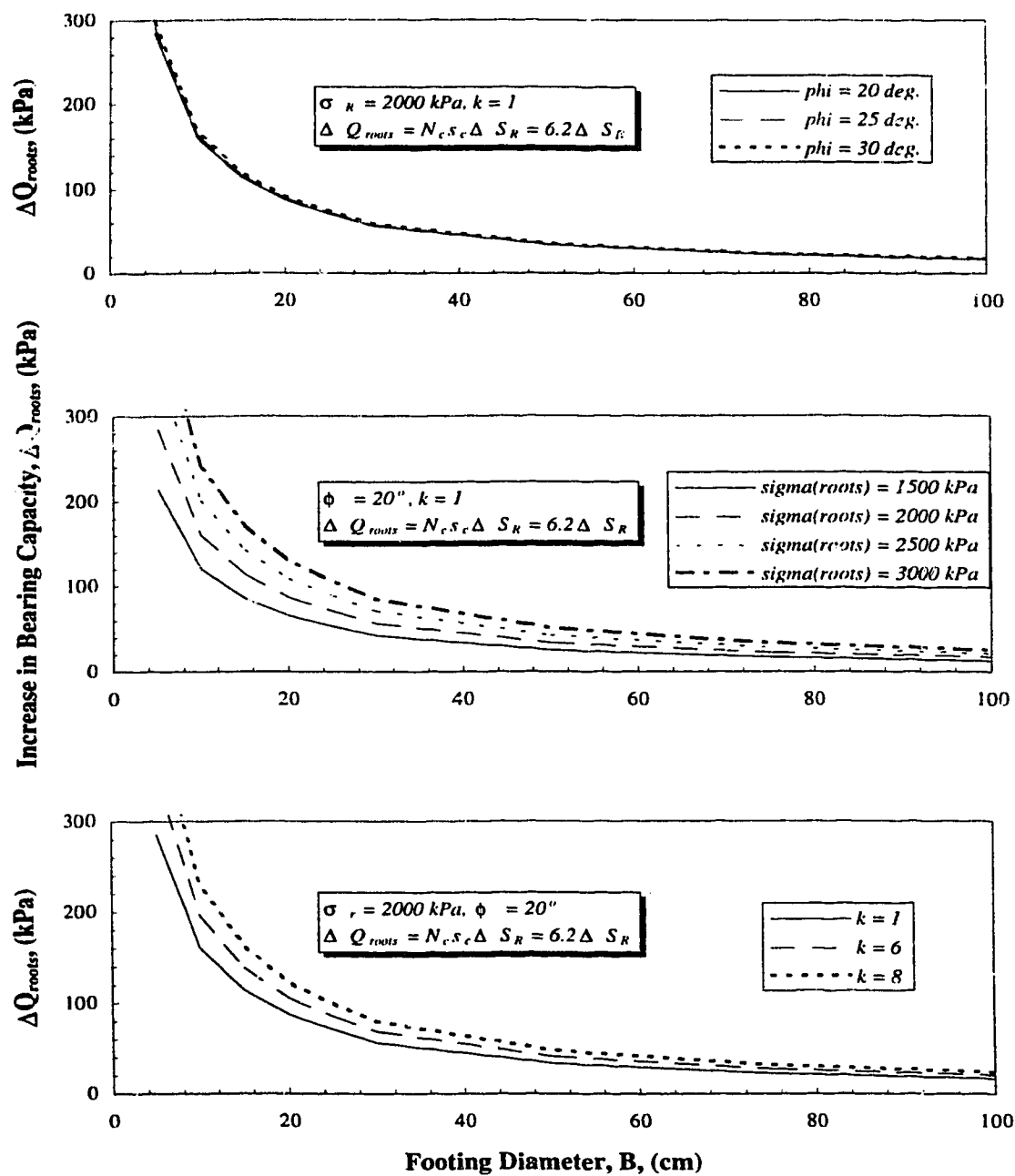


Figure E17

Parametric Analysis of Theoretical Increase in Bearing Capacity From Vegetative Root Systems - Coal Valley Tailings Beach - Site 3

**Figure E18**

Parametric Analysis of Theoretical Increase in Bearing Capacity From Vegetative Root Systems - Coal Valley Tailings Beach - Site 4

Appendix F

Correlations, Comparisons And Factors From Site Investigation Results

F.1. INTRODUCTION

The following appendix highlights extended analysis undertaken using site investigation results obtained along the beach portion of the Coal Valley tailings impoundment and within the Suncor NST Cells. The first section investigates the behavior of the Cone Penetration Test (CPT) and Spectral Analysis of Surface Waves (SASW) results with respect to a recently published Soil Behavior Type chart. The successive section investigates the integrity of the contrasting 1992 and 1994 SASW investigations at Coal Valley using published correlations. This is followed by a section discussing prediction of undrained shear strengths using CPT results, with subsequent correlation with field vane shear test (FVST) profiles. The concluding section explores the interaction of scale effect and fabric features by comparing the results of CPT soundings and Plate Load Test's (PLT's), and presents cone tip factors for root reinforced soils.

F.2. COMPRESSIBILITY CORRELATIONS

The CPT penetration resistance in sands is primarily a function of void ratio, *insitu* stresses, age, cementation, fabric, and compressibility. The shear wave velocity of sand is influenced in general by the same variables with some exceptions. Fabric is understood as having only a slight influence, and as a result of the small degree of strain realized during shear wave velocity

measurements, the large strain soil property of compressibility (Robertson *et al.* 1995) has little to no influence. To summarize some of the significant findings in Robertson *et al.* (1995), a trend is observed with the normalized shear wave velocity, V_{s1} (illustrated in [F1]) and void ratio of freshly deposited uncemented laboratory sand samples. Upon comparison of the normalized shear wave velocity and the normalized cone resistance, q_{c1} (illustrated in [F2]) a relationship is forwarded which compares normalized values as shown in [F3].

$$V_{s1} = V_s \left(\frac{P_a}{\sigma'_{vo}} \right)^{0.25} \quad [F1]$$

$$q_{c1} = q_c \left(\frac{P_a}{\sigma'_{vo}} \right)^{0.5} \quad [F2]$$

where: V_s = shear wave velocity
 q_c = cone penetration resistance
 P_a = atmospheric pressure (usually 100 kPa)
 σ'_{vo} = vertical effective stress

$$q_{c1} = \left(\frac{V_{s1}}{Y} \right)^4 \quad [F3]$$

where: q_{c1} is in MPa
 V_{s1} is in m/s

As discussed in Robertson *et al.* (1995), the Y parameter appears to be controlled by fabric, compressibility, age and cementation. Based on this parameter and the results of field seismic CPT tests and laboratory tests, an illustration is presented in Robertson *et al.* (1995) which relates Y to the inverse slope of the steady state line, $1/\lambda$, age, and compressibility. Based on previous research findings, a graphical representation of the normalized cone tip resistance, Q_t (Appendix C) versus the ratio G_o/q_t (where G_o is the small strain shear modulus determined from seismic CPT shear wave velocity measurements - Appendix D, and q_t is the corrected cone tip resistance - Appendix C) is proposed by Robertson *et al.* (1995) as illustrated in Figure F1. The

ratio G_o/q_t embraces the factors which control the γ parameter, but is influenced by a different exponent.

This results from the CPT and SASW field investigations at Coal Valley and Suncor were subjected to this extended graphical soil behavior type classification as illustrated in Figures F2 to F5 and F6 to F9 respectively. The data included in Figures F2 to F5 from Coal Valley Sites 1 through 4 were divided into the respective soil behavior type classifications defined in the CPT Q_t vs F_r charts in Appendix C. It is remembered that shear wave velocities from the SASW represent the sampling and forward modeling of a larger volume of soil than that sampled using the discrete shear wave velocities from the seismic CPT, which these charts are based upon. Several general comments based on these figures are presented below:

- In general, the material is grouped within and around the “Young Uncemented Soils” region, with a significant scatter outside this region observed at Sites 1, 2, and 3 (Figures F2, F3, and F4).
- The soil which exhibits (3) Clays - Clay to Silty Clay behavior in the Q_t vs F_r charts in Appendix C is generally represented in the “Clays” region in Figures F2 and F5.
- The slightly desiccated crust as a result of evaporation and evapotranspiration is generally represented above the “Young Uncemented Soils” region hedging towards the cementation region.
- As discussed in Appendix C, the Q_t vs B_q generally represent the CPT information from Coal Valley within the coarser regions than that from the Q_t vs F_r charts. Although the data locations would remain unchanged, the charts produced from the different point classifications obtained from the Q_t vs B_q charts in Appendix C would provide an interesting comparison. The value of such a comparison would be amplified if the shear wave velocities and computed G_o values were determined using more discrete method such as with the seismic CPT.

The CPT and SASW data obtained from the Suncor NST Cells is presented in Figures F6 to F9 and consider the two pore water pressure profiles (PWP 1 and PWP 2) represented in Appendix C. The G_o values were determined considering the “*With Crust*” shear wave velocity profiles illustrated in Appendix D. The specific data points defined along the G_o/q_t abscissa are unchanged considering the two pwp conditions. However, the Q_t values computed considering

the PWP 2 profiles are reduced from that considering the PWP 1 profiles due to the higher computed vertical effective stress denominator. In general, the data is represented within the “Clays” section of the charts, grouped within the “low void ratio” region. The data which appears to migrate in a vertical fashion from the lower boundary of the “Young Uncemented Soils” region represents the higher q_t and resulting Q_t data obtained within the upper approximately 0 to 0.4 m of the NST Cells. This upper region has experienced strength gain as a result of evaporation induced matric suction development.

Although definitive comments cannot be presented regarding the results in Figures F2 through F9 due to a variety of factors and issues as discussed in Appendix C and D and including contrasts in shear wave velocity measurement, and site heterogeneity, this soil behavior type chart appears encouraging. As discussed by Robertson *et al.* (1995), the chart not only helps establish material type, but may also signify unusual soils including cemented or aged soils, structured clays and fine grained soils with either high or low water content.

F.3. SHEAR WAVE VELOCITY CONFIRMATION

Appendix D highlighted that SASW investigations were conducted in 1992 at Coal Valley, however, the results were excluded due to their perceived erroneous nature. Qualification of this fact was fostered through a brief review of established empirical correlations within the literature. Hara *et al.* (1974) present a correlation which relates the small strain shear modulus, G_{ss} , with the undrained shear strength, S_u . The small strain shear modulus was determined from downhole seismic techniques and shear strengths were determined from undrained triaxial compression tests. Standard Penetration Test “N” values were recorded at the 25 sites which were included in the analysis and Hara *et al.* (1974) also provides correlations with G_o versus N and S_u versus N . The G_{ss} - S_u relationship shown in [F4] is based on soils with the following physical properties:

- Soils are cohesive, with a wide distribution range of plasticity index values
- The OCR ranges from 1.0 to 3.0
- The void ratios range from 0.5 to 3.0 with the majority of the data within the 1.0 to 2.0 range

- The degree of saturation ranges from 90% to 100% with the majority of the data nearly 100% saturated

$$G_o = 487 S_u^{0.928} \quad [F4]$$

where G_o and S_u are in kg/cm².

Extensive data analysis from 31 clay sites which include *insitu* measurements of initial tangent shear modulus G_{max} and CPT cone tip resistance, q_c is provided in Mayne and Rix (1993). The G_{max} values were obtained at the various sites from either the seismic cone penetration test (SCPT), crosshole (CHT), downhole (DHT), or spectral analysis of surface waves (SASW) techniques with the q_c obtained using the CPT with and without pore pressure measurements. As briefed by Mayne and Rix (1993), the data base represent clay deposits with a wide range in plasticity, sensitivity, stress history, and consistency. Following multiple regression analysis, a preliminary power function relating G_{max} , q_c , and initial void ratio, e_o , was developed as shown in [F5].

$$G_{max} = \frac{406}{e_o^{1.130}} (q_c)^{0.695} \quad [F5]$$

where G_{max} and q_c are in kPa.

Remembering Equation [C1] in Appendix C, and the shear strength formulation from the cone tip resistance outlined in Chapter 5, [F5] may be modified as shown in [F6].

$$G_{max} = \frac{406}{e_o^{1.130}} (\sigma_{vo} + S_u N_{kt} - (1-a)u)^{0.695} \quad [F6]$$

If one assumes shallow depths of investigation with relatively low pore pressures (i.e. σ_{vo} and $(1-a)u$ are small), [F6] converts to:

$$G_{max} = \frac{406 N_{kt}^{0.695}}{e_o^{1.130}} S_u^{0.695} \quad [F7]$$

which is of the same form as that shown in [F4] after Hara *et al.* (1974), however, S_u is dominated by a different exponent.

Equation [F4] was initially employed to investigate the validity of the contrasting 1992 and 1994 SASW investigations at Coal Valley. Equations [F4] and [F5] were manipulated as shown in [F8] and [F9] respectively to predict the shear wave velocities and compare them with the shear wave velocities determined from the SASW investigations. Equation [F8] assumes the shear strength predicted from the CPT cone tip resistance represents approximately the shear strength established from the triaxial tests used to develop [F4].

$$V_s = \sqrt{\frac{677.5}{\rho} \left[\frac{q_t - \sigma_{vo}}{N_{kt}} \right]^{0.928}} \quad [\text{F8}]$$

$$V_s = \sqrt{\frac{406}{\rho * e^{1.130}} [q_t - (1-a)u]^{0.692}} \quad [\text{F9}]$$

where q_t , u , and σ_{vo} are in kPa, ρ is in tonnes/m³, and V_s is in m/s.

The results from the 1994 CPT investigations from Coal Valley were subsequently subjected to the formulations in [F8] and [F9] with the resulting profiles included in Figures F10 to F13. These figures include the V_s profiles predicted from the CPT data, as well as the predicted V_s profiles from the 1992 and 1994 SASW investigations. The values required for the dependent variables in the formulations in [F8] and [F9] (i.e. N_{kt} , ρ , and e) are included in the figures. The link which affords utilization of cone tip resistance for prediction of S_u in the Hara *et al.* (1974) formulation (Equation [F4]) is through the appropriate N_{kt} factor. Based on comparison of CPT soundings with anisotropic consolidated triaxial tests, Luke (1995) found an average N_{kt} value of 10 for six Danish clay soils. Cavity expansion theories and strain path methods showed good agreement with this N_{kt} value (Luke 1995).

Based upon review of the contrasting trends of the 1992 and 1994 SASW V_s profiles in comparison with those predicted from the CPT soundings, abandonment of the 1992 SASW V_s profiles is supported. In all cases, the Hara *et al.* (1974) predicted shear wave velocity profiles

are less than that predicted using the Mayne and Rix (1993) formulation, with the difference increasing with depth. Furthermore, the 1994 SASW V_s profiles are generally less than that predicted from the CPT results, with the best agreement observed at Site 3 in Figure F12.

Although detailed discussion highlighting reasons for the contrast in profiles from Hara *et al.* (1974) and Mayne and Rix (1993) is prohibitive, two possible explanations are offered. Firstly, the Hara *et al.* (1974) formulation is based on shear strengths determined from triaxial compression tests whereas Mayne and Rix (1993) employ direct cone tip resistance. Secondly, the Hara *et al.* (1974) formulation is believed based on mainly on Japanese soils whereas the Mayne and Rix (1993) formulation is more global in nature.

The reader is advised that Hegazy and Mayne (1995) complimented the data base employed in Mayne and Rix (1993) with 31 additional sites which include 24 sand, 5 clay, and one tailings deposit(s). Multiple regression formulations are presented for clays, sands, and all sites which empirically predict V_s based on a variety of parameters including initial void ratio, e_0 , cone tip resistance, q_c , cone sleeve friction, f_s , and effective overburden stress, σ'_{vm} . Although these latest formulations deserved further investigation, they were not explored as part of this research since they would unlikely effect the outcome of this stream of analysis (i.e. to evaluate the contrasting 1992 and 1994 SASW investigations at Coal Valley and subsequently validate the 1994 profiles).

F.4. UNDRAINED SHEAR STRENGTH

Determination of the undrained strength, S_u , of a soil presents some difficulty due to the uniqueness of this parameter. As discussed by Wroth (1984), the S_u of a soil is dependent on a variety of factors including testing technique and resulting stress path, strain rate, and orientation of failure plane. An additional complication is the stress-strain behavior of the soil subjected to undrained shear with brittle to strain hardening responses establishing the range of behavior. The factors which affect the stress-strain response include sensitivity, stress-history, stiffness, as well as fissuring or other discontinuities.

In addition to the complications associated with soil properties, several different empirical and approximate theoretical formulations exist in the literature which attempt to predict S_u from CPT sounding information. Konrad and Law (1987) provide a summary of these formulations which employ the cone tip resistance, and introduce a new formulation which incorporates cavity expansion pressure and friction along the cone-soil interface.

Added to the various formulations in the literature, several reference S_u values have been used to compare with the CPT predictions including values determined from anisotropic consolidated triaxial tests (Luke 1995, Konrad and Law 1987) and field vane shear tests (Robertson and Van Impe 1987). The previous section discussed an N_{kt} value which correlates CPT results with S_u values from anisotropic consolidated triaxial tests. In the succeeding discussion (as recommended in Robertson and Van Impe 1987), the author has chosen to employ the shear strengths determined from the field vane shear test (FVST) results as a reference to those predicted from the CPT soundings.

The undrained shear strength, S_u , evaluated from the corrected cone tip resistance, q_r , is predicted using [F10]

$$S_u = \frac{q_r - \sigma_{vo}}{N_{kt}} \quad [\text{F10}]$$

where σ_{vo} is the total overburden pressure and N_{kt} is the cone tip factor. Several other similar formulations exist within the literature with slight modifications including using the uncorrected cone tip resistance q_c versus q_r , and/or replacing the total vertical stress σ_{vo} with the horizontal total stress σ_{ho} or the octahedral stress σ_{oct} . The subscripts associated with the cone tip factors in these other formulations are varied to reflect the different stress variables.

The common variable which influences the theoretically predicted cone tip factor (except factors developed from classical plasticity approach to bearing capacity) is the predicted rigidity index (I_r) of the soil defined as the shear modulus divided by the shear strength ($I_r = G/S_u$). Based on an estimated I_r of about 50 to 60 (Chapter 5), a preliminary cone tip factor of approximately 16

was selected. This cone tip factor was approximated from a theoretical relationship reproduced graphically in Robertson and Van Impe (1987). The predicted shear strengths from the CPT cone tip soundings from Coal Valley are compared with the vane shear profiles in Figure F14. This figure, which is similar to that produced in Chapter 5, illustrates that the predicted shear strengths are within the same range determined by the FVST, and that some of the heterogeneities at depth which exhibit higher or lower shear strengths are reflected in the companion CPT and FVST profiles.

The FVST strength profiles were directly cross-referenced with the CPT profiles to evaluate the distribution of mobilized N_{kt} factors. The results of this comparison are illustrated graphically in Figure F15. The computed N_{kt} cone factors are presented, with the stepwise average value profiles illustrated for each site. The stepwise profiles were computed on approximately 1 m intervals due to the increased uncertainty in the FVST shear strength profiles with increased depth as a result of enhanced rod friction as discussed in Appendix A. Although considerable scatter exists, the average N_{kt} value determined within the upper meter at Sites 1 through 3 is about 14.5. Site 4 exhibits the least amount of scatter with the computed average profile with depth shifting between 9.5 and 11 from near the surface to a depth of about 2.9 m.

The direct computed N_{kt} values in Figure F15 vary from about 5 to over 25. Although this represents considerable scatter, factors such as local heterogeneity and uncertainty in FVST results at depth are definite factors contributing to the dispersion.

Prediction of shear strength profiles from the CPT within the NST Cells provided a unique opportunity to employ both cone tip resistance and penetration pore pressure. The following quote is extracted from Robertson *et al.* (1986).

"In soft clays, the cone resistance can be very small and typically the cone tip load cell may be required to record loads less than 1% of rated capacity with an associated inaccuracy of up to 50% of the measured values. However, in soft clays, the pore pressures generated can be very large and the pressure transducer may record pressures up to 80% of its rated capacity with an associated accuracy of better than 1% of the measured value. Therefore, estimates of S_u in soft clays will inherently be more accurate using pore pressure data as opposed to the tip resistance."

The natural enhancement process of evaporation created a nonlinear strength profile within the NST Cells, with a relatively stiff surficial crust overlying weaker material. Prediction of S_u in the surficial crust was achieved using the cone tip resistance, whereas highlighted in the exert above, prediction of S_u in the underlying weaker material required the penetration pore pressure.

Prediction of S_u from penetration pore pressure is based on a semi-empirical solution using cavity expansion theory and includes effects of over consolidation and sensitivity through use of Skempton's pore pressure parameter at failure, A_f . The solution provided in Massarsch and Broms (1981) which predicts the pore pressure factor, $N_{\Delta u}$, which is the ratio of the change in pore pressure with the undrained shear strength is given as:

$$N_{\Delta u} = \frac{u - u_o}{S_u} = 4 \ln \frac{r}{\rho} + \ln I_r + 1.733 A_f - 0.577 \quad [\text{F11}]$$

Equation [F11] is based on cylindrical cavity expansion theory, with the pore pressure recorded behind the cone tip. The spherical cavity expansion solution presented in Massarsch and Broms (1981) is applied when the pore pressure element is located on the cone tip face. As previously defined, I_r is the rigidity index, r is the radius of the cylindrical cavity, ρ is the radial vector to a point within the plastic zone, u is the penetration pore pressure, and u_o is the *insitu* static pore pressure. The difference between the penetration and static pore pressure is often referred to as Δu . This equation has been graphically presented in Robertson *et al.* (1986) and Robertson and Van Impe (1987), with ranges of A_f values provided for very sensitive (quick) to highly overconsolidated clays.

The NST deposits may be considered as normally consolidated to very sensitive (or quick) clays with A_f values from 0.7 to 1.3 and 1.5 to 3.0 respectively (Robertson *et al.* 1986). Considering the CPT soil behavior type classification included in Appendix C, a preliminary approximate "mid-range" A_f value of 1.5 was selected. Using [F11], the cone pore pressure factor, $N_{\Delta u}$ of 6 is computed. This factor was used in [F12] to predict the S_u profiles based on the penetration pore pressure.

$$S_u = \frac{u - u_o}{N_{\Delta u}} \quad [F12]$$

The results of the shear strength predictions using the cone tip resistance (Equation [F10]) and the foregoing discussion using the penetration pore pressure are presented for the Suncor NST Cells 3 and 4 in Figures F16 to F19. These figures also include for comparison the shear strengths predicted from the FVST. As evidenced in these figures, the shear strengths predicted from the cone tip resistance below a depth of 0.4 to 0.6 m are consistently less than those determined from the FVST. Encouragingly, the undrained shear strength at depth, predicted using the pore pressure profiles, are very close to the strengths determined from the FVST. This excellent comparison is further amplified considering the very low range of shear strengths experienced within the NST Cells, and the fact that the initial pore pressure profile, u_o , was approximated through a shear strength ratio relationship (Appendix C). Although a circular argument exists through the establishment of u_o using FVST, profiles and using this profile to predict the S_u from the cone penetration pore pressure measurements, the predicted u_o is similar to that estimated from the pore pressure posts (except at the base of the Cells - Appendix C) and the encouraging results are uncompromised.

Boundary lines were established on Figure F16 through F19 at depths of between 0.4 m and 0.6 m. These boundaries approximately define the upper regions where the cone tip resistance is more applicable in defining S_u , versus the lower regions where the penetration pore pressure is more applicable. A cone tip factor, N_{kt} of 15 was selected to predict the FVST S_u in the upper surficial crust. Although FVST readings were not extend to the surface, some of the vane shear strengths in the upper layers (Figure F17 and F18) support the higher strength crust predicted from the CPT. The unsaturated nature of the surficial crust precludes confident utilization of the penetration pore pressures in shear strength prediction in the higher strength crust (bearing in mind that $N_{\Delta u}$ likely changes in the upper crust as a result of consolidation through matric suction development).

F.5. DISCONTINUITY EFFECTS

The previous section briefly mentioned the factors which influence the S_u of a clay including sensitivity, stress-history, stiffness, fissuring and other discontinuities. The following includes a brief discussion of the impact of fissures and other discontinuities (i.e. fabric features) on scale effects and mobilized *insitu* bearing capacity.

Powell and Quarterman (1988) present a relationship which illustrates the back calculated cone tip factor based on comparison with the mobilized bearing capacity from PLT's. The relationship included in Figure F20 illustrates the effect of plasticity, but more importantly fissures and associated CPT scale on the effective cone tip factor. The CPT soundings were conducted with a cone of standard dimensions, and the PLT's were conducted using circular plates. Although specifics regarding the plate diameters at each site were not provided, the authors discuss in the article plate diameters of from 140 mm, 292 mm, and 865 mm.

The fissures illustrated in Figure F20 represent planes or discontinuities of weakness. With closely spaced fissures, the mobilized cone tip resistance will depend upon the properties along the discontinuities. With increased fissure spacing, the mobilized cone tip resistance will be less compromised by the discontinuities and primarily record the properties of the intact soil. In the latter case of widely spaced fissures, the reduced sampling scale of the CPT fails to record the properties of the weak discontinuities. Since such discontinuities would control the behavior of large scale tests, the S_u employed for design must be reduced (higher N_c) to reflect the weak discontinuities.

The effect of discontinuities was also observed through comparison of the Coal Valley PLT and CPT investigations. In this case, the discontinuities are the vegetative root system, and contrary to fissures, serve to reinforce and strengthen the soil. The results of the comparison between the PLT's and CPT's are included in Figure F21. This figure represents the N_{kt} cone tip factor versus the % Roots with the Root Area Ratio (RAR) profile at Site 2 used as a bench mark. As illustrated in the caption in the upper left corner of the figure, an average q_t and σ_{vo} were obtained from the surface of the plate load test to a depth of $2D_p + s$ where D_p is the diameter of the plate and s is the amount of settlement. The computed N_{kt} values from the CPT and PLT

results range from about 8.5 to 11 with a lower value of about 6.5 recorded at Site 4. This range of values is below that illustrated in Figure F20, and is also below the average value of about 14.5 determined upon comparison with the FVST profiles at Site 1, 2, and 3 illustrated in Figure F15. The extreme heterogeneity at Coal Valley provides difficulty with respect to establishing the average plasticity index of the soil within the loaded zone for comparison with the results in Figure F20. However, as discussed in Chapters 2, 6 and 7, the grain size at D_{50} decreases, and percent fines $F\%$ increases in the downstream direction, with the maximum plasticity index of 35 % recorded within the pond (beyond Site 4).

Although insufficient data is available to confidently establish trends, it is hypothesized that the effect of roots on N_{kt} may exhibit a mirrored effect to that of fissures illustrated in Figure F20. The denser distribution of finer root patterns perhaps associated with grasses and legumes will have some influence on the cone tip resistance and the N_{kt} may resemble the values illustrated in Figure F21. As root species and morphology changes or matures with the development of larger and more robust vegetation patterns associated with deciduous or coniferous tree species, reduced N_{kt} factors below that determined in Figure F21 may be experienced.

It is recognized that rooting patterns are not uniform, with typically decreasing RAR with depth as illustrated in Appendix E. Although unconfirmed, it is envisioned that the N_{kt} factors may increase as the CPT sounding migrates downward through the vegetative zone. A similar increasing N_{kt} relationship with depth may perhaps also occur with fissured clays as illustrated in Figure F20, with the effects of weathering decreasing (fissure spacing increasing) with depth.

As a final comment, confirmation of these reduced N_{kt} factors associated with the higher strength discontinuities offered by vegetative root systems is an interesting area for future research initiatives. In addition, advances in CPT technology through the coupling of density and moisture content modules may eventually provide the opportunity to directly record and correlate changes in RAR and resulting N_{kt} with depth without the requirement for sampling. These potential developments may not only enhance reclamation activities and associated progress monitoring, but the promise of predicting the enhanced surface stability of vegetated environments with the CPT may also assist in resource and frontier development.

F.6. REFERENCES

- Hara, A., Ohta, T., Niwa, M., Tanaka, S., and Banno, T., 1974. Shear Modulus and Shear Strength of Cohesive Soil. *Soils and Foundations*, Japanese Society of Soil Mechanics and Foundation Engineering, **14**(3):1-12.
- Hegazy, Y.A., and Mayne, P.W., 1995. Statistical Correlations Between V_s and Cone Penetration Data for Different Soil Types. *Proceedings of the International Symposium on Cone Penetration Testing, "CPT'95"*, Linköping, Sweden, October 4-5, Vol. 2, pgs. 173-178.
- Konrad, J.M., and Law, K.T., 1987. Undrained Shear Strength from Piezocone Tests. *Canadian Geotechnical Journal*, **24**(3):392-405.
- Luke, K., 1995. The use of c_u from the Danish Triaxial Tests to Calculate the Cone Factor. *Proceedings of the International Symposium on Cone Penetration Testing, "CPT'95"*, Linköping, Sweden, October 4-5, Vol. 2, pgs. 209-214.
- Marsland, A., and Quarterman, R.S.T., 1982. Factors Affecting the Measurement and Interpretation of Quasistatic Penetration Tests in Clays. *Proceedings of the Second European Symposium on Penetration Testing*, Amsterdam, pgs. 697-702.
- Massarsch, K.R., and Broms, B.B., 1981. Pile Driving in Clay Slopes. *Proceedings of the Tenth International Conference on Soil Mechanics and Foundation Engineering*, Stockholm, Sweden, June 15-19, Vol. 3, pgs. 469-474.
- Mayne, P.W., and Rix, G.J., 1993. G_{max} - q_c relationships for clays. *Geotechnical Testing Journal*, The American Society for Testing and Materials **16**(1):54-60.
- Powell, J.J.M., and Quarterman, R.S.T., 1988. The Interpretation of Cone Penetration Tests in Clays, With Particular Reference to Rate Effects. *Proceedings of the Conference on Penetration Testing, ISOPT-1*, Florida, pgs. 903-909.
- Robertson, P.K., and Campanella, R.G., 1983a. Interpretation of Cone Penetration Tests. Part I: Sand. *Canadian Geotechnical Journal* **20**:718-733.
- Robertson, P.K., and Campanella, R.G., 1983b. Interpretation of Cone Penetration Tests. Part II: Clay. *Canadian Geotechnical Journal* **20**:734-745.
- Robertson, P.K., and Van Impe, W.F., 1987. Cone Penetration With Pore Pressure Measurement. *Belgisch Comité voor Ingenieursgeologie, B.C.I.G.*, Belgium, Dec. 1987, 60 pgs.

- Robertson, P.K., Campanella, D., Gillespie, D., and Greig, J., 1986. Proceedings of the ASCE Specialty Conference "IN-SITU 86". Use of In-situ Testing in Geotechnical Engineering, June, pgs. 1263-1280.
- Robertson, P.K., Fear, C.E., Woeller, D.J., and Weemee, I., 1995. Estimation of Sand Compressibility from Seismic CPT. 48th Canadian Geotechnical Conference, Vancouver, B.C., Sept. 26-29, Vol 1, pgs. 441-448.
- Teh, C.I., and Houlsby, G.T., 1991. An Analytical Study of the Cone Penetration Test in Clay. *Geotechnique*, **41**(1):17-34.

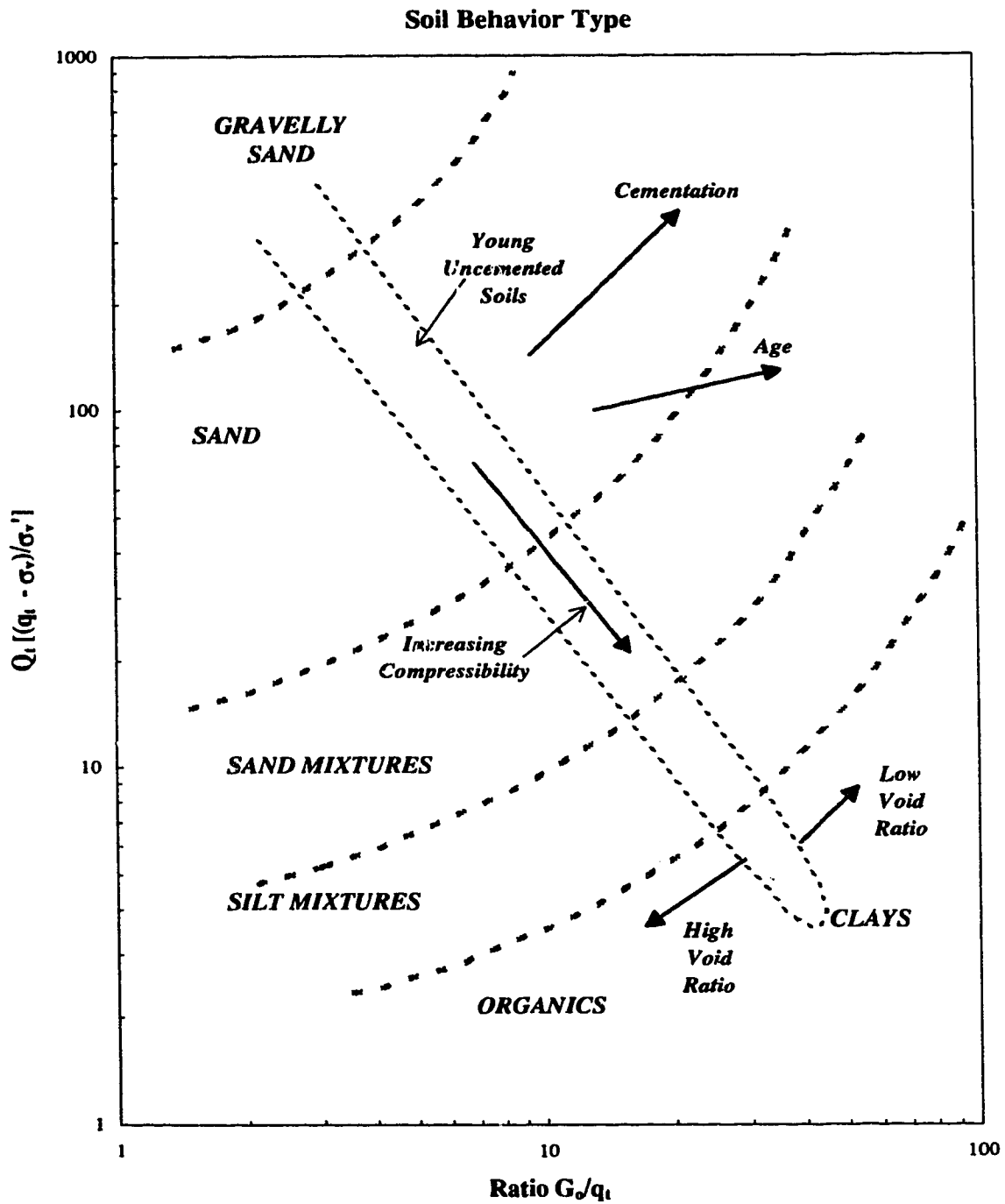


Figure F1 Proposed Soil Behavior Type Chart Based on Q_t and G_o/q_t (after Robertson et al. 1995)

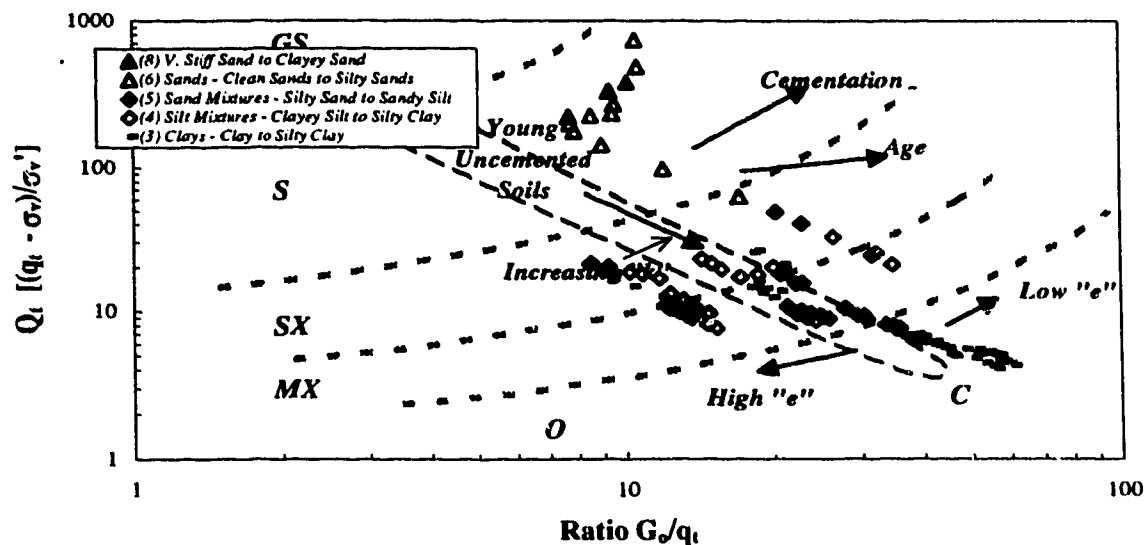


Figure F2 Q_t versus G_o/q_t Behavior Chart for Coal Valley Tailings Beach - Site 1

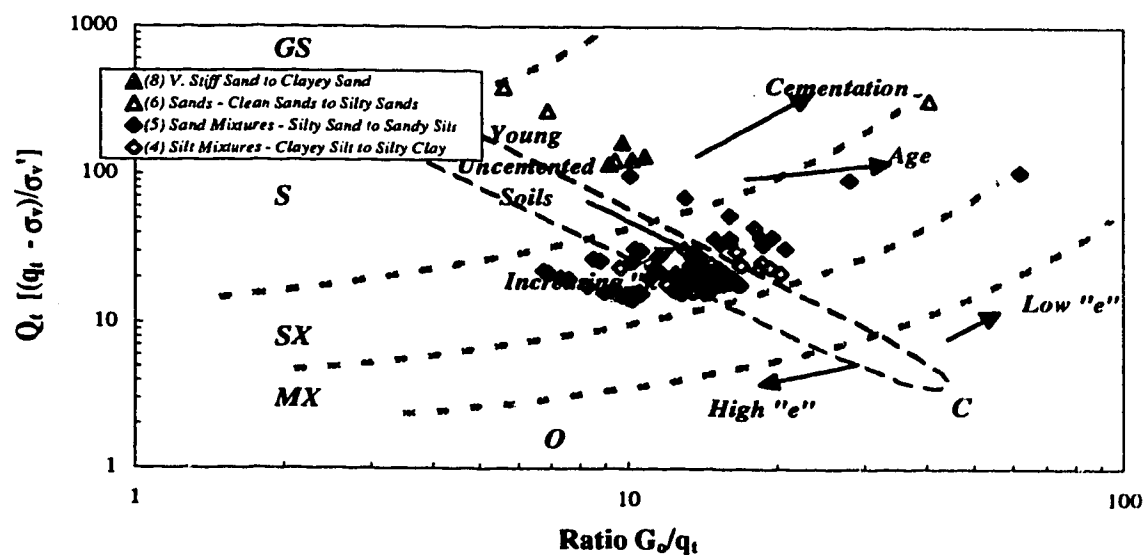


Figure F3 Q_t versus G_o/q_t Behavior Chart for Coal Valley Tailings Beach - Site 2

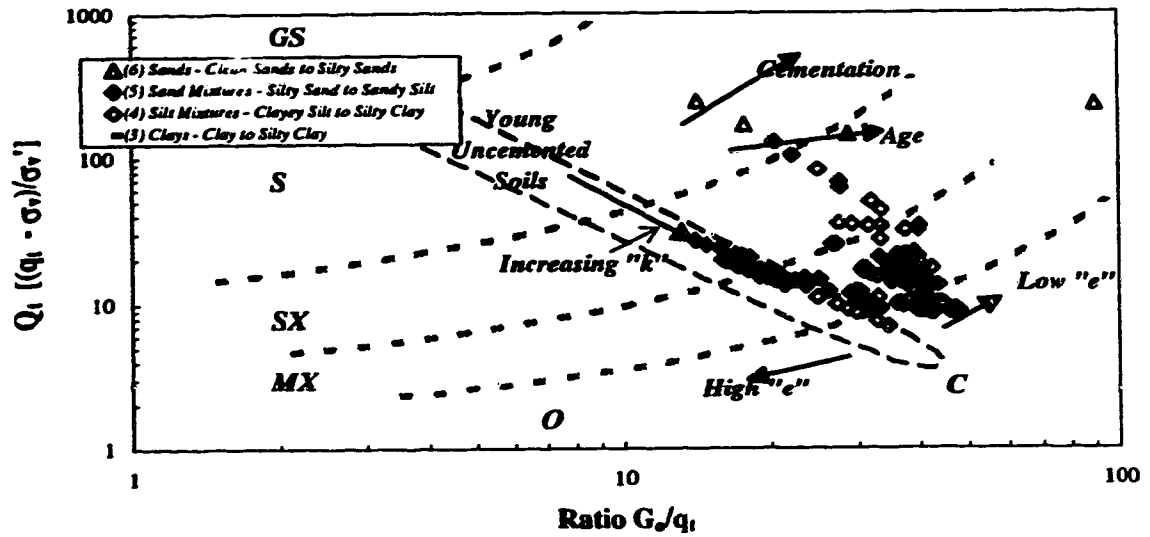


Figure F4 Q_r versus G_s/q_r Behavior Chart for Coal Valley Tailings Beach - Site 3

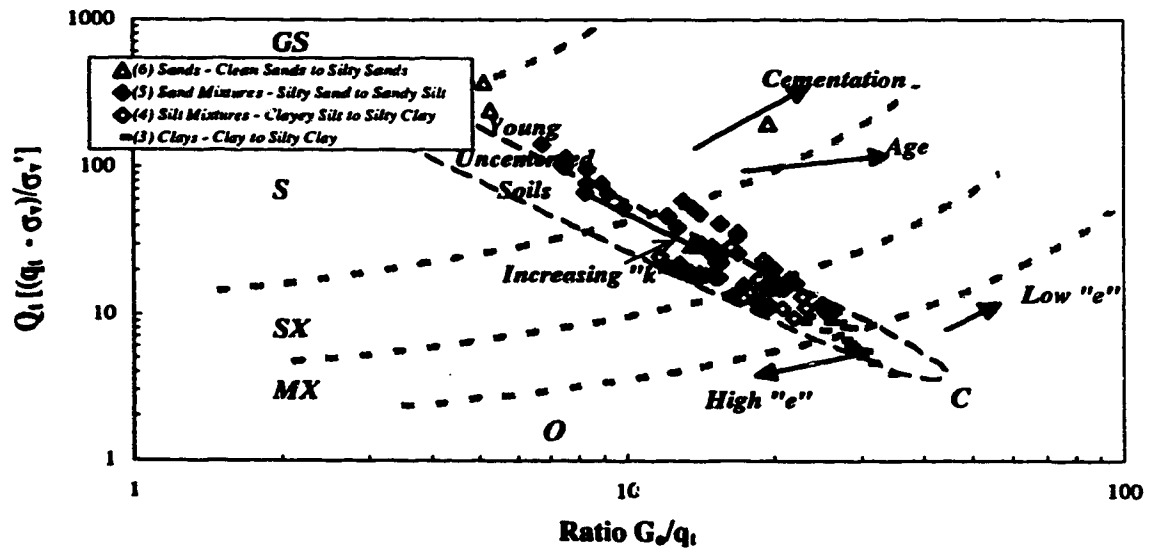


Figure F5 Q_r versus G_s/q_r Behavior Chart for Coal Valley Tailings Beach - Site 4

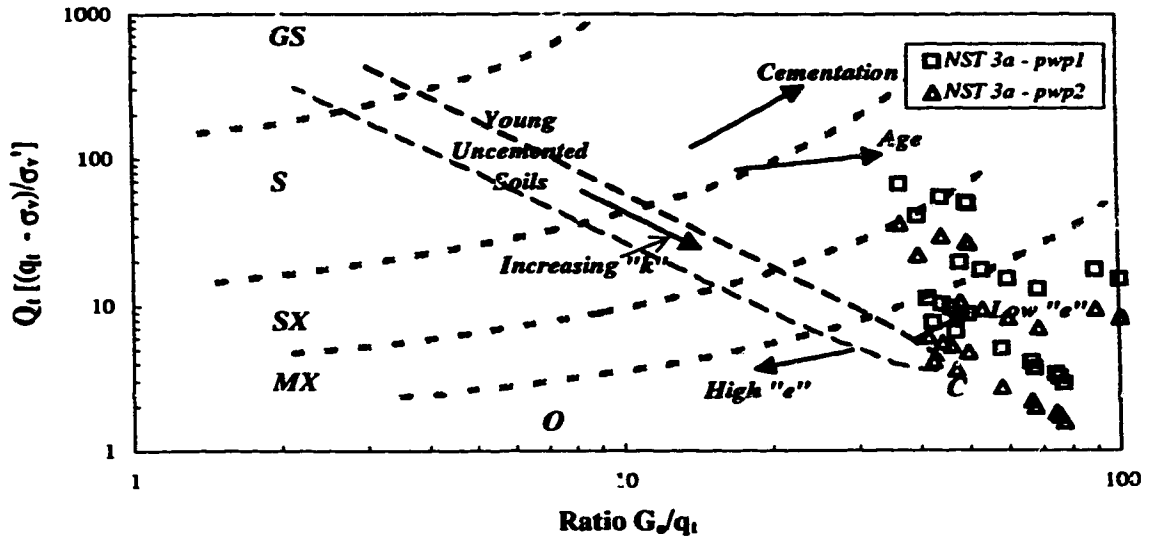


Figure F6 Q_t versus G_o/q_t Behavior Chart for Suncor NST Cell 3a

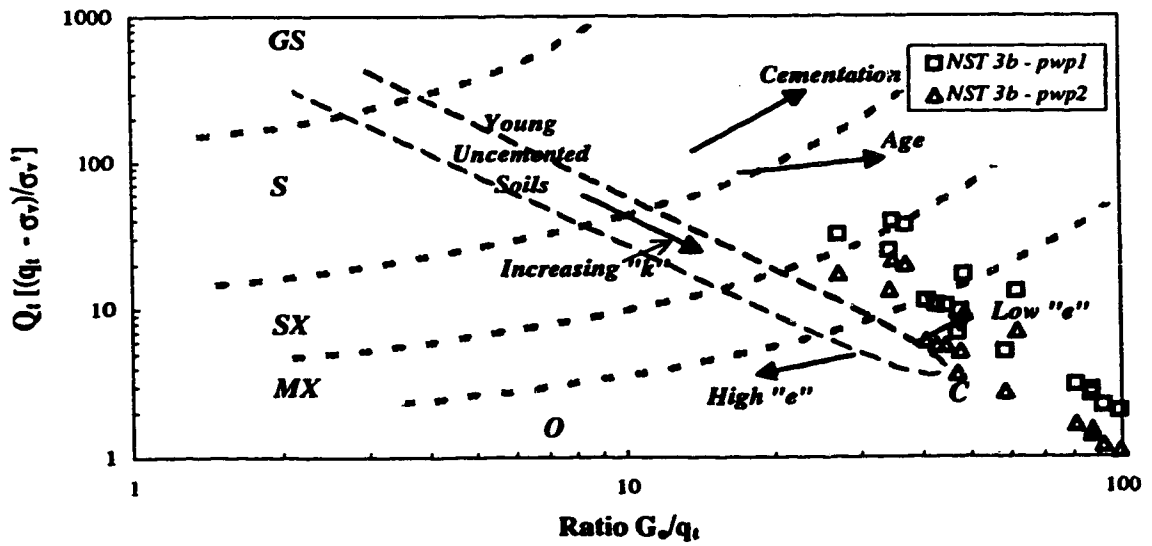


Figure F7 Q_t versus G_o/q_t Behavior Chart for Suncor NST Cell 3b

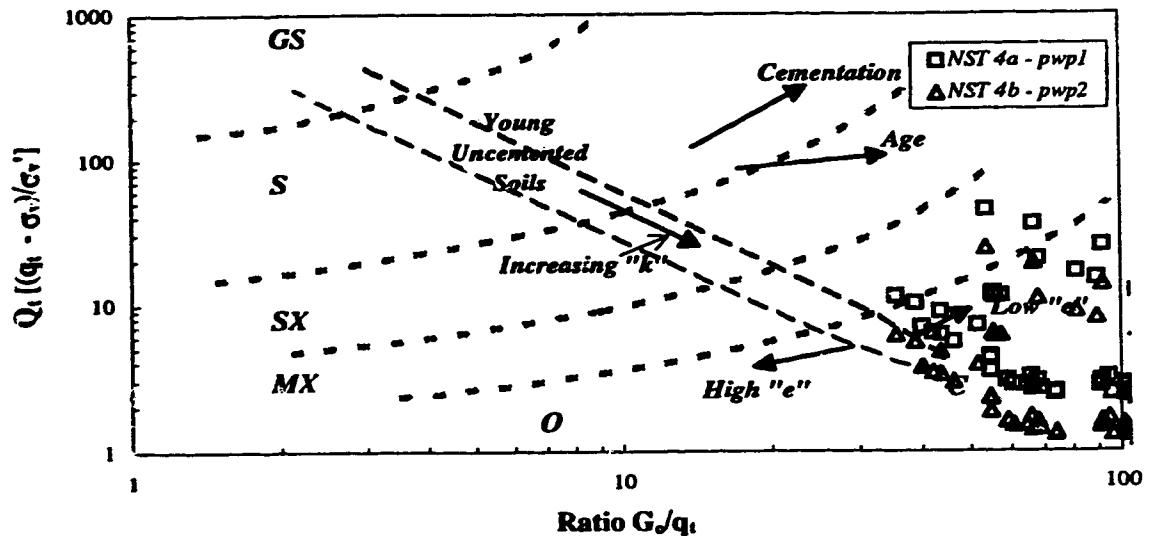


Figure F8 Q_1 versus G/q_1 Behavior Chart for Suncor NST Cell 4a

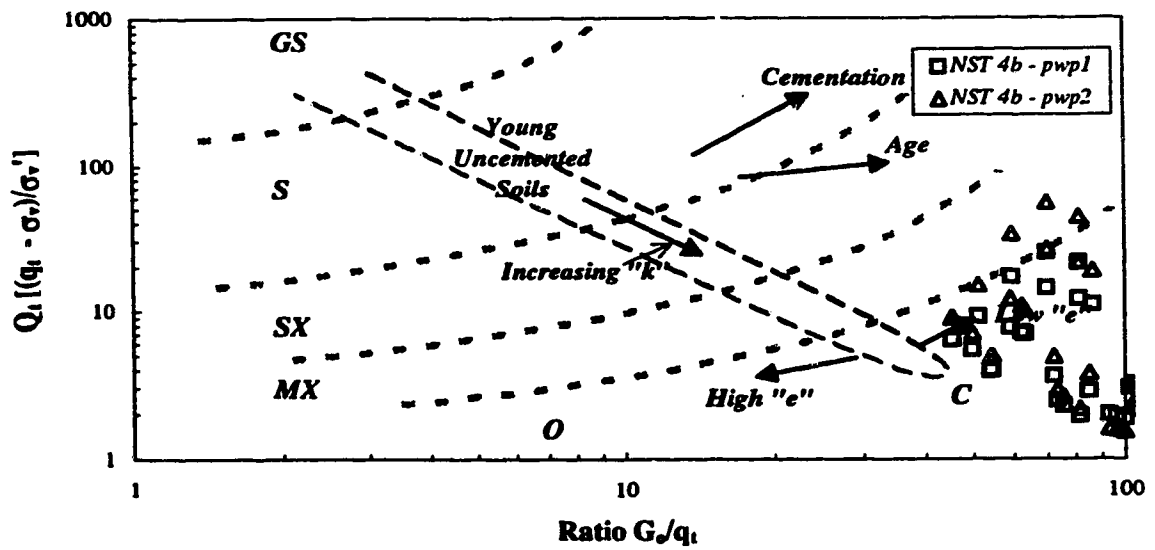


Figure F9 Q_1 versus G/q_1 Behavior Chart for Suncor NST Cell 4b

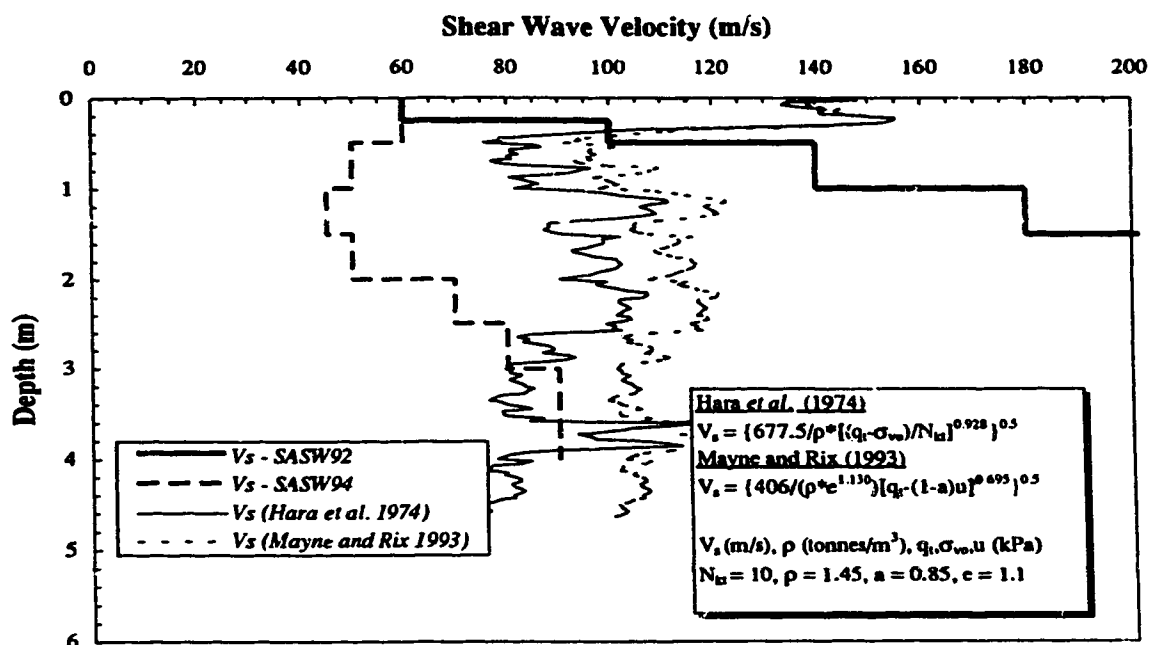


Figure F10 **Shear Wave Velocity Profiles from SASW Modelling and Predicted from CPT Soundings - Coal Valley Tailings Beach - Site 1**

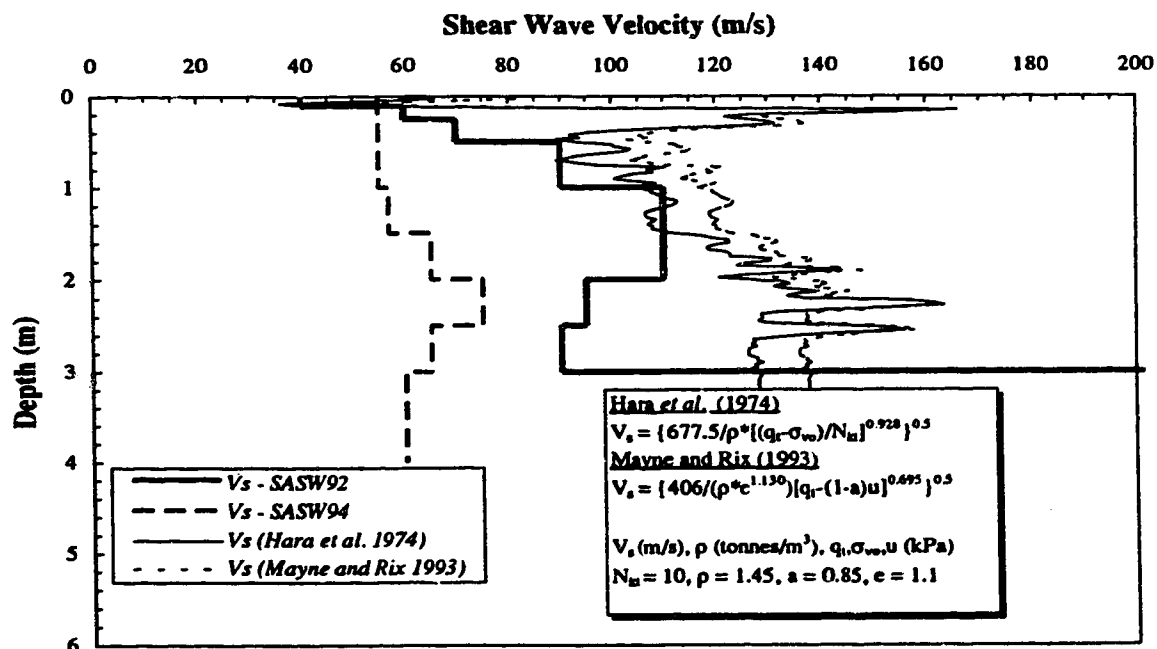


Figure F11 **Shear Wave Velocity Profiles from SASW Modelling and Predicted from CPT Soundings - Coal Valley Tailings Beach - Site 2**

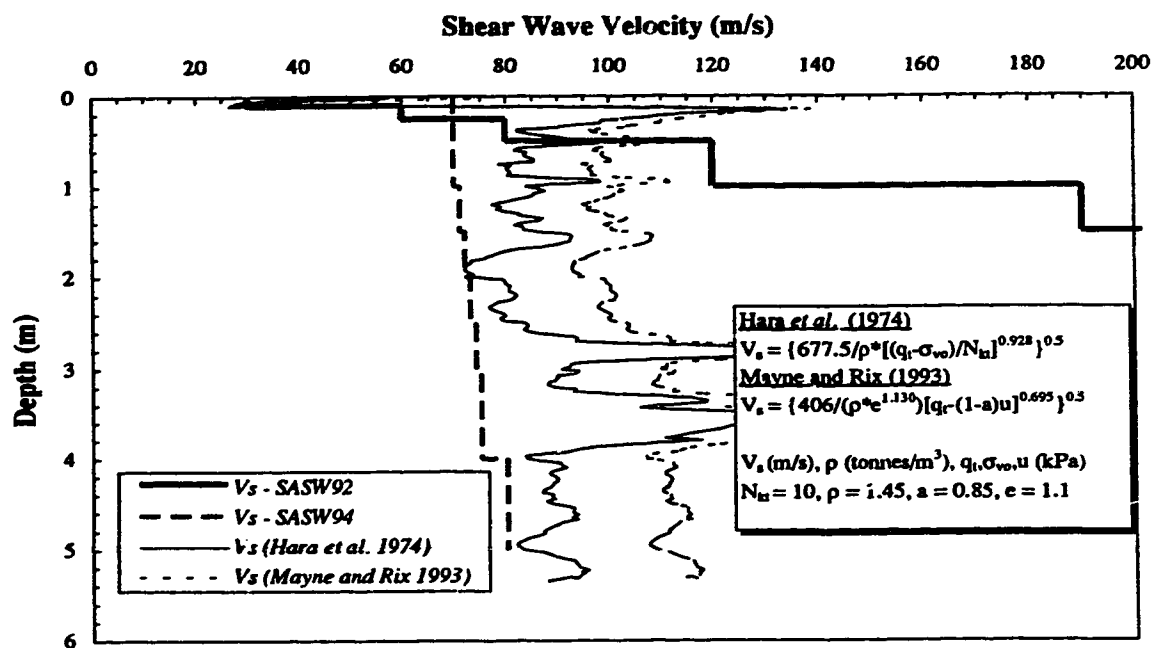


Figure F12 Shear Wave Velocity Profiles from SASW Modelling and Predicted from CPT Soundings - Coal Valley Tailings Beach - Site 3

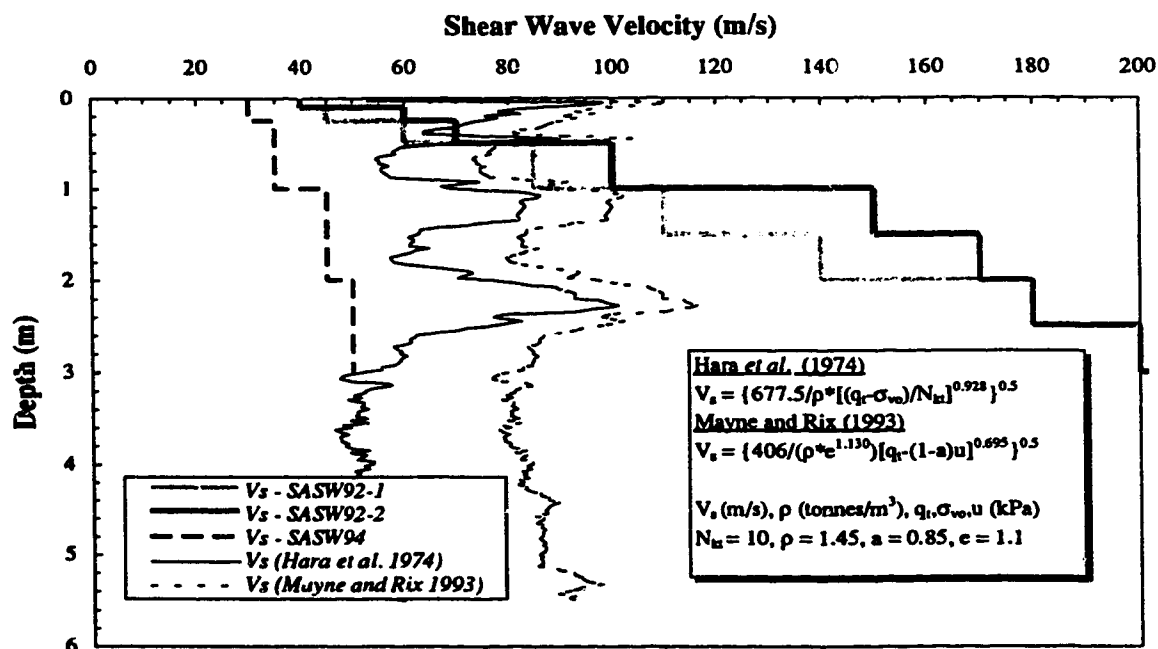


Figure F13 Shear Wave Velocity Profiles from SASW Modelling and Predicted from CPT Soundings - Coal Valley Tailings Beach - Site 4

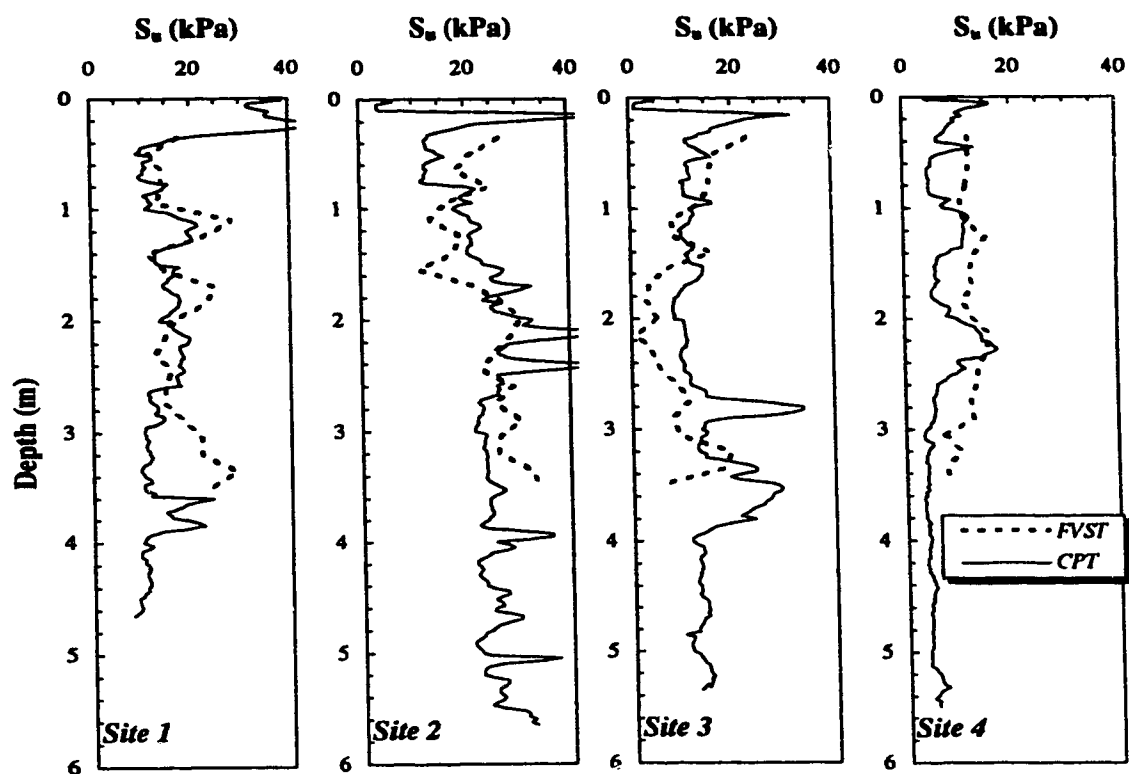


Figure F14 Shear Strength Profiles from FVST and CPT Soundings Along Coal Valley Tailings Beach

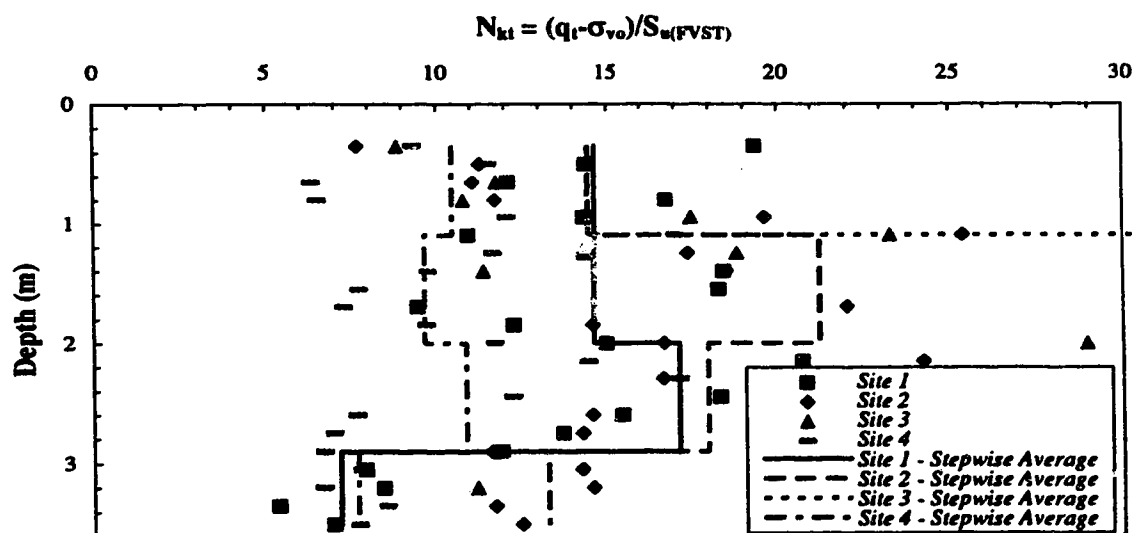


Figure F15 Computed N_{Kt} Cone Factors Based on Reference FVST Results Along Coal Valley Tailings Beach

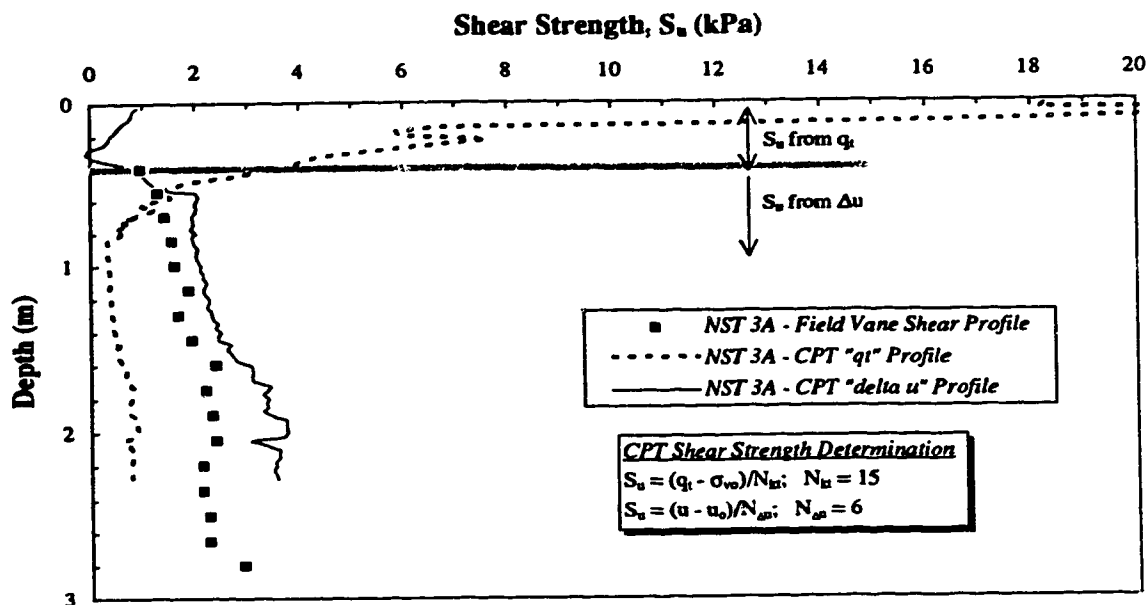


Figure F16 **Shear Strength Profiles from FVST and Predicted from CPT Soundings - Suncor NST Cell 3a**

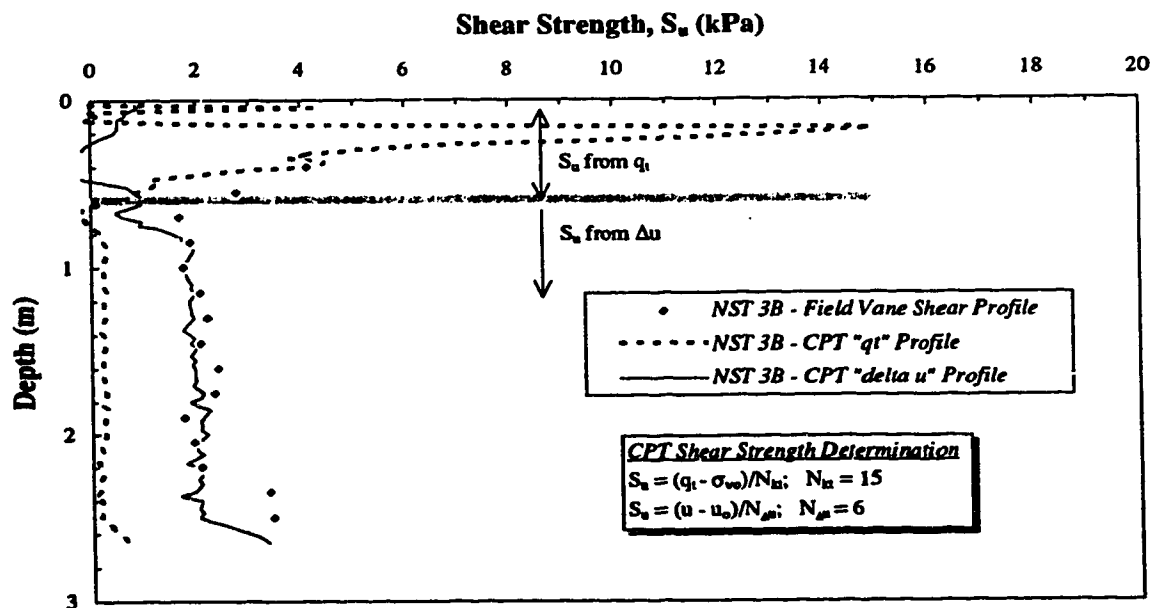


Figure F17 **Shear Strength Profiles from FVST and Predicted from CPT Soundings - Suncor NST Cell 3b**

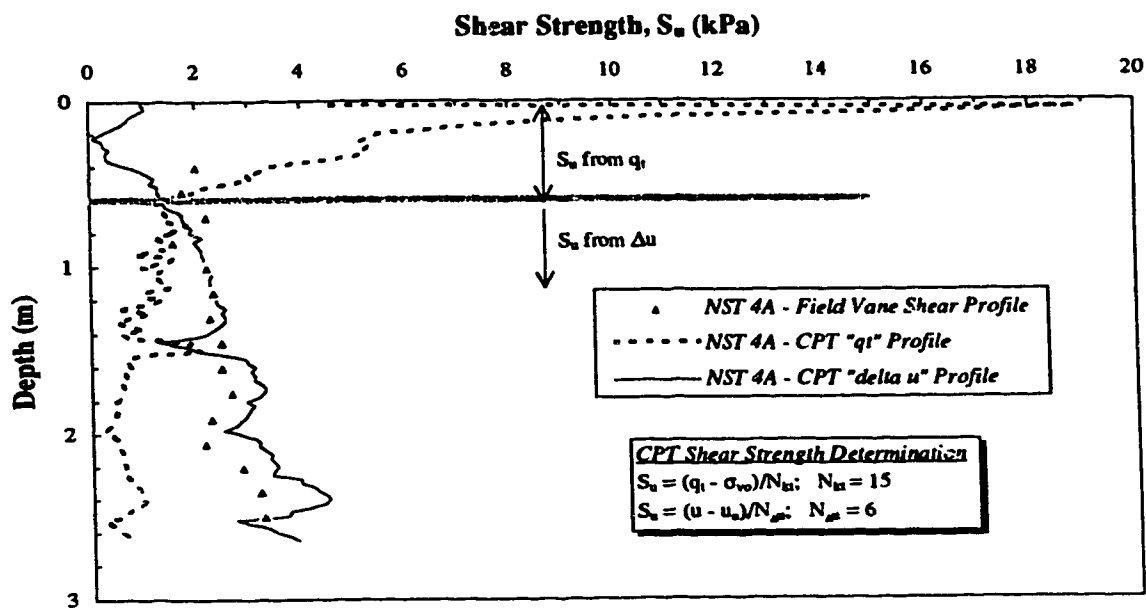


Figure F18 **Shear Strength Profiles from FVST and Predicted from CPT Soundings - Suncor NST Cell 4a**

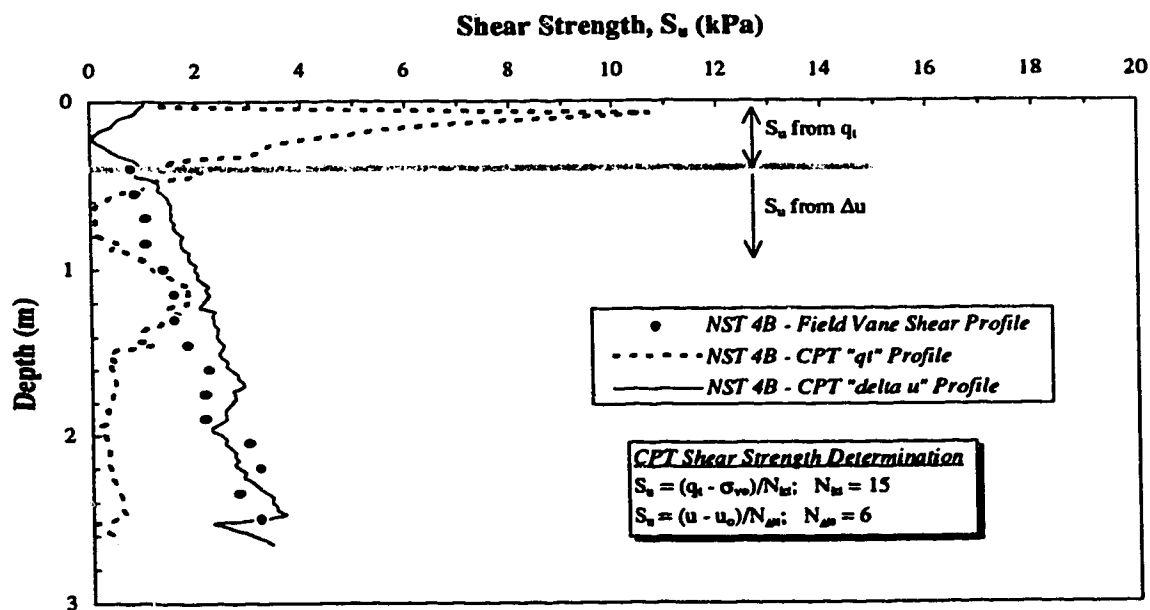


Figure F19 **Shear Strength Profiles from FVST and Predicted from CPT Soundings - Suncor NST Cell 4b**

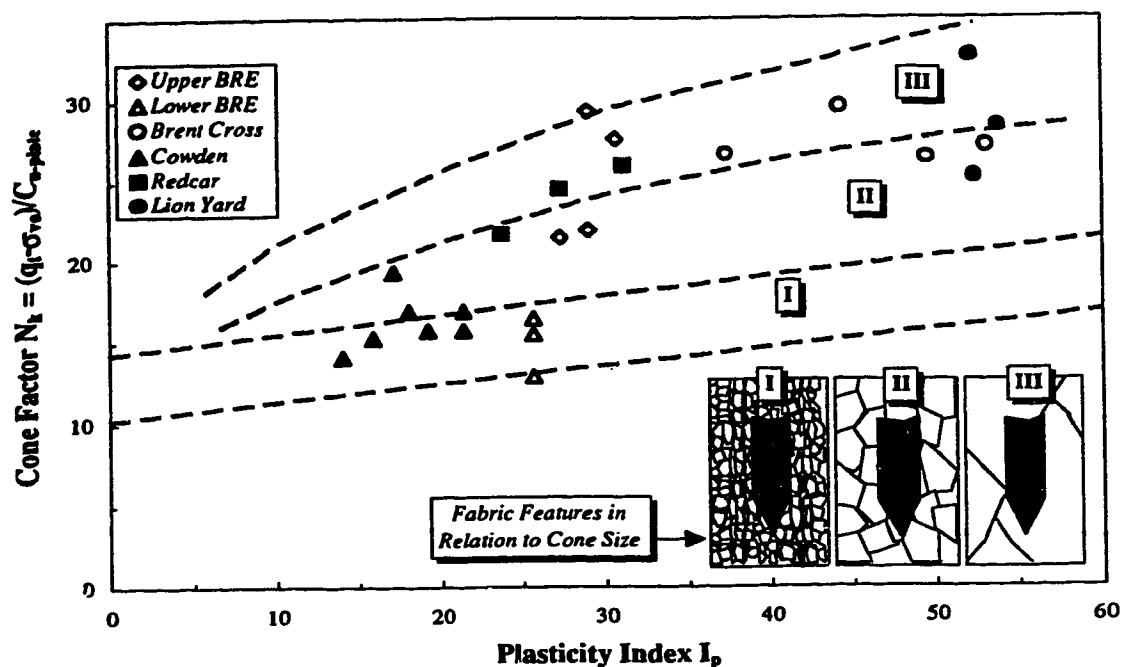


Figure F20 Cone Factors Based on Plate Load Tests Conducted in Clays with a Range in Scale of Fabric Feature (Discontinuities) (modified from Powell and Quarterman 1988)

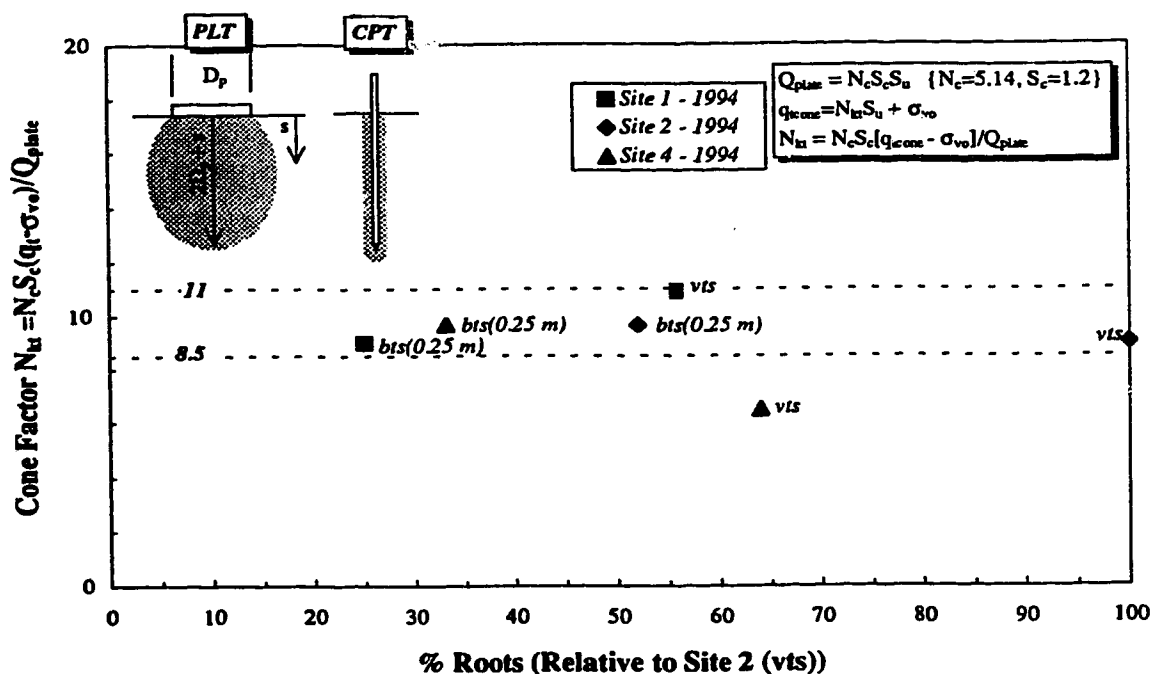


Figure F21 Cone Factors Computed from Plate Load Tests Conducted on Root Reinforced Soils Along Coal Valley Tailings Beach

***A Mans Finest Hour Is That Moment When He Worked His Heart
Out In A Good Cause And Lies Exhausted On The Field Of Battle,
Victorious.***

- Vince Lombardi -